Mesenchymal Stromal Cells: Mode of Action and Clinical Translation

Mónica Sofia Correia dos Reis

Submitted in partial fulfilment of the requirements for the degree of Doctor of Philosophy

Haematological Sciences

Institute of Cellular Medicine

Newcastle University, UK

August 2016

Abstract

Mesenchymal Stromal Cells (MSCs) are an extensively used cell type in clinical trials for the treatment of various diseases. In order to obtain clinically relevant numbers, MSCs need to be expanded *in vitro*, usually relying on the use of foetal calf serum (FCS), which is now not recommended by the regulatory authorities. In addition, the precise mechanism of action of MSCs remains unclear. The initial rationale for the therapeutic potential of MSCs was based on their engraftment and differentiation ability. It gets increasingly clear that MSCs exert their effects in a paracrine manner, by the release of soluble factors and extracellular vesicles (EVs). The aims of this study are: 1) to investigate the feasibility of replacing FCS with human platelet lysate (PLT) for the expansion of MSCs and assess its effect on MSC general characteristics and immunosuppressive potential; 2) to assess the immunoregulatory function of EVs derived from PLT-expanded MSCs (MSC-PLT).

Data presented in this thesis demonstrated that MSC-PLT maintained their general characteristics and immunosuppressive potential, while exhibiting enhanced proliferative properties compared to FCS-expanded MSCs (MSC-FCS). As the first comparative study on the global surface protein profile of MSC-FCS and MSC-PLT, we showed that PLT induced little changes on the expression of markers involved in the enhancement of proliferation and differentiation properties of MSCs. Furthermore, this study has demonstrated that MSC-derived EVs retained the immunosuppressive function of the parent cells, although with a lower potency. Here we also report for the first time, that MSC-EVs skewed DC maturation into a tolerogenic phenotype and impaired their phagocytic ability and migratory potential. We also found that MSC-derived EVs are rich in a wide variety of microRNAs that target a plethora of genes involved in various pathways related to development, trafficking and modulation of immune responses, including dendritic cell maturation and function. The findings in this study support the notion that PLT is a suitable supplement for *in vitro* MSC expansion and that MSC-PLT produce EVs with the ability to modulate immune responses.

Acknowledgements

I would like to express my gratitude to my supervisors, Dr. Xiao-nong Wang, Professor Anne Dickinson and Dr. Lindsay Nicholson for all the support and thoughtful input throughout my PhD. I am especially grateful to Dr. Xiao-nong Wang for believing in my ability and trusting my ideas and guiding me throughout my project. I am especially grateful for the trust given by Dr. Xiao-nong Wang when I proposed the study of MSC-derived extracellular vesicles as one of my main project objectives, despite the lack of expertise in this field within Haematological Sciences and Newcastle University in general.

I would also like to express my gratitude to the Marie Curie Initial Training Network Celleurope and to the European Commission who funded this work. A special thanks to all of the fellows, researchers and clinicians who were a part of this consortium and contributed to my work and knowledge.

I would like to thank Miltenyibiotec, in Bergisch Gladbach, Germany, for hosting me for 2 months during my secondment. I am especially grateful to Kathrin Godthardt and Sebastian Knöbel for their supervision and guidance during my time at Miltenyi.

I am also grateful to Clotilde Thery for allowing me to do an internship in her laboratory at Institute Curie, Paris, France, to learn how to isolate and characterise extracellular vesicles from culture supernatants. I am especially thankful to Joana Kowal and Mercedes Tkach for teaching me how to perform all the protocols. Thanks also to Newcastle's doctoral awards scheme, supported by Welcome Trust who funded this internship.

A special thanks to everybody who contributed to the generation of data presented in this thesis at Haematological Sciences, including Dr. Emily Mavin and Kile Green, who shared protocols and aided in the analysis of some data. Thanks to everybody at Haematological Sciences who, directly or indirectly, worked with me and helped on a daily basis.

Very special thanks to my family and friends who always supported and believed in me.

Author’s Declaration

The material contained in this thesis is entirely the work of this author, unless otherwise stated and has not been submitted for a degree previous to this or any other University.

Mónica Sofia Correia dos Reis, M.Sc.

August, 2016

List of Abbreviations

ADGRE(number)	Adhesion G protein-couple receptor (number)
ALP	Alkaline phosphatase
APC	Antigen presenting cell
APC	Allophycocyanin
ATP	Adenosine triphosphate
BCA	Bicinchoninic acid
BM	Bone marrow
BMP2	Bone morphogenetic protein 2
BSA	Bovine serum albumin
bFGF	Basic fibroblast growth factor
CBA	Cytometric bead array
CCL(number)	Chemokine (C-C motif) ligand (number)
CCR(number)	Chemokine (C-C motif) receptor (number)
CDCP1	CUB domain containing protein 1
cDNA	Copy deoxyribonucleic acid
C/EBP(greek)	CCAAT/enhancer binding protein (greek letter)
CFSE	Carboxyfluorescein succinimidyl ester
CFU-F	Colony forming units fibroblasts
CLA	Cutaneous lymphocyte antigen
Ct	Cycle threshold
CTL	Cytotoxic T lymphocyte
CTLA-4	Cytotoxic T lymphocyte antigen 4
DAPI	4’,6-diamidino-2-phenylindole
DC	Dendritic cells
DMEM	Dulbecco’s modified eagle medium
DMSO	Dimethyl sulphoxide
DNAM-1	DNAX accessory molecule 1
DPP4	Dipeptidyl peptidase-4
EDTA	Ethylenediaminetetraacetic acid
ESCRT	Endosomal sorting complexes required for transport
EGF	Epidermal growth factor
ERK(number)	Extracellular signal-regulated kinase (number)
EV	Extracellular vesicles
FACS	Fluorescence activated cell sorting
FCS	Foetal calf serum
FGF	Fibroblast growth factor
FITC	Fluorescein isothiocyanate
FoxP3	Forkhead box P3
GAG	Glycosaminoglycan
GM-CSF	Granulocyte macrophage colony stimulating factor

GMP	Good manufacturing practice
GPI	Glycophosphatidylinositol
GvHD	Graft versus host disease
HAS	Human autologous serum
hESC	Human embryonic stem cells
HCl	Hydrochloric acid
HGF	Hepatocyte growth factors
HLA	Human leukocyte antigen
HSA	Human serum albumin
HSP	Heat shock proteins
hUCBD	Human umbilical cord blood serum
ICAM-1	Intercellular adhesion molecule-1
IBMX	1-methyl-3-isobutyl-xanthine
IDO	Indoleamine 2,3-dioxigenase
IFN-γ	Interferon gamma
IGF-1	Insulin growth factor 1
IL-(number)	Interleukin-(number)
ILV	Intraluminal vesicle
iPS	Induced pluripotent stem cells
ISCT	International Society for Cellular Therapies
ITGA4	Integrin alpha 4 subunit
JNK	c-Jun N-terminal kinases
KIR	Killer immunoglobulin-like receptors
LAMP(number)	Lysosomal-associated membrane protein (number)
LPS	Lipopolysaccharide
MACS	Magnetic activated cell sorting
MAPK	Mitogen activated protein kinases
MCSP	Melanoma-associated chondroitin sulphate proteoglycan 4
miRNA	Micro ribonucleic acid
MSC	Mesenchymal Stromal Cells
MSCA1	Mesenchymal stem cell antigen 1
MLR	Mixed lymphocyte reaction
mRNA	Messenger ribonucleic acid
MVB	Multivesicular body
MVE	Multivesicular emulsion
NF-kB	Nuclear factor kappa-B
NGF	Nerve growth factor
NH	Non-haematopoietic
NTA	Nanoparticle tracking analysis
PBMC	Peripheral blood mononuclear cells
PBS	Phosphate buffered saline

PDGF	Platelet derived growth factor
PD-L1	Programed death ligand 1
PE	Phycoerythrin
PECAM1	Platelet and endothelial cell adhesion molecule 1
PFA	Paraformaldehyde
PGE2	Prostaglandin E2
PHA	Phytohaemagluttinin
PKB	Protein kinase B
PL (PLT)	Platelet lysate
PPARγ	Peroxisome proliferator-activated receptor gamma
PRP	Platelet rich plasma
PVR	Poliovirus receptor
RNA	Ribonucleic acid
RORγt	Retinoic-acid-receptor-related organ gamma T
RPMI	Roswell Park Memorial Institute
RT	Room temperature
Runx2	Runt-related transcription factor 2
SDS	Sodium dodecyl sulfate
SFM	Serum free medium
SI	Stain index
STAT(number)	Signal transducer and activator of transcription 5
TCR	T cell receptor
TEM	Transmission electron microscope
TGF-β	Transforming growth factor beta
Thy-1	Thymocyte differentiation antigen 1
TLR	Toll like receptor
TNF-α	Tumour necrosis factor alpha
TRAP	Thrombin receptor activating peptide
UTR	Untranslated region
VCAM1	Vascular cell adhesion molecule 1
VEGF	Vascular endothelial growth factor

List of Figures and Tables

Table of Contents

Chapter 1: Introduction and Study aims

“The Scientist is not a person who gives the right answers; he’s one who asks the right questions.”

- Claude Lévi-Strauss

Chapter 1: Introduction

1.1. Mesenchymal Stromal Cells

This chapter will introduce the current understanding in mesenchymal stromal cells (MSCs), regarding their expansion characteristics and immunoregulatory functions. Special focus will be given to the need for MSC expansion under xeno-free conditions and to the role of MSC derived extracellular vesicles (EVs) in MSC immunomodulatory effects.

MSCs are a heterogeneous subset of multipotent cells which undergo differentiation into cells of mesodermal lineage. Because of their trophic and immunomodulatory properties, MSCs are considered attractive cell sources for the treatment of various diseases, such as graft versus host disease (GvHD) and other autoimmune disorders, as well as for regenerative medicine (Le Blanc *et al.*, 2008; Pittenger *et al.*, 2015; Pers *et al.*, 2016) .

The presence of non-haematopoietic multipotent cells in the bone marrow (BM) was first hypothesized by Conheim and colleagues in the nineteenth century, who projected the existence of bone healing fibroblasts in the marrow (Prockop, 1997). However, it was not until the 1960s that Friedenstein and colleagues identified a population of cells within the bone marrow of guinea pigs that could rapidly adhere to plastic, had the characteristic spindle-shaped morphology of fibroblasts and could form colonies *in vitro* (Friedenstein *et al.*, 1966; Friedenstein *et al.*, 1970). This clonogenic capacity led to the designation of these cells as “Colony forming unit (CFU) fibroblasts”, however, the subsequent observation that the cells had the ability to differentiate into osteoblasts *in vitro* and could generate bone when ectopically implanted *in vivo*, categorised these cells as “Osteogenic stem cells” and “BM stromal stem cell” (Friedenstein *et al.*, 1974; Friedenstein *et al.*, 1987).

After Friedenstein’s findings, several laboratories focused on the expansion and characterisation of human BM derived stromal cells (Murray *et al.*, 2014), and in the 1990’s, Caplan introduced the term mesenchymal stem cells to describe these entities (Caplan, 1991). This nomenclature was later challenged by Dennis *et al* (1999) who proposed the term “mesenchymal progenitor cells” after verifying that these cells were progenitors rather than stem cells (Dennis *et al.*, 1999). In early 2000s, different groups suggested the implementation of the

terms “skeletal stem cells” and “multipotent adult progenitor cells” to describe their ability to differentiate into cells of mesodermal lineage (Bianco and Gehron Robey, 2000; Jiang *et al.*, 2002). Given the lack of consistency and evidence of *in vivo* differentiation of these cells, the Mesenchymal and Tissue Stem Cell Committee of the International Society for Cellular Therapy (ISCT) proposed that the most accurate designation to define MSCs should be “Multipotent Mesenchymal Stromal Cells” (Dominici *et al*, 2006). Recently, Caplan *et al* (2010) suggested the term “Medicinal Signalling Cells” to reflect the paracrine effects of these cells (Caplan, 2010) (**Fig.1.1**). Nonetheless, the acronym MSC is used worldwide and terms “Mesenchymal Stem Cells” and “Mesenchymal Stromal Cells” are often used to describe the same cell population.

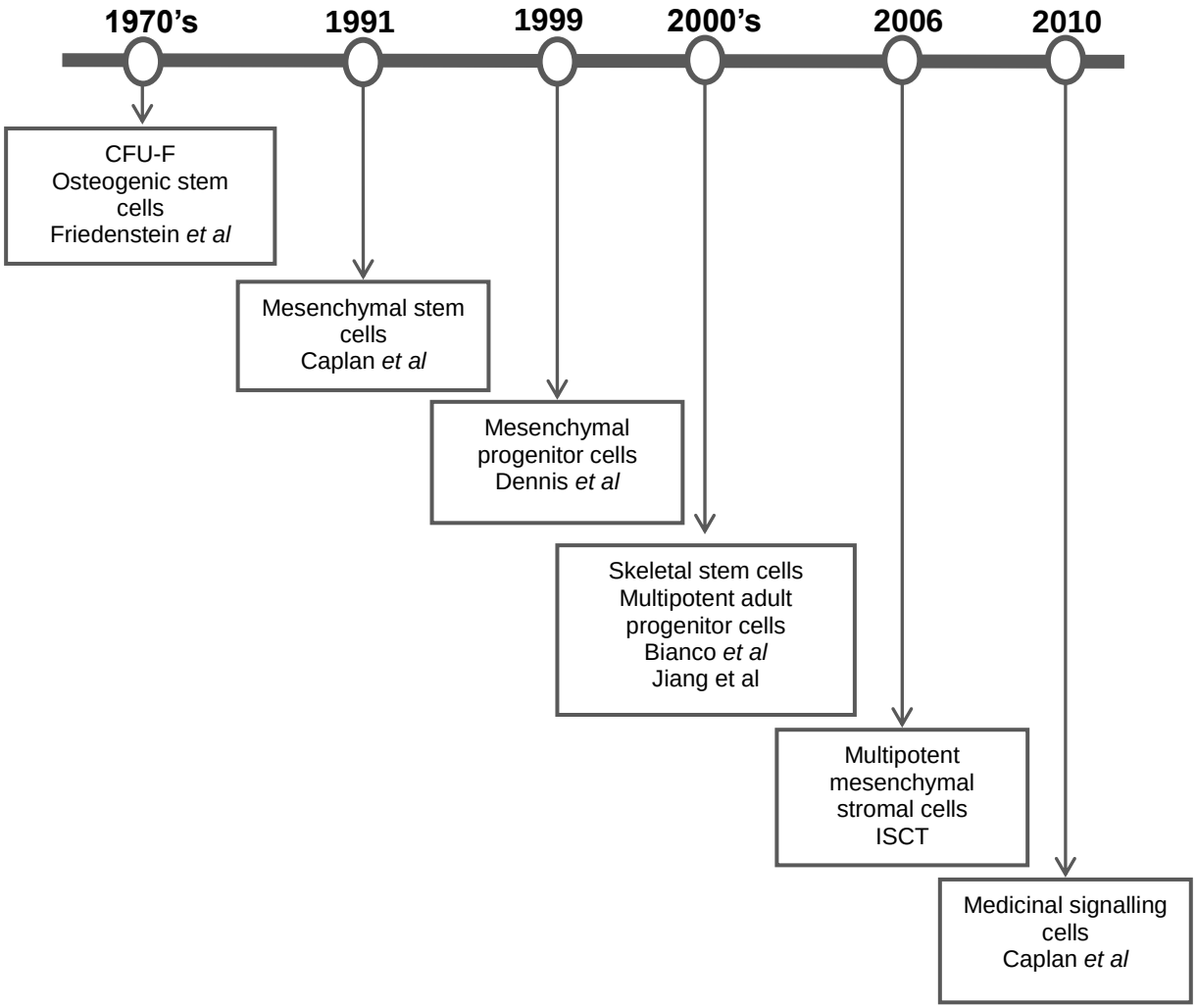

Figure 1.1: Historical overview of MSC nomenclature

1.1.1. Sources of MSCs

Since the original description of MSCs in the bone marrow, multipotent stromal cells have been isolated from the adherent fraction of many adult and embryonic sources. So far, MSCs have been identified in virtually all types of tissue, such adipose tissue (Zuk *et al.*, 2002; Xu *et al.*, 2005), umbilical cord (Rogers and Casper, 2004), dental pulp (Shi and Gronthos, 2003), among others (**Fig.1.2**). MSCs can also be generated *in vitro* by differentiation of human embryonic stem cells (hESCs) and induced pluripotent stem cells (iPS). Both hESC- and iPS-derived MSCs have been shown to present the same characteristics as those derived from adult sources (Fu *et al.*, 2015; Sheyn *et al.*, 2016).

This ubiquitous distribution of MSCs is widely thought to be needed to maintain the repair systems of the tissues from which they are derived (Grove *et al.*, 2004). Nonetheless, bone marrow-derived progenitors remain the most commonly used and better understood MSC type.

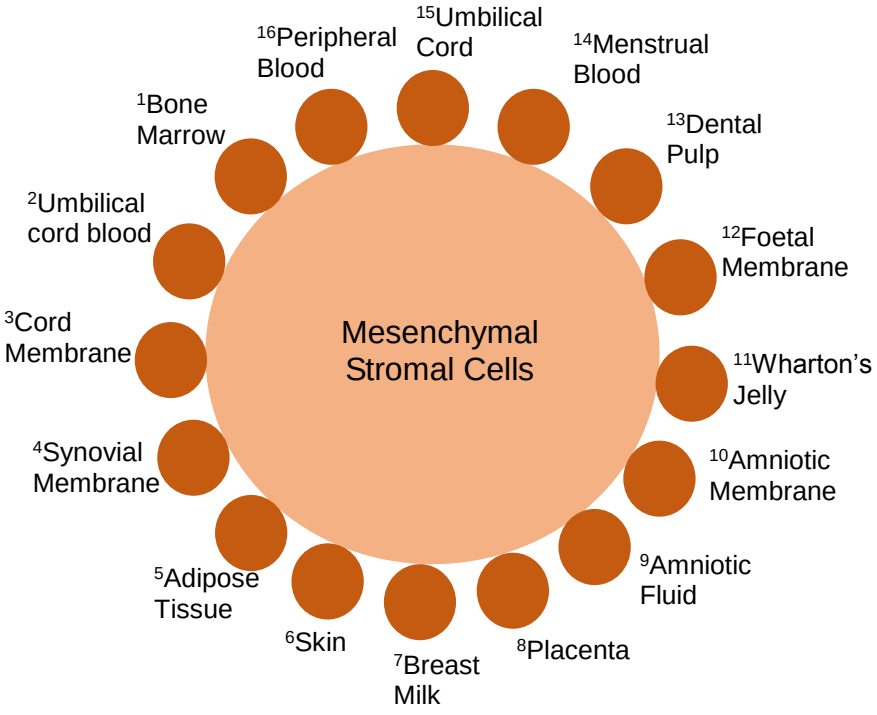

Figure 1.2: Sources of MSCs

1. (Friedenstein *et al.*, 1966); 2. (Sibov *et al.*, 2012); 3. (Lim and Phan, 2014); 4. (De Bari *et al.*, 2001); 5. (Zuk *et al.*, 2002); 6. (Toma *et al.*, 2001); 7. (Patki *et al.*, 2010); 8. (Talwadekar *et al.*, 2015); 9. (Wouters *et al.*, 2007); 10. (Corradetti *et al.*, 2014); 11. (Tsai *et al.*, 2004); 12. (Kmiecik *et al.*, 2013); 13.(Shi and Gronthos, 2003); 14. (Mou *et al.*, 2013); 15.(Rogers and Casper, 2004); 16. (Chong *et al.*, 2012); (illustration adopted from Van, 2011)

1.2. Characterisation of MSCs

To date, the defining characteristics of MSCs remain inconsistent among different laboratories. Variations in tissue sources, isolation and expansion protocols, donor age and gender have resulted in distinct features of the *ex vivo* generated cells (Sensebé *et al.*, 2013; Siegel *et al.*, 2013). This has made it challenging to compare results obtained from different experimental and clinical studies. To overcome these ambiguities the International Society for Cellular Therapies (ISCT) formulated the minimum criteria to identify these cells (Dominici *et al*, 2006). To be acknowledged as MSCs, these cells must:

1) Be plastic adherent and exhibit the characteristic spindle shaped morphology.
2) Be positive for the expression of cell surface antigens CD105, CD73 and CD90, and negative for the expression of CD45, CD34, CD14, CD11b, CD19 and HLA-DR as measured by flow cytometry.
3) Have the capacity to differentiate into osteocytes, adipocytes, and chondrocytes *in vitro*.

These guidelines were primarily set for human derived cells; however, other mammalian MSCs have met these criteria (Grzesiak *et al.*, 2011; Chong *et al.*, 2012). The ISCT also declared that the term mesenchymal stem cell should be reserved for a subgroup of these cells that exhibit stem cell activity (Horwitz *et al.*, 2005), nevertheless, these cells are still commonly referred as mesenchymal “stem cells” rather than “stromal cells”.

1.2.1. Phenotypic markers of MSCs

To date, there are no specific markers for MSCs, but the ISCT defined specific guidelines for the phenotypic characterisation of MSCs. An MSC should be ≥95% positive for the expression of cell surface markers CD105 or endoglin (part of the TGF-β receptor complex and involved in angiogenesis), CD73 or ecto 5’ nucleotidase, (converts adenosine monophosphate into adenosine), and CD90 or Thy-1 (a glycophosphatidylinositol (GPI)-anchored conserved cell surface protein, used as a marker for a variety of stem cells) and negative (≤2% positive) for the expression of cell lineage specific markers, CD45 or protein tyrosine phosphatase receptor type C – PTPRT (a pan-leukocyte marker), CD34 (primitive haematopoietic stem cell marker), CD11b or CD14

(macrophage and monocyte marker), CD19 or CD79α (B cell marker) and HLA-DR or MHC class II (only expressed on activated MSCs) (Dominici *et al.*, 2006).

Nonetheless, a diverse range of antigens, such as CD271, Stro-1 and TNAP, have been found on the surface of MSCs (Martens *et al.*, 2006; Battula *et al.*, 2009; Cox *et al.*, 2012). Many of these proteins are restricted to certain subsets of cells, rather than the whole MSC population, even at early passages. Accumulating studies have strengthened the notion that MSCs represent a heterogeneous mixture of cells containing a varied number of subpopulations that may have distinct biological activities (Yang *et al.*, 2013). A summary of the most well defined surface markers, including their biological functions, is described on **Table 1.1**.

In clinical settings, infusion of specific MSC subpopulations may be more advantageous and effective. It is noteworthy to mention that variation in the percentage of cells expressing the various markers differs between different laboratories due to source and culturing methodology differences. Currently, the influence of these different methodologies, e.g., MSC *in vitro* expansion in xeno-free medium, on the expression of many of these markers is still not well understood. In **Chapter 4** the effect of expansion of MSCs in human platelet lysate (PL)-supplemented media on the overall cell surface protein expression will be investigated.

Table 1.1: Summary of phenotypic markers of MSCs

Well defined markers for MSC identification			
Markers	**Other names**	**Biological functions in MSCs**	**Refs**
CD105	ENG	Enhanced myogenic differentiation	(Silva *et al.*, 2005)
CD73	Ecto-5'-nucleotidase	Regulator of osteo- and chondrogenic differentiation	(Ode *et al.*, 2013)
CD90	Thy-1	Marker for MSC differentiation	(Wiesmann *et al.*, 2006)
Stro-1	Endothelial antigen	Higher expression of pro-angiogenic factors	(Martens *et al.*, 2006; Psaltis *et al.*, 2010)
CD146	MCAM	Higher expression of osteo-related genes and osteogenic differentiation	(Sacchetti *et al.*, 2007)
CD271	LNGFR	Higher expression of immunosuppressive cytokines	(Kuci *et al.*, 2010; Mifune *et al.*, 2013)
CD106	VCAM1	Enhanced immunosuppressive properties	(Yang *et al.*, 2013a)
PDGFRα	CD140a	Enhanced migration and homing to skin lesions	(Tamai *et al.*, 2011)
CD44	HCAM	Enhanced proliferation and homing capacity	(Maleki *et al.*, 2014)
CD49a	ITGA1	Higher proliferative capacity	(Stewart *et al.*, 2003; Rider *et al.*, 2007)
CD49e	ITGA5	Increased osteogenic differentiation capacity	(Granéli *et al.*, 2014)
CD63	TSPAN30	Marker of primitive stromal cells; important regulator of EV secretion	(Stewart *et al.*, 2003)
CD166	ALCAM	Marker of primitive stromal cells	(Stewart *et al.*, 2003)
CD200	MRC OX-2 antigen	Increased immunosuppressive properties	(Pietila *et al.*, 2012)
CD309	KDR	Enhanced proliferative and immunomodulatory functions	(Liu *et al.*, 2006)
TNAP	ALPL	Enhanced proliferative capacity and osteo- and chondrogenic differentiation	(Battula *et al.*, 2009; Sobiesiak *et al.*, 2010)

Abbreviations: **ALCAM**: activated leukocyte cell adhesion molecule; **ALPL:** alkaline phosphatase liver/kidney/bone; **CD**: cluster of differentiation; **ENG**: endoglin; **ITGA1:** integrin, alpha 1; **ITGA5**: integrin, alpha 5; **KDR**: kinase insert domain receptor; **LNGFR**: low-affinity nerve growth factor homing receptor; **MCAM:** melanoma cell adhesion molecule; **TNAP**: tissue non-specific alkaline phosphatase; **TSPAN30**: tetraspanin 30; **VCAM1**: vascular cell adhesion molecule 1;

1.2.2. Differentiation capacity of MSCs

Initial work to demonstrate the multipotential of MSCs has been performed by Friedenstein and colleagues who showed that MSCs have the ability to differentiate into osteoblasts (Friedenstein *et al.*, 1987), but it was only in the late 1990's that Pittenger *et al* (1999) confirmed that these cells had the ability to differentiate into cells of mesodermal lineage such as, osteocytes, adipocytes and chondrocytes (Pittenger *et al.*, 1999). To date, MSCs have been successfully differentiated *in vitro*, into cartilage, bone, tendon, ligament, adipose tissue, marrow stroma and connective tissue, by supplementing cultures with a combination of lineage-specific growth factors (**Fig.1.3**) (Murray *et al.*, 2014). Additionally, mesodermal differentiation into adipocytes, osteocytes and chondrocytes is a pre-requisite for *in vitro* identification of MSCs. The general mechanisms underlying adipo-, osteo- and chondrogenic differentiation of MSCs will be further discussed in this section.

1.2.2.1. Adipogenenic differentiation

Adipocyte differentiation is accomplished by supplementing culture medium with dexamethasone, ascorbic acid and 1-methyl-3-isobutyl-xanthine (IBMX). The adipogenic process starts by the expression of the adipogenic regulator, the nuclear hormone receptor peroxisome proliferator-activated receptor gamma (PPARγ) (Nuttall and Gimble, 2004). This receptor activates the CCAAT/enhancer binding proteins (C/EBP) family of transcription factors. The binding of PPARγ to its ligands promotes the expression of C/EBPβ and C/EBPδ (Rosen *et al.*, 2002). These transcription factors induce the expression of C/EBPα which in turn activates the expression of several genes involved in the adipocyte phenotype including fatty acid-binding protein-4, lipoprotein lipase and adipokine, among others (Rosen *et al.*, 2000). This process induces a change in the morphology of MSCs, which are transformed into oval-shaped cells containing large lipid vesicles in the cytosol (Bunnell *et al.*, 2008).

1.2.2.2. Osteogenic differentiation

Osteogenesis is carried out by culturing the MSCs in a monolayer and culture in basal medium supplemented with β-glycerophosphate, dexamethasone, ascorbic acid and in some instances, additional bone morphogenic protein 2

(BMP2). Osteogenesis is a process involving three distinct stages: proliferation, matrix formation and mineralisation (Olsen *et al.*, 2000). In the proliferation stage, the master regulator of the osteogenic process, Runt-related transcriptional factor-2 (Runx2) is upregulated by the action of BMP2 and the activation of wnt/β-catenin signalling cascade (Jeon *et al.*, 2006; Deng *et al.*, 2008). In the matrix formation stage, Runx2 promotes the expression of alkaline phosphatase and other osteogenic related genes such as osteocalcin, osteopontin and collagen I, thus inducing a change in MSC morphology into an osteoblastic morphology, characterised by the presence of enlarged nucleus and Golgi apparatus and an extensive endoplasmic reticulum (Friedman *et al.*, 2006; Deng *et al.*, 2008). In the last stage calcium is deposited in the extracellular matrix (Friedman *et al.*, 2006).

1.2.2.3. Chondrogenic differentiation

The chondrogenic process is accomplished by pelleting the cells in spheroids and culturing them in TGF-β supplemented medium. This growth factor promotes the activation of intracellular signalling cascades, such as mitogen-activated protein (MAP) kinases, p38, extracellular signal-regulated kinases-(ERK-) 1 and c-Jun N-terminal kinases (JNK), which induce the activation of the transcription factors Sox-9 and scleraxis (Yu *et al.*, 2012). These transcription factors are then responsible for the upregulation of extracellular matrix genes, such as collagen type II and IX, proteoglycans, and glycosaminoglycans (GAGs) among others (Yu *et al.*, 2012; Giuliani *et al.*, 2013). During the chondrogenic process, MSCs lose their characteristic morphology as a result of increased deposition of extracellular matrix proteins and GAG biosynthesis (Yu *et al*., 2012; Giuliani *et al*., 2013).

1.2.2.4. Transdifferentiation of MSCs

Some reports have also shown that MSCs are not only committed to mesodermal differentiation, and, given the right cues, they are able to cross the germ layer boundary and transdifferentiate into cells of ecto- and endodermal lineages. Numerous reports have claimed that MSCs can differentiate *in vitro* into hepatocytes (Schwartz *et al.*, 2002), neurons (Cogle *et al.*, 2004; Tropel *et al.*, 2006), and cardiomyocytes (Pijnappels *et al.*, 2008). *In vitro*, differentiation into cells of ectodermal or endodermal lineages seems to be induced by

supplementation of medium with cocktails of small molecules and chemicals, by gene transfection or by co-culture of MSCs with cells of other germ layer origin, such as hepatocytes, cardiomyocytes and neural cells (Schwartz *et al*., 2002; Cogle *et al*., 2004; Tropel *et al*., 2006; Pijnappels *et al*., 2008). Initial belief suggested that *in vivo,* MSCs were capable of engrafting and transdifferentiating into myocardial, neural and hepatic tissues (Maltman *et al.*, 2011; Wu and Tao, 2012; Cashman *et al.*, 2013). The most recent consensus is that the therapeutic benefit of MSCs is due to paracrine interactions that lead to the recruitment and differentiation of existing tissue cells rather than true differentiation of the transplanted MSCs (Biancone *et al.*, 2012). This concept will be further discussed in more detail in **sections 1.7** and **1.9**.

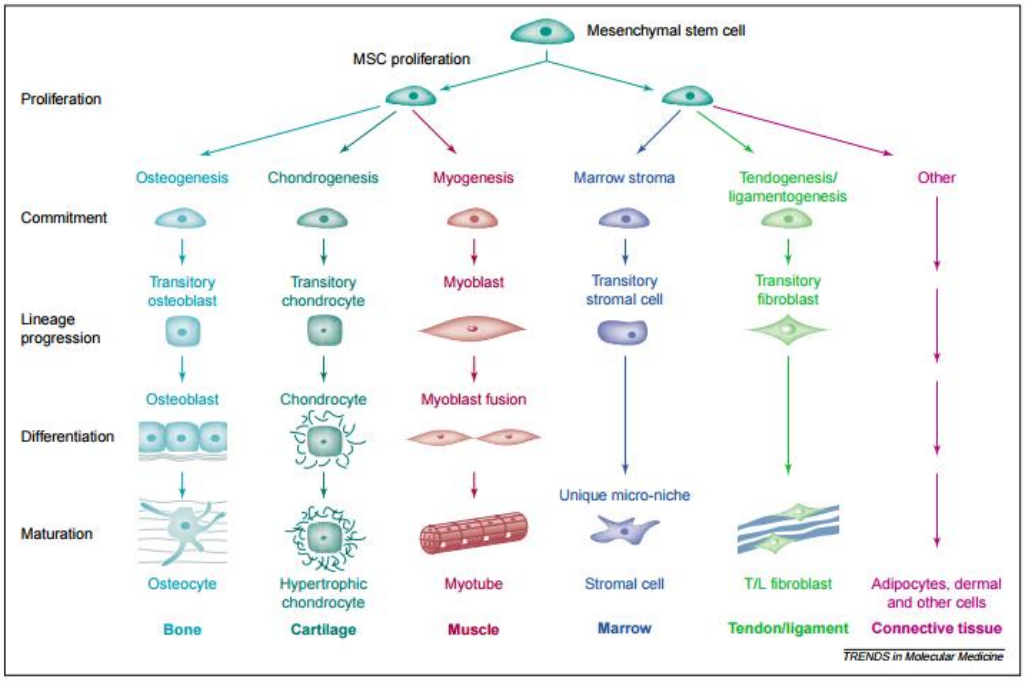

Figure 1.3: MSC multilineage differentiation potential

MSCs are able to undergo differentiation into a variety of mesodermal cell types, such as bone, cartilage, muscle, stroma, among others. Experimental evidence suggests MSCs can undergo transdifferentiation *in vitro* by the use of specific cues (adapted from Caplan and Bruder, 2001).

1.3. *Ex vivo* expansion of MSCs

Due to limited frequency of MSCs in the bone marrow (0.01 to 0.001%), *ex vivo* expansion of MSCs is pre-requisite to achieve the required cell numbers for functional research and clinical applications. Isolation of MSCs is typically accomplished by density gradient centrifugation followed by expansion under plastic adherence using standard medium containing 10% foetal calf serum (FCS) (Bernardo *et al.*, 2011). MSCs can then be expanded up to 35 to 50 population doublings (Neubauer *et al.*, 2012), under static and normoxic conditions, i.e., 20% O_2, or under hypoxia (3-5% O_2) (dos Santos *et al.*, 2010; Rosová *et al.*, 2008).

Laboratories worldwide developed protocols for expansion of MSCs that lack standardisation; however, most of them are consistent in the use of FCS-supplemented medium. FCS is a complex mixture of approximately 1000 biological molecules, including, growth factors, hormones, transport proteins, attachment/spreading factors, amino acids, vitamins, fatty acids, lipids and protease inhibitors, which contribute to the maintenance and proliferation of MSCs in culture (Kinzebach and Bieback, 2013). The use of FCS may carry potential clinical risks for patients. This reagent is, by nature, not very well defined and exhibits high batch-to-batch variability (Brunner *et al.*, 2010). It might also be responsible for the transmission of prions and undefined zoonoses. There is also an increased risk of development of immune reactions in the host and possible transplant rejection, as a result of MSC ability to internalise xenogenic proteins at high concentrations, especially if repeated infusions are required, (Bieback, 2013). In fact, sensitisation in a paediatric patient with *Osteogenesis Imperfecta* treated with repeated administration of FCS-expanded MSCs has been reported by Horwitz *et al* (1999). This sensitisation was characterised by the formation of alloantibodies against MSCs which led to transplant rejection (Horwitz *et al.*, 1999).

Due to these reasons, the use of FCS is being criticized by European Medical Agencies (EMEA CPMP/BWP/1793/02, 2003), nonetheless, its use is tolerated by regulatory agencies in clinical trials involving administration MSCs, especially in phase I clinical trials. There is, however, a high demand to develop defined GMP compliant, either serum-free or animal-free, medium that can be

standardised and used in both research and clinical trials, and possible future MSC manufacturing for therapeutic use, as a general culture condition.

1.3.1. Alternatives to FCS supplemented medium

With the aim of developing an animal-free medium, numerous laboratories have been focused on the development of medium formulations that use human blood-derived products, such as, human autologous or pooled allogeneic serum, cord blood serum and platelet derivatives (Tekkatte *et al.*, 2011). Although these reagents are still not well defined, they are isolated from healthy blood donors and can be screened for immunological and infectious parameters according to blood banking guidelines. Like FCS, they provide a plethora of molecules and growth factors that promote maintenance and MSC proliferation. Human plasma and human autologous serum (HAS) have been widely targeted as alternatives for xeno-free expansion of MSC. Lin *et al* (2005), showed that substituting FCS with 10% autologous serum or plasma and basic fibroblast growth factor (bFGF) and epidermal growth factor (EGF) maintained the proliferative and trilineage differentiation capacity of MSCs (Lin *et al.*, 2005). Some reports have demonstrated that the replacement of FCS with different concentrations of HAS resulted in faster proliferation with shorter population doubling times (Kobayashi *et al.*, 2005; Pérez-Ilzarbe *et al.*, 2009), improved osteogenic capacity (Stute *et al.*, 2004) and enhanced genetic and epigenetic stability (Dahl *et al.*, 2008). However, the difficulty in standardising the quality of autologous serum and limited availability restrict the application of autologous serum or plasma in clinical settings. To overcome these disadvantages, some laboratories turned their attention to allogeneic serum. Pooling serum from several donors can be used to produce a relatively stable and predefined product compliant with GMP criteria. Studies performed using pooled Human AB serum, have shown higher and faster proliferation when compared to FCS (Kocaoemer *et al.*, 2007; Bieback *et al.*, 2012). Although cells exhibited the same spindle-shaped morphology, they appeared to be smaller, while maintaining the characteristic differentiation capacity, frequency of colony-forming-units (CFU-F) and immunoregulatory properties as FCS expanded cells (Kocaoemer *et al.*, 2007; Bieback *et al.*, 2012). This specific morphology might

be an effect of the upregulation of stemness markers that conserves MSCs in a more premature state (Dahl *et al.*, 2008; Kinzebach and Bieback, 2013).

Allogeneic umbilical cord blood serum (hUCBD) is a complex combination of growth factors and cytokines, such as, EGF, FGF, nerve growth factor (NGF), vascular endothelial growth factor (VEGF), platelet-derived growth factor (PDGF), insulin like growth factor (IGF), transforming growth factor (TGF), interleukins, interferons; human serum albumin (HSA); transferrin and metabolism promoting factors like, α-2 macroglobulin and complement C3 and C5 precursors (Kinzebach and Bieback, 2013). This serum has also been shown to promote proliferation and differentiation (Kinzebach and Bieback, 2013), and to maintain the stemness of MSCs (Kim *et al.*, 2013).

There are also, numerous serum free media (SFM) formulations for the cultivation of MSC that support high proliferation rates, however, studies with SFM have shown that despite a higher proliferative capacity, MSCs were less potent in regulating the immune system (Gottipamula *et al.*, 2014).

Despite promising results with the above mentioned culture supplements, the use of platelet derivatives, such as platelet lysate, has illustrated the best results so far and extensive research with this supplement is being held in laboratories worldwide.

1.3.2. Use of platelet derivatives for MSC expansion

As indicated by the name, platelet derivatives are substances that derive from human platelets. Platelets are anucleate cells derived from megakaryocytes which, when physiologically activated, promote wound healing by releasing growth factors, cytokines and chemokines that support blood coagulation and stop bleeding (Burnouf *et al.*, 2016). Platelets are rich in a wide variety of substances including, immunologic molecules, adhesion molecules, and growth factors, among others (**Table 1.2**).

Table 1.2: Summary of platelet factors

Molecule Type	Molecules
Coagulation factors	Factor V; Factor XI; Factor XIII; Prothrombin; Antithrombin; α2-macroglobulin; α2- antiplasmin; plasmin; plasminogen; protein S; PAI-1; TFP1
Adhesion molecules	P-selectin; von Willebrand factor; vitronectin; fibrinogen; integrins, fibronectin
Immunologic molecules	Complement factors; platelet factor H; β1H globulin; factor D; C1 inhibitor; IgG; Thymosin-β4
Chemokines & cytokines	IL-8; NAP-2; RANTES; MCP-1, -3; MIP-1α; β-thromboglobulin
Growth & angiogenic regulators	bFGF; HGF; IGF-1; VEGF-A,-C; PDGF-AA,-AB,-BB; BDNF; angiostatin; PF4; thrombospondin; EGF; CTGF; TGF-β; angipoietin-1; SDF-1; MMP-1,-2,-9; Endostatin; TIMP-1,-4; BMD-2,-4,-6;

Abbreviations: **BDNF**, brain derived neurotrophic factor; **bFGF**, basic fibroblast growth factor; **BMP**, bone morphogenetic protein; C, complement; **CTGF**, connective tissue growth factor; **EGF**, epidermal growth factor; **HGF**, hepatocyte growth factor; **IGF-1**, insulin-like growth factor-1; **IL-8**, interleukin 8 (CXCL8); **MCP-1**, monocyte chemotactic protein-1 (CCL2); **MCP-3**, monocyte chemotactic protein-3 (CCL7); **MIP-1a**, macrophage inflammatory protein 1a (CCL3); MMP, matrix metalloproteinase; NAP-2, neutrophil-activating protein-2 (CXCL7); **PAI-1**, plasminogen activator inhibitor-1; **PDGF**, platelet derived growth factor; **PF4**, platelet factor 4 (CXCL4); **RANTES,** regulated on activation, normal T cell expressed and secreted (CCL5); **SDF-1**, stromal cell derived factor-1; **TFPI**, tissue factor pathway inhibitor; **TGF-β**, transforming growth factor-beta; **TIMP**, tissue inhibitor of metalloproteinases; **VEGF**, vascular endothelial growth factor.

There are two types of platelet derived compounds, platelet releasates and platelet lysate (Bieback, 2013):

Platelet releasate, or platelet rich-plasma (PRP) is produced by enrichment of platelets in plasma by centrifugation of anticoagulated whole blood. This compound is rich in growth factors which are released after platelet activation, such as, PDGF, TGF-β, IGF, VEGF, bFGF, hepatocyte growth factor (HGF) and EGF (Dugrillon *et al.*, 2002; Maynard *et al.*, 2007). Release of these factors is dependent on activation with several molecules, such as, thrombin, collagen, ADP/epinephrine and thrombin receptor activating peptide (TRAP) (Bieback, 2013). Early studies with PRP, showed higher proliferative and migratory capacity of MSCs while maintaining their multipotency (Bieback *et al.*, 2009; Müller *et al.*, 2009). Although promising, human platelet lysate seems to yield better results than its platelet releasate counterpart.

Platelet lysates (PL or PLT) are manufactured by platelet disruption using freeze/thaw protocols. Unlike PRP, platelet lysate contains all factors comprised by platelets. The first studies with PL were performed in the 1980s in various cell lines and tumour cells (Eastment and Sirbasku, 1980). Production of PL is a relatively easy, fast and cost-effective procedure that relies on the acquisition of platelet concentrates, derived from healthy blood donors, which go through a series of freezing and thawing procedures that give rise to PL. This reagent can be stored at -20 ºC for approximately 12 months and 2 years if stored at -80 ºC, while maintaining growth factor stability (Rauch *et al.*, 2011). Taking into account that the concentration of growth factors is limited and variable among different individuals, PL is produced by pooling platelet concentrates of several donors. This procedure gives rise to a more standardised and conserved product that can be manufactured under GMP compliant conditions (**Fig. 1.4**).

The first study using PL as medium supplement for MSC isolation and expansion was performed by Doucet *et al* (2005). Doucet showed that PL-expanded MSCs give rise to bigger colonies and sustains osteo-, adipo- and chondrogenic differentiation potential (Doucet *et al.*, 2005), and in 2007, Bernardo *et al* showed that supplementing basal medium with 5% of platelet lysate yielded higher clonogenicity when compared to 10% FCS supplemented medium, while multipotency and chromosomal stability was maintained

(Bernardo *et al.*, 2007). One of the main advantages of MSCs is their intrinsic characteristic of evasion of allo-recognition, i.e., low immunogenicity, due to the lack of HLA-DR expression. This low immunogenicity seems to be maintained even when cells are grown under PL-supplemented medium (Bieback, 2013). Moreover, preliminary studies testing the immunoregulatory characteristics of MSCs have presented comparable results to the ones previously obtained with MSCs expanded in FCS-medium in terms of alloantigen-induced cytotoxicity and promotion of regulatory T cell proliferation (Bernardo *et al.*, 2007; Flemming *et al.*, 2011). However, the inhibitory effect of PL-expanded MSCs on alloantigen-induced T cell proliferation remains controversial with some studies showing lower suppressive effect of these MSCs (Abdelrazik *et al.*, 2011b; Copland *et al.*, 2013). Nonetheless, studies applying human derived reagents in the manufacturing of MSCs show a promising outcome. These reagents are already being applied in clinical trials for a variety of diseases, such as, GvHD, invertebral disc disease, maxillary cyst and adult periodontitis (Wang *et al.*, 2012). Altogether, the results obtained so far suggest that PL is a promising candidate for the replacement of FCS in the expansion of MSCs; however, further studies are needed to better understand the effect of this supplement in MSC characteristics and function, both *in vitro* and *in vivo*. Issues regarding xeno-free expansion of BM derived MSCs using platelet lysate supplemented media, and its effect on morphological and immunomodulatory functions of MSCs will be further discussed in **Chapter 3**.

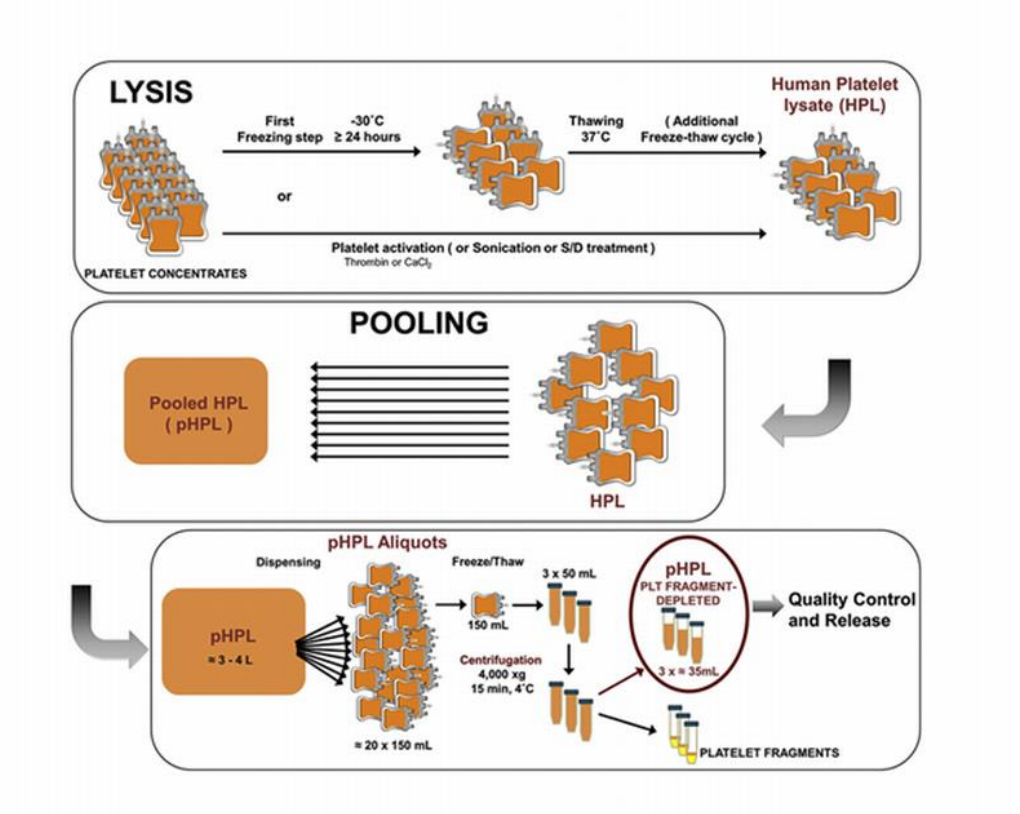

Figure 1.4: Preparation of allogeneic pooled human PLs.

Platelet concentrates obtained from healthy donors are lysed using a freeze/thaw protocol. Platelet activation is accomplished by addition of thrombin of $CaCl_2$ or other methodologies. Lysed platelets are then pooled and centrifuged for depletion of platelet fragments (adapted from Burnouf *et al.,* 2016)

1.4. Clinical applications of MSCs

As a result of their immunomodulatory properties, tissue repair potential and low immunogenicity MSCs are exploited in many preclinical and clinical settings. Broadly, the clinical application of MSCs is mainly focused on 3 unique areas: tissue regeneration for cartilage, bone, muscle, tendon and neuronal cells; improvement of hematopoietic stem cell engraftment; and treatment of immune-related diseases such as, rheumatoid arthritis (RA), Crohn's disease, multiple sclerosis and GvHD (Wang *et al*., 2012). The first clinical trial using *ex vivo* expanded MSCs was performed in 1995 to test the safety and feasibility of using these cells in clinical settings. In this study, 15 patients suffering from haematological malignancies were infused with autologous BM-MSC and showed no adverse effects or toxicity related to MSC expansion (Lazarus *et al.*, 1995). Since then, MSCs have been further explored for a wide range of clinical applications.

Currently, there are a range of registered clinical trials in various phases aimed at evaluating MSC therapeutic effects in both immune and non-immune related diseases. Based on the most up to date information published on www.clinicaltrials.gov, the current ongoing 430 clinical trials are summarised in **Fig.1.5**.

MSCs have been vastly used to treat bone related diseases, including osteoarthritis (110 studies), neurodegenerative diseases (e.g. Parkinson's and Alzheimer's disease, 77 studies), various heart related diseases (36 studies) and immune related diseases, like GvHD (26 studies), among others. MSC application in other conditions has also been noted, but studies with less than 10 registered trials were not included in this graph. In general, the clinical data reports no association between MSC therapy and organ complications, death or malignancy (Wang *et al*, 2012).

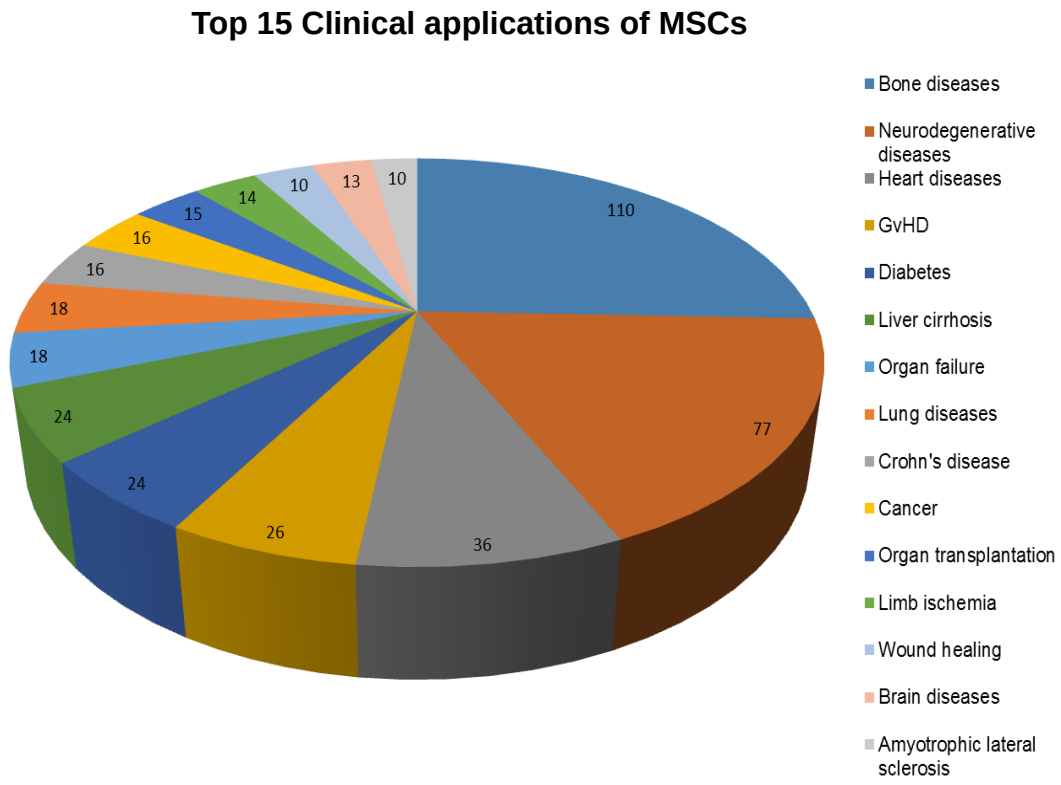

Figure 1.5: Clinical trials using MSC based on types of diseases

Ongoing clinical trials using MSCs were assessed on the public trials database www.clinicaltrials.gov (as for 05/2016) using the search terms: “mesenchymal stem cells”. The clinical trials that were suspended, terminated or completed were excluded from this analysis.

Despite encouraging reports there are still some limitations to be overcome in the use of MSCs in therapeutic applications. Firstly, there are still controversial observations regarding MSC characteristics and functional potency, as a result of the lack of standardisation of expansion protocols. Clinical-grade MSCs have been isolated from various sources and generated using different extraction methodologies, culture protocols and characterisation approaches. Secondly, until the first clinical trial utilising PL expanded MSCs to treat acute GvHD in 2009, trials relied on the generation of MSCs using FCS-containing medium, a condition no longer recommended by the regulatory requirements for GMP production of MSCs. Current studies show a trend towards the use of PL to generate GMP-compliant MSCs. As illustrated by **Fig.1.6**, there are now 11 clinical studies, commenced between 2012 and 2016, utilising MSCs expanded in PL for the treatment of various diseases.

Collectively the evidence from preclinical and clinical studies have demonstrated the beneficial effect of MSCs, however, given the differences in production and characterisation of MSCs interpretation and comparison of the different clinical outcomes remains difficult. Future focus on standardisation of GMP-compliant MSC production and immunological assessment is necessary to consolidate these cells as robust and reliable therapeutic agents.

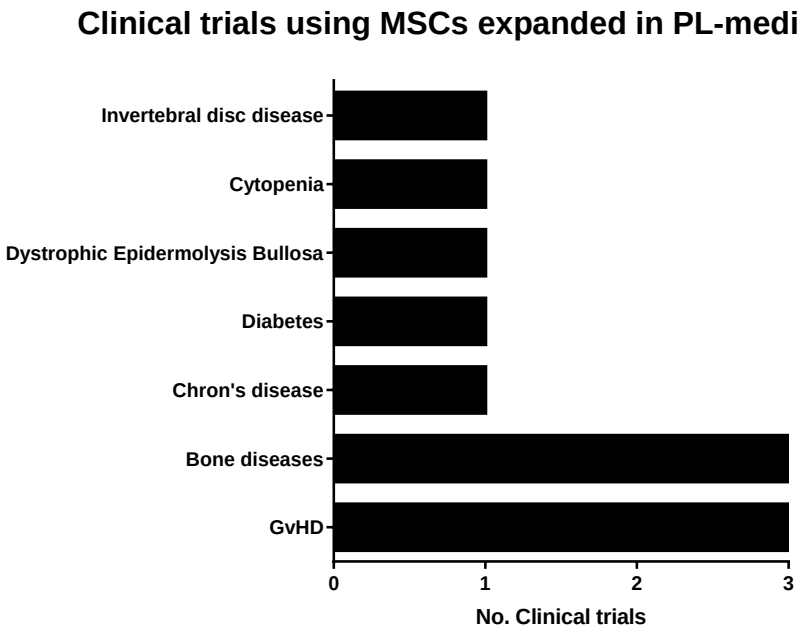

Figure 1.6: Clinical trials using MSCs expanded in PL-medium

Clinical trials utilising PLT expanded MSCs were compiled using the www.clinicaltrials.gov (as for 05/2016) database using the search terms: “mesenchymal stem cells” and “platelet lysate”. This analysis resulted in 11 studies, exhibiting start dates between 2009 and 2016. This bar graph shows the studies grouped according to diseases.

1.5. Immunomodulatory properties of MSC

The immunomodulatory properties of MSCs have been extensively studied in the past decade. They are generally described as a “universal” suppressor of the immune system since they show modulatory effect towards a wide range of cells, including, macrophages, T lymphocytes, monocyte-derived dendritic cells (moDC), B lymphocytes and NK cells (Wang *et al.*, 2014). Although the mechanisms of MSC mediated immunomodulation are not yet fully understood, MSCs seem to interact with innate and adaptive immune cells which culminate in immunosuppression, anergy and induction of tolerance (Uccelli *et al*., 2008; Wang *et al*., 2014). This section will focus on the immunomodulatory effect of MSCs on T cells, DCs and NK cells.

1.5.1. Immunoprivilege of MSCs

As discussed previously, the lack of HLA class II expression by MSCs is one of their main phenotypic characteristics. In addition, MSCs express low levels of HLA class I molecules and lack the expression of the co-stimulatory molecules CD40, CD80 and CD86 (Jacobs *et al.*, 2013b). This is of importance for clinical application of these cells in various diseases, as it is the premise for the use of allogeneic MSCs in therapeutics. The absence of HLA class II molecules and low expression of HLA class I molecules, prevents the generation of allogeneic immune responses. These are characterised by the binding of HLA class I and II and antigen complexes with the T cell receptor (TCR) on the surface of $CD4^+$ and $CD8^+$ T cells (Choo, 2007). After the TCR signalling is triggered, the co-stimulatory signalling cascade directs the T cell fate and function. Without co-stimulation, the T cell becomes anergic rather than activated (Chen and Flies, 2013). There are two main families of co-stimulatory molecules, the B7 family and the tumour necrosis factor (TNF) receptor superfamily (Chen and Flies, 2013). Members of the B7 family include, e.g., molecules like CD86 and CD80. These molecules are usually expressed by antigen presenting cells (APCs) and interact with CD28 or cytotoxic T-lymphocyte antigen 4 (CTLA-4), which is an inhibitory ligand, on T cells (Chen and Flies, 2013). CD40 belongs to the tumour necrosis factor (TNF) receptor superfamily. This molecule is usually expressed on APCs and binds to its ligand, CD40L on the T cells. Altogether, ligand-receptor engagement promotes a signalling cascade and activation of pathways

involved in cell growth, activation and survival of effector T cells (Appleman and Boussiotis, 2003; Chen and Flies, 2013). These signals can direct the T cell activation towards a stimulatory or regulatory phenotype, depending on the molecules and ligands involved (Appleman and Boussiotis, 2003).

Ideally, autologous MSC transplantation is the most suitable option, as they pose no immunological risk to the patients, however, there are numerous challenges associated with this approach. As mentioned before, the MSC fraction obtained from the bone marrow is of limited amount, and expansion is a prerequisite to obtain the cell numbers for therapeutic application. Additionally, MSCs derived from the patient may carry the disease therefore they may be inappropriate for transplantation.

On the other hand, allogeneic MSCs overcome these challenges since they can be harvested from healthy donors, expanded and stored until use. Several *in vitro* and *in vivo* studies have reported on the feasibility of using allogeneic MSCs in therapeutics, and accounted their efficacy to their immunomodulatory properties and immunoprivilege. Bartholomew *et al* (2002) reported no adverse effect of allogeneic MSCs in a MHC-mismatched primate model (Bartholomew *et al.*, 2002). In a Phase II clinical trial, Le Blanc *et al* (2008) investigated the effect of treating 55 patients suffering from acute GvHD with both haplo-identical and mismatched MSCs over a 6 year period. This study reported no side effects during MSC treatment and demonstrated their immunosuppressive capacity (Le Blanc *et al*., 2008). However, given the fact that these patients underwent myeloablative conditioning, which inactivates the patient's immune system, these studies did not in fact test the immunoprivilege of MSCs, since there was no active immune system to recognise them in the first place. Murine models of GvHD challenged Le Blanc's findings by showing the failure of allogeneic MSCs to prevent GvHD after intravenous administration, and that allogeneic MSCs were rejected after subcutaneous implantation in immunocompetent mice (Eliopoulos *et al.*, 2005; Liu *et al.*, 2006; Sudres *et al.*, 2006). In these models, the sites of injection were infiltrated with host $CD8^+$ and NK cells, which have been shown to lyse MSCs in *in vitro* experiments (Eliopoulos *et al*., 2005). Comparative studies using syngeneic and allogeneic MSCs in a murine model for bone marrow transplantation demonstrated that

while syngeneic MSCs enhanced long-term engraftment and increased tolerance, allogeneic MSCs were associated with increased rejection (Huang *et al.*, 2010). The concept of immunoprivileged MSCs is therefore controversial. Several studies have demonstrated poor engraftment of MSCs after transplantation, despite the detection of prolonged MSC-derived immunosuppressive effects, which are believed to be mainly due to MSC secretome (Lavoie and Rosu-Myles, 2013). MSC paracrine effects will be further discussed in more detail in **section 1.7**.

1.5.2. The effect of inflammatory environment in MSC function

Upon transplantation, the immunomodulatory properties of MSCs are dependent on the inflammatory milieu they encounter. Initial studies hypothesized that, upon injury, MSCs perceive inflammatory cues. They can be licensed directly, via toll like receptor (TLR) engagement, or indirectly, via stimulation with pro-inflammatory cytokines, such as IFN-γ and TNF-α. Licenced MSCs can then engage in pathogen clearance or immunomodulatory effects (English, 2013). A series of studies has shown that pre-incubation of MSCs with both IFN-γ and TNF-α enhances the anti-proliferative effects of MSCs (English *et al.,* 2007; Krampera *et al.,* 2005; Noone *et al.,* 2012). In a murine model of GvHD, MSCs were revealed to be more efficient when vigorous inflammation is in progress, which is characterised by augmented IFN-γ release during the early stages of GvHD (Polchert *et al.*, 2008). Conversely, this immunosuppressive effect was not as effective when MSCs were administered at the time of bone marrow transplantation when inflammation was yet to be elicited (Polchert *et al.*, 2008). Further studies on the crosstalk between inflammation and immunosuppressive capacity of MSCs further intensified this notion (Le Blanc *et al.*, 2003; Krampera *et al.*, 2005; Dazzi and Marelli-Berg, 2008). This has led to the development of a paradigm which describes the environmental-dependent polarisation of MSCs into a MSC1 pro-inflammatory phenotype or a MSC2 immunosuppressive phenotype as illustrated in **Fig. 1.7**. These two populations showed differences in their differentiation capacity and soluble factor secretion, including IDO and PGE-2 expression and also in TGF-β signalling pathway. Additionally, while MSC2 suppress T cell proliferation, MSC1 exacerbate

inflammation by promoting T cell activation and clonal expansion (Bunnell *et al.*, 2010; Waterman *et al.*, 2010).

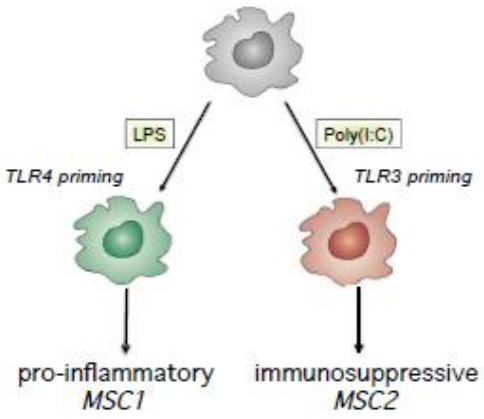

Figure 1.7: Polarisation model of MSCs (adapted from Bunnell *et al.,* 2010).

1.5.3. MSC and T cells

T lymphocytes are the primary cellular effectors of the adaptive immune system. Upon TCR engagement, T cells proliferate and exert several functions, such as cytokine release by $CD4^+$ T cells, and cytotoxicity mediated by $CD8^+$ T cells. Some of the T cells develop a memory phenotype, which is responsible for the rapid response to secondary encounters with the same antigens, while other cells acquire a regulatory phenotype which is responsible for the maintenance of self-tolerance and homeostasis (Germain, 2002). *In vitro*, MSCs suppress T cell proliferation in a dose dependent manner, with the highest inhibitory capacity being achieved at higher concentrations of MSCs. This effect occurs regardless of whether T cells have been stimulated with allogeneic DCs or peripheral blood mononuclear cells (PBMCs), or non-specific mitogens such as phytohaemagluttinin (PHA) or lipopolysaccharide (LPS) (Krampera *et al.*, 2003; Le Blanc *et al.*, 2004; Vellasamy *et al.*, 2013).

A large amount of evidence shows that allogeneic and autologous MSCs have the ability to influence T cell activation, proliferation and function *in vitro* and *in vivo* (English and Wood, 2013). This inhibition seems to be executed by cell cycle arrest of the T cells in the G0/G1 phase (Benvenuto *et al.*, 2007). This suppression leads to a decrease in IFN-γ production both *in vitro* and *in vivo* and increased IL-4 production, indicating a shift in the balance from a pro-inflammatory Th1 phenotype to a more anti-inflammatory Th2 phenotype

(Aggarwal and Pittenger, 2005; Uccelli *et al.*, 2008). In addition, MSCs induce T cell anergy which leads to cessation of proliferation and cytokine secretion in response to the antigenic stimulation, most likely, due to insufficient co-stimulatory signals (Zappia *et al.*, 2005). MSCs have also been implicated in the inhibition of Th17 differentiation in a PGE-2- and IDO-dependent manner (Duffy *et al.*, 2011). MSCs can also trigger the generation of regulatory T cells. Regulatory T cells are a subset of T cells that help maintain the homeostasis and safeguard the tolerance to self-antigens by suppressing the activation of the immune system (Sakaguchi *et al.*, 2008). MSCs manipulate T cell plasticity by suppressing the Th17 transcription factor retinoic-acid-receptor-related organ receptor-gamma T (RORγt) and upregulating the master transcription factor forkhead box P3 (FoxP3) for regulatory T cells (Uccelli *et al.*, 2008; Duffy *et al.*, 2011). Moreover, data from co-culture demonstrated that MSCs induce the proliferation of regulatory T cells in a HLA-G5 dependent manner (Selmani *et al.*, 2008). The effect of MSCs in cytotoxic T lymphocytes (CTL) has also been tested *in vitro* in co-culture experiments. Effects on CTLs seem to be dependent on the time of addition of MSCs. When added in the beginning of a MLR, they inhibit the formation of CTLs, however, this effect is not observed if MSCs are added days after the MLR started (Rasmusson *et al*., 2007).

1.5.4. MSC and Dendritic Cells

Dendritic cells act as sentinel cells and present antigens and activate antigen-specific helper T cells thus leading to the generation of an immune response (Waisman *et al*., 2016). MSCs can interfere with conventional and plasmacytoid DCs. One of the main mechanisms of MSC suppression of effector T cell function relies on the modulation of DC maturation. Several reports have shown that MSCs can inhibit differentiation of monocytes and $CD34^+$ progenitors into DCs (Chen *et al*., 2007; Kronsteiner *et al*., 2011). DCs generated in the presence of MSCs show decreased expression of MHC class II and co-stimulatory molecules such as CD40, CD80 and CD86, decreased expression of IL-12 and hampered ability to induce T lymphocytes activation (Aggarwal and Pittenger, 2005; Uccelli *et al.*, 2008). These effects on DCs seem to be caused predominantly by the release of soluble factors such as IL-6, PGE2 and/or IL-10. (English and Wood, 2013). Additionally, MSCs have also been shown to interfere with the homing capacity of DCs. *In vitro*, DCs show

down-regulation of the C-C chemokine receptor 7 (CCR7), and consequently, lower migratory capacity, when co-cultured with MSCs (Consentius *et al.,* 2015; English *et al*., 2008). MSCs reprogram DCs into a tolerogenic phenotype, characterized by the production of higher levels of anti-inflammatory cytokines, such as IL-10, and lower levels of pro-inflammatory cytokines like IL-12, IFN-γ and TNF-α (Consentius *et al.*, 2015; English and Wood, 2013;). This leads to an enhanced capacity of these DCs to generate regulatory T cells, indicating that in contact with MSCs, DCs acquire an immunoregulatory function (Uccelli *et al.*, 2008; English and Wood, 2013)

1.5.5. MSC and NK cells

In addition to modulating adaptive immune responses, MSCs also interact with innate immune cells. Natural Killer (NK) cells are one such example. NK cells play an important role in immunological defences against pathogens and tumours. They are also important regulators of adaptive immune responses due to their interaction with DCs. These cells are the major producers of IFN-γ during an immune response and exert their cytotoxic abilities by recognising cells expressing stress-induced signals or that have low expression of MHC class I molecules. In humans, these cells can be found in the peripheral blood, spleen and in lymph nodes (Vivier *et al*., 2008). Unlike B and T cells, NK cell function relies on the balance between the binding of their receptors to activating and inhibitory ligands. NK cells express killer immunoglobulin-like receptors (KIRs) which recognise MHC class I molecules. This recognises the target cell as “self” and leads to the inhibition of NK cell function. In the absence of the inhibitory signal, i.e., MHC class I expression, an activating KIR will bind to its ligand and lead to NK cell mediated cytotoxicity (Thielens *et al*., 2012). Several studies have demonstrated that MSCs can inhibit IL-2 or IL-15 induced proliferation of resting NK cells and IFN-γ production in *in vitro* co-culture experiments (Rasmusson *et al*., 2003; Spaggiari *et al*., 2006). This inhibitory effect was primarily mediated by secreted PGE-2, IDO and TGF-β1 and resulted in down-regulation of activating NK cell receptors (Noone *et al.*, 2013; Spaggiari *et al*., 2006; Spaggiari *et al.*, 2008). Alternatively, *in vitro* co-culture assay of IL-2 activated NK cells with MSCs has demonstrated that NK cells can also effectively lyse both autologous and allogeneic MSCs, despite their

inherent expression of MHC class I molecules. This is due to the expression of multiple ligands to the activating receptors NKG2D and DNAX accessory molecule (DNAM)-1 (Noone *et al*., 2013; Spaggiari *et al.*, 2006; Giuliani *et al*., 2014). Interestingly, IFN-γ primed MSCs are less susceptible to NK cell mediated lysis, partly due to the upregulation of MHC class I molecules and other inhibitory ligands on the surface of MSCs (Noone *et al*., 2013; Giuliani *et al*., 2014).

1.6. Recent understanding in the mechanisms of MSC mediated immunoregulation

Despite strong evidence supporting MSC potency in regulating immune responses, the mechanism of action of these cells is still not fully understood. These effects were initially proposed to be a result of the collaboration between cell-to-cell contact and release of trophic and paracrine factors. This notion has been challenged by recent studies reporting lack of incidence and engraftment of MSC shortly after administration. Infused MSCs have been shown to be trapped in the spleen, lung and liver, and their survival was reported to be less than 1% in several *in vivo* studies (von Bahr *et al.*, 2012). Current available experimental approaches, such as bioluminescence imaging, intra-vital microscopy, donor DNA and RNA analysis, have detected limited survival of MSCs with the majority of the cells dying within 48h of systemic infusion (Gholamrezanezhad *et al.*, 2011; von Bahr *et al*., 2012, Ringden *et al*., 2006).

These observations were also seen in clinical trials involving MSCs as therapeutic agents. In one such study, MSCs from normal siblings were intravenously administered into 5 children with *Osteogenesis imperfecta*, a genetic disorder that mainly affects bone and tissue formation due to mutations in the genes for type I collagen. After MSC infusion, 4 of the 5 children showed increased growth and strengthening of the bones, however, less than 1% of the donor MSCs was found in the bone, skin and other tissues of the patients (Horwitz *et al*., 2010). Similar observations were detected in clinical trials of MSCs for the treatment of acute GvHD. For example, in 2006, Ringden *et al* performed a study where 8 patients suffering from steroid-refractory GvHD, grades III-IV, were infused with allogeneic MSCs. Complete remission of aGvHD was detected in 6 out of 8 patients, however, MSC donor DNA could only be detected in colon and lymph nodes of one of the eight patients (Ringden *et al*., 2006).

This body of work suggests the efficacy of MSC therapy can be predominantly accounted to their secretome. MSC secretome includes an array of bioactive proteins, such as, cytokines, growth factors and chemokines, and secreted membrane vesicles, generally termed, extracellular vesicles (EVs).

1.6.1. MSC derived soluble factors

Many soluble factors have been reported to be involved in MSC-mediated immunoregulation. They are constitutively expressed by MSCs or induced upon MSC activation. The most well-characterised soluble factor-derived mechanisms are, Indoleamine 2,3-dioxigenase (IDO), Prostaglandin E2 (PGE2), Nitric oxide (NO), Human leukocyte antigen G5 (HLA-G5), Transforming growth factor β1 (TGF-β1), and Interleukin-10 (IL-10).

Indoleamine 2,3-dioxigenase (IDO) is an enzyme that catabolises tryptophan, which is essential for T cell proliferation, into kynurenine metabolites. IDO expression by MSCs is induced by IFN-γ or TLR3 and TLR4 activation (English *et al.*, 2007). MSC secreted IDO has been linked to the induction of polarisation of macrophages into the M2 phenotype (François *et al.*, 2012), induction of tolerogenic dendritic cells and regulatory T cells *in vivo*, promotion of Th2 phenotype and inhibition of T and NK cell proliferation (Mellor and Munn, 1999; English, 2013).

Prostaglandin E2 **(PGE2)** is a small lipid mediator that is produced by the cleavage of arachidonic acid into prostaglandin H2 via COX-1 and COX-2 enzymes, followed by conversion of prostaglandin H2 into prostaglandins through the action of prostaglandin synthases (English, 2013). Production of PGE2 by MSC is constitutive; however, it is upregulated upon IFN-γ and TNF-α priming (English *et al.*, 2007). PGE2 seems to be involved in suppression of T cell activation and proliferation both *in vitro* and *in vivo*, and in DC and macrophage repolarisation (Kronsteiner *et al.,* 2011). MSC-produced PGE2 has also been shown to inhibit Th17 differentiation by binding to the PGE2 receptor 4 (EP4) (Duffy *et al.*, 2011; English, 2013).

Nitric oxide **(NO)** is a produce derived from the enzymatic reaction of inducible NO synthase. NO production by MSCs is induced by IFN-γ and TNF-α or IL-11 stimulation (Ren *et al.*, 2008). This molecule has been linked to suppression of T cell proliferation and apoptosis (Ren *et al.*, 2008). These effects are more evident in murine models than in humans, however, it aids in the understanding of the mode of action of small molecules produced by MSCs.

Human leukocyte antigen G5 **(HLA-G5)** is another molecule that is involved in MSC immunomodulation. Production of HLA-G5 by MSCs has been shown to inhibit T cell proliferation and NK cell and CTL cytotoxicity and to induce the generation of regulatory T cells (Selmani *et al.*, 2008; Uccelli *et al.*, 2008).

Transforming growth factor β1 **(TGFβ1)** is a cytokine which regulates proliferation, differentiation, adhesion and migration of several cell types. TGF-β1 is constitutively expressed by MSCs and diminishes allogeneic-T lymphocyte proliferation (Di Nicola *et al*., 2002), mediates the generation of $CD4^+CD25^+FoxP3^+$ Tregs and reduces the proliferation of NK cells (Kyurkchiev *et al*., 2014).

Interleukin-10 **(IL-10)** is an anti-inflammatory cytokine which inhibits the activity of Th1 cells, NK cells and macrophages and influences maturation of dendritic cells (Couper *et al.,* 2008). Expression of IL-10 by MSCs is controversial. Several reports have shown that IL-10 can be expressed by human and murine MSCs, while others report in inability of these cells to produce this cytokine (Bernardo et al., 2013; Ivanova-Todorova *et al.,* 2012; Park *et al.,* 2009). Despite conflicting results, MSC-produced IL-10 downregulates Th1 cytokine expression and stimulates the expression and secretion of HLA-G5 (Ivanova-Tadarova *et al.*, 2012). IL-10 also mediates the generation of $CD4^+CD25^+FoxP3^+$ Tregs by MSCs (Bernardo *et al*., 2013; Bassi *et al*., 2011) and impairs the maturation and function of DCs by suppressing IL-12 production by these cells (Ivanova-Tadarova et al., 2009; Ivanova-Tadarova et al., 2012).

Overall, these soluble factors have been shown to mediate MSC modulatory effects, however, none could sufficiently account for the complete efficacy of MSC-mediated regulation. Timmers *et al* (2007) used MSC-conditioned medium (MSC-CM) to treat myocardial ischemia and reperfusion in a porcine model. This study showed that MSC-CM was capable of reducing infarct size by approximately 50%. Posterior fractionation studies revealed that the active components providing cardio-protection were large complex structures of 50-100nm in diameter rather than small single molecules. These structures were later identified as phospholipid vesicles by electron microscopy analysis (Timmers *et al.*, 2007). These observations have led to an increasing interest in

MSC derived-extracellular vesicles (EVs) and in their potential to be used as a safe cell-free, “off-the-shelf” therapy.

1.6.2. Extracellular vesicles

Extracellular vesicles (EVs) represent a heterogeneous family of membrane vesicles originating from the plasma membrane or endosomes. EVs were first described by Pan and Johnstone in 1983 as part of a disposal mechanism to discard unwanted proteins and genetic material from the cells (Pan and Johnstone, 1983). Subsequent research demonstrated that these vesicles also represent a mechanism of intercellular communication involved in the delivery of bioactive material that modifies physiological processes in the target cells (Gyorgy et al., 2011; Raposo *et al*., 1996). EV release is a conserved cellular function that has been documented in many types of prokaryotic organisms, and eukaryotic cells, including dendritic cells, T cells, and MSCs. Their presence has also been detected in a variety of bodily fluids, such as, blood and urine (Colombo *et al*., 2014). Vesicles released by different cells have similar biology, including, mechanisms of biogenesis and uptake by recipient cells. This section will report on the general biology of EVs which is common to all cell types, including MSCs.

1.6.3. Features and composition of EVs

EVs are composed of a lipid bilayer containing transmembrane proteins and cell specific receptors. They can enclose a plethora of cytoplasmic components which includes genetic material, such as short non-coding RNAs, microRNAs (miRNA) and mRNA, and several bioactive proteins, e.g., enzymes, cytokines and growth factors (Colombo *et al.*, 2014) (**Fig 1.8**). By virtue of their size, electron microscopy is the only available methodology to visualise their morphology. When analysed by ‘whole-mount’ electron microscopy, EVs appear cup-shaped (Raposo *et al.*, 1996). This feature is often utilised to characterise vesicles of sizes ranging from 30 to 100 nm, however, rather than an intrinsic feature, this morphology is an artefact of fixation, contrasting and embedding procedures. Further analysis using cryo-microscopy showed that these vesicles appear spherical with a well-defined lipid bilayer (Raposo *et al.*, 2013).

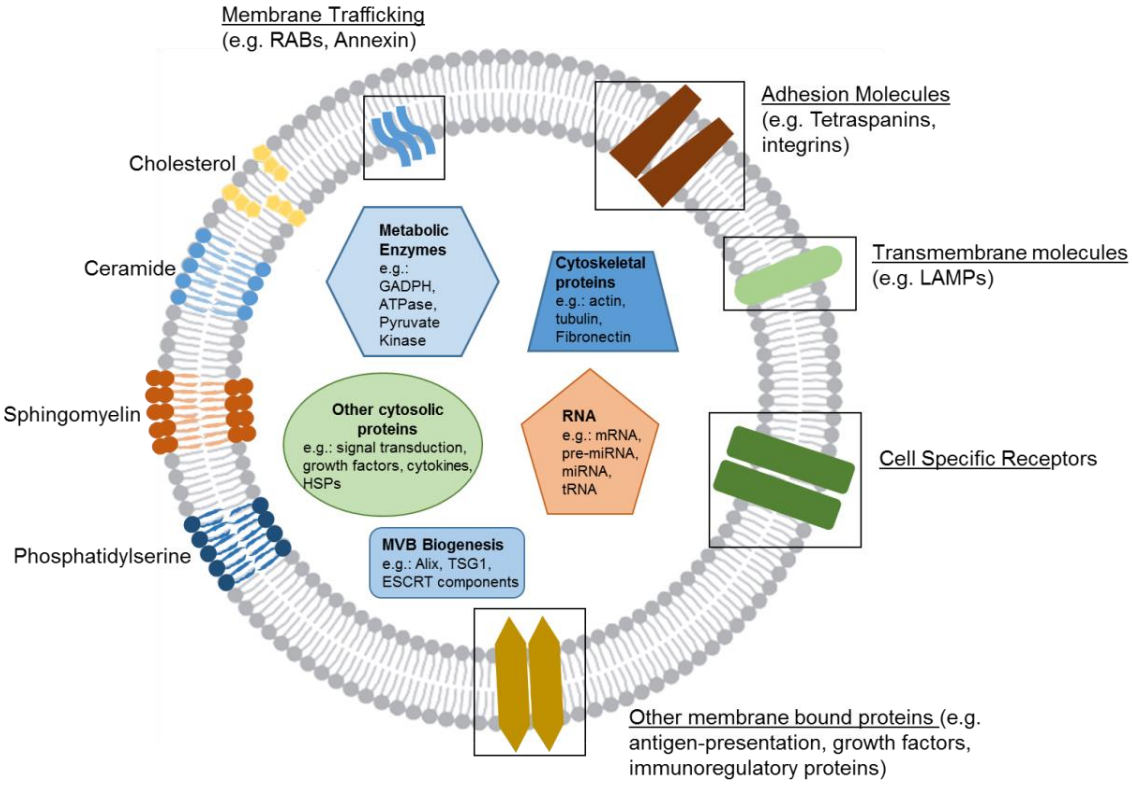

Figure 1.8: Schematic composition of extracellular vesicles

EVs are composed of a lipid bilayer rich in transmembrane proteins (e.g. CD63, CD9, CD81), adhesion molecules (e.g. integrins), membrane trafficking proteins (e.g. RABs, annexin) and other cell specific receptors and/or membrane bound proteins. These vesicles enclose a wide variety of proteins (e.g. cytoskeletal proteins, enzymes and other cytosolic proteins) and a plethora of RNA species, including mRNA, microRNA and tRNA.

Since the infancy of the EV field, research has been focused on characterising the proteome and the RNA content in these particles. As a result, extensive lists of EV-associated components have now been generated. Details of these studies are catalogued in various online databases, including Vesiclipedia (www.microvesicles.org) (Kalra *et al.,* 2012), EVpedia (www.evpedia.info) (Kim *et al*., 2013) and ExoCarta (www.exocarta.org) (Keerthikumar *et al.,* 2016).

In general, EV preparations comprise a mixture of vesicles ranging 30-1000nm in size with a variety of cargos. Within an EV preparation, three types of vesicles can be detected: exosomes, microvesicles and apoptotic bodies (Colombo *et al.*, 2014). A general description of the three major types of EVs and their general characteristics are described in **Table 1.3**.

Table 1.3: Nomenclature and classification of the different types of vesicles

Adopted from Colombo *et al.,* 2014 and Rani *et al.,* 2015

Characteristics	Exosomes	Microvesicles	Apoptotic Bodies
Size	20-100nm	50-1000nm	500-5000 nm
Shape	Cup shaped	Irregular	Heterogeneous
Sedimentation	100,000xg	Size dependent at 100,000xg, 10,000xg and 2000xg	Size dependent at 100,000xg, 10,000xg and 2000xg
Sucrose gradient	1.13-1.19 g/ml	1.04-1.07 g/ml	1.16 and 1.28 g/ml
Markers	Tetraspanins (CD63/CD9), Alix, TSG1, ESCRT components, flotilin	Integrins, tetraspanins, selectins and CD40 ligand	Histones
Lipids	Cholesterol, sphingomyelin, ceramide, lipid rafts, phosphatidylserine	Phosphatidylserine	High amounts of phosphatidylserine
Origin	Endolysosomal pathway; Intraluminal budding into multivesicular bodies and released by fusion of the multivesicular bodies with the cell membrane	Cell surface; outward budding of cell membrane.	Cell surface; outward blebbing of apoptotic cell membrane
Contents	mRNA, microRNA, and other non-coding RNAs; cytoplasmic and membrane proteins (including HSP, and cell specific receptors	mRNA, microRNA (miRNA) and other non-coding RNAs; cytoplasmic proteins and membrane proteins, including cell specific receptors	Nuclear fractions and cell organelles

The two main types of vesicles are microvesicles and exosomes. These two types can be distinguished based on their mode of formation, however, they display overlapping composition, markers, density and size (Colombo *et al.*, 2014). Due to these characteristics, the International Society for Extracellular Vesicles (ISEV) suggested that the term EV should be used to describe vesicle preparations from bodily fluids and cell cultures. Furthermore, in 2014, Lötvall and colleagues established the basic criteria to characterise EV preparations. According to this position paper EVs must be purified from extracellular fluids (e.g. conditioned medium and bodily fluids). These EVs must express at least 3 proteins that recapitulate their mode of biogenesis (e.g. CD9, CD63 and CD81); and their size and morphology must be analysed to provide information about the heterogeneity of the EV preparation in study (Lötvall *et al*., 2014). One of the main features used to classify the two main types of EVs is based on their mode of formation and release. While exosomes are formed within the endosomal complex, microvesicles are formed by outward budding of plasma membrane.

Exosomes have a diameter of 30-100 nm, can be sedimented by ultracentrifugation at 100,000xg and concentrated by sucrose gradient at a density of 1.13-1.19 g/ml. These vesicles are of endosomal origin and constitutively secreted by most cells. During the maturation of early endosome into late endosomes, intraluminal vesicles (ILVs) accumulate in their lumen. These ILVs are formed by invagination of the early endosomal membrane, also known as multivesicular emulsion (MVE). This process leads to the segregation of specific cargo and vesicle arrest, giving rise to multivesicular bodies (MVBs). MVBs bearing the tetraspanin CD63 and other lysosome-associated proteins such as LAMP1 and LAMP2 are translocated to the plasma membrane in an ensodomal sorting complex required for transport- (ESCRT-) dependent or independent way. They then fuse directly with the plasma membrane and are exported to the extracellular milieu (Colombo *et al.,* 2014).

Microvesicles are a heterogeneous subset of EVs, with sizes ranging from 50 to 1000 nm in diameter, which can be sedimented by centrifugation at different centrifugal speeds, ranging from 2,000-100,000xg, and concentrated on a sucrose cushion at a density of 1.04-1.07 g/ml. Release of these vesicles

usually requires *stimuli* induction leading to a calcium-dependent remodelling of the cytoskeleton. This remodelling leads to outward budding and fission of the cell membrane, resulting in the release of these microvescles to the extracellular environment (Colombo *et al.*, 2014) (**Fig.1.9**)

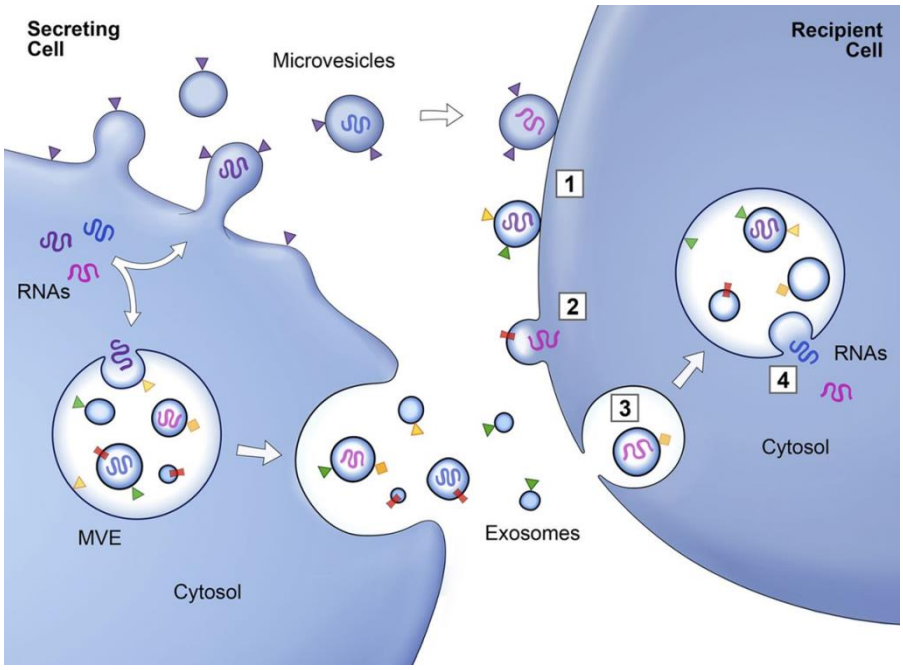

Figure 1.9: Biogenesis and release of exosomes and microvesicles and uptake by target cells.

Membrane-associated (triangles) and transmembrane proteins (rectangles) and RNAs (curved symbols) are selectively incorporated into the ILV of MVEs or into MVs budding from the plasma membrane. MVEs fuse with the plasma membrane to release exosomes into the extracellular space. Uptake by target cells is performed by (1) interaction with cell receptors (2) phagocytosis and (3) vesicle fusion with the membrane of an endocytic compartment (4). This leads to a delivery of proteins and RNA into the membrane or cytosol of the target cell (image adapted from Raposo *et al*., 2013)

1.6.4. EV interaction with the target cells

EV interaction mechanisms with the target cells are still not well defined, however, 3 mechanisms of EV uptake by the target cells have been proposed: 1) interaction of membrane proteins with cell receptors; 2) phagocytosis by target cells and 3) vesicle fusion with the endocytic compartment of the target cells in a clathrin- or caveolin-mediated endocytosis. Surface receptors on the outer membrane of EVs are responsible for their biodistribution, by binding to their specific ligands on the cell surface or extracellular matrix. This interaction

is sufficient to trigger signalling pathways that modify physiological processes within the target cells. Alternatively, EVs may be internalised by the target cells, by vesicle fusion with the endocytic compartment of target cells, or, as it is more commonly described, by phagocytosis. These processes seem to be executed in specific parts of the cell membrane, i.e., the lipid rafts, which present the same membrane fluidity of EVs. Lipid rafts are microdomains within the plasma membrane rich in proteins and sphingolipids that are tightly ordered and, in consequence, more rigid than the rest of the plasma membrane. They are also rich in cholesterol, which is involved in the clathrin- and calveolin-mediated mechanism of endocytosis (Colombo *et al*., 2014; Raposo *et al.,* 2013, Théry *et al.,* 2011). Upon internalisation, EVs release their content onto the cytosol of the target cell (**Fig. 1.9**).

1.6.5. EV isolation methods

EVs can be isolated from cell culture supernatants and other bodily fluids by differential ultracentrifugation. This protocol was first used in 1987 by Johnston *et al* to purify reticulocyte EVs from cell culture conditioned medium. In 2006, Thery *et al* described this protocol in detail and established the gold standard for EV purification worldwide. This protocol is based on a series of centrifugations at different speeds to eliminate cell debris and protein contaminants (Théry *et al.,* 2006). Several studies report variations on this method which can include higher-speed ultracentrifugation (e.g. 140,000xg), longer centrifugations at maximum speed (e.g. 4-7 hours) and inclusion of filtration methods or size-exclusion chromatography to recover particles larger than 50,000kDa to eliminate debris and contaminating proteins (Baj-Kryworzeka *et al.,* 2006; Muralidharan-Chari *et al*., 2009). This protocol only allows enrichment of EV types and does not separate different types of vesicles. One way to address this issue is by using a sucrose gradient, which separates vesicles according to their flotation properties (see **Table 1.3** for flotation density details). One of the major drawbacks of this methodology is the recovery rate of EVs. Despite separating EVs according to their size, there is also a high loss of material after sucrose separation which may influence downstream applications (Momen-Heravi *et al.,* 2013). Recently, commercially available kits based on polymer-precipitation and immune-capture using antibody-coated magnetic beads have been released. The first method

precipitates a wide range of vesicles; however it may display concomitant precipitation of protein contaminants. The second method is a more refined technology based on the use of magnetic beads coated with antibodies against specific EV markers, such as CD63, CD9 and CD81. However, this method precipitates a restricted fraction of the EV population and neglects others that may harbour therapeutic potential (Momen-Heravi *et al.,* 2013). Current research in the EV field is focused on the refinement of the abovementioned protocols to allow for a more robust and pure isolation of EVs.

1.6.6. MSC-derived EVs

MSC-EVs are constitutively secreted by MSCs and easily isolated from culture supernatants. They can be identified by transmission electron microscopy as cup-shaped nanovesicles with sizes ranging from 20-150 nm in diameter (Lai *et al.,* 2016). MSC-EVs are rich in a variety of adhesion molecules, such as intercellular adhesion molecule-1 (ICAM-1), lysosomal-associated membrane 2 (LAMP-2), tetraspanins (e.g. CD9, CD63, CD81), integrins (e.g. CD49c, CD49d), heat shock proteins, cytoskeletal proteins, and membrane trafficking proteins such as “Ras-related in brain” and annexins (Kim *et al.*, 2012; Tan *et al.*, 2013). Moreover, they express MSC-specific molecules, including CD73, CD44 and CD105 and enclose proteins involved in MSC proliferation and differentiation (GF, Wnt, TGF-β, MAPK, BMP, etc) (Kim *et al.*, 2012). MSC-EVs carry a wide variety of genetic material, including mRNA and non-coding RNA (pre-miRNA, miRNA, tRNA, piRNA) (Chen *et al.*, 2010; Tomasoni *et al.*, 2013; Baglio *et al.*, 2015). MSC-EVs lipid composition is still unknown; however, Lai and colleagues have reported an enrichment of phosphatidylserine in MSC-EVs. This lipid has been described as a canonical EV component present in all types of vesicles.

The packaging of the secreted MSC-EVs is however, related to the environmental cues. EVs from MSCs that have gone through hypoxic or inflammatory conditioning exhibit distinct protein and RNA content when compared to those purified from conditioned medium of steady-state MSCs (Anderson *et al.,* 2016). In depth proteome analysis of MSC-EVs from cells expanded in hypoxic conditions revealed an enrichment of components involved in EGFR, FGF, PDGF pathways and enhancement of NF-κB pathway activity, in

comparison to the MSC-EVs from the normoxic expanded MSCs (Anderson *et al.,* 2016). Moreover, MSCs subjected to inflammatory conditioning with IFN-γ and TNF-α show increased levels of tolerogenic receptors and anti-inflammatory microRNAs, such as let-7b (Kilpinen *et al.,* 2013; Ti *et al*., 2015).

1.6.7. Immunomodulatory potential of MSC-derived EVs

Since the initial identification of EVs in the conditioning medium of MSCs, increasing studies have demonstrated that MSC-EVs harness therapeutic effects. MSC-derived EVs have been shown to recapitulate the therapeutic effect of the parent cells in models of cardiac, kidney and brain injuries (Lai *et al.*, 2010; Gatti *et al.*, 2011; Zhang *et al.*, 2015). The importance of MSC-EVs in immunomodulation has also been identified as one of the mechanisms of MSC immunomodulation. MSC-EVs have been reported to modulate proliferation and differentiation of T-cells, B-cells and monocytes (**Fig 1.10**). Budoni *et al* (2013) demonstrated that the effect of MSCs on B-cell proliferation and differentiation could be fully reproduced by MSC-EVs. In the presence of MSC-EVs, proliferation and differentiation of B lymphocytes in a CpG-stimulated peripheral blood mononuclear cell co-culture system, was inhibited in a dose-dependent manner (Budoni *et al.*, 2013).

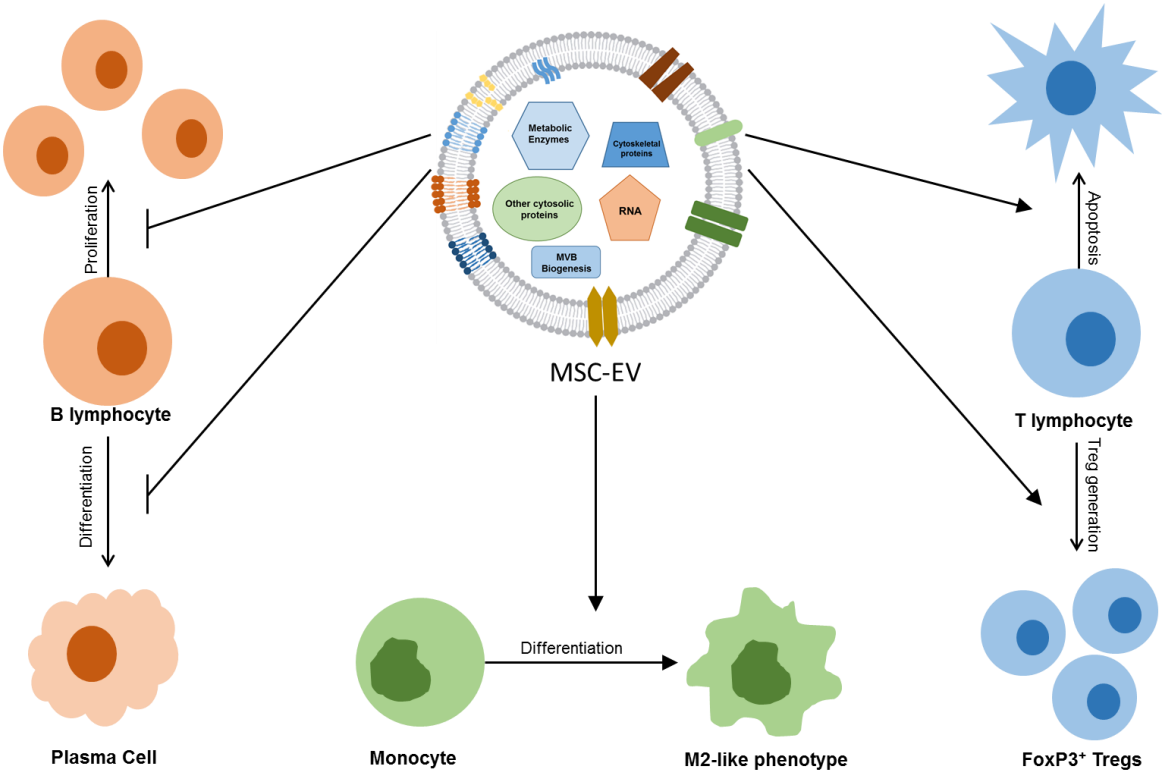

Figure 1.10: Immunomodulatory effects of MSC-EVs on lymphocytes and monocytes

MSC-EVs inhibit proliferation and differentiation of B cells into plasma cells; they induce apoptosis of T lymphocytes and tolerogenic responses by prompting the generation of $CD4^{+}CD25^{hi}FoxP3^{+}$ T cells and the differentiation of monocytes into a M2-like phenotype characterised by high production of IL-10 and decreased secretion of IL-12.

The effect of MSC-EVs on T lymphocytes was initially investigated by Mokarizadeh *et al* in 2012. Initially, the effects of MSC-EVs were shown to be due to specific ligand-receptor interactions with the target cells and induction of tolerogenic responses. MSC-EVs were shown to express regulatory receptors, such as programmed death ligand 1 (PD-L1), galectin-1 and membrane bound TGF-β1. When added to auto-reactive lymphocytes, they inhibited proliferation and induced apoptosis of T lymphocytes. Concomitantly, an increase in IL-10 and TGF-β1 secretion was detected (Mokarizadeh *et al*., 2012). Further studies demonstrated that MSC-EVs induced *de novo* generation of $CD4^{+}CD25^{+}FoxP3^{+}$ Tregs (Blazquez *et al.,* 2014; Favaro *et al.,* 2016). Despite these findings, the direct targeting of MSC-EVs on T lymphocytes is still controversial. Some reports show that MSC-EVs fail to suppress T cell proliferation, even when added to the co-cultures at high concentrations (Di Trapani *et al.,* 2016;

Gouveia de Andrade *et al.,* 2016). Similarly, uptake analysis of MSC-EVs by the different subtypes of immune cells, such as, monocytes, B cells, NK cells and $CD3^+$ T cells revealed a preferential uptake of EVs by monocytes, followed by B, NK, and T cells respectively (Di Trapani *et al.,* 2016).

The effect of MSC-EVs on monocytes is still widely unexplored, and little is known about their influence in dendritic cell maturation and function. Recent studies performed by Zhang *et al* (2015) demonstrated that MSC-EVs were preferentially taken up by BALB/cJ mice-derived splenocytes. MSC-EV treatment induced a tolerogenic $IL\text{-}12^{lo}IL\text{-}10^{hi}$ M2-like phenotype. These macrophages were then responsible for the polarisation of activated $CD4^+$ T-cells to that of a $CD4^+CD25^+FoxP3^+$ Treg phenotype (Zhang *et al.*, 2015). Recently, Favaro and colleagues demonstrated that MSC-EVs impaired *in vitro* maturation of DCs. These EV treated DCs were characterised by lower expression of co-stimulatory molecules CD86, CD80 and CD83, and increased IL-10 production (Favaro *et al.*, 2016).

MSC-EVs have also been tested in the context of HSCT and GvHD. A recent study has provided initial evidence that MSC-EV treatment combined with HSCs contributes to faster reconstitution of the hematopoietic microenvironment. In this study, MSC-EVs were shown to be enriched in miRNAs that promote UCB-$CD34^+$ migration and engraftment in the BM niche (De Luca *et al.*, 2015). Amarnath *et al* (2015) detected CD73-expressing EVs in MSC recipients in a mouse model of GvHD. These EVs were found to metabolise extracellular ATP into adenosine and, as a consequence, to inhibit Th1 cell effector function. (Amarnath *et al.*, 2015). Accumulation of adenosine leads to the activation of extracellular signal-regulated kinases (ERK) and protein kinase B (PKB/AKT) signaling pathways, which in turn mediate cell survival and proliferation signaling mechanisms (Amarnath *et al.*, 2015). In 2014, Kordelas *et al*, was the first to administer MSC-EVs in a therapy-refractory GvHD patient. MSC-EV preparations were shown to contain high concentrations of anti-inflammatory molecules IL-10, TGF-β and HLA-G and were administered to the patient at intervals of 2 or 3 days for a period of 2 weeks. MSC-EV infusion was well tolerated and no side effects were reported. The patient exhibited a 50%

decrease in the production of the pro-inflammatory cytokines IL-1β, TNF-α, and IFN-γ and concomitant with the cytokine profile, a reduction in the volume of diarrhea and cutaneous and mucosal GvHD, which remained stable for more than 4 months post MSC-EV treatment (Kordelas *et al*., 2014).

Despite the efficacy of MSC-EV treatment, the key mechanisms of action remain ill-defined. These vesicles are rich in a variety of proteins, lipids and RNA that altogether influence a multitude of networks and cellular components. It is unlikely that the beneficial effects can be accounted to only a limited amount of MSC-EV related molecules. Further work dissecting the interactome is essential to fully understand their functional potential. The immunomodulatory properties of MSC-EVs, specifically on the modulation of dendritic cell maturation and function will be further dissected in **Chapter 5**.

1.7. MSC- EV enclosed microRNA

As described above, EVs contain a variety of molecules including proteins, lipids and genetic material. A diverse range of genetic material has been detected in EVs, including DNA, mRNA, piRNA, tRNA and microRNAs (miRNAs). Significant importance has been given to EV enclosed miRNAs, due to their regulatory function in gene expression. MicroRNAs are 17-24 nucleotide small non-coding RNAs produced by animal and plant cells. These RNAs regulate gene expression by binding to the 3'untranslated region (UTR) or open reading frame (ORF) region of target mRNAs thus targeting them for degradation and repressing translation. The human genome encodes over 1000 miRNAs, which collectively target about 60% of mammalian genes (Bartel, 2004). In MSCs, the role of miRNAs has been linked to the control of differentiation, proliferation, survival and paracrine activity (Clark *et al.,* 2014).

1.7.1. Biogenesis and maturation of microRNAs

Genes for miRNA are distributed in clusters of identical or closely related mature miRNAs in the genome. These clusters are transcribed as polycistronic primary transcripts that contain at least two genes. This organisation leads to simultaneous expression of similar miRNAs, which share similar functional effects. The biogenesis of microRNAs can be performed via canonical and non-canonical pathways, with the canonical pathways being the most common (Melo and Melo, 2014).

The canonical pathway starts with the transcription of these clusters into a long transcript, the primary miRNA (pri-miRNA), typically by the action of RNA polymerase II. These transcripts are polyadenylated at the 3' end and capped at the 5' end and structurally, they consist of at least one hairpin structure, each containing a stem and a terminal loop. While still in the nucleus, the pri-miRNA is "cropped" into pre-miRNAs, consisting of ~70nt hairpin structure. This process is catabolised by the activity of a protein complex known as microprocessor, which contains Drosha, an RNase III enzyme, and DGCR8 (DiGeorge syndrome critical region 8), a double-stranded RNA-binding protein. The DGCR8 protein binds to the flanking single-stranded RNA (ssRNA) region of the stem and Drosha cleaves the stem ~11 nt away from the stem-ssRNA junction. The resulting pre-miRNA contains a 5'phosphate and a 2 nt 3'

overhang. The 3' overhang is then recognized by exportin-5 and translocated from the nucleus to the cytoplasm via Ran-GTP-dependent mechanism (Melo and Melo, 2014; Winter *et al.,* 2009).

In the cytoplasm, pre-miRNAs are further processed into ~22 nt miRNA duplexes by the action of Dicer. Dicer is secreted in the cytoplasm and recognises the 5'phosphate and the 3'overhang of the pre-miRNA. This enzyme associates with other proteins, including trans-activator RNA (tar)-binding protein (TRBP) and Argonaute. Dicer cleaves the double-strand at the terminal base pairs of the pre-miRNA. The resulting RNA duplex (miRNA-5p:miRNA-3p) is separated into single strands, the miRNA-5p and miRNA-3p. The miRNA-5p strand associates with argonaute proteins and is incorporated in the RNA-induced silencing complex (RISC) which is then guided to repress target mRNAs (Melo and Melo, 2014; Winter *et al.,* 2009) (**Fig.1.11**).

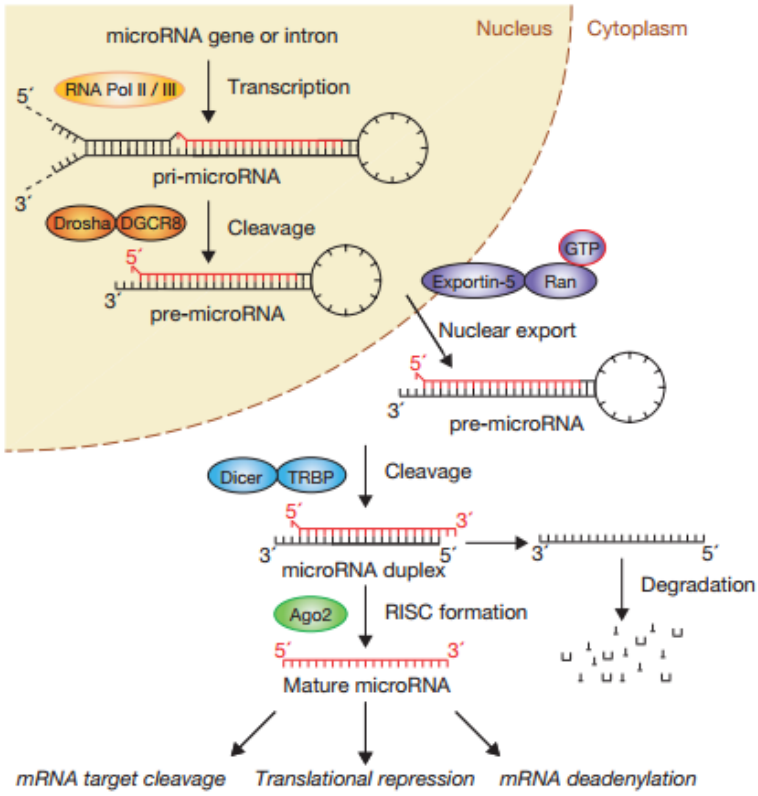

Figure 1.11: Canonical pathway of miRNA processing and function

The process starts with the transcription of the microRNA genes via the action of RNA polymerase II or III, giving rise to the pri-miRNA transcript. This transcript is then cleaved by the action of Drosha/DGCR8 and translocated to the cytoplasm in an Exportin-5/Ran-GTP dependent manner. In the cytoplasm the pre-miRNA is cleaved by Dicer and complexed with argonaute 2 into RISC to form the mature miRNA complex (adapted from Winter *et al.,* 2009)

1.7.2. Sorting of miRNAs into EVs

MicroRNAs have been shown to be transferred from donor to receptor cells and to influence gene expression in the recipient cells. One of the main mechanisms of intercellular transport of miRNAs is by packaging into extracellular vesicles. By being enclosed in extracellular vesicles, the miRNA is protected from degradation by the action of RNases and trypsin. Although the underlying mechanisms of miRNA sorting into EVs are not yet fully understood, there are four proposed pathways:

1) Via the action of neural-sphingomyelinase 2 (nSMase2). A previous study has shown increased miRNA secretion into extracellular vesicles upon nSMase2 overexpression (Kosaka *et al.*, 2013).
2) Via the action of sumoylated heterogeneous nuclear ribonucleoproteins (hnRNPs). These sumoylated hnRNPs have affinity to motifs in the 3'-end of the miRNA which causes sorting of the bound miRNAs into EVs (Villarroya-Beltri *et al.,* 2013).
3) Via the sorting of specific 3'-end of the miRNAs. Previous reports demonstrated that miRNAs with an uridylated 3'-end were preferentially sorted into EVs while adenylated 3'-end miRNAs remained in the parent cells (Koppers-Lalic *et al.*, 2014).
4) Via the action of microRNA induced silencing complex (miRISC). This complex is composed of miRNAs, miRNA-repressible mRNA, GW182 and Argonaute 2 (AGO2), and co-localises with the MVBs in the cytoplasm. AGO2 has been linked to specific sorting of miRNAs into EVs, and has been identified in proteomic analysis of EVs. A decreased of specific miRNAs in EVs has been detected in $AGO2^{-/-}$ models. The blockade of MVB formation and turnover resulted in loss or over-accumulation of miRISC, respectively (Frank *et al.,* 2010; Melo *et al.,* 2014).

1.7.3. The role of MSC-EV enclosed microRNA on MSC paracrine effects

The research on MSC-EV derived miRNA is only in its infancy. Initial microarray analysis detected specific packaging of miRNAs into MSC-EVs. A microarray analysis of MSC-conditioned medium (-CM), MSC-EVs and respective parent cells showed that miRNAs were preferentially present in the EVs when compared to the MSC-CM and detected a miRNA cargo that partially

recapitulated the parent cells miRNA content, with 45 of 60 miRNAs identified in EVs, being equally present in MSCs (Chen *et al*., 2010). Further microarray analysis performed by several other groups identified microRNAs that were specifically sorted in EVs, indicating that this mechanism is selective rather than random (Baglio *et al.,* 2015; De Luca *et al.,* 2015). Gene ontogeny analysis showed that many of these microRNAs were associated with regulation of the immune system (Baglio *et al.,* 2015; Phinney *et al.,* 2015). In addition, the MSC protective effect on diseases, such as acute kidney injury, has been shown to be abolished by RNase treatment in both *in vitro* and *in vivo* models (Biancone *et al.,* 2012; Bruno and Camussi, 2013). These data prompted the investigation of functional effects of MSC-EV shuttled miRNAs, and so far, their role on MSC therapeutic effects has been experimentally analysed in the context of several disease models, such as cancer, cardiac, kidney and brain injury.

The anti-tumour effect of MSC-EV shuttled miRNA was described in several studies. Lee *et al* (2014) demonstrated that MSC-EVs suppressed angiogenesis by breast cancer cells by shuttling miR-16, which inhibited VEGF expression both *in vitro* and *in vivo* (Lee *et al.,* 2014). Similarly, *in vitro* co-culture experiments of MSC-EVs with breast cancer cell line BM2 showed that these vesicles promoted cell dormancy by transferring miR-23b (Ono *et al.,* 2014). This microRNA suppressed the expression of myristoylated alanine-rich C-kinase substrate (MARCKS), a protein involved in cell cycling and motility (Ono *et al.,* 2014). Other studies have explored the possibility of using MSC-EVs as drug delivery vehicles. MSCs transfected with miR-122 were shown to secrete EVs containing this miRNA. The microRNA, miR-122 was detected in hepatocellular carcinoma cells after co-culture with MSC-EVs; moreover treatment with these EVs prompted suppression of α-disintegrin and metalloproteinase domain-containing protein 10 (ADAM10), insulin-like growth factor receptor 1 (IGFR1) and cyclin G1 (CCNG1) genes which led to an increased chemosensitivity by the tumour cells (Lou *et al.,* 2015). Furthermore, MSCs transfected with miR-146b produced EVs enriched in this miRNA, which caused glioma shrinkage in a rat model of primary brain tumour (Katakowski *et al.,* 2013).

MSC-EVs have been shown to recapitulate the therapeutic effect of their parent cells in preclinical models of cardiac, kidney and brain injury (Gatti *et al.*, 2011; Lai *et al.*, 2010; Zhang *et al.,* 2015). Transplanted MSC-EVs have been reported to efficiently reduce infarct size in animal models of myocardial ischemia, protect from acute and chronic kidney injury in glycerol induced mouse models and contributed to tissue repair in rat models of stroke (Gatti *et al.,* 2011; Lai *et al.,* 2010; Liu *et al.,* 2013). These effects were shown to be at least partially mediated by microRNAs.

MSC-EV shuttling of miR-19a was demonstrated to be involved in the protective effect of these vesicles in models of cardiac injury (Katare *et al.,* 2011). Similarly, miR-22 and miR-221 loaded MSC-EVs were found to promote cardiac remodelling by targeting methyl CpG binding protein 2 (*MecP2*) and suppressing the expression of p53 upregulated modulator of apoptosis (*PUMA*) (Yu *et al.,* 2015).

In kidney injury, the effect of MSC-EVs can be attributed mainly to their anti-inflammatory properties. As described previously, MSC-EVs partially carry the immunosuppressive properties of their parent cells. In murine models of acute kidney injury, these vesicles induced up-regulation of anti-apoptotic genes, such as baculoviral IAP repeat containing 8 (*BIRC8*), B-cell lymphoma-extra-large (*Bcl-xL*) and B-cell lymphoma 2 (*Bcl2*), and down-regulation of apoptotic genes Lymphotoxin alpha (*LTA*), Caspase-1 (*Casp1*) and Caspase-8 (*Casp8*), thus promoting cell survival and maintenance of renal function (Rani *et al.,* 2015). Recently, Collino *et al* (2010), demonstrated that this effect could be abrogated by inhibiting microRNA secretion in MSCs and derived EVs. In their study, Drosha-knockdown MSCs were shown to produce the same amounts of EVs as wild type MSCs, however, in comparison with the latter, the knockdown MSCs exhibited global downregulation of microRNAs (Collino *et al.,* 2010). Further *in vivo* experiments showed that only wild type derived EVs were capable of promoting kidney recovery, indicating these small RNAs play an important role in kidney repair (Collino *et al.,* 2010).

MSC-EV enclosed microRNAs have similar functional effects in treating brain injury. Xin *et al* (2013) recently found that MSC-EVs containing miR-133b contributed to the protective effect of MSCs on stroke models. MiR-133b is

commonly found in midbrain dopaminergic neurons and regulates the production of tyrosine hydroxylase and domapine transporters (Heyer *et al.,* 2012). In their study, this microRNA was increased in astrocytes after MSC-EV treatment, but not detected when MSCs were treated with an miR-133b inhibitor. In addition, miR-133b transfer by EVs was accompanied by an induction of neurite outgrowth (Xin *et al.,* 2013).

In addition, a recent study by De Luca *et al* (2015) analysed the effect of MSC-EV derived microRNAs on gene expression patterns of umbilical cord blood (UCB) derived $CD34^+$ cells. Their study reported a correlation between the EV enclosed miRNAs and the down-regulated genes on UCB-$CD34^+$ cells. This differential gene expression was further shown to be associated to increased cell survival and migratory capacity of the cord blood cells to the BM niche (De Luca *et al.,* 2015). In one other study, Phinney *et al* (2015) reported that MSC-EVs inhibited macrophage polarisation by shuttling microRNA which suppressed Toll-like receptor signalling (Phinney *et al.,* 2015). Similarly, MSC-EVs were shown to contain high amounts of Let-7b after LPS conditioning (Ti *et al.*, 2015). The let-7 family represents a group of highly conserved microRNAs across species in both sequence and functions. Dysregulation of these microRNAs has been linked to impairment of cellular differentiation and development of cancer (Su *et al.,* 2012). This microRNA was responsible for the polarisation of monocyte-derived THP-1 macrophages into a tolerogenic M2 like phenotype, by the regulation of the TLR4/NFκB/STAT3/AKT pathway (Ti *et al.,* 2015).

Altogether, these data indicate miRNAs are one of the main bioactive components of MSC-EVs. Despite promising data, the functional effect of EV microRNAs on the immunoregulatory functions of MSCs is still widely unexplored. Further exploration of MSC-EV derived microRNA and their functional properties will be further discussed in **Chapter 6** in the context of novel data collected from this PhD.

1.8. Future direction of MSC clinical application

As discussed so far, the immunomodulatory and trophic properties of MSCs have been the key factors for their use in clinical applications. Considerable data indicates that MSCs mediate their long-term effects in a paracrine manner, by the secretion of soluble factors and extracellular vesicles. Apart from developing standardised protocols for MSC generation and functional assessment, two major developments are underway to facilitate more effective use of MSC therapy in the future: 1) the replacement of FCS with PLT for the *ex vivo* expansion of MSCs and 2) the exploration of MSC-EV potential to be used as an "off-the-shelf" cell-free therapeutic product.

In the most recent years, research suggests that MSC-EV based therapy could potentially have significant clinical relevance. In comparison with MSCs, secreted vesicles are less immunogenic as a result of lower expression of membrane-bound molecules, including membrane histocompatibility complex (MHC). By virtue of their encapsulated cargo, EVs provide added protection to their contents from *in vivo* degradation, thus preventing problems associated with rapid breakdown of soluble molecules, such as cytokines, growth factors and RNAs. In contrast to cell-based therapy, MSC-EV therapy can be easier to manufacture and safer, as they are devoid of cells and hence impose no danger of ectopic tissue formation. In addition, they can be stored in non-toxic cryopreservatives at -20^{o}C for 6 months with maintenance of biological activity (Webber and Clayton, 2013).

Despite these advantages, for clinical translation to be considered it is essential to elucidate the biological properties and the constituents of these vesicles, in terms of proteins and RNAs. MSC-EVs, as cellular products, are influenced by the secreting cells; therefore, it is inevitable that MSC heterogeneity will impact on EV cargo and biological effects. Distinct MSCs have been shown to display different abilities to produce cytokines and to respond to inflammatory licensing (Castro-Manrreza and Montesinos, 2015). Moreover, donor age and gender also affect the functional characteristics of MSCs (Siegel *et al.*, 2013). Current studies have not clarified the effect of inter-individual variability of MSC-EVs, and only a few studies have shown the effect of MSC licensing with inflammatory cytokines on the immunomodulatory potential to the EVs

(Mokarizadeh *et al.*, 2012; Ti *et al.*, 2015). Furthermore, considerations regarding the immunomodulatory potency of the vesicles in relation to their cellular counterparts need to be taken into account. A recent report on the immunosuppressive effect of BM-MSCs and their derived EVs has shown that the latter were considerably less potent in suppressing T-cell proliferation and preventing B-cell differentiation (Conforti *et al.*, 2014). MSC-EVs were also seen to be not as effective in modulating DC maturation as their parent cells (Favaro *et al.*, 2016). In the future, it will be important to investigate the effect of MSC variability and licensing on the molecular signature of their derived vesicles. Notwithstanding, data indicates that MSC-EVs are capable, at least in part, of mediating immunomodulatory responses; however, further research is needed to unravel their mode of action and the development of standardized EV purification, characterization and potency assays is essential to predict the real potential of using MSC-EVs for clinical applications.

1.9. Research aims

The overall aim of this study is to add new knowledge to facilitate the development of future MSC therapies under xeno-free conditions. This research also aims to advance the understanding of the mode of action of MSC mediated immunomodulation. Firstly, this study investigated the effect of xeno-free expansion using platelet lysate supplemented medium on MSC general characteristics, global surface protein profiles and immunomodulatory properties, in comparison with conventionally FCS-expanded MSCs. Secondly, this project further investigated the effects of EVs derived from platelet lysate expanded MSCs on allo-immune responses, with particular focus on their potential to suppress T cell proliferation and to modulate the maturation and function of monocyte derived dendritic cells. Thirdly, this project elucidated on the molecular basis underlying the functional effect of MSC-EV mediated immunomodulation. The investigation has been conducted by:

1) Generation of BM-derived MSC using human platelet lysate supplemented media and comparing them to FCS expanded MSCs in terms of proliferative capacity, morphology, trilineage potential, phenotype and immunomodulatory properties.
2) Investigation of the effect of MSC expansion in PLT-supplemented media on the expression of over 300 surface proteins in comparison to FCS expanded MSCs.
3) Purification and characterisation of EVs derived from PLT-expanded MSCs and investigation of the effect of MSC-EV treatment on allogeneic stimulated T cell proliferation and on monocyte derived DC maturation and function.
4) Screening and validation of a signature list of microRNAs on EVs and corresponding parent cells and identification of downstream miRNA targets for the identified microRNA list.

Chapter 2: General Materials and Methods

“If we knew what it was we were doing, it would not be called research, would it?”

-Albert Einstein

Chapter 2 – General Materials and Methods

2.1. Samples sources and ethics declaration

All samples were acquired from healthy donors with informed consent and under approval of the local ethics committee (Project 6980, Improving hematopoietic stem cell outcome through studies of alloreactivity, immune reconstitution, biomarkers and novel therapies: 14/NE/1136)

2.2. General Tissue culture methods

2.2.1. General Cell culture media and buffers

General culture media (RF10) included Roswell Park Memorial Institute (RPMI) medium 1640 supplemented with 100 IU/ml penicillin, 100 µg/ml streptomycin, 2 mM L-glutamate and 10% Heat Inactivated Foetal Calf Serum (Hi-FCS) (Sigma). Basal medium for MSC expansion consisted of Dulbecco's modified eagle medium (DMEM, Sigma) supplemented with 100 IU/ml penicillin, 100 µg/ml streptomycin and 2 mM L-glutamate and StemMACS (Miltenyi). Fluorescence activated cell sorting (FACS) buffer contained phosphate buffered saline (PBS) (Sigma), 2% HI-FCS and 1mM endotoxin free Ethylenediaminetetraacetic acid (EDTA) (Invitrogen). Magnetic activated cell sorting (MACS) buffer included PBS supplemented with 0.5% HI-FCS and 1mM EDTA.

2.2.2. General Cell culture

All cultured cells were incubated at 37^{o}C in a humidified incubator with 5% CO_2 (Flow Laboratories IR 1500 incubator). Cell culture was carried out in class II containment cabinets using aseptic technique.

2.2.3. Source of peripheral blood mononuclear cells (PBMCs) and bone marrow derived mononuclear cells (BM-MNC)

Peripheral blood mononuclear cells (PBMC) were isolated from heparinised peripheral blood or leukocyte reduction system (LRS) cones (obtained from the National Blood Transfusion Service, Newcastle upon Tyne) from healthy donors and BM-MNCs were isolated from healthy bone marrow aspirates, surplus to transplantation requirements (obtained from the Newcastle Cellular Therapy Facility).

2.2.4. Cell counting

Cell number and viability was assessed by Trypan blue (Gibco) dead cell exclusion method. Cells were washed in appropriate media/PBS and 20 µl of cell suspension were then mixed with trypan blue at a 1:1 ratio. Counting was executed using an Improved Neubauer cell counting chamber (Weber Scientific International). The number of cells within the central square was counted and cell concentration per ml was determined by multiplying the cell counts by 10^4.

2.2.5. Cell cryopreservation

Isolated cell populations were cryopreserved in a freezing solution containing 90% Hi-FCS (Sigma) and 10% dimethyl sulphoxide (DMSO, Sigma). PBMCs were cryopreserved in 70% RPMI, 20% HI FCS and 10% DMSO. All cells were frozen in cryovials (Nunclon, UK) and stored at -80 ºC for 24h and then transferred to -140 ºC for long term storage.

2.2.6. Cell Thawing

When necessary, cell populations were thawed by swiftly submerging the cryovials in a 37 ºC water bath and washing in pre-warmed culture medium. Cells were then counted as described previously and re-suspended in appropriate volume of cell culture media for use in experiments and/or expansion.

2.3. Cell isolation/depletion

2.3.1. Isolation of PBMC and BM-MNC

Both cell populations were isolated by density centrifugation using Lymphoprep™ (Axis-Shield). Briefly, whole blood or bone marrow aspirated were diluted 1:1 with PBS and layered over the Lymphoprep™ solution. Samples were centrifuged at 800g for 15 minutes at RT. Most of the top phase was discarded and PBMC/BM-MNC layer was collected from the interface using a sterile Pasteur pipette. Cells were then washed 2 times in sterile PBS and re-suspended at an appropriate cell concentration in cell culture media.

2.3.2. Magnetic cell isolation

Cell isolation of $CD3^+$ T cells, $CD14^+$ monocytes and NK cells was carried out using the MACS microbeads technology. This technology is a column-based immune-magnetic separation. Cells are labelled with the MACS microbeads which are then applied to a MACS column. Unlabelled cells pass through the column (negative fraction) while the labelled cells are retained in the column (positive fraction). After washing, the columns are removed from the magnet and the retained cells can be eluted. This technique was used for both positive and negative selection of cell populations. A summary of the type of isolation and respective isolation kit for each cell population can be found in **Table 2.1.**

Table 2.1: Summary of the type of isolation and respective isolation kits for each cell population. PBMCs were isolated from Leukocyte reduction system (LRS) cones by density centrifugation and subjected to magnetic separation.

Cell Type	Type of isolation	Isolation kit	Cat No.	Supplier
$CD3^+$ T cells	Depletion of non $CD3^+$ T cells	Pan T cell Isolation kit, human	130-096-535	Miltenyi
$CD14^+$ cells	Positive selection of $CD14^+$ cells	CD14 microbeads, human	130-050-201	Miltenyi
NK cells	Depletion of non-NK cells	NK cell isolation kit, human	130-092-657	Miltenyi

2.4. *In vitro* cell culture

2.4.1. *In vitro* expansion of BM-MSC

Human mesenchymal stromal cells were generated from healthy BM donors using the plastic adhesion method. For comparison purposes, MSC expansion was performed by splitting the initial MNC fraction into equal parts and seeding in either conventional MSC expansion medium, supplemented with FCS, or xeno-free medium, supplemented with human platelet lysate. This product was purchased from Mill Creek (PLTMax, Mill Creek, Life Sciences) and manufacturing details are as published previously (Crespo-Diaz *et al.*, 2011). For ease of understanding, MSCs expanded in –FCS and -PLT supplemented medium will be referred as MSC-FCS and MSC-PLT, respectively.

Briefly, MNC were plated at a density of $2x10^7$cells/flask in T-25 flasks (Falcon BD) in non-haematopoietic medium (NH medium; Miltenyi Biotec) supplemented with 10% FCS, 100IU/ml penicillin and 100 µg/ml streptomycin or in basal medium supplemented with 5% PLT and 2 IU/ml Heparin-EDTA, at 37 ºC and 5% CO_2 in a humidified atmosphere. On day 3 after seeding, the non-adherent cells were discarded and fresh medium was added to the adherent cells. Thereafter, medium was changed every 3 days. When the cells reached sub-confluence (~80%) they were washed with PBS and detached from the flask with Trypsin-EDTA (Sigma-Aldrich) for 5 minutes in a 37 ºC incubator. Harvested cells were re-plated at a density of $3x10^5$cells/flask in a T-75 flask. This procedure was repeated until passage 3. Further expansion was performed by seeding $1x10^5$cell/flask in T-25 flasks.

2.4.2. Generation of monocyte derived dendritic cells

Monocyte derived DC were generated from magnetically isolated $CD14^+$ monocytes. Isolated $CD14^+$ monocytes (5×10^5 cells/ml) were cultured in RF10 supplemented with GM-CSF and IL-4 (both, 50 ng/ml, Immunotools) for 6 days in 24-well plates and matured with LPS (0.1 µg/ml, Immunotools) for a further 24h.

2.5. Isolation of Extracellular Vesicles from MSC supernatants

2.5.1. Preparation of EV-depleted medium

Standard MSC expansion requires growth supplements for maintenance of proliferation and viability of the cells. In this work, MSC-EVs were purified from xeno-free expanded MSC supernatants. Prior to purification, MSC growth medium was depleted for its content in EVs derived from the platelets. In brief, basal medium was supplemented with 10% PLT and 2 IU/ml Heparin-EDTA. The medium was added to polycarbonate ultracentrifuge tubes (Beckman Coulter) and centrifuged at 100,000xg for at least 16h using a 45Ti Rotor (Beckman Coulter) and L-7 Beckman Ultracentrifuge (Beckman Coulter). Medium was then sterile filtered using a 0.22 µm sterile vacuum filter unit (Millipore) and stored for future use.

2.5.2. Conditioning of MSC with EV-depleted medium

MSC conditioning for EV purification was performed as previously described (Thery *et al.,* 2006, Lai *et al.,* 2010). In summary, conditioning medium was prepared by diluting EV-depleted PLT supplemented medium with serum free medium at a 1:1 ratio. MSCs were expanded up to passage 3 to 70-80% confluency. Medium was removed and the MSC monolayer was thoroughly washed with 1X PBS and conditioned medium was added to the cells. MSCs were then incubated at 37^{o}C and 5% CO_2 humidified atmosphere for 48h, after which MSC-EV purification was performed.

2.5.3. Purification of MSC-EV

MSC-EVs were purified from culture supernatants using differential ultracentrifugation as described by Thery *et al* (2006). A general overview of EV purification workflow is depicted in **Figure 2.1**.

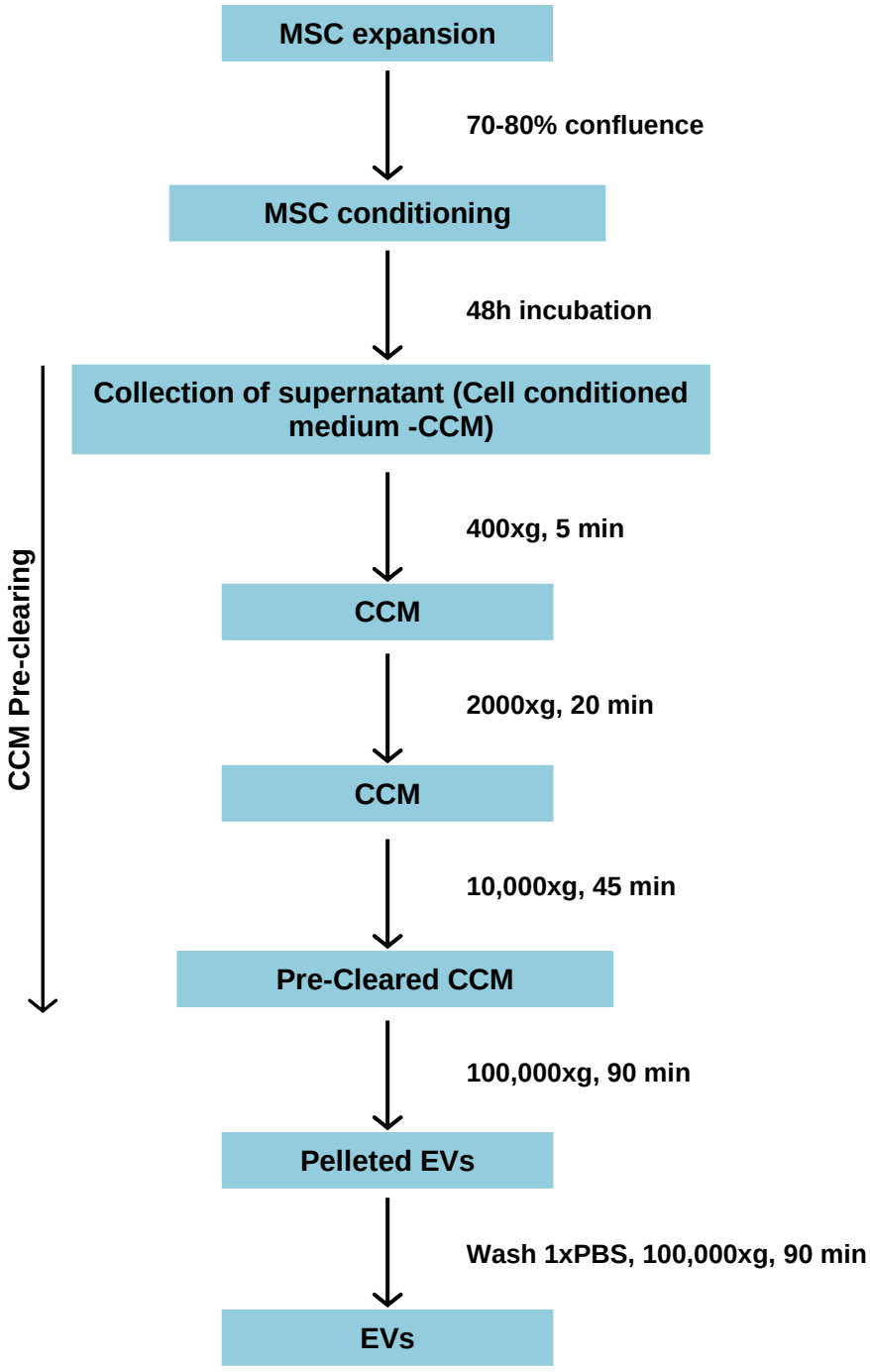

Figure 2.1: Workflow chart for MSC conditioning and EV purification

MSCs were expanded until P3 and conditioned for 48h with EV-depleted medium. After 48h incubation, Culture supernatant (Cell conditioned medium – CCM) was collected and EVs were purified using differential ultracentrifugation. The speed and length of each centrifugation are indicated on the right of each arrow. The pellets derived from the first three centrifugations (cells, dead cells, debris, apoptotic bodies) were discarded and the cleared supernatant was centrifuged at 100,000xg for EV pelleting. After the first 100,000xg centrifugation, the pellet was suspended in PBS and centrifuged again at 100,000xg. The derived pellet was suspended in PBS and used for downstream analysis.

2.6. Flow Cytometry

Flow cytometry is a laser-based technology employed in multi-parametric analysis of cells, including cell size, cell type, complexity and viability. These characteristics are determined using an optical-to-electronic system that records how the cell scatters incident laser light and emits fluorescence. A flow cytometer is usually made up of three main systems: the fluidics system which consists of a central channel that presents the sample and removes the waste; optics and detectors that scatters and detects the light/fluorescence emission; and a computer system that collects and stores the data.

One of the main characteristics of flow cytometry is the capacity to measure the properties of individual particles by means of hydrodynamic focusing, in which, the sample fluid is enclosed by an outer sheath fluid that is under high pressure. The movement of the sheath fluid creates a drag effect which causes the sample fluid to narrow in the central core thus creating a single stream of particles. Lasers then produce a single wavelength of light at one or more discreet frequencies which scatters when in contact with the single file of particles. Side scatter and forward scatter are used to assess granularity and size of cells, respectively. Larger and more granular particles originate higher side and forward scatter than smaller and less complex ones. The use of antibodies labelled with fluorochromes allows for the identification and quantification of specific markers either on the surface of the cell or intracellularly. The use of distinct fluorochromes with specific excitation and emission spectra allows for the analysis of several markers at once. When several fluorochromes are used in multi-parameter analysis compensation is required due to spectral overlap of several fluorochromes resulting in false positive signal. Compensation can be easily achieved by the use of single-stained beads or cells for each fluorochrome used in one multicolour analysis. Unless otherwise stated $3x10^5$ – $1x10^6$ cells were re-suspended in FACS buffer and incubated with appropriate concentrations of antibodies at 4 ºC for 20-30 minutes. Afterwards, cells were washed in FACS buffer and re-suspended in 400 µl of FACS buffer. For viability analysis, 50 µl of DAPI was added prior to flow cytometry analysis. All flow cytometry data was acquired on BD Canto II

flow cytometer (BD Biosciences), and analysed using the FlowJo software, version 7.4 or 10 (TreeStar).

Table 2.2: Used antibodies in flow cytometry. Summary table showing markers, fluorochromes, species, isotype, clone and supplier.

Marker	Fluorochrome	Species	Isotype	Clone	Supplier
CD1a	APC	Mouse	IgG1	HI149	BD Biosciences
CD3	PerCPCy5.5	Mouse	IgG1	SK7	BD Biosciences
CD4	V500	Mouse	IgG1	RPA-T4	BD Biosciences
CD8	APC	Mouse	IgG1	SK1	BD Biosciences
CD8	APC-Cy7	Mouse	IgG1	SK1	BD Biosciences
CD9	PerCPCy5.5	Mouse	IgG1	M-L13	BD Biosciences
CD14	FITC	Mouse	IgG2b	MϕP9	BD Biosciences
CD14	FITC	Mouse	IgG2a	M5E2	BD Biosciences
CD19	FITC	Mouse	IgG1	4G7	BD Biosciences
CD25	PECy7	Mouse	IgG1	2A3	BD Biosciences
CD25	APC	Mouse	IgG1	M-A251	BD Biosciences
CD34	FITC	Mouse	IgG1	581/CD34	BD Biosciences
CD38	PE	Mouse	IgG1	HIT2	BD Biosciences
CD45	FITC	Mouse	IgG1	2D1	BD Biosciences
CD56	APC	mouse	IgG1	AF12-7H3	MiltenyiBiotec
CD56	APC	Mouse	IgG1	B159	BD Biosciences
CD63	PE	Mouse	IgG1	H5C6	BD Biosciences
CD69	PECy7	Mouse	IgG1	FN50	BD Biosciences
CD73	PE	Mouse	IgG1	AD2	BD Biosciences
CD80	PE	Mouse	IgG1	L307.4	BD Biosciences
CD80	FITC	Mouse	IgG1,k	L307.4	BD Biosciences
CD81	APC	Mouse	IgG1	JS-81	BD Biosciences
CD83	FITC	Mouse	IgG1	HB15e	BD Biosciences
CD83	APC	Mouse	IgG1,k	HB15e	BD Biosciences
CD86	PEcy7	Mouse	IgG1	2331	BD Biosciences
CD90	PerCPCy5.5	Mouse	IgG1	5E10	BD Biosciences
CD105	APC	Mouse	IgG1	266	BD Biosciences
CD107a	PE	Mouse	IgG1	H4A3	BD Biosciences
CCR7	PECy7	Mouse	IgG2a	G043H7	Biolegend
CLA	FITC	Rat	IgM	HECA-452	BD Biosciences
HLA-ABC	FITC	Recombinant human	REA control	REA230	Miltenyibiotec
HLA-ABC	FITC	Mouse	IgG1	G46-2.6	BD Biosciences
HLA-E	PE	Mouse	IgG1	3D12	eBiosciences
HLA-DR	APC	Mouse	IgG2a	G46-6	BD Biosciences
HLA-DR	PerCP	Mouse	IgG2a	L243	BD Biosciences
DAPI					BD Biosciences

2.6.1. Phenotypic assessment of MSC

MSCs were harvested as previously described and labelled with CD14-, CD19-, CD34- and CD45- FITC, along with CD73- PE, CD105-APC, CD90-PerCPCy5.5 and HLA-DR-APC. Appropriate isotype controls were used as negative controls.

2.6.2. Phenotypic assessment of $CD3^+$ T cells

All T cells used in this work were obtained as described in **2.3.2**. Evaluation of $CD3^+$ T cell purity was checked prior and after isolation by flow cytometry. For this, PBMCs and enriched $CD3^+$ T cells were treated with an anti-CD3 antibody. Details about the used antibodies are described in **Table 2.2**.

2.6.3. Phenotypic assessment of monocyte derived DCs

Phenotypic assessment of moDCs was performed before and after isolation, prior to and after maturation. Assessment of $CD14^+$ monocyte purity was evaluated by labelling PBMCs and enriched $CD14^+$ monocytes, with CD14-FITC and CD1a-APC. Evaluation of moDC maturation was then assessed by staining the cells, before and after maturation with LPS, with CD80-PE, CD83-FITC, CD86-PeCy7 and HLA-DR-PerCP. Details about the used antibodies can be found in **Table 2.2**.

2.6.4. Assessment of activation markers on T cells

The level of activation of $CD3^+$ T cells was assessed by analysing the expression of the markers CD25 and CD69 by flow cytometry. The expression of the early activation marker CD69 was assessed 24h after initiation of MLR. The late activation marker, CD25 was examined on day 5 after stimulation.

2.6.5. CBA analysis of culture supernatants

Flow cytometry can be equally used to detect soluble proteins present in the serum, plasma or supernatants. The Cytometric Bead Array (CBA) system employs a series of particles with discrete fluorescence intensity, to which a specific alpha-numeric position is assigned, to detect multiple soluble proteins from a single sample of serum, plasma, or culture supernatants. The soluble protein of interest is “captured” by a capture bead. This protein-bead complex is incubated with a PE-conjugated antibody and then detected by flow cytometry.

The concentration of an unknown soluble protein is then calculated by comparison to a standard curve specific for each protein. Following acquisition the sample results are generated in graphical and tabular format using the BD FCAP array software (**Fig.2.2**).

A)

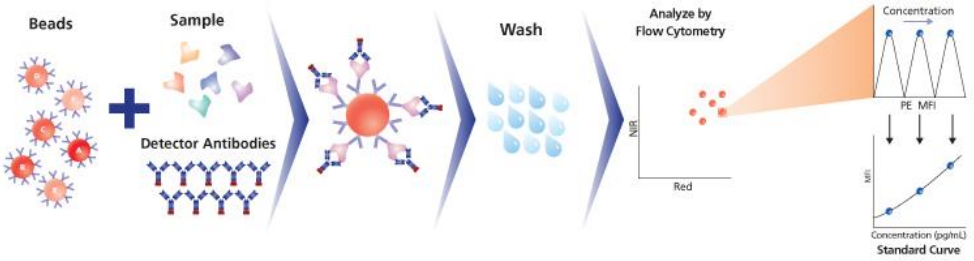

B)

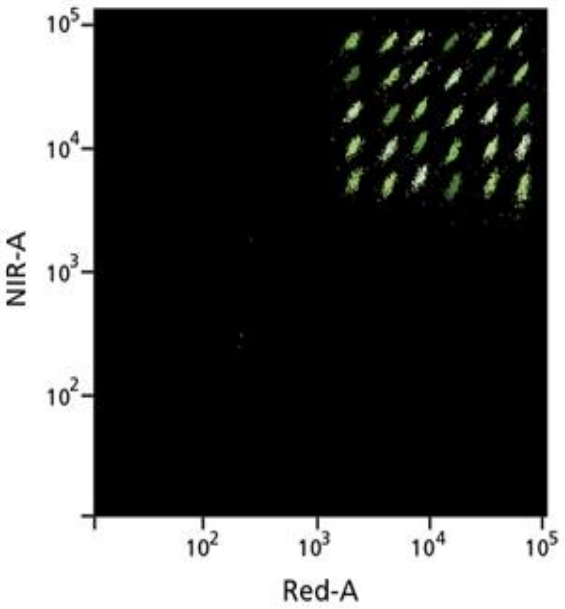

C)

Product Description	Bead Position	Cat. No.
IFNγ flex set human	E7	558269
TNFα flex set human	D9	558273
IL-6 flex set human	A7	558276
IL12p70 flex set human	E5	558283
IL-1β flex set human	B4	558279
IL-10 flex set human	B7	558274
IL-17A flex set human	B5	560383
TGF-β1 flex set human	B6	560429
Human soluble protein master buffer kit		558267

Figure 2.2: Diagram of the process of a CBA assay

A) The protein of interest is captured on a bead. The detector antibodies are then added. These bind to the beads and form a complex which has a distinct fluorescence intensity to which a specific alpha-numeric position is assigned. **B)** Alpha-numeric positions of all the beads as they appear after flow cytometry. Mean fluorescence intensity is calculated and compared to the standard curve to calculate the protein concentration. Image adapted from www.bdbiosciences.com/. **C)** Summary of CBA flex-sets used, including bead positions and catalogue numbers.

2.7. Assessment of MSC and MSC-derived EV immunosuppressive properties

Mixed Lymphocyte Reactions (MLRs) were used to evaluate the immunosuppressive effect of MSC-FCS and MSC-PLT. $CD3^+$ T cells were stimulated with allogeneic monocyte-derived DCs, either in the presence or absence of third party MSCs or MSC-EVs. $CD3^+$ T cells alone were used as negative controls and allo-DC stimulated T cells as positive control. For co-incubation, MSC-FCS and MSC-PLT on passage 3 were irradiated with 20 Gy, using a Gammacell Irradiator, and seeded in RF10 medium at different ratios in wells of a round bottomed 96-well plate, and allowed to attach overnight. On day 2, $CD3^+$ T cells and DCs were added to the MSCs. When MSC-EVs were used, a titrated dose of MSC-EVs was added to MLR directly. A description of the cell concentrations can be found in **Table 2.3**. Suppression of $CD3^+$ T cells activation by MSCs and MSC-EVs was assessed using flow cytometry by measuring the expression of the activation markers, CD69 and CD25, while proliferation was determined using 3H-Thymidine incorporation and carboxyfluorescein diacetate succinimidyl (CFSE) dilution.

Table 2.3: Cell concentrations, used in co-culture assays with MLR. MLR reactions were cultured in RF10

	$CD3^+$	moDC	MSC
CD3	1×10^6 cells/ml	-	-
+moDC	1×10^6 cells/ml	1×10^5 cells/ml	-
+5:1 MSC	1×10^6 cells/ml	1×10^5 cells/ml	2×10^5 cells/ml
+10:1 MSC	1×10^6 cells/ml	1×10^5 cells/ml	1×10^5 cells/ml
+20:1 MSC	1×10^6 cells/ml	1×10^5 cells/ml	5×10^4 cells/ml

2.7.1. 3H-Thymidine incorporation

Radioactive 3H-Thymidine incorporation methodology is used to measure the proliferation of cells. Each time a cell replicates it incorporates radioactive thymidine and this is then analysed as an indicator of proliferation. On day 4

after co-culture at 37 ºC in a 5% humidified CO_2 incubator, the culture wells were pulsed with 10 µl of 3H-Thymidine (0.185 MBq/ml, Perkin Elmer) and incubated for further 16h. The cells were then harvested onto a filter mat with an INOTECH cell harvester (CH-5610 Wohlen). The filter was left to dry at room temperature for 24h and then sealed in a plastic pocket with scintillation fluid (PerkinElmer). $CD3^+$ T cells were then assessed for their proliferation levels by counting radioactivity using a Direct Beta Counter (MATRIX 9600, Packard Instrument). The whole procedure was carried out after the appropriate training and following all local rules and the safe use of radioactive material.

2.7.2. CFSE dilution

CFSE dilution was used to measure the proliferation of allo-stimulated T cells. CFSE is an effective means of monitoring cell divisions. This reagent establishes covalent bonds of long-lived intracellular molecules with the fluorescent dye, carboxyfluorescein. When a CFSE-labelled cell divides, its progeny carries half the number of carboxyfluorescein-tagged cells. Each cell division can then be assessed by measuring the decrease in cell fluorescence using flow cytometry. Briefly, $CD3^+$ T cells were labelled with CFSE (Invitrogen) on day 0. Cell labelling was carried out by incubating with 1 µM CFSE in PBS for 5 minutes in the dark, at room temperature. Cells were then washed 3 times with RF10 and used to set up MLR reactions as previously described. After 5 days, proliferation was assessed using flow cytometry.

2.8. RNA extraction and gene expression

2.8.1. Total RNA Extraction

Total RNA was extracted from cell lysates using the Qiagen RNAeasy mini kit (Qiagen) (**Fig. 2.3**). Initially, the pelleted cells were re-suspended in Lysis buffer consisting of RLT buffer with 0.01% of β-mercaptoethanol. To homogenise the sample, the lysate was passed through a blunt 20-gauge needle at least 5 times. RNA extraction was then performed by adding 1 volume of 70% ethanol to the lysate followed by thorough mixing. The mix (700 µl) was then transferred to an RNeasy filter cartridge placed in a 2 ml collection tube, centrifuged for 15s at 10,000xg and the flow through was discarded. The wash buffer 1 (RW1) was added to the filter, spun down as previously mentioned. The flow through was once again discarded and total RNA was washed twice with wash buffer 2 (RPE buffer) and centrifuged for 1 minute at 10,000xg for complete removal of the buffer. The filter was then transferred to a new RNase free Eppendorf and at least 30 µl of RNase-free water was used to elute the RNA by centrifugation at 10,000xg for 1 minute. The total RNA was analysed for purity and quantity using NanoDrop (NanoDrop®, ND-1000) and stored at -80ºC for future use.

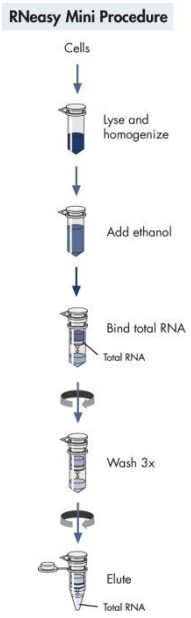

Figure 2.3: Total RNA extraction from cell lysates performed using the RNeasy mini kit. Total RNA extraction from cell lysates involves three main steps; (1) Cell lysis and homogenisation; (2) Total RNA binding to filter cartridge and washing; (3) Total RNA elution. Illustration adapted from Qiagen (www.qiagen.com)

2.8.2. Quantitative Real-time PCR

Quantitative Real-Time PCR was performed using Taqman® gene expression assays. Taqman reactions use a two-step reverse transcription polymerase chain reaction. In the first step the RNA is reverse-transcribed to complementary DNA. Using the Applied Biosystems High capacity cDNA reverse transcriptase kit, cDNA was generated by reverse transcription of 1.5 µg of total RNA using an equal volume of cDNA master mix containing random primers, RT buffer, dNTP mix, RNase inhibitor, MultiScribe^{TM} reverse transcriptase and Nuclease-free H_2O. All steps were performed on ice and cDNA synthesis was performed on a thermal cycler (Applied Biosystems, 2720 Thermo Cycler) using the following settings: 25^{o}C for 10 minutes, 37^{o}C for 120 minutes and 85^{o}C for 5 seconds. Generated cDNA was then stored at -20^{o}C until used for quantitative Real-Time PCR.

In the second step, this cDNA undergoes standard PCR. Taqman® assays use a fluorogenic process to detect the gene of interest as they are produced. The probe sets, containing a fluorescent dye on the 5' end and a quencher dye on the 3'end, anneal downstream from one of the primer sites. The 3' quencher dye reduces the fluorescence from the reporter dye by fluorescence resonance energy transfer (FRET). During each cycle, the 5' to 3' nucleolytic activity of DNA polymerase cleaves the hybridised probe between the reporter and the quencher dye, thus increasing the fluorescence signal. The fluorescence intensity is therefore proportional to the amplification of a product. In this study, Taqman® gene expression assays were used to measure the expression of several genes of interest summarised in **Table 2.4**. Reactions were carried out in triplicate using a 7900HT Fast Real Time PCR system and standard thermal cycling conditions (Applied Biosystems). C_T values, i.e, the number of cycles where the number of amplified targets crosses the threshold, were normalised to the reference gene using the comparative C_T threshold method (ΔC_T), as described in Applied Biosystems Bulletin 2.0.

Table 2.4: Summary of genes and primer/probe sets used for gene expression

Gene of Interest	Primer/probe set
GAPDH	Hs99999905_m1
VCAM1	Hs01003372_m1
ALPL	Hs01029144_m1
CDCP1	Hs01080405_m1
DDP4	Hs00897391_m1

2.9. Statistical analysis

Unless otherwise stated, all statistical analysis was performed using Graphpad Prism™ software. Paired t tests or Mann-Whitney U tests were used with a p-value of less than 0.05 being considered significant.

2.10. Ingenuity pathway analysis

Markers (n=12) and microRNAs (n=79) that showed a ≥ 1.5 fold change and a p-value<0.05 incorporated into the pathway mining analysis using Ingenuity pathway analysis (IPA). The IPA software represents a computational platform that can be used for pathway mining (www.ingenuity.com; Ingenuity Pathway Analysis – IPA). A core analysis and a microRNA target filter analysis were performed for the selected markers and microRNAs, respectively. Canonical pathway analysis identified the pathways from the IPA library of pathways that were most significant to the data set. The markers from the data set that met the fold-change cut-off of 2 in association with a canonical pathway in ingenuity knowledge base were considered for analysis. The significance of the association between the data set and the canonical pathways was analysed in 2 ways: 1) a ratio of the number of molecules from the data set that map to the pathway divided by the total number of molecules that map to the canonical pathway, and 2) Fisher exact test that was used to calculate a p-value

determining the association probability between the genes in the data set and the canonical pathway.

Network analysis was used to exhibit relationships between the selected molecules. The software generates a network by limiting the number of molecules in the network to 35 and displaying only the most important ones based on the number of connections for each selected molecule. Each identifier was mapped to its corresponding object in Ingenuity's Knowledge Base and the networks of these molecules were algorithmically generated based on their connectivity. Molecules or microRNAs are represented as nodes, and the biological relationship between two nodes if represented as an edge (line). All edges are supported by at least one reference from the literature or from canonical information stored in the ingenuity pathways knowledge base. The intensity of the node colour indicated the degree or up- (red) or down-regulation (green). Nodes are displayed using various shapes that represent the functional class of a gene product and edges with numerous labels describe the nature of the relationship between two nodes. A comprehensive list of the molecular functions and relationships used in the generation of the canonical pathways and networks are described in **Fig.2.4**.

For microRNA analysis, the IPA software scans a wide variety of databases, including targetscan (targets are predicted using the Targetscan algorithm by searching for the presence of conserved 8mer and 7mer sites that match the seed region of each microRNA), Tarbase (database containing experimentally demonstrated microRNA/mRNA interactions), miRecords (database containing experimentally validates human, rat and mouse microRNA-mRNA interactions) and the Ingenuity® knowledge database (microRNA related findings manually generated from published literature by ingenuity scientific experts). To limit the number of targets presented for the microRNAs, only the experimentally verified and highly predicted targets were analysed.

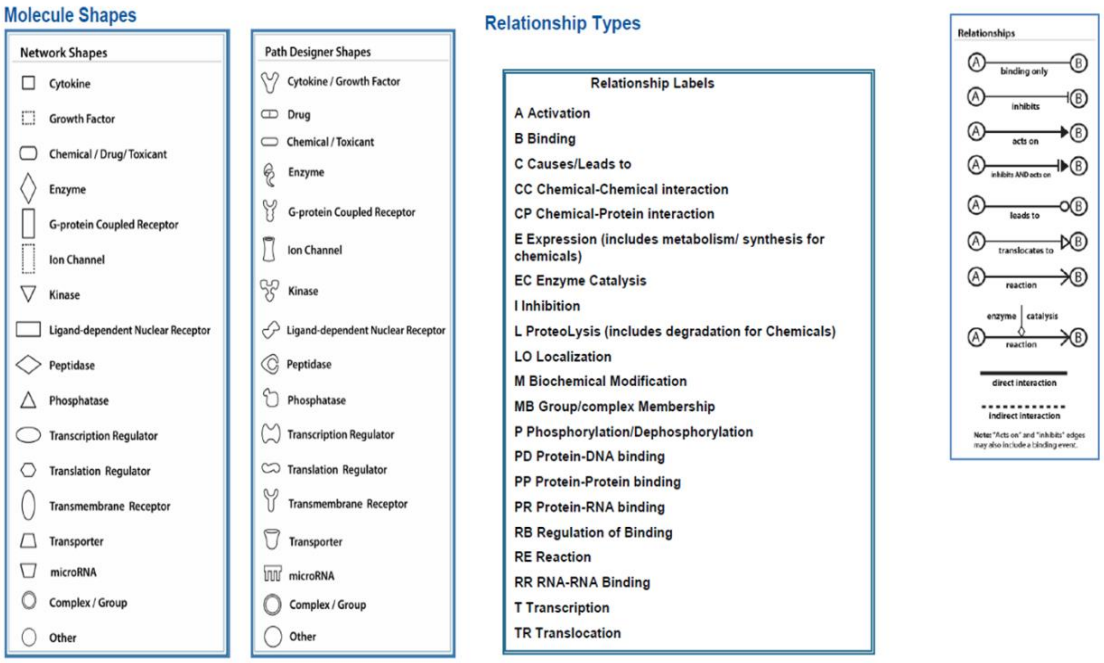

Figure 2.4: The legend shows the main symbols and lines used to generate networks and canonical pathways using IPA (adapted from www.ingenuity.com/)

Chapter 3: Generation and characterisation of human PLT-expanded MSCs

"To raise new questions, new possibilities, to regard old problems from a new angle, requires creative imagination and marks real advance in science"

– Albert Einstein

Chapter 3 – Generation and characterisation of human PLT-expanded MSCs

3.1. Introduction

Mesenchymal stromal cells (MSC) are multipotent progenitor cells. They attract great interest for clinical applications due to their capacity to modulate immune responses and promote tissue regeneration (Uccelli *et al*., 2008). Their application in clinical trials has shown beneficial effects in a wide variety of therapeutic applications, including GvHD (Le Blanc *et al.,* 2008; Ringden *et al.,* 2006). MSCs have been shown to inhibit proliferation and differentiation of several immune cells, such as T cells, Dendritic Cells and NK cells, and to promote the differentiation of $CD4^+$ T cell subsets expressing a regulatory T cell phenotype (Uccelli *et al.,* 2008). These cells can be isolated from several tissues; however, bone marrow remains the most common source. In the bone marrow, MSCs represent 0.01-0.001% of the total population of nucleated cells (Wexler *et al.*, 2003), therefore, clinical application is only possible after *in vitro* expansion. Conventional expansion of MSCs relies on the use of FCS supplemented medium; however, FCS raises ethical, scientific and safety concerns when used for clinical applications (Bieback *et al.,* 2013; Brunner *et al.,* 2010). To date, large-scale expansion of MSCs for therapeutic use is still based on the use of FCS-supplemented medium, however, current GMP guidelines recommend the replacement of this supplement with xenogeneic-free alternatives (EMEA CPMP/BWP/1793/02, 2003).

In the past decade, several groups have invested their efforts into finding efficient replacements for xeno-free expansion of MSCs. Human PL, herein denominated PLT, has attracted most attention as an effective substitute to FCS for MSC expansion. PLT is obtained by mechanical disruption of activated platelets and is enriched in growth factors, such as, TGF-β, PDGF, bFGF, IGF-1 and VEGF, which promote cellular expansion (Dugrillon *et al.*, 2002; Maynard *et al.*, 2007). PLT expanded MSCs are endowed with increased proliferative capacity while maintaining their characteristic phenotype, morphology and tri-lineage differentiation potential (Crespo-Diaz *et al.,* 2011; Doucet *et al.,* 2005). This factor is favourable for MSC therapy since, in the clinical setting, at least $1x10^6$ MSC/Kg are required (Wang *et al.,* 2012); therefore, increased cell

numbers in shorter periods of time represent an attractive advantage to expansion of MSCs using PLT. Despite these advantages, results regarding their immunomodulatory potential have been contradictory (Doucet *et al.,* 2005; Abdelzarik *et al.,* 2011; Flemming *et al.,* 2011). It is therefore necessary to further elucidate on the effect of MSC expansion using PLT supplemented medium in their general characteristics and in their trophic and immunosuppressive properties. In view of these issues, this chapter aimed at investigating the feasibility of replacing FCS with PLT-supplemented medium and testing the effect of this culture condition in MSC characteristics and function. The specific aims of this chapter were:

- To generate xeno-free MSC from BM derived MNCs by expanding these cells in PLT supplemented medium
- To compare the growth kinetics of PLT expanded MSCs with conventionally FCS expanded MSC
- To characterise PLT generated MSCs in comparison with FCS expanded MSCs as described by the ISCT guidelines
- To compare the immunosuppressive capacity of –PLT and –FCS expanded MSCs to modulate innate and adaptive immune cells using *in vitro* assays
- To examine the susceptibility of PLT-expanded MSCs to NK cell mediated lysis *in vitro*.

3.2. Specific methods

The majority of methods are presented in **Chapter 2**; additional methods used only in this chapter are described below. For ease of understanding, MSCs expanded in PLT and in FCS supplemented medium will be termed MSC-PLT and MSC-FCS from this point onwards.

3.2.1. Assessment of proliferative potential of paired MSCs

Proliferative potential of MSC-PLT was assessed by comparing their growth rate with the conventionally FCS expanded MSCs. Growth was assessed after passage 1 by measuring the population doubling, i.e., the number of times the cells have doubled in number since their primary isolation, and doubling time, i.e., the period of time required for the population to double in number. Cumulative Population doubling (CPD) and doubling time (DT) were calculated using the following *formulae* (Crespo-Diaz *et al.,* 2011):

$$CPD = \frac{Log(H) - Log(S)}{Log(2)} \qquad DT = \frac{\Delta T\ Log(2)}{Log(H) - Log(S)}$$

Where, H = cell number harvested, S = cell number seeded and ΔT= time until confluence at a given passage. Assessment of cell viability was assessed by trypan blue exclusion method as described in **section 2.2.4**.

3.2.2. Trilineage differentiation of paired MSC

3.2.2.1. Adipogenic differentiation

MSCs were seeded in a well of a sterile 6-well plate at a density of $1x10^5$ cells/ml in basal medium. When cells reached confluence, medium was substituted with adipogenic medium (Miltenyi) and cells were maintained in culture for 21 days with medium replacement every 3 days. On day 21, cells were fixed with 10% formalin for 30-60 minutes, incubated with 60% isopropanol for 5 minutes, stained with 0.3% Oil-Red-O for 5 minutes and histochemically assessed for lipid droplet deposition.

3.2.2.2. Osteogenic differentiation

Cells were seeded into a well of a 6 well plate at a density of $3x10^4$ cells/well in Osteo differentiation medium (Miltenyi). After 24h, medium was completely replaced with fresh differentiation medium and cells were maintained in culture for 21 days with medium replacement twice weekly. On day 21, cells were evaluated by alkaline phosphatase (ALP) detection and by the Von Kossa method for mineralisation assessment. Briefly, cells were fixed with 10% formalin for 10 minutes at 37ºC and 5% CO_2, washed 2x with 0.2M Tris-HCL buffer and stained overnight in a 37ºC incubator with ALP substrate. On day 2, cells were washed 3X with dH_2O and covered with 3% silver nitrate solution for at least 1 hour under a lamp. Cells were washed 3X with dH_2O and imaged under an inverted microscope.

3.2.2.3. Chondrogenic differentiation

Chondrogenesis was accomplished by re-suspending $2.5x10^5$ MSCs in basal medium in 15 ml polypropylene conical tube and centrifuging for 5 minutes at 150g, RT. The medium was completely removed and cells were re-suspended with pre-warmed Chondro differentiation medium (Miltenyi). Cells were centrifuged and incubated at 37 ºC and 5% CO_2 as a pellet for 24 days with medium replacement every 2 to 3 days. On day 24, the cell pellet was washed twice with PBS and fixed in 10% formalin for at least 3h at room temperature. After fixation, pellet was washed with dH_2O and paraffin-wax embedding and sectioning into 5µm thin slices was performed by Newcastle University Biobank service. The slides were then deparafinised by soaking in Xylene for 10 minutes, followed by soaking in decreasing concentrations of ethanol (100%, 95% and 70%) for 5 minutes each. Slides were washed in 0.1N HCl for 1 hour and incubated with 0.1 % Alcian Blue solution overnight. The slides were then washed with 0.1N HCl and microscopically assessed for proteoglycan.

3.2.3. Immunophenotyping of paired MSCs by flow cytometry

The immunophenotype of MSCs was assessed by Flow Cytometry as described on **section 2.6**.

3.2.4. Assessment of immunosuppressive potential of xeno-free MSCs

The majority of the methods for assessment of the suppressive potential of paired MSCs on allo-stimulated T cell proliferation are thoroughly described in **Chapter 2**. Specific methods for examining the immunosuppressive potential of MSC-PLT and MSC-FCS on NK cells and their resistance to NK cell mediated lysis will be herein described.

3.2.4.1. Maintenance of K562 target cell

K562 cells, a human myeloid cell line, commonly used to examine non-allo-specific cytotoxicity mediated by NK cells, were used as target cells. The K562 cell line was maintained in RF10 media at $2x10^5$ /ml; cells were regularly split to maintain log phase of expansion of 48 to 96h, for use in assays.

3.2.4.2. Generation of effector NK cells

NK effector cells were generated by negative enrichment as described in **Chapter 2**. Freshly purified $CD56^+/CD3^-$ cells, (>90% purity) as detected by flow cytometry, were cultured overnight at $1x10^6$ /ml in RF10 with 100U/ml of IL-2 (Immunotools). Effector NK cells were directly used in functional assays. To evaluate the suppressive effect of paired MSCs on NK cell mediated cytotoxicity, NK cells were cultured in the presence or absence of paired MSC samples at a 4:1 ratio. Assessment of NK cell mediated lysis of MSCs was performed by co-culturing paired MSC samples with NK cells at effector/target cell ratio of 10:1 for 3h at 37^0C. A schematic representation of these assays can be found in **Fig. 3.1**.

3.2.4.3. Assessment of NK cell degranulation and target cell death

To assess the functional abilities of MSC-treated NK cells, they were added to 96 well U-bottomed plates with a range of K562 cells in RF10. If required, CD107a, a marker for degranulation, was added at this point. Plates were then spun down to ensure cell-cell contact and incubated for 3h to assess degranulation and target cell death. To assess the susceptibility of paired MSCs to NK cell mediated lysis, the first were used as targets. K562 mediated lysis was used as positive control to demonstrate NK cell functionality. Both degranulation and target cell death were assessed by flow cytometry. Gating

strategies for are shown in **section 3.3.5**. Additionally, paired MSCs were assessed for their expression in HLA-ABC which is a known NK cell ligand that confers resistance to NK cell mediated cytotoxicity.

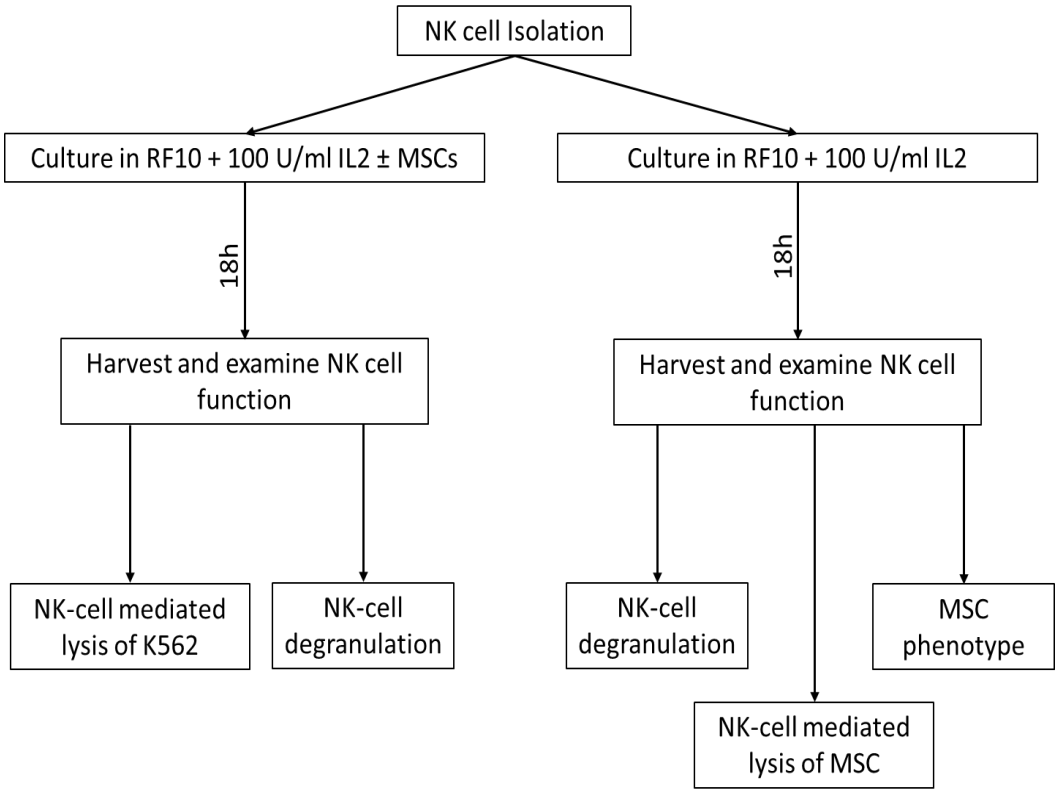

Figure 3.1: Experimental design to test the effect of paired MSC on NK cell cytotoxic capacity (left arm) and to test the susceptibility of paired MSCs to resist NK cell mediated lysis (right arm).

3.3. Results

3.3.1. Comparison of the proliferative kinetics of MSC-PLT and MSC-FCS

To evaluate the effects of PLT expansion on MSC characteristics and cell growth, BM-MNCs were plated in parallel in PLT and FCS (control) expansion medium. The human PLT utilised in this work contains a plethora of growth factors, such as, TGF-β, IGF-1, EGF, PDGF, VEGF, and FGF, at relatively conserved concentrations (**Fig. 3.2**). Paired cultures were maintained until passage 7, when they were terminated. Characterisation of paired samples was performed along passages and functional assessment was assessed at passage 3 cells, which is the commonly used passage for clinical application of MSCs (von Bahr *et al.,* 2012).

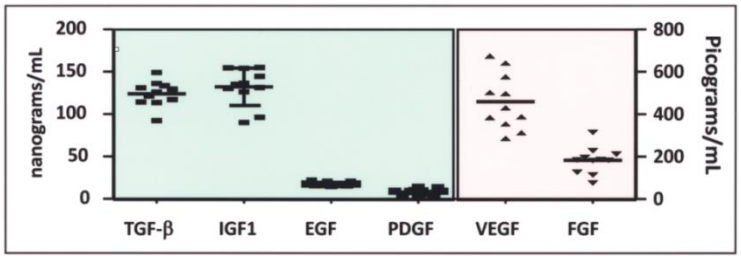

Figure 3.2: PLTmax composition.

ELISA analysis performed by Crespo-Diaz *et al* 2011 revealed conserved expression of PLT growth factors TGF-β (125 ± 15 ng/ml), IGF-1 (130 ± 25 ng/ml), EGF (20 ± 3ng/ml), PDGF (10 ± 3 ng/ml), VEGF (450 ± 130 pg/ml) and FGF (195 ±100 pg/ml). (Crespo-Diaz *et al.*, 2011b)

Both media formulations supported MSC expansion, however, MSCs expanded in PLT medium exhibited higher proliferative capacity. Overall, MSC-PLT showed higher cumulative population doublings (CPD) than MSC-FCS (p=0.005) (**Fig.3.3A**). At passage 3, MSC-PLT showed a CPD of 11.03 ± 0.52 in comparison with 8.71 ± 0.42 CPD of MSC-FCS (p=0.002). The time taken to reach passage 7 was not significantly different between MSC-PLT and MSC-FCS (**Fig.3.3B**). After passage 4, MSC-PLT showed lower doubling times (DTs), however these differences were not statistically significant. Additionally, no differences were detected in cell viability of the paired samples along passages, with cells exhibiting a viability of >80%, regardless of the expansion medium (**Fig3.2C**).

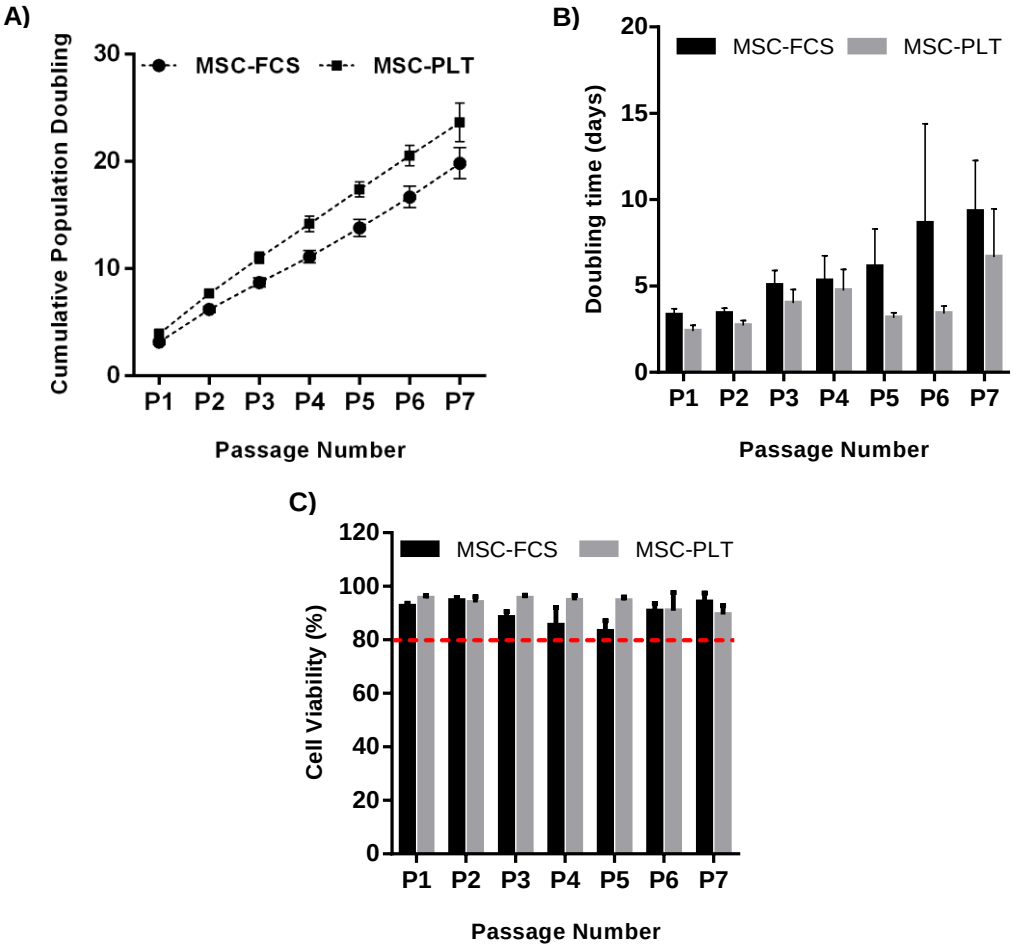

Figure 3.3: MSC-PLT exhibit higher proliferative capacity than their –FCS counterparts.

A) Cumulative population doubling of MSC-FCS and MSC-PLT; **B)** doubling time of both cell populations along passages; **C)** Viability of MSC-FCS and MSC-PLT are maintained above 80% (red dashed line) regardless of the passage. Results express mean ± SEM of 13 different donors.

3.3.2. Characterisation of MSC-PLT as defined by the ISCT criteria

To ensure the identity of the generated MSCs, paired samples were characterised as described by the ISCT guidelines. The surface phenotype of the cells was examined by flow cytometry using the methods described in **Chapter 2**. As shown in **Fig. 3.4**, at passage 3, the phenotypic profile of paired samples was comparable and in agreement with the current guidelines, i.e., ≥95% positive for the expression of the surface markers CD73, CD105 and CD90, and ≤2% negative for the expression of lineage specific markers, CD14, CD19, CD34 and CD45 and HLA-DR.

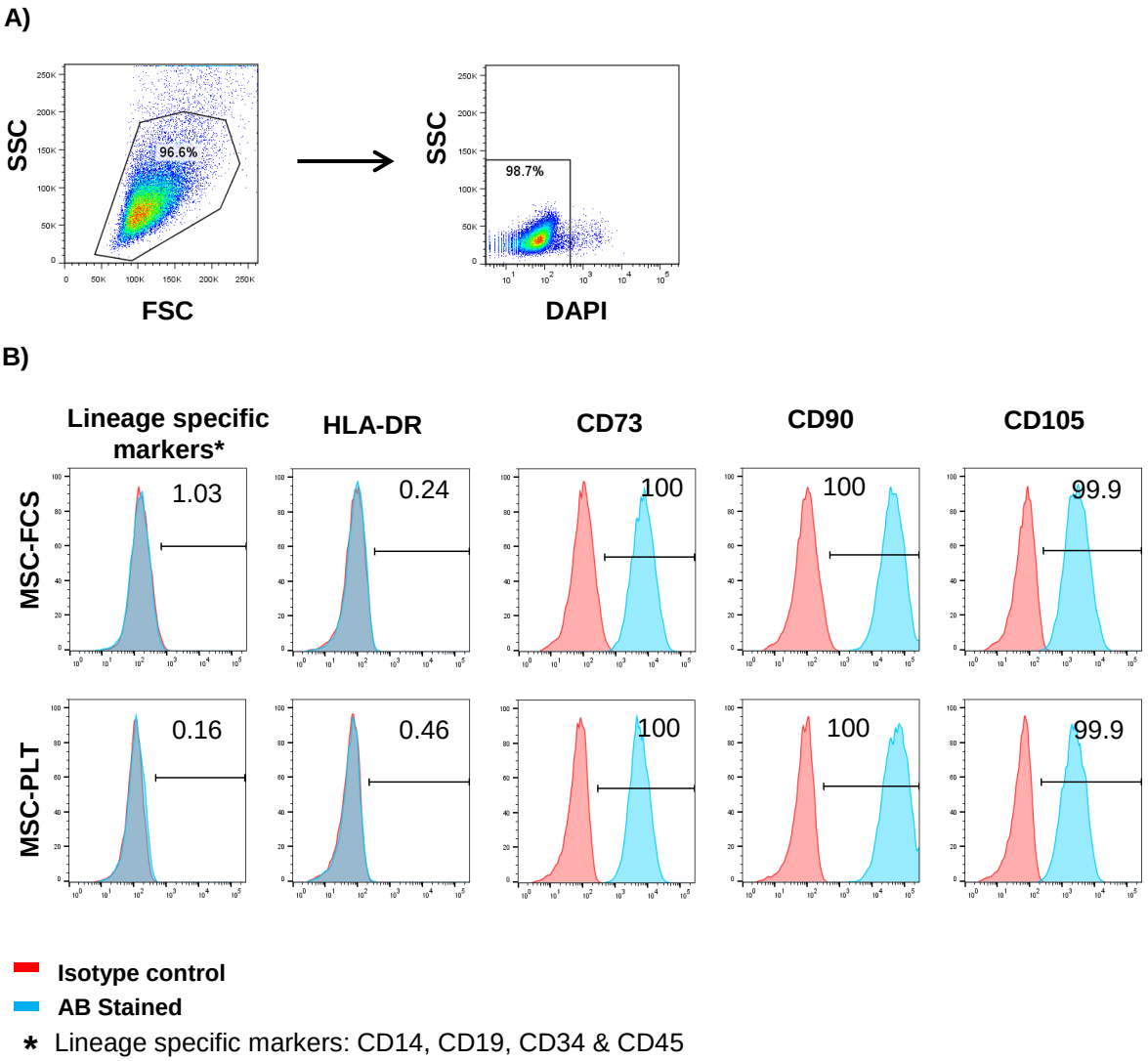

Figure 3.4: Flow Cytometric characterization of MSC phenotype. MSCs maintained in –FCS and –PLT exhibited typical MSC surfer marker expression.

A) Gating strategy for MSC to SSC/FCS and DAPI negativity and **B)** Representative histograms of MSCs expanded in FCS and PLT media as determined by the expression of negative (HLA-DR and lineage specific markers CD14, CD19, CD34 and CD45), and positive markers (CD73, CD90 and CD105) of passage 3 MSC-FCS and MSC-PLT. Red histograms represent the isotype controls and the blue histograms the specific cell marker.

To study the effects of cell passage on MSC-PLT, the phenotype of paired samples was analysed on passages 1, 3 and 6. As evidenced by **Fig. 3.5**, the phenotype of MSC-FCS and MSC-PLT was similar and no changes were detected in the expression of the positive and negative markers on MSCs across the different passages.

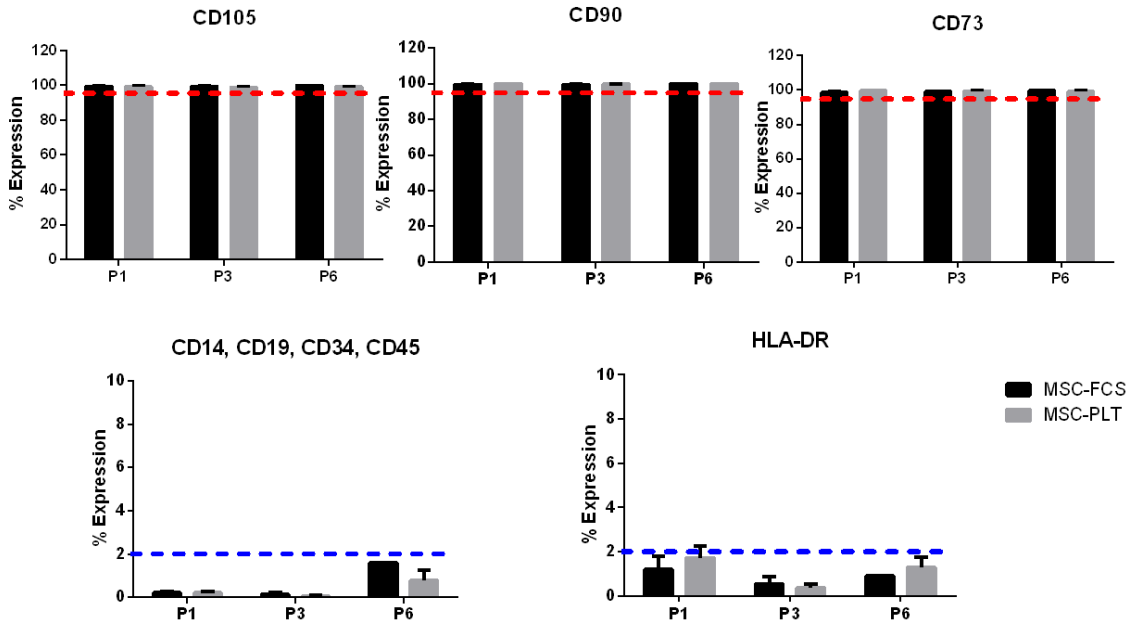

Figure 3.5: MSCs expanded in –FCS and –PLT retain the characteristic phenotype along passages.

Graphs showing the expression of positive and negative markers on MSC-FCS (black) and MSC-PLT (grey) on passages 1, 3 and 6. Red and Blue dashed lines represent the threshold percentage for positive and negative markers, respectively, as defined by the ISCT criteria. Results show mean ± SEM of >6 independent experiments and p-value>0.05

To further confirm the identity of MSCs, morphology and tri-lineage differentiation potential was monitored at passage 3. As shown by **Fig. 3.6A and B,** MSC in different media exhibited fibroblast-like morphology. However, cells cultured in PLT appeared slightly smaller and more elongated than the cells expanded in FCS medium. After passage 4, FCS cells gradually lost their spindle shaped morphology and exhibited a more flattened morphology whereas PLT cells maintained spindle-shaped morphology throughout passages (**Supplementary Figure S3.1**).

Differentiation of paired MSCs was induced by culturing the cells in specific differentiation media. Tri-lineage differentiation of MSCs into adipocytes, osteocytes and chondrocytes was observed in both cases as determined by oil-red-O (**Fig 3.6 C and D**), alkaline phosphatase activity and Von Kossa (**Fig 3.6 E and F**) and proteoglycan staining (**Fig 3.6 G and H**), respectively.

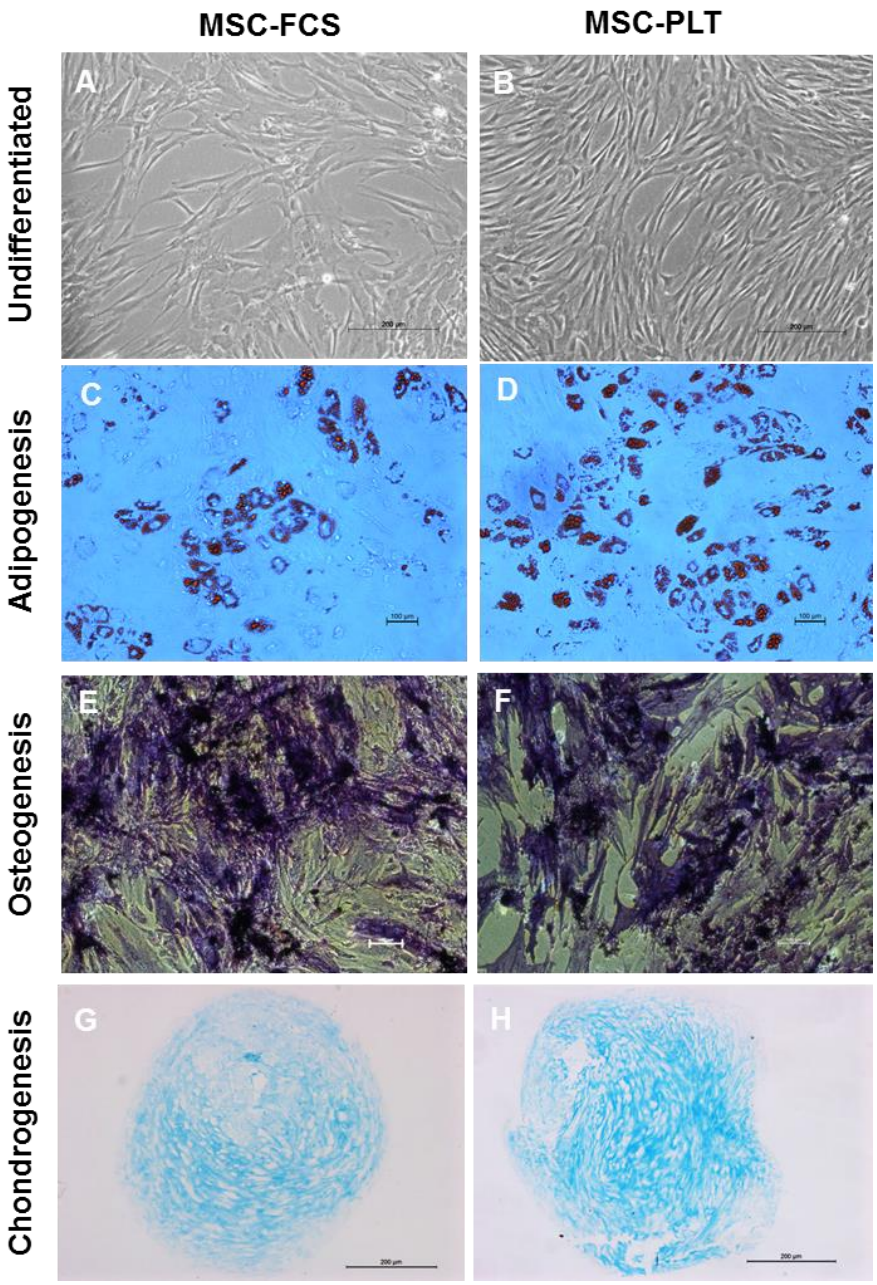

Figure 3.6: MSC-FCS and MSC-PLT have comparable morphology and tri-lineage differentiation potential.

Representative photographs of paired MSC morphology and tri-lineage differentiation at passage 3 as acquired by inverted microscopy. (**A-B**) paired MSCs display fibroblast-like morphology; (**C-D**) Differentiation into adipocytes is revealed by lipid droplet detection by Oil-Red-O. (**E-F**) Osteogenesis is demonstrated by detection of alkaline phosphatase detection (purple) and calcium deposition (dark brown). (**G-H**) Chondrogenic differentiation is confirmed by proteoglycan detection. Magnification = 20x and scale bars represent 200 or 100 µm.

3.3.3. MSC-PLT and MSC-FCS equally suppress T cell proliferation

To examine the immunosuppressive property of MSCs expanded in PLT, they were added to a Mixed Lymphocyte Reaction (MLR), consisting of allo-DC stimulated $CD3^+$ T cells, in parallel with MSCs expanded in FCS. Their effect on T cell proliferation and activation was assessed after 5 days of the co-culture. T cell proliferation was measured using 3H-TdR incorporation as described in **Chapter 2**. T cells cultured alone were used as background control. T cells stimulated with allo-DCs in the absence of MSCs served as positive control.

Both MSC-PLT and MSC-FCS were strong suppressors of alloreactive T cell proliferation and their suppressive potency was dose dependent. All doses showed significant suppression with highest dose exhibiting the strongest suppression (%inhibition of T cell proliferation = 81.7 and 74.3% for MSC-FCS and MSC-PLT, respectively). In addition, no significant difference was observed between MSC-FCS and MSC-PLT in their ability to inhibit T cell proliferation (p=0.090, 0.307 and 0.309 for 1:5, 1:10 and 1:20 ratio respectively (**Fig. 3.7**).

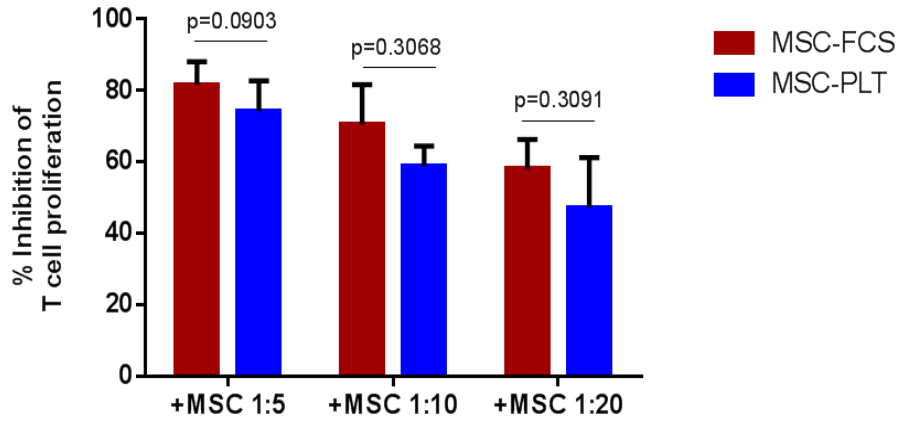

Figure 3.7: MSC-FCS and MSC-PLT have similar capacity to inhibit T cell proliferation

Paired MSCs were added to MLR at different MSC:TC ratios and assessed for their suppressive potential. The inhibition rate was illustrated as percent of non-proliferating cells compared to the MLR in the absence of MSCs. Results are expressed as mean ± SEM of n=3.

3.3.4. MSC-PLT and MSC-FCS inhibited T cell activation

Activation of $CD3^+$ T cells following allo-DC stimulation results in increased expression of CD69 and CD25. To evaluate the effect of MSC-PLT on T cell activation, paired MSCs were co-cultured with allo-DC simulated T cells and CD69 and CD25 expression was evaluated by flow cytometry. The early activation marker CD69, increased in expression after 24h after allo-DC stimulation from 13.3% ± 4.6 and 8.9% ± 6.9 to 35.4% ± 6.2 and 30.5% ± 5.7 in the CD8 and CD4 populations, respectively. After co-culture with MSC-FCS and MSC-PLT there was a significant increase of CD69 expression in both CD8 and CD4 populations. No differences were detected between MSC-FCS and MSC-PLT in their ability to enhance CD69 expression (P>0.05) (**Fig. 3.8**)

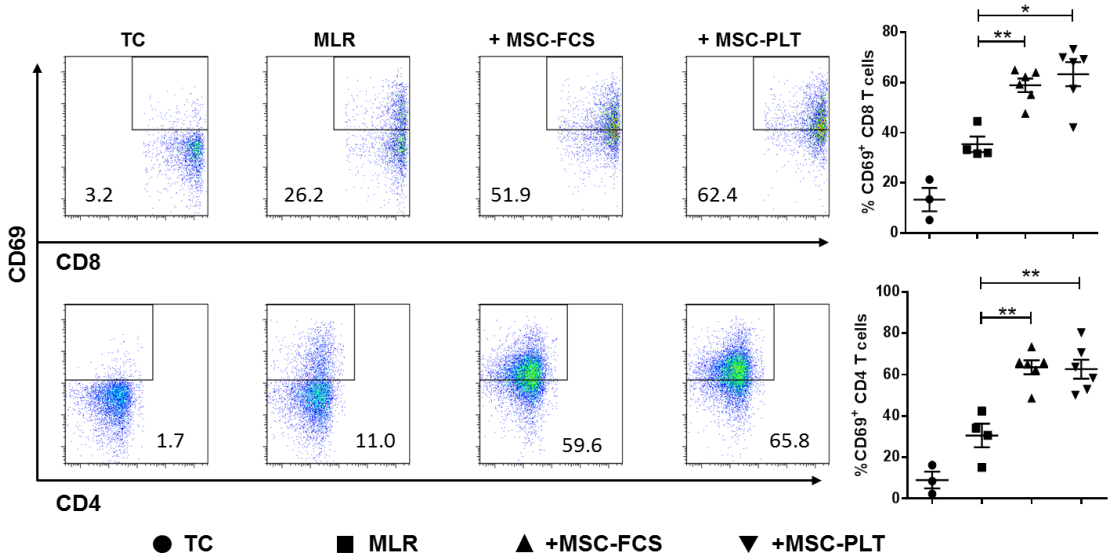

Figure 3.8: MSC-FCS and MSC-PLT equally induce CD69 expression on allo-stimulated T cells

Paired MSC were added to a MLR consisting of allo-DC and $CD3^+$ T cells at MSC:TC ratio of 1:5. CD69 expression was assessed by flow cytometry after 24 of co-culture by flow cytometry. Cells were gated based on SSC/FSC and then based on $CD8^+$ T cells prior to representative plots shown. $CD8^-$ cells were considered CD4. MLR and T cells alone used as positive and negative controls, respectively .Results express mean ± SEM of 4 independent experiments; ** P<0.01 and *P<0.05.

After 5 days, significant up-regulation of CD25 expression was observed in $CD4^+$ and $CD8^+$ T cells. In the presence of MSCs, there was a decrease of CD25 expression in both CD4 and CD8 populations. These differences were more evident in the $CD8^+$ population, with the a reduction of CD25 from 46.0% ± 4.6 in the allo-stimulated T cells to 12.43% ± 2.7 and 14.71% ± 4.7 in the

presence of MSC-FCS and MSC-PLT, respectively ($p<0.01$). For the CD4 population, both MSC-PLT and MSC-FCS showed an inhibition of CD25 expression, although it did not reach statistical significance ($p>0.05$). No differences were detected between MSC-FCS and MSC-PLT in their ability to inhibit CD25 expression on T cells (**Fig. 3.9**).

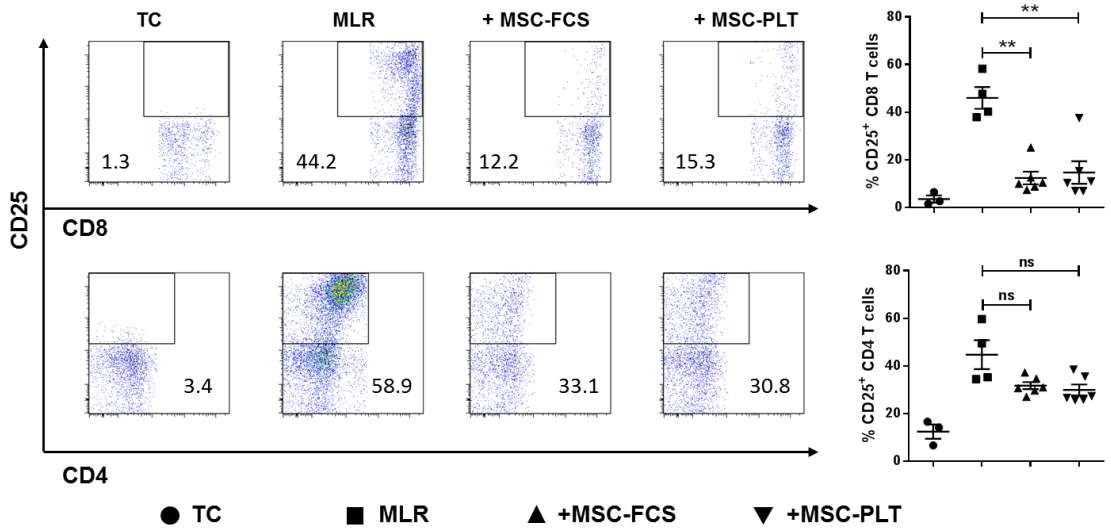

Figure 3.9: MSC-FCS and MSC-PLT have similar ability to reduce CD25 expression on allo-stimulated T cells

$CD3^+$ T cells were stimulated with allogeneic DCs. Paired MSCs at a MSC:TC 1:5 ratio were added to the co-culture wells and CD25 expression was assessed after 5 days by flow cytometry. Cells were gated according to SSC/FSC and then based on $CD8^+$ T cells prior to representative plots shown. $CD8^-$ cells were considered CD4. CD25 expression was then compared to the expression of allo-DC stimulated T cells. Results express mean ± SEM of 4 independent experiments; ** $P<0.01$

Additionally, the effect of the MSC-FCS and MSC-PLT on cutaneous lymphocyte antigen (CLA) expression was assessed. CLA is a skin homing receptor, expressed by activated T cells, which binds selectively to the vascular lectin endothelial-leukocyte adhesion molecule 1 (ELAM 1) thus allowing migration of T cells to cutaneous sites of inflammation (Fuhlbrigge *et al.,* 1997). CLA expression by CD8 and CD4 T cells increased upon stimulation with allo-DCs from 1.2% ± 0.9 and 2.5% ± 0.6 to 16.8% ± 4.9 and 9.3% ± 1.7, respectively (**Fig. 3.10**). In the presence of MSCs, regardless of the MSC culture condition, there was a significant decrease in CLA expression in both

CD8 and CD4 T cell populations ($p<0.05$), with levels being similar to those detected with the background control.

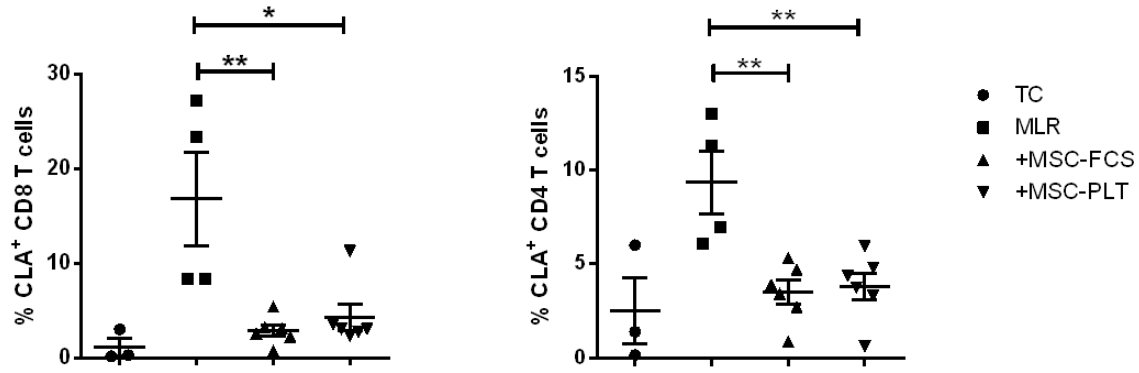

Figure 3.10: CLA expression is decreased in the presence of paired MSCs

CLA expression was assessed on allo-DC stimulated T cells cultured in the presence or absence of paired MSC (MSC:TC ratio of 1:5) for 5 days. Allo-DC stimulated T cells and T cells alone were used as positive and negative controls respectively. Results express mean ± SEM of n=4; ** $P<0.01$ and * $P<0.05$.

3.3.5. Effect of paired MSCs on cytokine production by activated T cells

In addition to analysing the effect of paired MSCs on T cell proliferation and activation, the effect of the first on the pro-inflammatory cytokines was assessed by CBA after 5 days of co-culture. Allogeneic stimulation of T cells with DCs is accompanied by an increase in the secretion of pro-inflammatory cytokines, such as IFN-γ and TNF-α (Chen *et al.,* 2013).

Secreted levels of IFN-γ and TNF-α were significantly higher after co-culture with allogeneic DCs in comparison with the background control (p=0.05 for both). In the presence of MSCs, the secreted concentration of IFN-γ was lower; however these results did not reach statistical significance. Soluble levels of TNF-α were significantly decreased in supernatants from allo-DC stimulated T cells in the presence of MSCs (p<0.05). No significant differences were detected in the ability of MSC-PLT and MSC-FCS to inhibit secretion of IFN-γ and TNF-α (p=0.676 and 0.236, respectively).

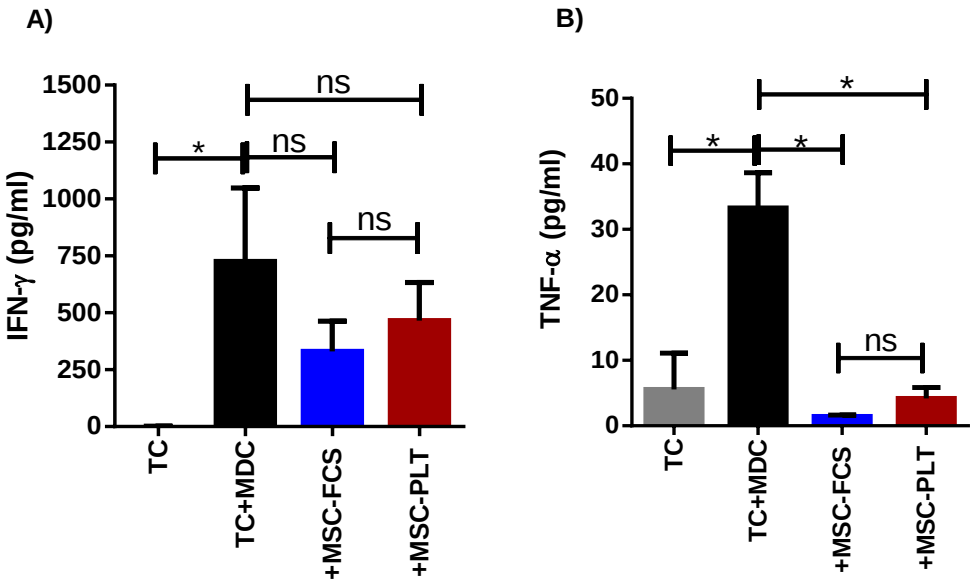

Figure 3.11: CBA analysis of secreted cytokines after MLR co-culture with paired MSCs

Cell culture supernatants were collected after 5 days of co-culture of allo-DC (MDC) stimulated $CD3^+$ T cells and paired MSCs. Supernatants were analysed by CBA flex. Data was acquired by flow cytometry and analysed with FCAP array. Error bars indicate SEM, n=3 and *p<0.05

3.3.6. MSC-PLT and MSC-FCS have similar capacity to modulate NK cell functions

Since MSCs have been previously shown to inhibit NK-cell cytotoxicity (Spaggiari *et al*., 2006; Spaggiari *et al*., 2008), the functional properties of MSC-PLT on NK cell functionality in comparison with MSC-FCS were tested. For this, NK cells were co-incubated overnight with paired MSC samples at a ratio of 4:1, which was identified as the most appropriate NK:MSC ratio in a pilot study. NK cell function was assessed by flow cytometry as previously described (Kim *et al.*, 2007). To assess NK cell mediated lysis, the K562 cell line was used as target cell. K562 cell line is a human chronic leukemia cell line, positive for the Philadelphia Chromosome, which is devoid of HLA-ABC expression, making them susceptible to NK cell mediated lysis, due to their "missing self" status (Lozzio and Lozzio, 1975). The gating strategy used to assess NK cell cytotoxicity after treatment with the paired MSC samples was shown in **Fig.3.12**. NK cells, identified as $CD3^{-}CD56^{+}$ cells, were measured for degranulation by assessment of CD107a expression after co-incubation with target cells (**Fig. 3.12A**). CD107a (lysosome-associated membrane protein-1–LAMP-1), is a well-recognised functional marker for NK cytotoxicity, which is transported into the cell membrane as degranulation occurs (Aktas *et al.,* 2009; Alter *et al.,* 2004). Assessment of K562 cell death was carried out by gating HLA-ABC negative target cells and posterior identification of dead cells by DAPI or PI (**Fig. 3.12B**). To standardise the data, cell death was represented as fold increase in death above the background death of K562 only cell culture.

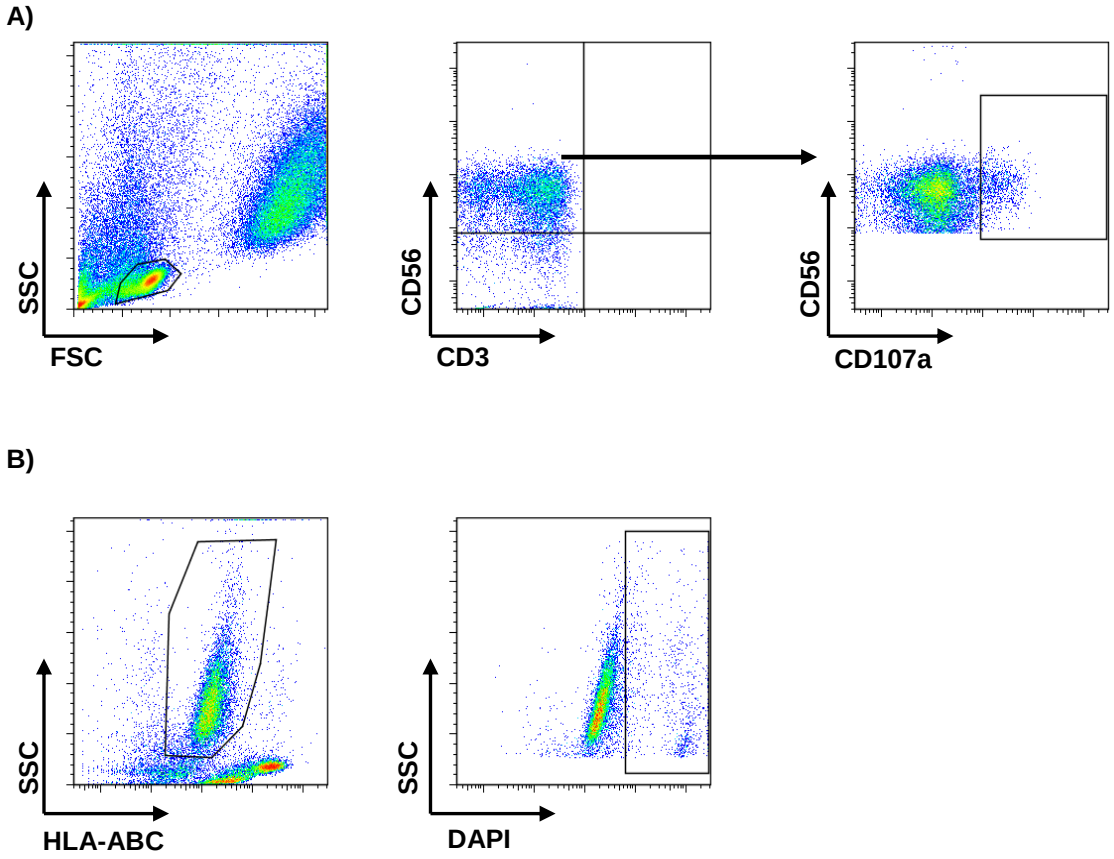

Figure 3.12: Gating strategy to assess NK cell functions

A) Effector cells were selected based upon $CD3^{-}CD56^{+}$ and then assessed for CD107a expression. B) Target cells were selected based on negative expression of HLA-ABC and cell death was then assessed by DAPI or Propidium iodide (PI) staining. Appropriate isotype controls were used to determine gating strategies.

Results showed that MSC-FCS and MSC-PLT were similarly capable of decreasing NK cell mediated lysis of K562 cells (**Fig. 3.13**). A decrease in target cell death was observed at all NK:K562 ratios for the NK cells treated with MSCs compared to untreated NK cells. At NK:K562 ratio of 2:1 the fold increase in target cell death were 13.9 ± 11.9 vs 8.35 ± 5.5 and 8.2 ± 6.5 for untreated NK cells, MSC-FCS and MSC-PLT treated NK cells respectively. At 5:1 ratio, the fold increase in target cell death were 10.7 ± 11.9 vs 7.9 ± 4.2 and 6.5 ± 3.1 for untreated NK cells, MSC-FCS and MSC-PLT treated NK cells, respectively.

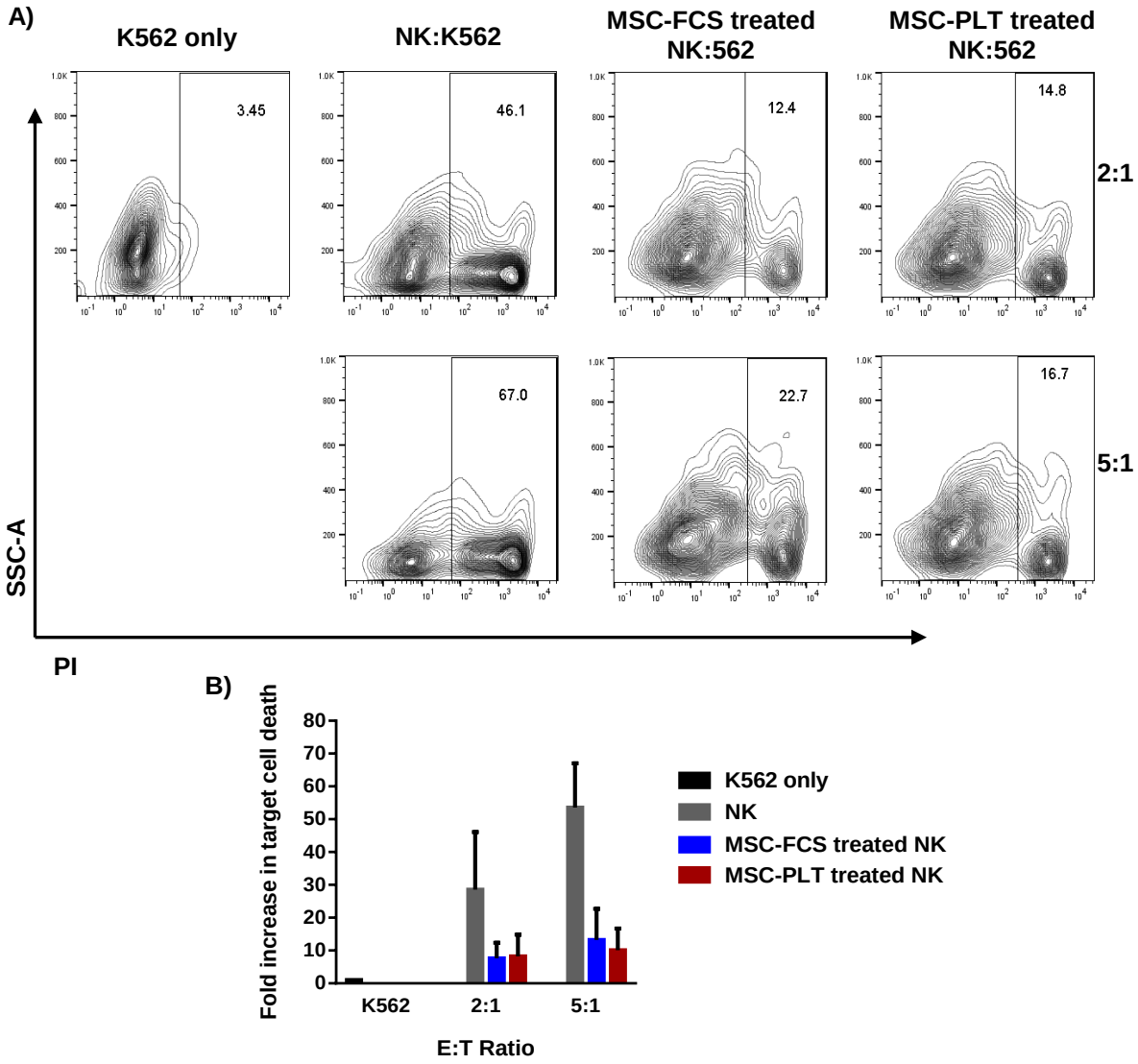

Figure 3.13: MSC-FCS and MSC-PLT equally impair NK cell mediated target cell death.

Untreated NK cells, MSC-FCS and MSC-PLT treated NK cells were co-cultured with a range of K562 cells for 3 hours. K562 viability was measured with PI and calculated as fold increase over K562 only cell death. **A)** Representative plots of K562 cell death after co-incubation with NK cells and **B)** Cumulative data from two independent experiments (mean ± SEM).

In addition to target cell death, NK cell degranulation was analysed as measurement of NK cell function. CD107a has been described as an important marker of $CD8^+$ T cell and NK cell degranulation following engagement with target cells. CD107a expression positively correlates with cytokine secretion and target cell lysis (Aktas *et al.,* 2009; Alter *et al.,* 2004). A reduction in the percentage of degranulating NK was observed when they were treated with either MSC-FCS or MSC-PLT. In the absence of target cells, NK cells did not exhibit CD107a expression (<5% $CD107a^+$ cells). At NK:562 ratios of 2:1 and

5:1, untreated NK cells exhibited a degranulation of 40.3% ± 6.9 and 28.8% ± 5.1, while MSC-FCS and MSC-PLT showed a percentage of degranulating cells of 21.0% ± 4.4 and 22.4% ± 3.5 at 2:1, and 15.3% ± 1.7 and 16.2% ± 0.4 at 5:1, respectively (**Fig. 3.14**). Moreover, MSC-PLT and MSC-FCS displayed comparable efficacy in inhibiting NK cell degranulation.

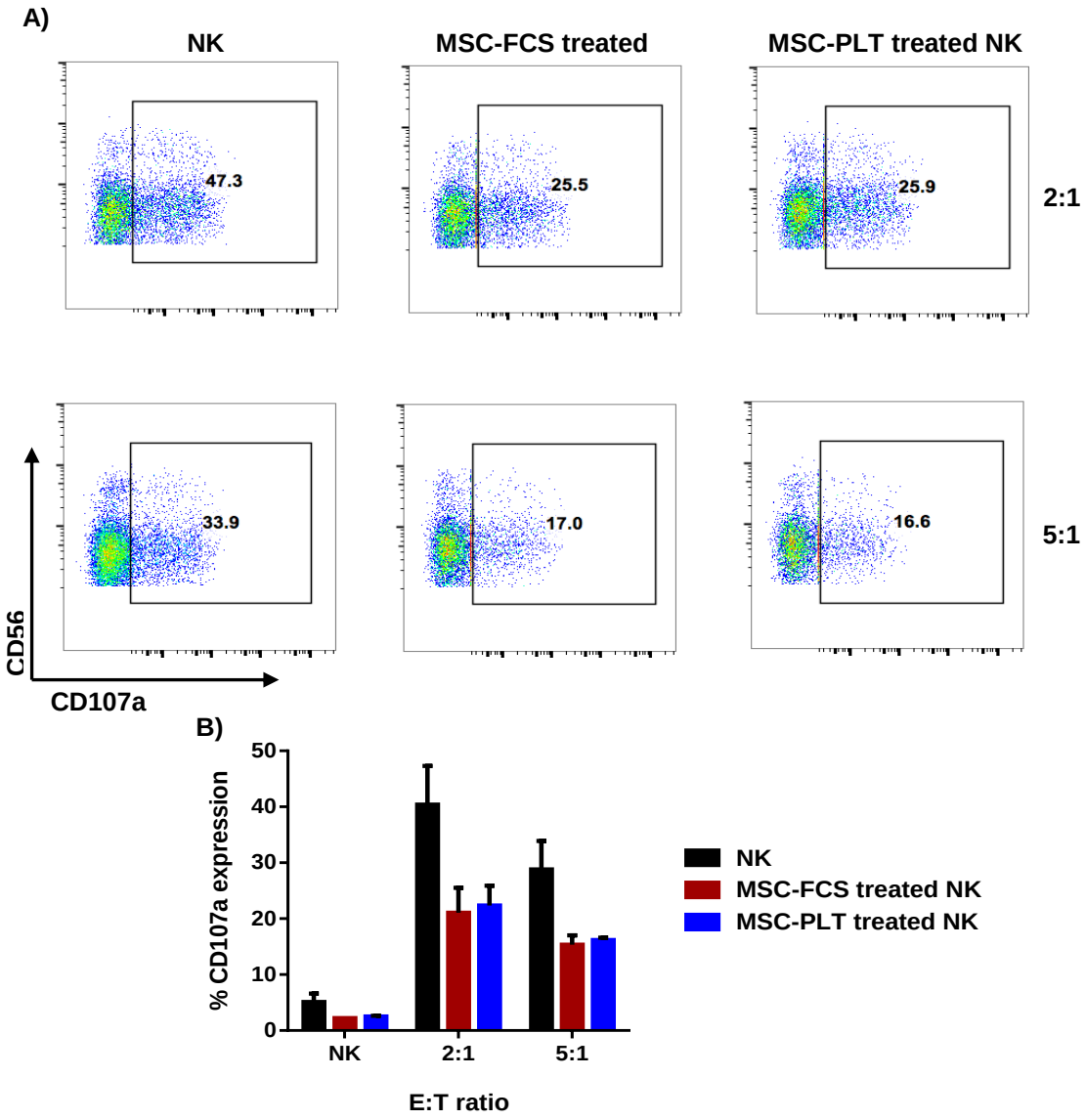

Figure 3.14: NK cell degranulation is reduced upon treatment with MSC-FCS and MSC-PLT

Untreated NK cells, MSC-FCS and MSC-PLT treated NK cells were co-cultured with a range of K562 cells for 3 hours. CD107a expression was assessed by flow cytometry. **A)** Representative plots of CD107a expression of untreated and MSC treated NK cells **B)** Cumulative data from two independent experiments (mean ± SEM). NK cells in the absence of target cells were used as negative controls.

3.3.7. MSCs express NK cell inhibitory molecule HLA-ABC

MSCs have been shown to influence NK cell cytotoxicity upon co-culture with NK cells during IL-2 activation of the latter, however, IL-2 activated NK cells are also capable of inducing MSC killing. This factor can result in potential disadvantages to MSC mediated therapy, since, upon transplantation, the inflammatory environment wherein MSCs reside, may lead to activation of the regional NK cell population. To test whether MSCs are capable of resisting NK cell killing, paired MSC samples were assessed for their expression of NK cell inhibitory marker HLA-ABC, and the fold increase of MFI was calculated as fold increase above the MFI of the isotype control. MSC-FCS and MSC-PLT were positive for the expression of HLA-ABC (**Fig. 3.15**). The results show that PLT expansion of MSCs results in a significant increase surface expression of HLA-ABC molecules in comparison with MSC-FCS, as evidenced by MFI fold increase of 43.88 ± 2.73 vs 17.00 ± 2.67, respectively (p=0.002).

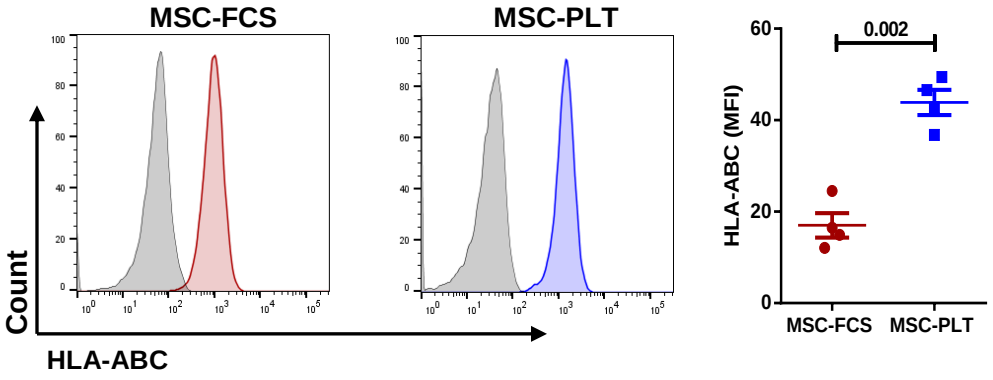

Figure 3.15: MSC-PLT have higher expression of NK cell inhibitory marker HLA-ABC

Expression of HLA-ABC was assessed by flow cytometry on MSC-FCS (red histogram) and MSC-PLT (blue histogram). Representative plots and cumulative data of MFI fold increase of HLA-ABC in comparison to isotype controls are shown. Results express mean ± SEM of 4 independent experiments.

3.3.8. Paired MSCs are equally susceptible to NK cell mediated lysis

To investigate the effect of MSC expansion in PLT-medium on their susceptibility to be lysed by NK cells, paired MSC samples were co-cultured with IL-2 activated NK cells at a NK:MSC ratio of 10:1 for 3 hours, and MSC death was assessed by flow cytometry. NK cell cytotoxic ability was confirmed by co-culture with K562 cells at a 4:1 ratio for 3 hours as a positive control. CD105 and HLA-ABC were used to gate MSCs and K562 cells, respectively, and the percentage of dead cells was determined by DAPI staining. Cellular death was determined as fold increase in cell death above the background death of MSC or K652 only cell culture. Results showed that IL-2 activated NK cells induced cytolysis of paired samples (**Fig. 3.16A**). Cumulative data showed that the fold increase of MSC cell death after co-incubation with NK cells was comparable to that of the control condition using K562 cells (**Fig. 3.16B**). Additionally, no differences were detected in the susceptibility of MSC-FCS and MSC-PLT to NK cell mediated lysis, with a fold increase of 3.27 ± 0.48 and 3.39 ± 0.82, respectively (p=0.889) (**Fig. 3.16B**).

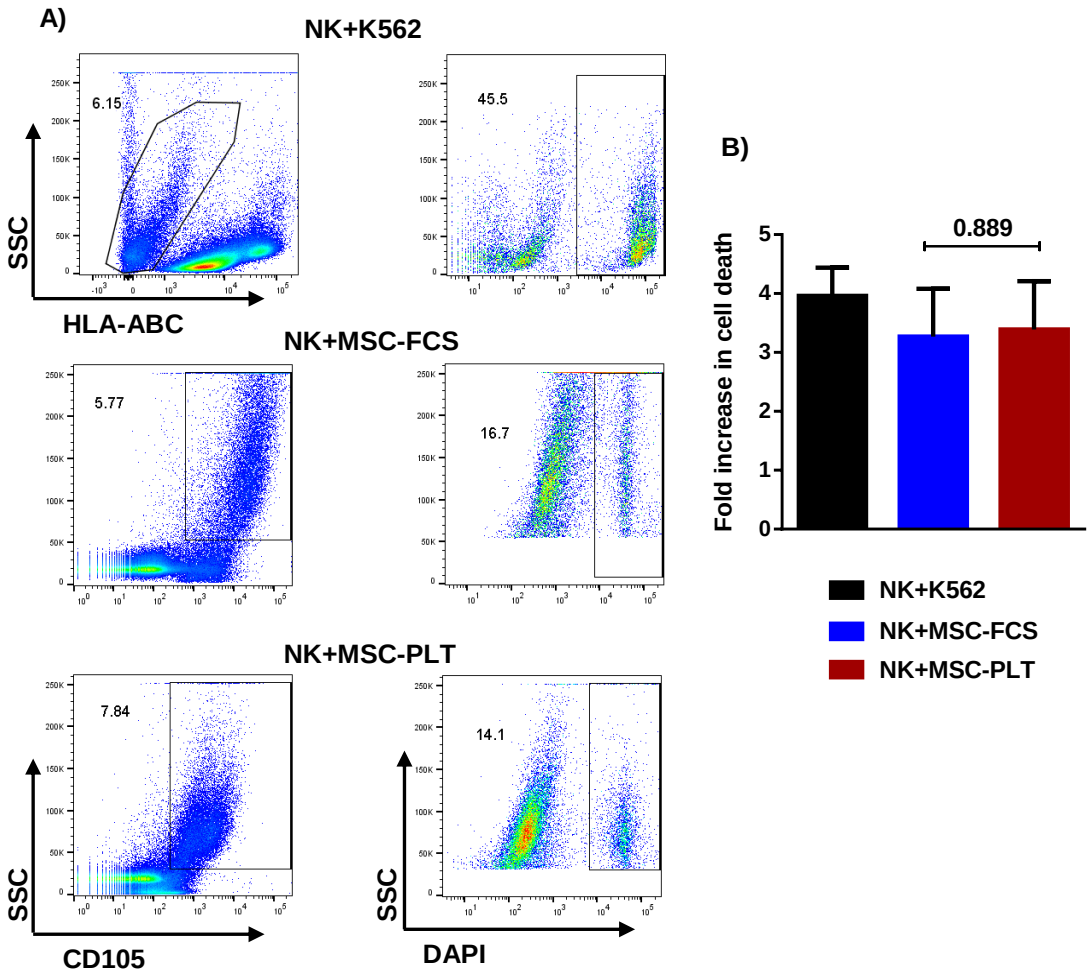

Figure 3.16: MSC-FCS and MSC-PLT are equally killed by activated NK cells.

IL-2 activated NK cells were co-cultured with MSC-PLT and MSC-FCS for 3 hours. **A)** Representative plots showing MSC killing by NK cells as assessed by cells selection based on CD105 expression and viability was then assessed by DAPI staining. **B)** Cumulative data showing fold change in cell death from n=4 (mean ± SEM) of MSC-FCS, MSC-PLT and K562 (positive control).

To further investigate NK cell cytotoxic activity towards MSCs, degranulation of NK cells by CD107a assessment was performed. CD107a expression was assessed on NK cells after 3h incubation with paired MSC samples. Analysis was carried out as previously described on **Fig. 3.12**. NK cells alone, which are almost unable to express CD107a, and NK cells co-incubated with K562 cells, were used as negative and positive control, respectively. The results showed that NK cell degranulation was similar when in the presence of MSC-FCS or MSC-PLT (**Fig 3.17A**). The percentage of CD107a expression was 11.91% ±

3.16 and 9.96% ± 3.27 for NK cells in the presence of MSC-FCS and MSC-PLT, respectively (p=0.370) (**Fig. 3.17B**). Overall, MSC-FCS and MSC-PLT show similar susceptibility to NK cell mediated lysis.

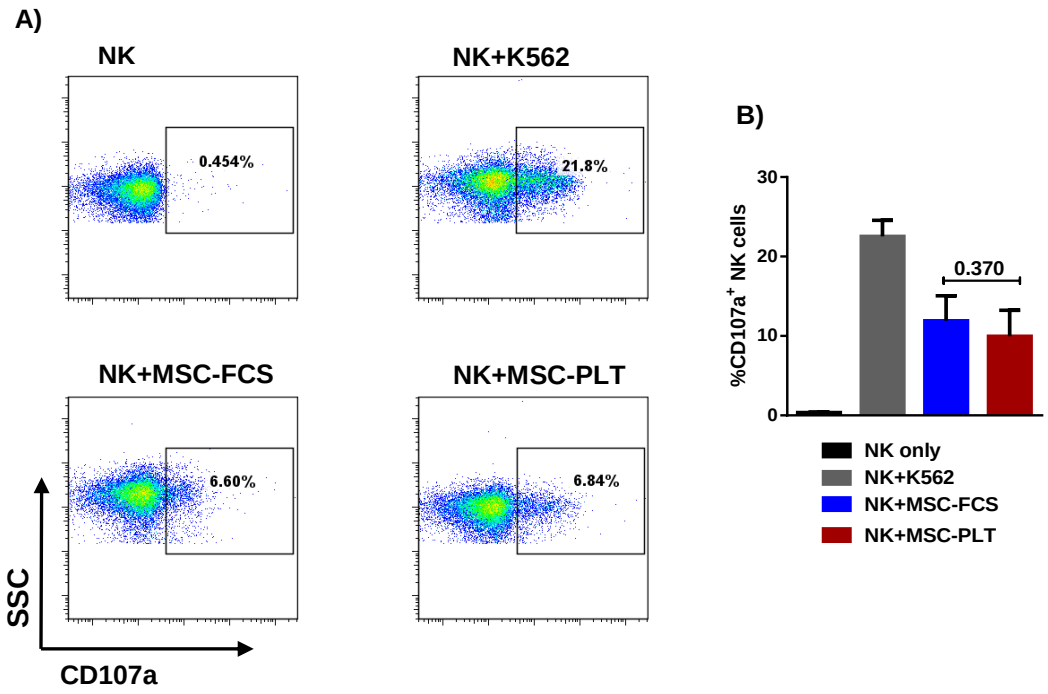

Figure 3.17: NK cell degranulation upon interaction with MSC-FCS and MSC-PLT

IL-2 activated NK cells were co-cultured with either paired MSCs or K562 cells (positive control). **A)** Representative graphs showing CD107a expression of NK cells alone and NK cells after co-incubation with paired MSC samples and K562 cells. **B)** Cumulative data of CD107a expression from 4 independent experiments. NK cells alone and NK cells co-incubated with K562 cells were used as negative and positive controls respectively. Data represented as mean ± SEM of n=4.

3.4. Discussion

This work demonstrates the feasibility of replacing FCS, a conventional MSC expansion supplement, with human PLT for xeno-free expansion of MSCs. Due to their potential to modulate immune responses and to promote tissue regeneration; MSCs have been widely tested in clinical trials for the treatment of a plethora of diseases. *In vitro* expansion of MSCs typically relies on the use of FCS as a source of mitogenic growth factors; however, the administration of animal products to humans is undesirable because it may lead to the transmission of prions and unidentified zoonosis, and possible adverse immune reactions (Bieback *et al.,* 2013). Spees *et al* (2004) reported that rat MSCs grown in 20% FCS supplemented medium induced humoral responses after repeated administrations to rats (Spees *et al.,* 2004). Similarly, FCS antibodies have been detected in individual patients that have received two allogeneic BM derived MSC infusions (Horwitz *et al.,* 2002). Additionally, the establishment of a standardised protocol based on FCS is intrinsically difficult due to its complex composition which is usually ill-defined and variable from batch-to-batch (Brunner *et al.,* 2010). And, although there are currently GMP-compliant batches of FCS, its use is critically rated by the regulatory authorities (EMEA CPMP/BWP/1793/02, 2003).

In view of these considerations, several groups have shifted towards xeno-free expansion of MSCs using human PLT, which has been shown to enhance proliferative capacity of MSC while maintaining their morphological and functional characteristics (Doucet *et al.,* 2005; Bernardo *et al.,* 2007; Crespo-Diaz *et al.,* 2011). In this study, MSCs expanded in culture media with relatively low concentrations of PLT (5%) were shown to have an accelerated cell growth, with significantly increased cumulative population doublings and a moderate decrease in doubling times, when compared with MSCs expanded in 10% FCS culture medium. This increased proliferative rate is likely due to the higher concentration of growth factors present in PLT, such as, bFGF, IGF1, PDGF and TGF-β, than those in most batches of FCS. These growth factors have been shown to enhance MSC proliferation rate *in vitro* (Bernardo *et al.,* 2007; Crespo-Diaz *et al.,* 2011; Doucet *et al.,* 2005; Iudicone *et al.,* 2013).

Additional characterisation demonstrated that PLT expanded MSCs, fulfilled the minimal criteria for MSC identification, as defined by the ISCT guidelines (Dominici *et al*, 2006). Phenotypically, early passage MSC-PLT were ≥ 95% positive for the expression of CD73, CD105 and CD90 and ≥2% negative for the expression of lineage specific markers, CD19, CD14, CD34 and CD45 and for HLA-DR. This phenotype was maintained throughout passages and was comparable to their FCS expanded counterparts and in accordance with previous studies using PLT as growth supplement (Bieback *et al.,* 2009; Crespo-Diaz *et al.,* 2011). Previous studies have documented that factors such as EGF and PDGF induce HLA-DR expression by MSCs thus leading to the stimulation of $CD4^+$ cells (Bocelli-Tyndall *et al.*, 2010), however, MSCs herein expanded, were negative for the expression of HLA-DR at all tested passages indicating that PLT maintained phenotypic stability of MSCs.

Morphologically, MSC-FCS and MSC-PLT exhibited the typical fibroblast-like morphology. At later passages, while MSC-PLT retained the characteristic spindle-shape morphology, MSC-FCS appeared enlarged, flatter and grainier. These changes were detected after passage 6, and are in agreement with previous studies (Bonab *et al.*, 2006; Griffiths *et al.,* 2013). Griffiths *et al* (2013) demonstrated that FCS expanded MSCs, which exhibited a flatter and ragged morphology after P10, had increased expression of the senescence marker β-galactosidase in comparison to the PLT expanded cells. Other studies have shown that FCS expanded MSCs had chromosomal aberrations that were not found in their PLT expanded counterparts, and that the enlarged cell size found on the MSC-FCS was correlated to inefficient *in vitro* differentiation of MSC (Bernardo et al., 2007; Bonab *et al.,* 2006; Lee *et al.,* 2013; Lennon *et al.,* 2012). Altogether, these results indicate that PLT is beneficial for MSC expansion conferring added proliferative capacity to these cells while preventing cellular ageing.

One of the main characteristics of MSCs is their ability to differentiate into cells of mesodermal origin, such as, adipocytes, osteocytes and chondrocytes. This study concurs with previous reports and indicates that PLT maintains the differentiation potential of MSCs (Bernardo *et al.,* 2007; Crespo-Diaz *et al.,* 2012; Doucet *et al.,* 2005). *In vitro* differentiation of MSCs into adipocytes,

osteocytes and chondrocytes was successful with both media formulations and no apparent differences were detected between the paired samples.

One of the most attractive properties of MSCs is their ability to modulate immune responses. Studies focused on comparison of different MSC expansion media have so far been contradictory regarding the immunosuppressive potential of PLT expanded MSCs. Initial studies performed by Doucet *et al* (2005) reported that PLT expanded MSCs were capable of suppressing allogeneic T cell responses as efficiently as FCS expanded MSCs (Doucet *et al.*, 2005). Further studies have confirmed these observations and showed that both MSC populations were competent immunosuppressors (Flemming *et al.*, 2011, Bernardo *et al.,* 2007). Conversely, other studies have shown that PLT expanded MSCs are less inhibitory than their FCS expanded counterparts. Abderlzarik *et al* (2011) has shown that expansion of MSCs in PLT supplemented medium induced decreased production of PGE2, resulting in a reduced suppressive capacity of T cell proliferation and NK cell cytotoxic ability (Abdelzarik *et al.,* 2011). Copland *et al* (2013) corroborated these observations and demonstrated that PLT expanded cell were also poor secretors of IDO (Copland *et al.,* 2013). Results in this chapter indicate that PLT expanded MSCs are at least, as immunosuppressive as FCS expanded MSCs. MSC-PLT were strong suppressors of T cell proliferation and inhibited CD25 expression by $CD3^+CD4^+$ and $CD3^+CD8^+$ T cells. Moreover, MSC-PLT and MSC-FCS demonstrated similar ability to inhibit production of IFN-γ and TNF-α by allo-moDC stimulated T cells. MSC dependent modifications in immune cell cytokine secretion have been previously reported. These reports have demonstrated a dose dependent inhibition of TNF-α and IFN-γ secretion by immune cells after co-culture with MSC-FCS (Aggarwal and Pittenger, 2005; Zheng *et al.,* 2007). One such report compared the effect of PLT expansion of MSCs on their ability to inhibit secretion of the abovementioned cytokines by T cells. Similarly to the findings reported in this chapter, both MSC-FCS and MSC-PLT showed comparable ability to inhibit the secretion of the abovementioned cytokines (Flemming *et al.,* 2011).

Interestingly, MSC-PLT and MSC-FCS were equally capable of increasing CD69 expression by $CD3^+CD4^+$ and $CD3^+CD8^+$ cells. CD69 is a target of

canonical nuclear factor kappa-B (NF-κB) signalling and is transiently expressed upon T cell activation (Werfel *et al.,* 1997). Stable expression of the CD69 marker has been linked to cells with immunoregulatory properties (Cortés *et al.,* 2014). Saldanha-Araujo *et al* (2011) have shown that upon MSC treatment *in vitro*, T cells had increased and stable expression of CD69 marker, in a mechanism that was regulated by the non-canonical NF-κB signalling pathway. It has been demonstrated that CD69 deficiency in mice leads to increased production of pro-inflammatory cytokines, such as TNF-α, IFN-γ and IL-21, and reduced $FoxP3^+$ regulatory T cell function (Radulovic *et al.*, 2012). CD69 was shown to promote activation of Jak3-signal transducer and activator of transcription 5 (STAT5) signalling pathway which leads to the inhibition of TH17 differentiation and promotion of regulatory T cells (Martin *et al.*, 2010). In this regard, current evidence provides the basis for the potential of MSCs to induce a regulatory pattern of T cells by dampening CD25 expression while promoting CD69 expression (Ciccocioppo *et al.,* 2015). The effect of MSC treatment on expression of CLA showed that both MSC-FCS and MSC-PLT had similar ability to downregulate its expression on T lymphocytes. CLA is a fucose-containing carbohydrate that facilitates T cells migration to inflamed skin (Fuhlbrigge *et al.,* 1997). Our results provide evidence that MSCs can influence CLA-expression by T cells and may have impact on their homing capacity into the sites of cutaneous injury.

MSC-FCS have been demonstrated to be strong inhibitors of NK cell mediated cytotoxicity. NK cells are cytotoxic lymphocytes with an important role in innate immunity and play an important role during allogeneic transplantations (Vivier *et al.*, 2008). By inhibiting NK cell cytotoxicity MSCs may prevent graft rejection. Spaggiari *et al* (2006) have shown that MSCs are capable of inhibiting IL-2 induced NK cell proliferation and hampering cytotoxic capacity of these cells by downregulation of the activating NK cell receptors NKp30, NKp44 and NKG2D via production of IDO and PGE2 (Spaggiari *et al.,* 2006). Other factors, including, IL-10, TGF-β and HGF have also been shown to be involved in this effect (Casado *et al.,* 2013; Spaggiari *et al.,* 2008). Further studies corroborated these findings and demonstrated the efficacy of MSCs in impairing NK cell mediated cytotoxicity (Consentious *et al.,* 2015; Giuliani *et al.,* 2014). Few studies have looked into the effect of PLT expanded MSCs on NK cell functions.

Abdelzarik *et al* (2011) demonstrated that PLT expanded cells were not as potent as FCS expanded MSCs in suppressing NK cell functions. In their study, MSC-PLT treated NK cells had higher cytotoxic capacity than the NK cells treated with FCS expanded MSCs (Abdelzarik *et al.,* 2011). Our study contradicts these observations. MSC-PLT were as efficient as FCS expanded MSCs in suppressing NK cell cytotoxicity against K562 cell targets as evidenced by the lower percentage of lysed target cells and degranulating NK cells, as indicated by the expression of CD107a. Upon contact with the target cells, a synapse is formed between the effector and the target cells. As a result, the lysosome vesicles, which are rich in lysosomal-associated membrane glycoproteins (LAMPs), such as CD107a (LAMP-1) are polarised and migrate towards the synapse where they fuse with the cytotoxic cell membrane. Effector cell degranulation ensues by the release of cytotoxic granules into the synapse where they lead to the lysis of the target cell (Aktas *et al.,* 2009; Alter *et al.,* 2004). Altogether, our results indicate that MSC-FCS and MSC-PLT treated NK cells exhibit similar impairment of NK cell cytotoxicity.

On the other hand, despite their inherent low immunogenicity, culture expanded MSCs can be lysed by activated NK cells (Giuliani *et al*., 2014; Spaggiari *et al.,* 2008). This effect may hinder the outcome of MSC therapy as a consequence of direct elimination of MSCs *in vivo*. NK cell activity is regulated by a balance of inhibitory and activating signals. Upon interaction with MSCs, which express ligands for both inhibitory and activating signals, the outcome is determined by the prevalent signals (Reinders *et al.,* 2014). Culture expanded MSCs express HLA-ABC, which offers partial resistance to NK-cell mediated lysis as they are identified as “self” by the NK cells. However, HLA-ABC expression is not sufficient for full protection. Contrary to the previously reported study, that indicated a lower susceptibility of MSC-PLT cells for NK cell killing (Abdelzarik *et al.,* 2011), results in this chapter indicate that MSC-FCS and MSC-PLT have comparable susceptibility to NK cell mediated lysis, as evidenced by similar MSC death rates and NK cell degranulation. Abdelzarik *et al* (2011) demonstrated that PLT expansion of MSCs downregulates the expression of NK cell activating ligands, Nectin-2 and poliovirus receptor (PVR) (DNAM-1 ligands) and ULBP-3 (NKG2D ligand) thus conferring higher resistance to NK cell mediated lysis to MSC-PLT. This discrepancy between the studies might be

due to the differing sources of MSCs and concentration of PLT used for expansion (10%). In our study, expression of HLA-ABC was significantly higher in MSC-PLT. The higher expression of HLA-ABC did not correlate with higher resistance to NK cell mediated lysis, indicating that these signals are not sufficient for full protection of MSCs.

Overall, our study provides evidence that PLT expansion of MSCs may be a feasible option to produce xeno-free MSCs for future therapeutic use. It is important to note that the differences found between the different studies in terms of phenotype and immunomodulatory capacity may be due to variance in samples and experimental methodology. Different groups have used not only, different MSC sources and different isolation and expansion methodologies, but also different experimental approaches for testing the immune potency of MSCs. Ultimately, one of the most pressing issues in MSC therapeutic application is the development of standardised assays for expansion and potency assessment that will allow an effective comparison between independent studies. Nonetheless, our study and work of others have demonstrated that human PLT is a promising candidate to replace FCS for MSC expansion. This research outcome is further supported by the fact that PLT expanded MSCs have been increasingly used in early clinical trials (Introna *et al.,* 2014; Lucchini *et al.,* 2010). The ultimate confirmation of MSC expansion in PLT will depend on the long term follow up of the clinical trials.

Acknowledgments

Diashati Mardiasmo for performing some NK cell experiments under my supervision during her MRes project.

Chapter 4: Phenotypic characterisation of MSC-PLT by high-throughput flow cytometry

“Everything is theoretically impossible, until it is done.”

-Robert A. Heinlein

Chapter 4: Phenotypic characterisation of MSC-PLT by high-throughput flow cytometry

4.1. Introduction

Conventional expansion of MSCs relies on the use of FCS as culture supplement which provides the cells with essential nutrients and growth factors (Bieback, 2013). Concerns raised by the regulatory authorities regarding its use in therapeutics have prompted laboratories worldwide to look for xeno-free alernatives for MSC expansion. In the past decade human PLT has emerged as one of the most suitable replacements for FCS for the expansion of MSCs. MSCs expanded in PLT-containing medium have been shown to maintain their general characteristics and immunomodulatory properties (Bernardo *et al.,* 2007; Crespo-Diaz *et al.*, 2011; Doucet *et al.,* 2005). As a result, they have been increasingly used in clinical trials (Lucchini *et al.*, 2010; Introna *et al.*, 2014).

The effect of PLT expansion of MSCs on their general characteristics, including general phenotype, trilineage potential, morphology and immunomodulatory properties, has been reported in **Chapter 3**.

Despite observations that PLT expanded cells comply with the minimal criteria similarly to FCS-expanded cells, the effect of PLT on a wide range of cell surface markers expressed by MSC is still not well characterised. Given the importance of cell surface proteins to a plethora of biological functions, there is a need to characterise the phenotypic profile of MSCs expanded in PLT-culture media in comparison to conventional FCS-expanded MSCs. Platforms like mass spectrometry have been widely used to screen for a variety of protein compounds within a mixture of samples (Kupcova, 2013), however, although this analysis allows for the detection of many different compounds, it does not allow for the investigation cell surface proteins in a target cell. One of the technologies that have emerged as an attractive tool for this analysis is high-throughtput (HTP) flow cytometry. This analysis platform is a reproducible discovery-orientated screening technology that allows for the identification of surface proteins using panels of hundreds of CD markers. This tool can also be combined with fluorescent cell barcoding that allows for parallel analysis of

distinct populations (Ramirez *et al.*, 2003; Black *et al.*, 2011; Gedye *et al.*, 2014). This platform takes advantage of the general characteristics of conventional flow cytometry for cell surface protein expression analysis but incorporates a high-speed sample loading device that allows for fast analysis of a range of antibodies, usually arrayed in 96- or 384-well plates (Black *et al.*, 2011; Gedye *et al.*, 2014). This technology also enables the use of multiplexed assays thus allowing for the analysis of several cell populations in the same well (Black *et al.*, 2011; Gedye *et al.*, 2014). To date, no high throughput flow cytometry analysis of PLT expanded MSCs has been reported, despite such analysis being used to screen for surface markers in MSCs expanded in FCS-culture media (Baer *et al.*, 2013; Donnenberg *et al.*, 2015; Walmsley *et al.*, 2015). This chapter focuses on the phenotypic profiling of cell surface proteins expressed on MSC-PLT in comparison to MSC-FCS by high-throughput flow cytometry.

Research reported in this chapter aimed to characterise the overall surface phenotypic “fingerprint” of PLT-expanded MSCs and to identify differentially expressed markers between MSC-PLT and MSC-FCS. The specific objectives of this chapter were the following:

- To screen for over 300 surface marker proteins on paired MSC-PLT and MSC-FCS
- To identify a signature of surface markers that is differentially expressed on the surface of MSC-PLT and MSC-FCS
- To perform bioinformatics analysis on the differentially expressed surface proteins in order to identify pathways that are enriched/influenced by these markers
- To generate a searchable database of markers expressed by MSCs grown under different culture conditions that can be used as a resource to appreciate the heterogeneity and functional diversity of the MSC lineage.

4.2. Specific methods

General methods for this chapter are described in **Chapter 2**. Additional methods specific to this chapter are herein described.

4.2.1. Cell barcoding for MSC population discrimination

To discriminate between FCS- and PLT-expanded MSCs, MSC-PLT were labelled with CellTrace™ Violet (Life Technologies) and MSC-FCS were kept unlabelled. In brief, MSC-PLT and MSC-FCS, at passage 3, were harvested as described in **section 2.4.1**. MSC-FCS were suspended in PEB buffer, consisting of PBS with 2 mM of EDTA and 0.5% BSA and used directly. MSC-PLT were washed in in PBS and re-suspended in a 0.2 µM solution of CellTrace™ violet at a cell density of $1x10^4$cells/µl. Cells were incubated for 5 minutes at room temperature in the dark, washed twice with PEB and re-suspended in the same buffer for subsequent analyses.

4.2.2. Surface protein screening using Lyoplate system

Non-labelled MSC-FCS and CellTrace labelled MSC-PLT were pooled together at a 1:1 ratio and analysed using Miltenyi 96 well human antibody panel (Miltenyi), containing APC-conjugated antibodies with specificity for 350 human cell surface markers and 7 isotype controls, arrayed on four round bottom 96 well plates. Details about the antibodies are illustrated in **Supplementary Tables S4.1-4**. Staining and plate preparation was performed as described by the manufacturer's protocol. In brief, the lyophilized antibodies were reconstituted with 25 µl of deionized water. The previously prepared MSCs were added to each well of the 96 well plates at a density of $5x10^4$cells/well. Cell incubation with the antibodies was carried out for 10 minutes in the dark at 4^oC. Next, cells were washed twice with PEB and centrifuged at 300xg for 5 minutes. Cell pellet was then re-suspended in 50 µl of PEB and samples were analysed using an automated MACSQuant flow cytometer (Miltenyi) where 35 µl of sample were analysed and at least 10,000 events per well were collected.

4.2.3. Data analysis

Data acquisition was performed using the MACSQuant analyser v10 software (Miltenyi) and analysis was performed using either MACSquant or FlowJo

software (TreeStar). An initial analysis template was created to select different MSC populations and to analyse each population for its positivity for APC. Briefly, a gate was manually drawn to select MSC and eliminate debris based on Forward Scatter (FSC) and Side Scatter (SSC) profiles. Subsequently, MSC-FCS and MSC-PLT were selected as negative and positive CellTrace Violet^{TM} populations respectively, and finally, one-dimensional histograms for APC were drawn based on fluorescence intensity for each MSC population. The gate for positive events was determined such that all negative controls (isotype control) represented less than 1% of clean events. These gates were then applied to all individual wells within an experiment without posterior alteration. When necessary, gates were adjusted to account for fluorescence intensity variances between the different isotype controls. Analytical data (event count, percentage of APC positive clean events, median fluorescence intensity and standard deviation) were exported to Microsoft Excel and associated with sample ID, plate number, row and column.

4.2.4. Reverse transcription and Quantitative Real-Time PCR

Total RNA was extracted from three paired MSC samples at passage 3 as described in **section 2.8.1**. Quality and quantity of extracted RNA was assessed using Nanodrop 2000 (Thermo Fisher Scientific). The quality of the total RNA extracted was assessed by determining the 260/280 and 260/230 ratios. These ratios are used to assess the purity of RNA, with values of ~2.0 being considered “pure”, indicating the absence of contaminants, such as, phenol and proteins. A summary of RNA quality for each paired sample can be found on **Table 4.1**. Quantitative PCR was then performed as described in **section 2.8.2**, using the primer/probe sets illustrated on **Table 2.4**.

Table 4.1: Total RNA extracted from MSC-PLT and MSC-FCS was of high purity

Sample	260/280	260/230
MSC-FCS 1	2.07	2.15
MSC-PLT 1	2.10	2.21
MSC-FCS 2	2.07	2.10
MSC-PLT 2	2.02	1.92
MSC-FCS 3	2.08	2.00
MSC-PLT 3	2.08	2.01

4.3. Results

4.3.1. HTP flow cytometry screening identified markers with equally high expression in MSC-PLT and MSC-FCS

Surface marker analysis of MSC-PLT and MSC-FCS, using cells at passage 3, was assessed by flow cytometry using the Lyoplate system consisting of a panel of monoclonal antibodies specific for over 350 human surface proteins. To decrease experimental variability, each paired sample was analysed in parallel by pre-labelling one of the populations with a different colour fluorescent marker, in a process termed “barcoding”. In this work MSC-PLT sample were tagged with CellTrace Violet™ whereas MSC-FCS samples were left unlabelled. The paired MSC samples were combined in a single tube and then added at a density of $5x10^4$cells/well to a 96-well plate where APC-conjugated antibodies for each specific cell surface marker and correspondent isotype controls were arrayed. The workflow and gating strategies for the flow cytometric data analysis is depicted in **Fig. 4.1**.

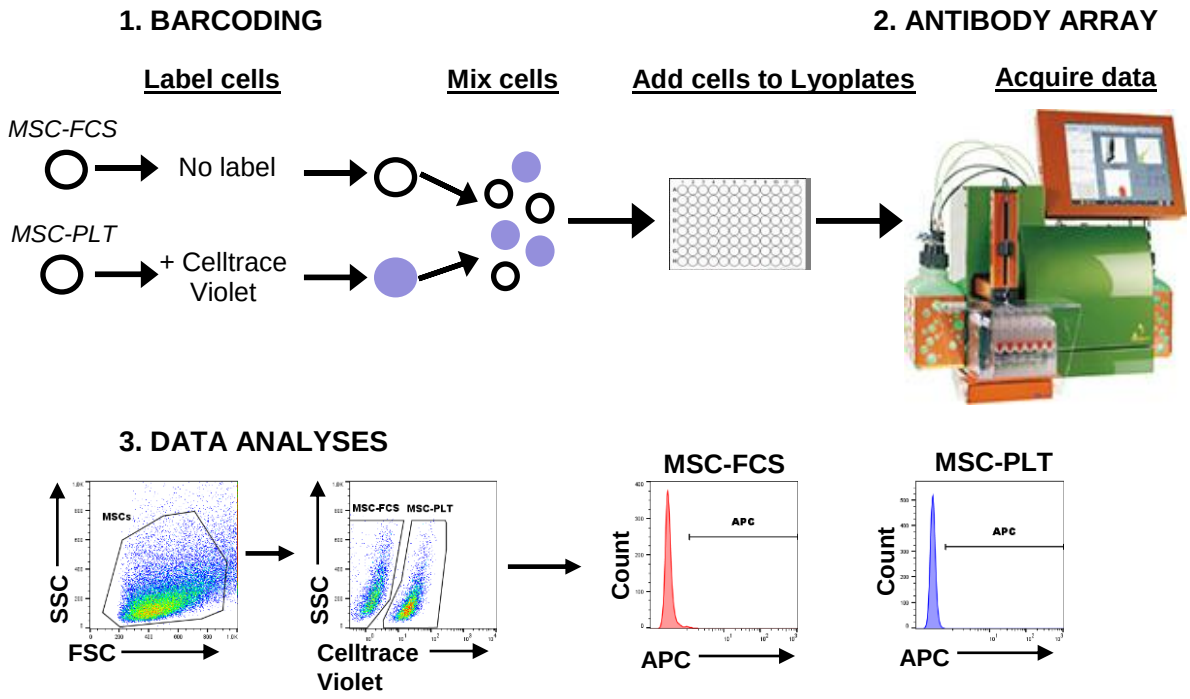

Figure 4.1: Schematics showing experimental overview of surface marker screening of MSCs using the lyoplate technology

MSCs were selected according to SSC/FSC properties. MSC-FCS and MSC-PLT were gated as Celltrace™ violet negative and positive populations, respectively and the percentage of positive cells for each antibody was determined based on gates drawn for each specific isotype control.

An initial surface marker screening was performed on one paired sample to select the markers that were expressed in at least 5.5% of one or both cell populations. Overall, 97 out of 350 markers were expressed on ≥5.5% of one or both cell populations. Both MSC populations were shown to express their characteristic markers, such as CD73, CD44 and CD29 but did not express haematopoietic lineage markers, such as CD3, CD4 and CD11b, suggesting the reliability of this platform. To further confirm these results, the 97 markers that were considered as “positive” by flow cytometry and a selected group of markers considered “negative” (n=36) in the first screening were investigated on two additional paired MSCs using the Lyoplate system.

Surface marker analysis of the three MSC samples from different bone marrow donors identified 3 groups of surface markers. Two polarised groups showed high or no expression on both MSC-PLT and MSC-FCS (n=51 and 46, respectively) (**Fig.4.2A and C**). Another group had variable expression between MSC-PLT and MSC-FCS (n=36) (**Fig.4.2B**).

Markers expressed on both MSC-PLT and MSC-FCS were identified as having >70% of cells in the positive gate. They included common MSC markers, such as, CD73, CD44, CD29, CD105 and CD90, as well as recently reported phenotypic markers for MSCs such as, CD46, CD47, CD49a, CD9, CD81, CD63, CD47, among others (Abdelrazik *et al.*, 2011; Baer *et al.*, 2013; Donnenberg *et al.*, 2015; Walmsley *et al.*, 2015). Markers were defined as negative for both MSC-PLT and MSC-FCS based on threshold of <5.5% cells in the positive gate. For the purpose of this present study, the group of markers with variable expression between the two MSC populations is the most interesting (**Fig.4.2**).

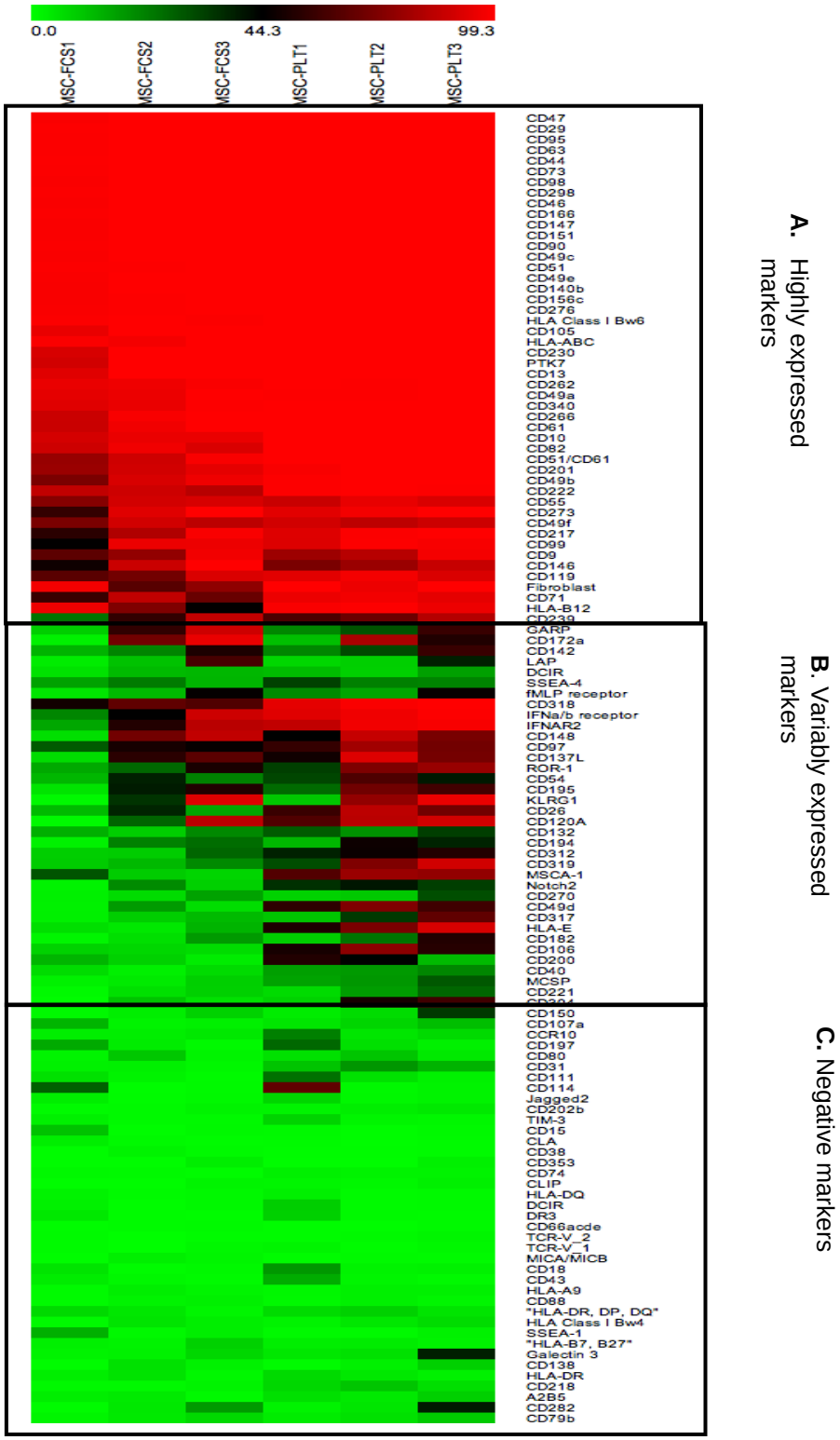

Figure 4.2: Three groups of surface markers with varied expression levels

The heat-map showed three distinct groups of markers. (**A**) Highly expressed markers on both MSC-PLT and MSC-FCS; (**B**) variably expressed markers between the two MSC populations; (**C**) negative on both MSC populations.

We further studied the highly expressed markers using the Kyoto encyclopedia of genes and genomes (KEGG) enrichment pathway analysis to catalogue the molecular pathways associated with these proteins. According to the molecular functions most of these proteins are associated with maintenance of haematopoietic cell lineages (10%) cell adhesion molecules (9%), focal adhesion (9%) and ECM-receptor signalling (9%) (**Fig. 4.3**)

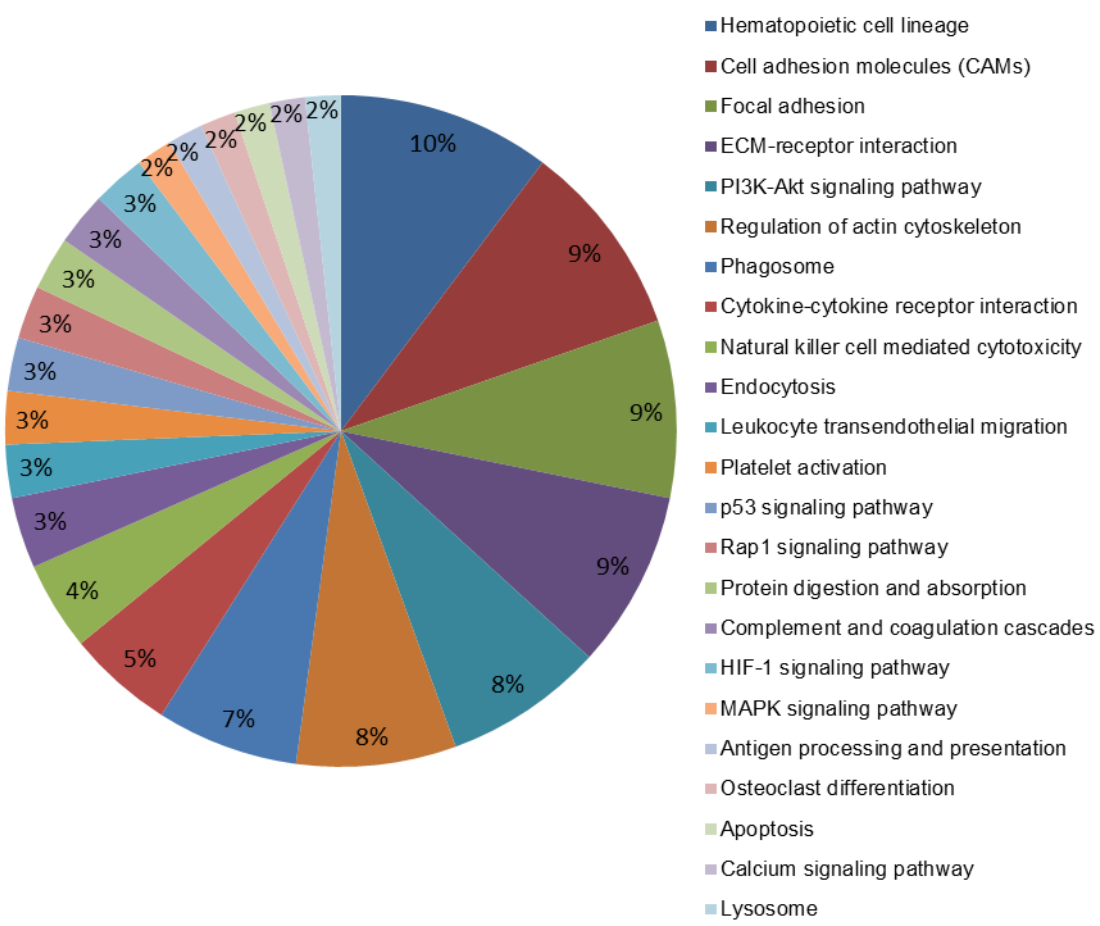

Total: 51 markers

Figure 4.3: Functional analysis of surface markers commonly expressed on both MSC-PLT and MSC-FCS

The pie chart depicts the molecular pathways identified for the highly expressed markers on both MSC-PLT and MSC-FCS (n=3) (queried on KEGG).

4.3.2. HTP flow cytometry screening identified 13 markers that were overexpressed by MSC-PLT

Examination of the surface marker array profiles of MSC-PLT and MSC-FCS across the different donors revealed that MSC-FCS has a higher intra-variability than MSC-PLT. PCA of the two first components of the expressed markers on the three different donors showed that while MSC-PLT clustered together on lower left quadrant, the three MSC-FCS samples were spread across the other 3 quadrants (**Fig.4.4A**), with coefficient of variation ranging from 3.3-88.9% and 17.8-114.5% in MSC-PLT and MSC-FCS, respectively (**Supplementary Table.S4.6**).

Further analysis of the variably expressed markers revealed 13 markers that were significantly overexpressed on MSC-PLT, defined according to the following criteria: at least two out of three samples had more than 5.5% of the cells in the positive gate in at least one of the paired MSC populations, an average fold change of ≥1.5 and a p-value <0.05. These included, CD318 (CUB domain containing protein 1; CDCP1), the mesenchymal stem cell antigen-1 (MSCA-1; alkaline phosphatase, liver/kidney/bone; ALPL), CD26 (dipeptidyl peptidase-4; DPP4), CD106 (vascular cell adhesion molecule 1; VCAM1), CD40 (TNF receptor superfamily member 5), CD31 (platelet and endothelial cell adhesion molecule 1; PECAM1), CD54 (intracellular adhesion molecule 1; ICAM-1), MCSP (melanoma-associated chondroitin sulphate proteoglycan 4, CSP4), CD312 (adhesion G protein-couple receptor 2, ADGRE2), CD97 (adhesion G protein-couple receptor 5, ADGRE5), CD49d (integrin α4 subunit, ITGA4) and Notch2. With the selected 13 markers, a hierarchical clustering using percent-positive values was performed. Cell surface protein expression differences stratified the samples into two clusters related to their expansion media (**Fig.4.4B**). Examples of representative histograms for these markers are presented in **Fig.4.4C.** Amongst these 13 markers, CD318, MSCA-1 and CD26 showed the higher enrichment in MSC-PLT, with a fold increase in percentage of positive cells of 10.5, 10.3 and 8.6, respectively (p=0.008, p=0.043 and p=0.003) (**Fig.4.4D**).

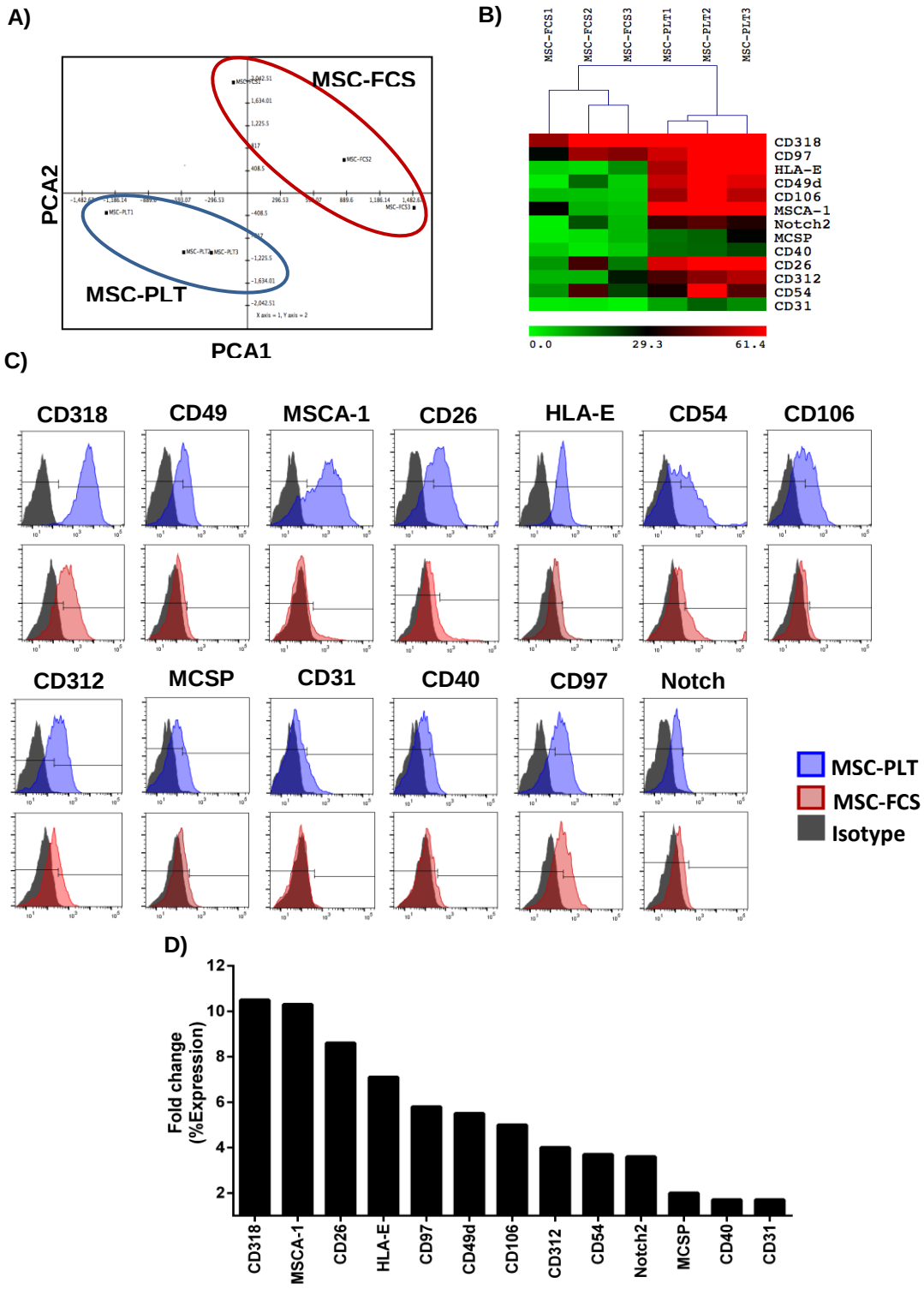

Figure 4.4: Lyoplate analysis identified 13 overexpressed markers on MSC-PLT

A) Principal component analysis (PCA) of the MSC-PLT (blue circle) and MSC-FCS (red circle) samples analysed using the lyoplate technology; **B)** hierarchical clustering of percent-positive marker expression significantly overexpressed on MSC-PLT; **C)** representative histograms of cell surface markers upregulated in MSC-PLT as obtained by flow cytometry; **D)** Fold increase of percent-positive marker expression on MSC-PLT. Data from n=3. Results were considered significant when a fold change >1.5 and a P-value<0.05 was detected.

To quantify the level of expression between of the 13 markers overexpressed on MSC-PLT, we analysed the differences in staining intensity, herein expressed as stain index. The stain index (SI) is a measure that allows the comparison of the relative brightness of a fluorochrome. The SI takes into consideration the background fluorescence which can be influenced by population autofluorescence, nonspecific staining, electronic noise and optical background from other fluorochromes (Frings, 2012). Previous reports have shown that PLT expanded MSCs are significantly smaller in cell size and less complex than MSCs maintained in FCS expansion media (Griffiths *et al.*, 2013). In the present study, MSC-PLT were shown to have smaller size (forward scatter) and less granularity (side scatter) than MSC-FCS, which influenced the background fluorescence of each MSC population with MSC-FCS exhibiting a 13-fold higher background fluorescence than MSC-PLT (p=0.029, **Fig.4.5**).

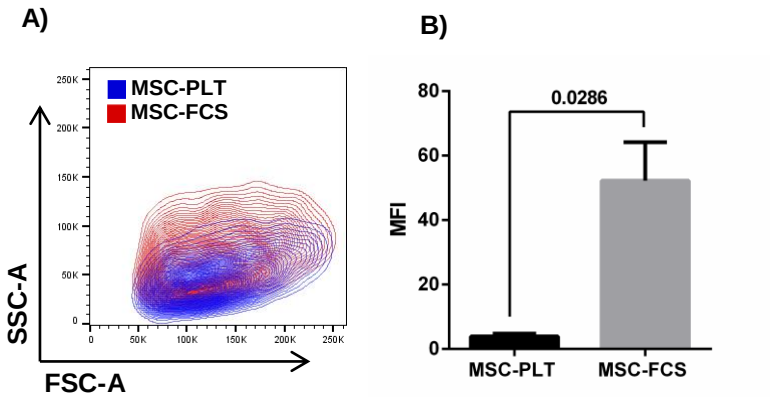

Figure 4.5: Differences in background fluorescence in MSC-PLT and MSC-FCS

A) Side scatter (SSC-A) and Forward Scatter (FSC-A) of MSC-PLT (blue) and MSC-FCS (red); **B)** background fluorescence levels in MSC-PLT and MSC-FCS detected in the APC channel. Results are expressed as mean ± SEM of n=3.

In general, higher stain index in MSC-PLT were detected across all 13 markers, compared to MSC-FCS (**Fig.4.6A**). CD318 and CD26 were the most differentially expressed markers between both populations with MSC-PLT exhibiting a 9.2 and a 7.1-fold higher SI than MSC-FCS ($p<0.05$ for both). Significantly higher expression of the markers CD106, CD312, CD49d, HLA-E and CD97, was also detected in MSC-PLT, showing a 6.3 to 1.6 fold higher SI than MSC-FCS ($p<0.05$). MSCA-1, one of the markers that was detected to be expressed in higher percentage of PLT expanded cells showed a concomitant 2.2-fold higher expression, however, this fold change failed to reach statistical significance ($p>0.05$). The remaining markers, MCSP, Notch2, CD54 and CD40, also showed higher expression levels in MSC-PLT, however, the difference in fold increase did not reach statistical significance ($p<0.05$, **Fig. 4.6B**).

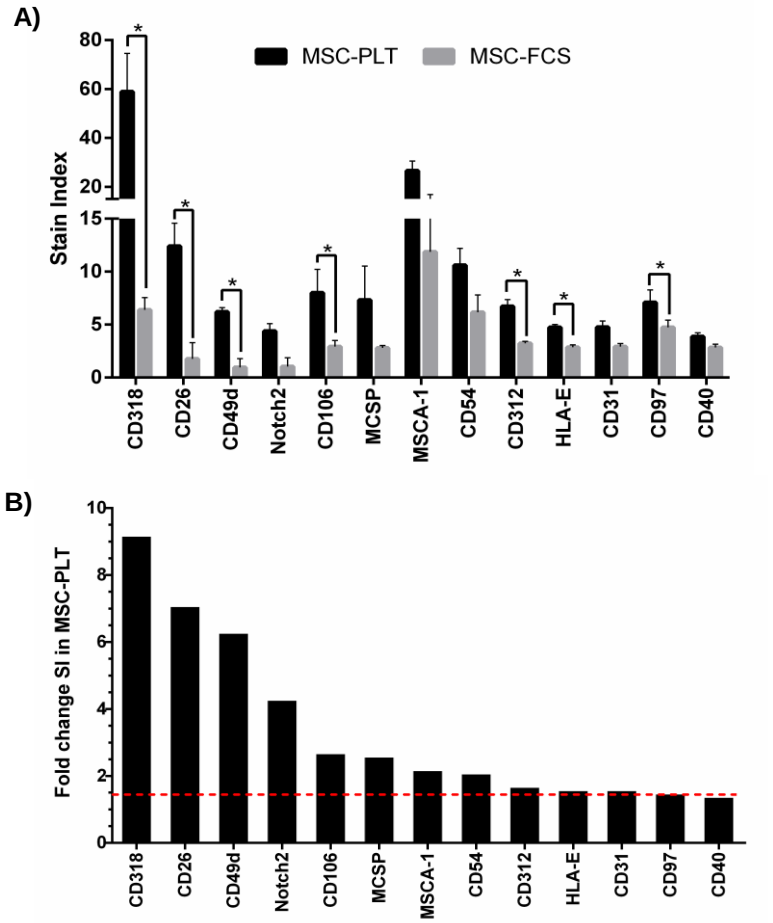

Figure 4.6: The level of expression of the significantly overexpressed markers in MSC-PLT.

The expression levels of each surface marker were determined by comparing the SI of each marker for MSC-PLT and MSC-FCS. The stain index was calculated by normalising the brightness of the signal for each antigen, i.e., the Median Fluorescence Intensity (MFI), to the background fluorescence of each cell population; **A)** Stain index of MSC-PLT in comparison to MSC-FCS for each marker; **B)** stain index fold increase in MSC-PLT. Data from n=3, representing mean ± SEM. Results were considered significant with fold increase compared to MSC-FCS > 1.5; *p-value <0.05.

4.3.3. Validation of surface marker expression by qPCR

To validate the overexpressed surface markers in MSC-PLT using the Lyoplate analysis, we investigated if these differences could be detected at mRNA level. For this analysis, 4 of the 13 significantly overexpressed markers were examined. The markers CD318 (CDCP1), CD26 (DPP4) and MSCA-1 (ALPL) were chosen based on their higher percentage of positive cells in the three analysed samples. The other analysed marker was CD106 (VCAM-1), due to its role in MSC immunomodulatory functions (Yang *et al.,* 2013). Analysis by qPCR of three paired MSC samples revealed that MSCA-1 and CD26 are significantly overexpressed at mRNA level ($p<0.05$). Conversely, the mRNA levels of CD106 and CD318 are similar between MSC-FCS and MSC-PLT ($p>0.05$) (**Fig.4.7**).

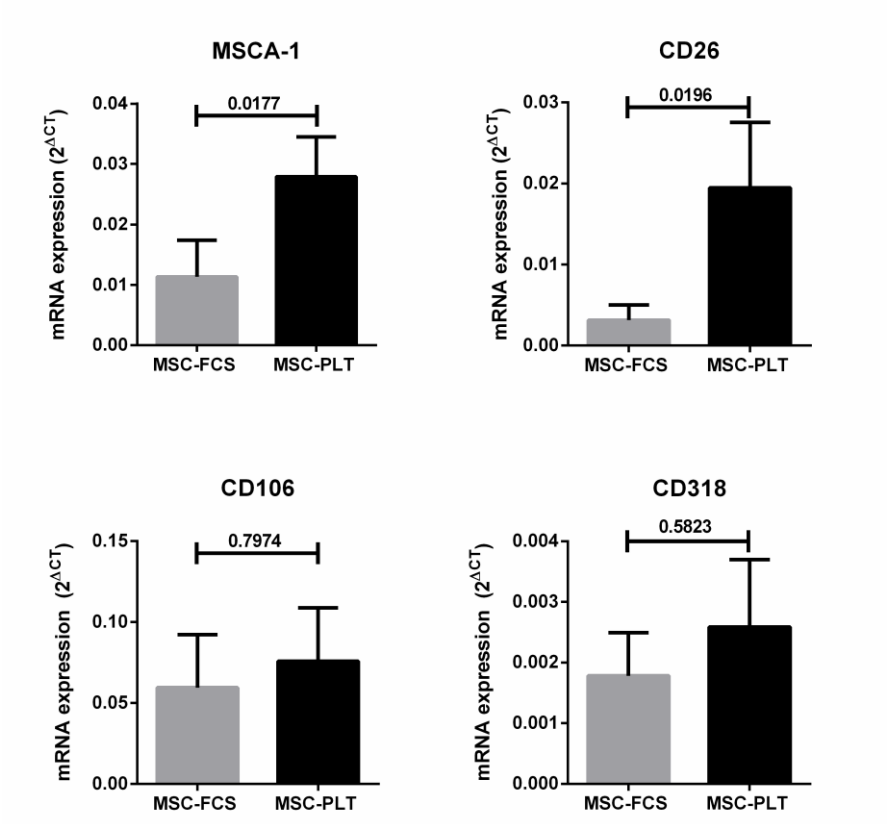

Figure 4.7: mRNA expression of 4 selected markers that were significantly upregulated on MSC-PLT as assessed by the Lyoplate technology.

Gene expression of MSCA-1, CD26 , CD106, and CD318 were measured by qPCR and normalised to GADPH. Results represent mean ± SEM of n=3.

4.3.4. Pathway and Network enrichment analysis

The 13 overexpressed markers in MSC-PLT were used to identify enriched pathways and associated networks based on a calculated probability score of ≥2 and a p-value of <0.05 using ingenuity pathway analysis (IPA) software application. The top enriched canonical pathways identified by the IPA software are described in **Fig. 4.8**. The pathways “Leukocyte extravasation signalling”, “CD40 signalling” and TREM1 signalling” were the most significantly upregulated pathways in MSC-PLT.

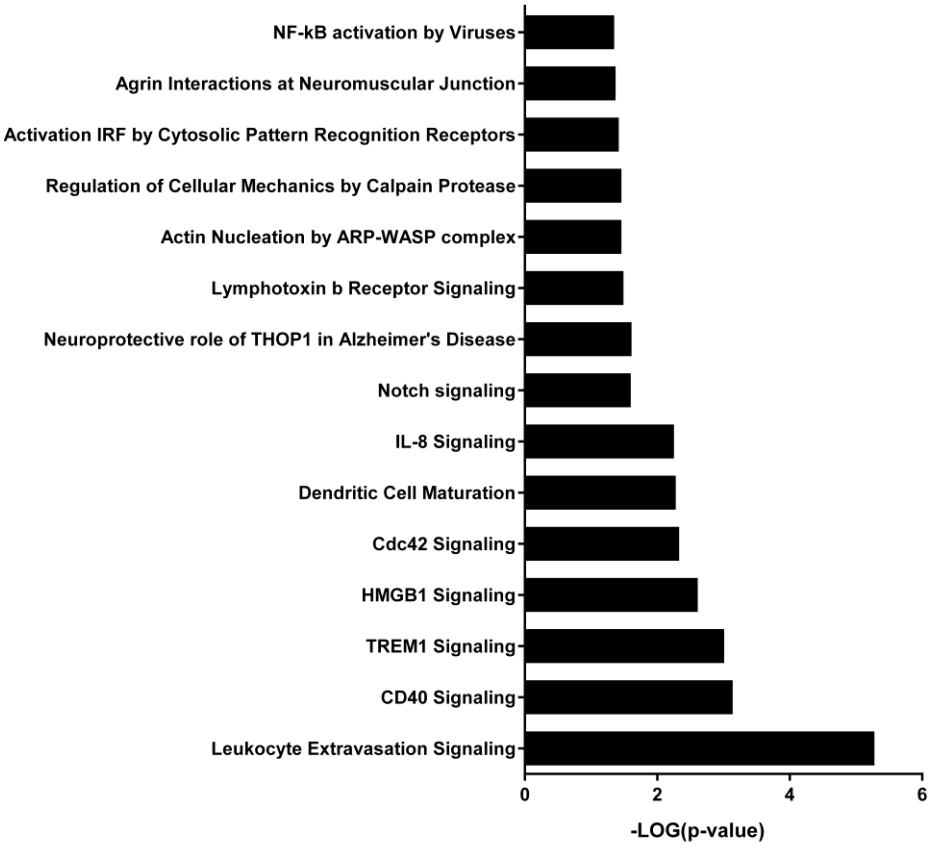

Figure 4.8: Top 15 canonical pathways influenced by the markers upregulated in MSC-PLT.

The 13 overexpressed markers were queried on IPA software. The height of the bars represents the number of genes associated with that specific canonical pathway which exhibited a p-value <0.05. The x axis shows the negative log of the p-value and the y axis displays the canonical pathways.

Network analysis revealed the association of these markers in 3 different networks. The first network, with a score of 24, included 9 of 13 the markers and is associated with inflammatory responses. This network's key components included the P38 mitogen-activated protein kinases (MAPK), the extracellular signal-regulated kinase (ERK) 1/2, TGF-β, interferon- (IFN-) γ and tumour necrosis factor- (TNF-) α families (**Fig. 4.9**). The second network, scoring 9, is associated with the carbohydrate metabolism, and contains 4 of the 13 markers. This network's key component is the G-protein-coupled receptor (Gpcr) family, which act as mediators of the energy metabolism and lead to the activation of pathways like the vascular endothelial growth factor (VEGF) (Richard *et al.*, 2001) and the insulin growth factor (IGF) pathway (Rozengurt *et al.*, 2010) (**Fig. 4.10**). The third network, with a score of 4, is associated with cellular mobility and migration and includes 3 of the 13 markers. This network is a central component of the guanosine triphosphatase (GTPase) family which regulate the actin cytoskeleton and the mobility of various cells, including MSCs and lymphocytes (Murali and Rajalingam, 2014) (**Fig. 4.11**). A summary of all the components of the three different pathways is described in **Supplementary Table S4.7**.

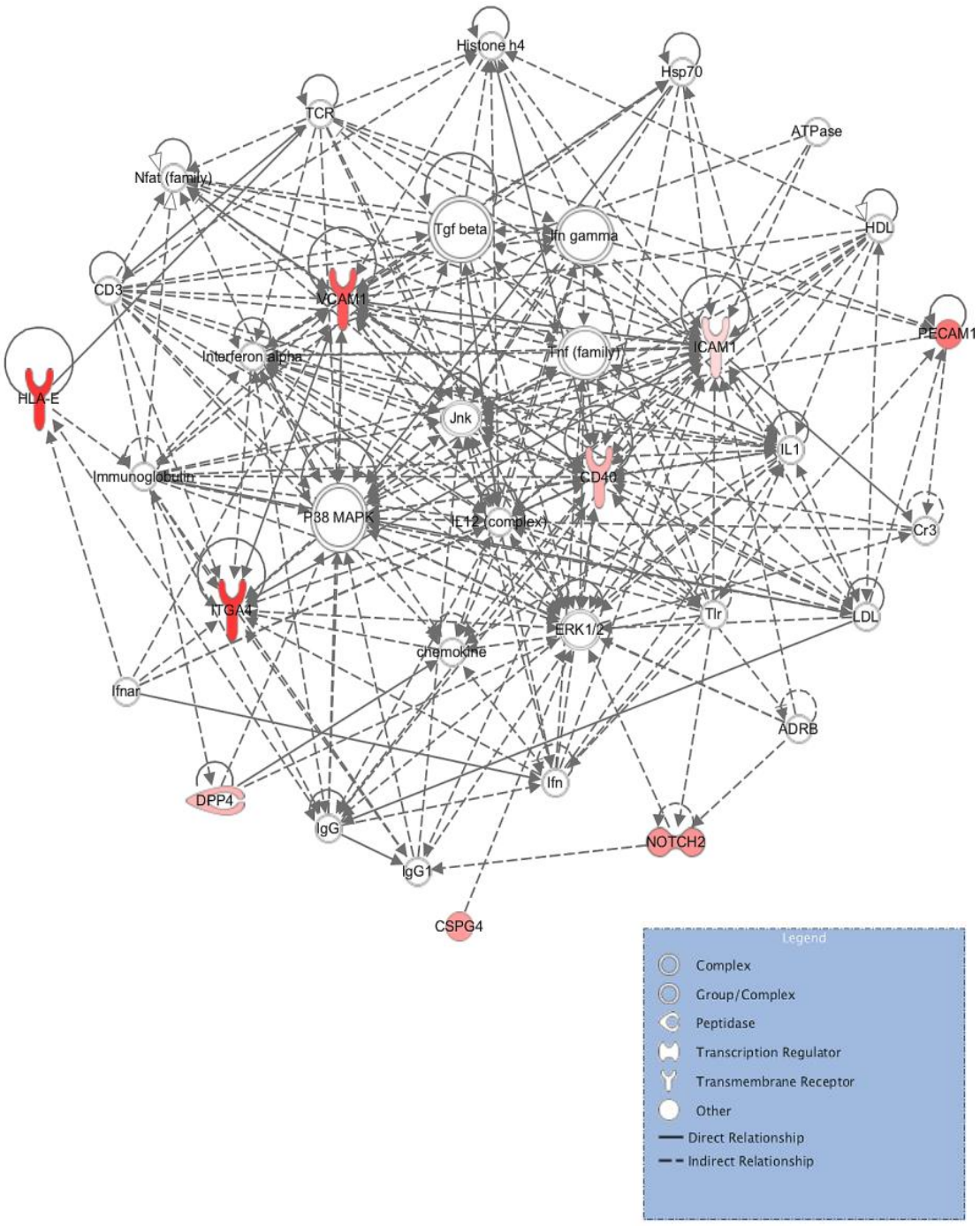

Figure 4.9: Network 1 shows the most significant interactions of 9/13 upregulated markers in MSC-PLT with genes involved in inflammatory responses

Network 1, with a score of 21, is related to inflammatory responses Dark red: upregulated markers with highest fold-increase; light red: upregulated markers with lower fold-increase.

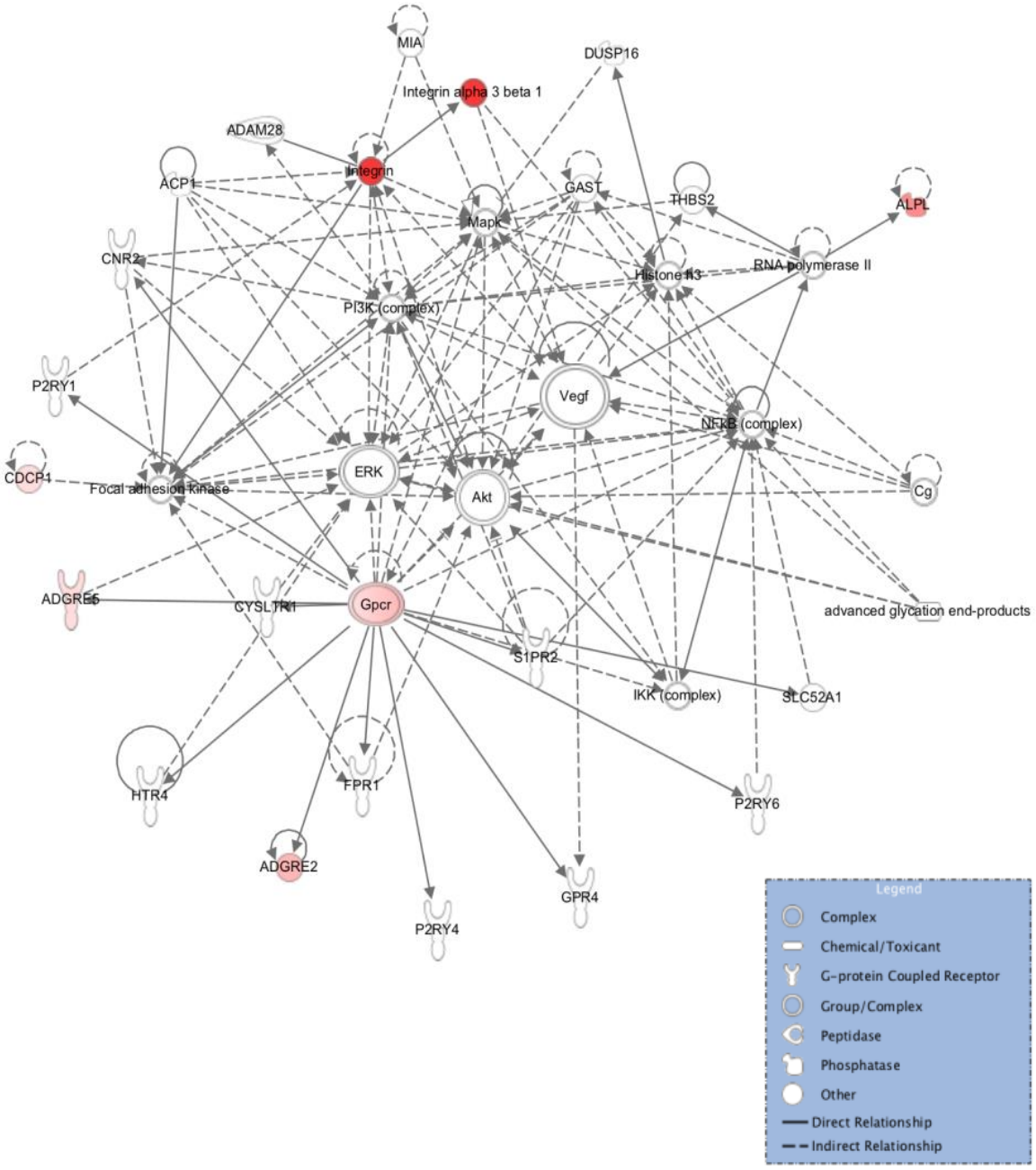

Figure 4.10: Network 2 shows the most significant interactions of 4/13 upregulated markers in MSC-PLT with genes involved in carbohydrate metabolistm

Network 2, with a score of 9, is related to carbohydrate metabolism Dark red: upregulated markers with highest fold-increase; light red: upregulated markers with lower fold-increase.

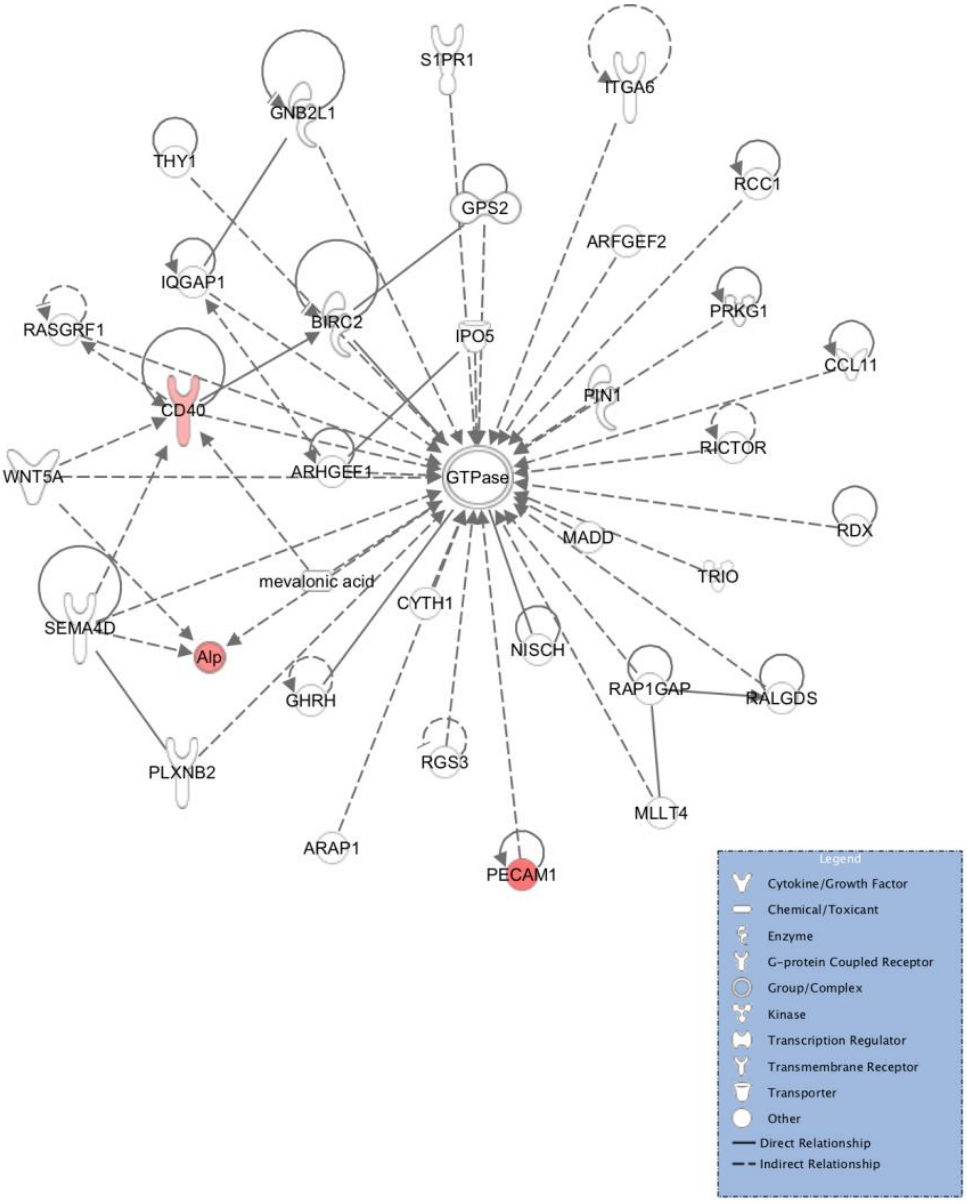

Figure 4.11: Network 3 shows the most significant interactions of 3/13 upregulated markers in MSC-PLT with genes involved in cellular motility

Network 3, with a score of 4 is connected to cell movement. Dark red: upregulated markers with highest fold-increase; light red: upregulated markers with lower fold-increase.

4.4. Discussion

In this study, we present the first comprehensive surface marker characterisation of MSCs expanded in PLT supplemented medium in comparison to FCS expanded MSCs. Over 300 surface markers were screened using high-throughput flow cytometry. The aim of this study was to characterise the phenotype of MSC-PLT and to identify markers that were differentially expressed by PLT and FCS expanded MSCs.

Using the lyoplate analysis, we verified that PLT-expansion does not induce marked changes in the expression of the main characteristic markers. Three distinct groups of markers were identified with the lyoplate analysis. Two groups included markers that were highly expressed or not detected on the surface of MSC-PLT and MSC-FCS, and the third group identified a subset of markers with variable expression between both MSC populations. PLT-expanded MSC phenotype was compliant with the ISCT criteria (Dominici *et al.*, 2006) and expressed other markers commonly detected on the surface of MSCs, such as CD44, CD29, CD10, CD13, CD95, among others. These observations are in accordance with previous studies which have shown no significant differences in the expression of proteins commonly found on the surface of MSCs (Abdelrazik *et al.*, 2011; Azouna *et al.*, 2012). Interestingly, in our study, no differences were detected in the expression of CD155 between MSC-FCS and MSC-PLT. This provides a logical explanation for the discrepancy in the resistance of MSC-PLT to NK cell mediated killing observed in our study and the study of Abdelzarik *et al* (2011) which has been reported in **Chapter 3**. CD155, also known as poliovirus receptor, (PVR) acts as ligand to DNAM-1, a transmembrane glycoprotein that upon cross-linking with its ligands, transduces activating signals that trigger NK- and CTL- mediated cytotoxicity (Pende *et al.*, 2005). Abdelzarik *et al* (2011) showed that PLT-expansion induced lower expression of CD155 on the surface of MSCs thus conferring higher resistance to NK cell mediated killing (Abdelrazik *et al.*, 2011). In our study the expression of CD155 was similar between MSC-PLT and MSC-FCS, supporting the comparable ability of both MSC populations in resisting NK-cell mediated cytotoxicity.

Previous studies have shown that the function and phenotype of BM-MSCs from different donors is highly dependent on the donor age and gender (Siegel *et al.*, 2013). PCA analysis of the different analysed samples revealed high individual variability within the MSC-FCS samples while MSC-PLT clustered together, suggesting that PLT may induce uniform upregulation of several surface markers, thus decreasing the variability between samples.

Globally, this study identified 13 markers (CD40, HLA-E, MSCA-1, CD97, CD106, CD54, Notch2, CD318, CD26, CD312, MCSP, CD31 and CD49d) that were differentially expressed between MSC-PLT and MSC-FCS. These differences were unidirectional showing an increased expression by MSC-PLT. To assess if this upregulation was at the mRNA level, expression of MSCA-1, CD318, CD26 and CD106 were validated using qPCR. Only CD26 and MSCA-1 showed significantly higher levels of mRNA in MSC-PLT than MSC-FCS. No significant differences were observed in the other two markers at mRNA levels between MSC-PLT and MSC-FCS. This validation was performed on three independent MSC samples. The low correlation of mRNA data and the surface protein expression analysis may be due to sample variability, protein turnover differences by MSC-PLT and MSC-FCS and post-transcriptional or post-translational modifications.

Analysis of the 13 overexpressed markers with the IPA database yielded 15 canonical pathways that were upregulated by overexpression of these markers. The four most representative pathways, “Leukocyte extravasation signalling”, “CD40 signalling”, “triggering receptor expressed on myeloid cells 1 (TREM1) signaling” and “high mobility group protein B1 (HMGB1) signalling”, are involved in the transendothelial migration, inflammatory responses and osteoblast differentiation. This indicates that PLT-expanded MSCs have higher migratory capacity towards the sites of injury than MSC-FCS (Colonna and Facchetti, 2003; Elgueta *et al.*, 2009; Liu *et al.*, 2013; Lin *et al.*, 2016). Migration of MSCs has been shown to be enhanced by expansion in medium supplemented with platelet lysate or platelet-rich plasma, in comparison to MSC-FCS (Moreira Teixeira *et al.*, 2012; Murphy *et al.*, 2012). These effects are mainly attributed to the high concentration of growth factors present in platelet derivatives, such as, FGF, EGF, TGF-β1, PDGF, IGF-1, and VEGF (Crespo-Diaz *et al.*, 2011).

Collectively, these growth factors are involved in repair mechanisms by the activation of signalling pathways involved in cell proliferation, recruitment and motility thus promoting wound healing and neovascularisation (Ball *et al.*, 2007; Ng *et al.*, 2008; Chiara Barsotti *et al.*, 2013).

Additional network mining associated the 13 upregulated markers on MSC-PLT into three distinct networks. The first network, yielding the highest score, comprises 9 of the 13 differential markers, including, HLA-E, CD40, CD49d (ITGA4), CD26 (DPP4), CD31 (PECAM1), Notch2, MCSP (CSPG4), CD54 (ICAM1) and CD106 (VCAM1). This network includes protein complexes and cytokines that play major roles in inflammatory responses, such as, IFN-γ, TNFα and p38 MAPK (Herlaar and Brown, 1999; Cantaert *et al.*, 2010). This data indicates MSC-PLT may have compromised immunosuppressive capacity than their FCS-expanded counterparts, by eliciting pro-inflammatory immune responses. It is well established that MSCs are potent suppressors of immune responses. One premise for this effect is the lack of expression of co-stimulatory molecules such as CD80, CD83, CD86 and CD40 (Jacobs *et al.*, 2013a). In our study, PLT expanded MSCs did not express CD80, CD83 or CD86, however, they showed increased expression of CD40. This marker binds to its ligand, CD40L and contributes to the pro-inflammatory signalling cascade (Elgueta *et al.*, 2009). Results presented in **Chapter 3** demonstrated that MSC-PLT and MSC-FCS have similar capacity to suppress immune responses, indicating that increased expression of CD40 on MSC-PLT does not influence their immunomodulatory properties. The expression of the co-stimulatory markers seemed to be counter-balanced by the upregulation of markers that confer higher suppressive capacity to these cells. One such marker, having a key node in the network, is CD106 which has been associated with enhanced immunoregulatory properties in MSCs (Ren *et al.*, 2010; Yang *et al.*, 2013b). CD106 is a marker used to select MSCs with increased clonogenic CFU-F ability and higher differentiation capacity. Recent studies by Yang *et al* (2013) demonstrated that $CD106^{+}$ MSCs had higher capacity to modulate T cell responses (Yang *et al.*, 2013). Noteworthy, one of the key proteins in this network is TGF-β. This growth factor confers increased proliferation and a bias towards chondrogenic and osteogenic differentiation by MSCs (Roelen and Dijke, 2003).

The second network includes 4 of the 13 markers, CD318 (CDCP1), MSCA-1 (ALPL), CD312 (ADGRE2) and CD97 (ADGRE5). These markers are associated with carbohydrate metabolism and have the G protein-coupled receptor (Gpcr family) as the central node. This family encompasses a variety of receptors involved in the regulation of cellular and physiological processes by regulating the metabolic activity in the cells (Choi *et al.*, 2015). In stem cells, these receptors are implicated in higher proliferative and migratory capacity (Doze and Perez, 2013). Additionally, this network contains, as an important node, the MSCA-1 (ALPL) marker. $MSCA1^{+}$ MSCs are effective at differentiating into osteoblasts and chondrocytes (Estève *et al.,* 2016).

The third network contains CD40 and PECAM1 and is associated with cell movement. It has as central node the Rho family of guanosine triphosphatases (GTPases). Members of this family play important roles in cytoskeletal rearrangements that are crucial in a set of specialised functions, including, self-renewal, adhesion and migration (Murali and Rajalingam, 2014). In MSCs, the Rho-GTPase signalling regulates commitment into osteogenic and adipogenic differentiation (Sherwin *et al.*, 2014). Taken together, this data indicates an upregulation of pathways related to self-renewal and mesodermal differentiation by MSCs expanded in the presence of PLT.

Overall, data presented in this Chapter further supports the notion that PLT is a suitable replacement for FCS in the expansion of MSCs. Here we identified several markers that were significantly upregulated on the surface of MSC-PLT. The promoting effects on MSC proliferation, migration and regenerative potential make PLT an ideal expansion supplement for applications in regenerative medicine and tissue repair. To our knowledge, data presented in this chapter is the first to describe differences in the expression of these markers at surface protein levels between PLT- and FCS- expanded cells. Nonetheless, this screening is in accordance with previous reports in MSC-FCS and shows that MSCs represent a heterogeneous population of cells with many different subpopulations that could potentially have different functional abilities. In the future, further studies need to be performed to investigate the functional ability of these subpopulations with the aim of identifying the ideal subsets for MSC therapeutic application.

Chapter 5: Isolation and characterisation of MSC-derived extracellular vesicles and assessment of their immunosuppressive capacity

“Somewhere, something incredible is waiting to be known”

– Carl Sagan

Chapter 5: Isolation and characterisation of MSC-derived extracellular vesicles and assessment of their immunosuppressive capacity

5.1. Introduction

Despite their multiple potential, MSC mode of action remains unknown. Various observations demonstrated that MSCs are sequestered in the lungs, spleen and liver, shortly after administration (von Bahr *et al.,* 2012). As a result, the initial paradigm envisaging MSC engraftment into the sites of injury has shifted towards an effect mainly accounted to their secreted factors (Liang *et al.,* 2014). These include a wide variety of secreted proteins, including cytokines, growth factors, and EVs.

Research focused on MSC-EVs is fairly recent. It was not until Timmers *et al* (2007) identified EVs as the main active component in MSC-supernatants for the treatment of myocardial ischemia, that laboratories worldwide have started exploring their therapeutic potentials. EVs are bilipid membrane vesicles enclosing a variety of bioactive proteins, such as cytokines, growth factors and enzymes, and genetic material, including microRNA and mRNA, among others (Colombo *et al.,* 2014). There are three main types of EVs: exosomes, microvesicles and apoptotic bodies (Colombo *et al.,* 2014). Their sizes, biogenesis and characteristics have been thoroughly described in **Chapter 1**. Particular focus has been given to the two main types of EVs, exosomes and microvesicles, due to their promising therapeutic effects.

MSC-EVs have been shown to reproduce the effects of their parent cells in models of myocardial ischemia and acute kidney reperfusion (Gatti *et al.,* 2011; Lai *et al.,* 2010). Treatment with MSC-EVs in ischemia/reperfusion preclinical models has been mainly attributed to the induction of pro-survival stimuli and angiogenesis. These effects seem to be a direct result of the delivery of proteins and genetic material (e.g. miRNA and mRNA), increased ATP production and activation of AKT signalling (Arslan *et al.,* 2013).

Recent studies have reported the beneficial effect of MSC-EVs in modulating immune responses. MSC-EVs has been shown to inhibit proliferation and differentiation of B lymphocytes and to cause T cell apoptosis and induce tolerogenic responses by promoting the generation of $CD4^+CD25^+FoxP3^+$

regulatory T cells (Budoni *et al.,* 2010; Del Fattore *et al.,* 2015; Mokarizadeh *et al.,* 2012). Studies with macrophages have shown that MSC-EVs induce an M2 anti-inflammatory phenotype characterised by the production of anti-inflammatory cytokines IL-10 and consequent generation of regulatory T cells (Zhang *et al.,* 2014). To date the effect of MSC-EVs on dendritic cell phenotype and function has not been explored. This chapter sought to examine MSC-EV mediated phenotypic and functional changes in dendritic cells. This investigation was focused on the following areas:

- Isolation and characterisation of MSC-EVs
- The uptake of MSC-EVs by immune cells
- The capacity of MSC-EVs to suppress allogeneic T cell responses
- The effect of MSC-EV treatment on DC maturation and function, including:
    - Phenotype of MSC-EV-treated DCs
    - The ability of MSC-EV-treated DCs to process antigens
    - The ability of MSC-EV-treated DCs to stimulate allo-reactive T cell proliferation
    - The profile of cytokine production by MSC-EV-treated DCs
    - The migration capacity of MSC-EV-treated DC

5.2. Specific methods

5.2.1. Conditioning and purification of MSC-derived EVs

Conditioning and purification of MSC-EVs was performed as described in **Chapter 2**. Purified EVs were thoroughly washed in PBS, suspended in 100-200 µl of sterile PBS and stored at -80^{0}C until required.

5.2.2. Characterisation of MSC-EVs

5.2.2.1. Protein quantification

MSC-EV protein quantification was performed using the micro Bicinchoninic Acid (BCA) protein assay kit (Thermo Fisher Scientific). The micro BCA assay is a detergent-compatible solution for the quantification of dilute protein samples (0.5-20 µg/ml). This assay involves an initial reaction where Cu^{2+} ions are reduced to Cu^{+} by the peptide bonds in the protein sample in a temperature dependent reaction. Afterwards, two molecules of BCA chelate with each Cu^{+} ion, forming a purple-coloured product that absorbs light at a 562 nm wavelength. The amount of protein in the solution is quantified by measuring the absorption spectra and comparing with protein solutions, with known concentrations, to a standard curve, using y = mx+b equation, where y = absorbance, x = protein concentration of sample (µg/ml), b = intercept and m = standard curve slope.

Protein quantification was performed as per the manufacturer's protocol. Briefly, a serial dilution of bovine serum albumin (stock = 2 µg/ml, ThermoFisher Scientific), ranging 0.625 – 1.6 µg/ml was used as the standard. MSC-EV samples were first diluted at 1:15 ratio in PBS + 2% Sodium Dodecyl Sulfate (SDS), followed by the addition of micro BCA working reagent at a 1:1 ratio. The plates were then incubated for 120 minutes at 37^{o}C and finally read at 575 nm using a Multiskan Ascent plate reader (Thermo, Labsystems).

5.2.2.2. Transmission Electron Microscopy

Transmission electron microscopy was used to analyse the morphology of MSC-EVs. The transmission electron microscope (TEM) uses electrons as "light source", which makes it possible to get a better resolution than a light microscope, due to the lower wavelengths of electrons. Objects detected by

TEM can be as small as a few angstroms (10^{-10}m). Briefly, 10 µl of PBS suspended MSC-EVs were adsorbed for 1 minute onto a carbon-coated grid. Excess liquid was removed with a filter paper (Whatmann no. 1), and samples were stained with 1% uranyl acetate for 30 seconds. After excess uranyl acetate solution was removed, the MSC-EV loaded carbon-coated grids were dried by exposure to glow discharge. Grids were then examined using a Philips CM100 TEM and images were acquired using an AMTV540 camera (Philips).

5.2.2.3. Nanoparticle tracking analysis of MSC-EVs

Size and particle concentration was measured by Nanosight LM10 (Malvern). The nanosight, with nanoparticle tracking analysis (NTA) software visualises and analyses particles suspended in liquids from 10 to 2000 nm in diameter by tracking the Brownian motion of the particles, i.e., the irregular movement of particles suspended in a fluid, caused by collisions between these particles and the molecules of the fluid. The light is scattered by the nanoparticles with laser illumination being captured by a digital camera, and the motion of each particle is tracked from frame to frame. Particle movement is then related to a sphere-equivalent hydrodynamic radius as measured by the Stokes-Einstein principle (**Fig.5.1**). In this study, MSC-EV pellets were diluted at a 1:100-1:500 ratios with sterile-filtered PBS and MSC-EV size and particle concentration was analysed using NTA. For accuracy and statistical analysis, at least 3 videos were acquired per sample and processed using NTA 2.3 software (Malvern).

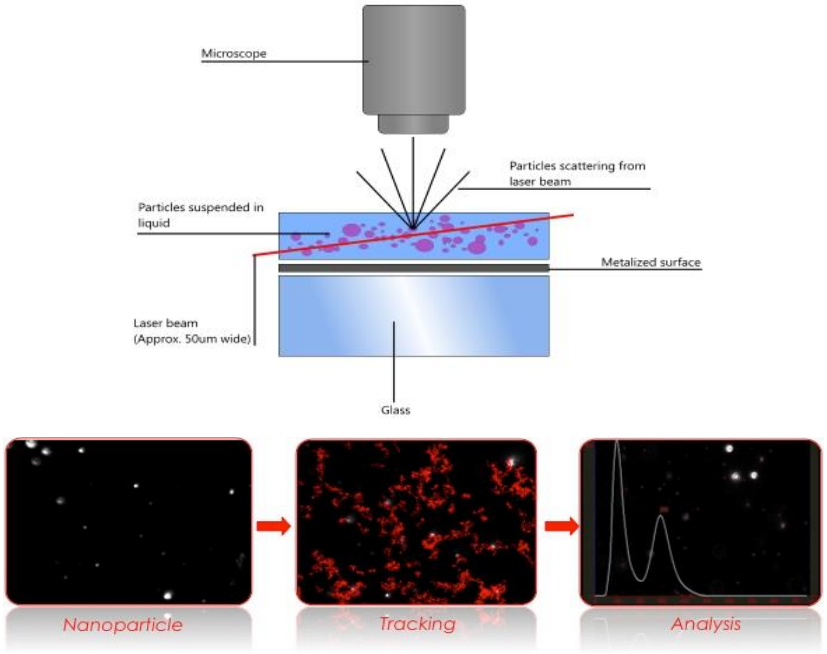

Figure 5.1: **Schematics of Nanosight principle.**

Laser is scattered and the diffracted light is captured by a camera perpendicular to the fluid pane. Nanoparticle movement is tracked according to their Brownian motion, with small particles moving faster than larger particles. Particle size and concentration is then calculated through application of the Stokes-Einstein equation (images adapted from www.malvern.com/products/product-range/nanosight-range/)

5.2.2.4. Analysis of MSC-EVs by Flow cytometry

Flow cytometry was used to analyse the expression of commonly used EV markers on the surface of MSC-EVs. Although the measurement of larger vesicles has been reported by flow cytometry, this methodology is not sensitive enough to detect smaller vesicles. To overcome this issue, detection of MSC-EVs was accomplished by coupling MSC-EVs to latex which is detectable by the flow cytometer. The MSC-EVs were then labelled with fluorochrome-conjugated antibodies and analysed by flow cytometry. Briefly, 1-5 µg of MSC-EV suspension were incubated with 2 µl of 4 µm latex beads (Life Technologies). The MSC-EV-bead mix was topped up to 1000 µl with sterile PBS and incubated overnight on a rotary wheel at RT. The reaction was blocked 1M glycine (Sigma) for 30 minutes at RT. The MSC-EV-bead complex was washed with PBS with 0.5% FCS and centrifuged twice at 5000 rpm for 4 minutes. The pellet was then suspended with FACS buffer and labelled with

CD63-PE, CD81-APC, CD9-PerCPCy5.5 and correspondent isotype controls as described **in Chapter 2**.

5.2.3. Assessment of MSC-EV immunosuppressive capacity

MSC-EV ability to suppress allogeneic-T cell responses was performed as described in **Chapter 2**. MSC-EVs were added to a MLR, consisting of $CD3^+$ T cells and allogeneic DCs at concentrations of 2, 4 and 20 µg/ml. The cells were incubated for 5 days at 37^0C, and T cell proliferation was assessed by 3H–thymidine incorporation or by CFSE dilution as previously described. MLR without MSC-EVs and $CD3^+$ T cells were used as positive and negative controls, respectively.

5.2.4. Assessment of MSC-EV uptake by immune cells

5.2.4.1. MSC-EV fluorescent labelling

Fluorescent labelling of EVs was carried out using PKH26 membrane linker dye (Sigma), following the manufacturer's protocol, with some modifications. Briefly, MSC-EV suspension was pelleted at 100,000xg for 90 minutes and re-suspended in 500 µl of Diluent C, provided by the kit. Another 500 µl of Diluent C were mixed with 2 µl of PKH26 dye. The MSC-EV suspension was then mixed with this stain solution and incubated for 5 minutes, with regular mixing in the dark, at RT. The labelling reaction was stopped with an equal volume of sterile 1% BSA (Sigma) and labelled MSC-EVs were washed twice with filtered PBS at 100,000xg for 90 minutes. MSC-EV pellet was then re-suspended in RPMI 1640 medium and added to the target cells.

5.2.4.2. Uptake of MSC-EVs by immune cells

Investigation of the uptake kinetics of MSC-EVs by immune cells was analysed using immunofluorescence microscopy. Briefly, 20 µg/ml of PKH26 labelled EVs were added to either DCs alone or a co-culture of DCs and TCs. After 24h of incubation at 37^0C in a 5% CO_2 humidified atmosphere, the cells were washed in PBS, suspended in serum-free media and $2x10^5$ cells were seeded onto a poly-L-lysine coated coverslip. The cells were incubated for 15 minutes at 37^oC to allow for attachment to the coverslip. Cells were then fixed with 2% paraformaldehyde (PFA) for 15 minutes at room temperature, washed twice

with PBS and blocked with antibody diluent, consisting of PBS with 0.1% Triton and 0.5% BSA, for 30 minutes at 4^{o}C. Staining of the DC and TC co-culture was carried out by incubating the cells with the primary antibody anti-CD3 (BD Biosciences, 1:100) overnight at 4^{o}C. The coverslips were washed twice with wash buffer, consisting of PBS with 0.1% Triton (Sigma) and 0.1% BSA, and incubated with secondary antibody Dy649 (Jackson Immunoresearch), at a 1:300 dilution for 2h at 4^{0}C in the dark. The coverslips were washed twice and incubated with a HLA-DR-FITC (BD Biosciences, 1:20) for an additional 4h, as previously mentioned. When MSC-EVs were co-incubated with DCs only, cells were treated as previously and co-incubated for 4h with HLA-DR-FITC. After washing with PBS, the samples were mounted with DAPI mounting medium (Vector Laboratories) for nuclei counter-staining. The immunofluorescence stained specimens were imaged using Axioimager Z2 fluorescence microscope with axiovision software V4.8 (Zeiss). PKH26 treated vehicle only (sterile PBS) was used as negative control.

5.2.5. Effect of MSC-EV treatment on DC maturation and function

The experimental workflow used to assess the effect of MSC-EV treatment on DC maturation and function is described in **Fig.5.2**. The majority of the methods are described in **Chapter 2**; specific methods used in these experiments are described below.

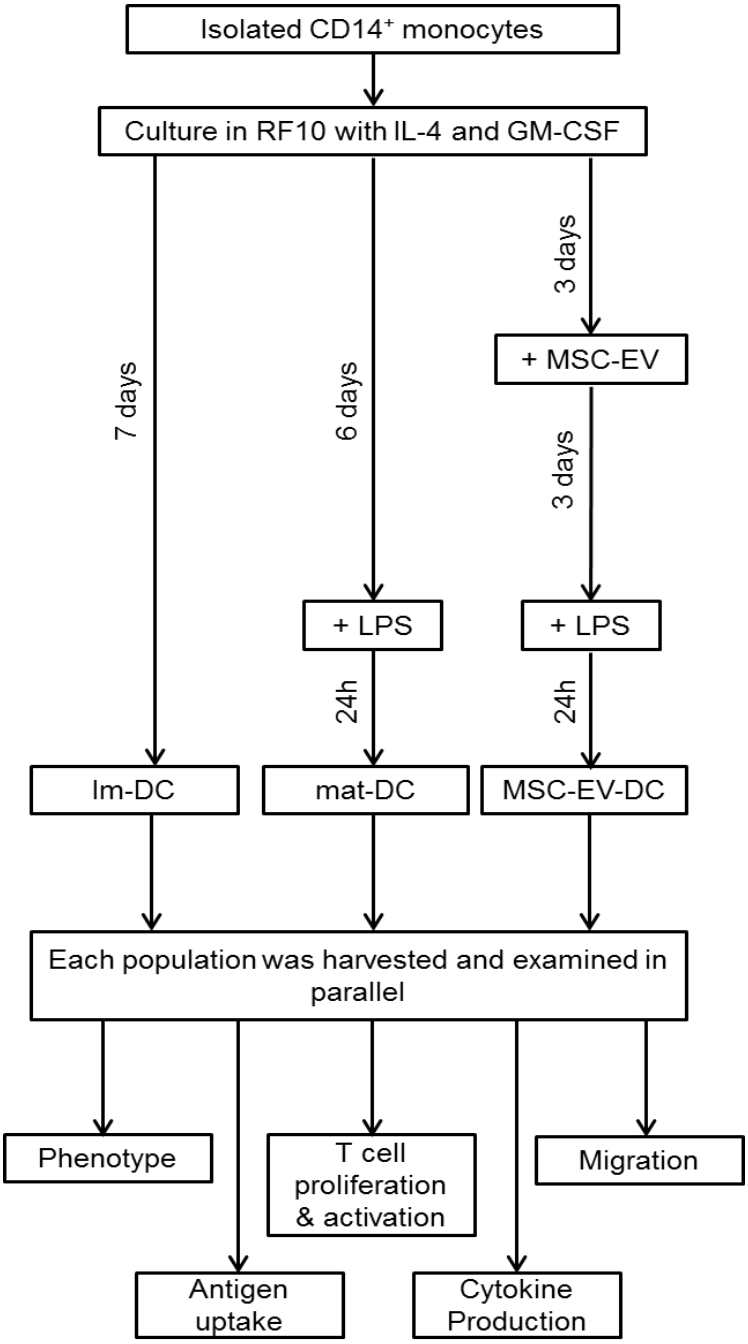

Figure 5.2: **Summary for experimental workflow for assessment of MSC-EV modulatory effect on DC**

Phenotype was assessed by flow cytometry; antigen uptake was assessed by FITC dextran uptake by immature DCs; Migration was assessed using Transwell system. T cell proliferation and activation was assessed following MLRs with third-party $CD3^+$ T cells and cytokine secretion was assessed by flow cytometry from analysis of supernatants collected from DC and MLR cultures.

5.2.5.1. Generation of MSC-EV-treated DCs

Monocyte-derived immature and mature DCs were generated according to conventional protocols with IL-4 and GM-CSF as described in **Chapter 2**. MSC-EV-treated DCs were generated by adding a titrated dose of MSC-EVs to DCs on day 3 of generation, as described by **Fig.5.2**. Untreated DCs were used as controls.

5.2.5.2. Antigen uptake assay

The phagocytic ability of immature DCs was performed by FITC-dextran uptake (Sigma-Aldrich). In brief, $5x10^4$ immature, mature and MSC-EV-treated DCs were incubated for 1h at 37^0C or 4^0C in RF10 with 1 mg/ml FITC dextran. Cells were washed three times with cold FACS buffer and the amount of FITC dextran taken up by DCs was analysed by flow cytometry.

5.2.5.3. Assessment of MSC-EV-treated DC migratory potential

DC migration was assessed as described by Anderson *et al* (2009) with small modifications to the protocol. Briefly, migration was measured using a transwell system, where at least 1 x 10^5 DCs suspended in RPMI 1640 medium, were added to the upper chamber (pore size 8 µm, Corning Life Sciences), and medium with or without CCL21 (250 ng/ml, R&D systems) was added to the lower chamber. DC migration was assessed after a 24h incubation period at 37^0C by harvesting the cells in the lower chamber and counting using a Neubauer chamber. Migration efficiency was expressed as the percentage of input DCs that had migrated. Mature DCs migrating towards medium with or without CCL21 were used as positive and negative controls, respectively.

5.3. Results

5.3.1. MSC conditioned with EV-depleted medium maintain phenotype and viability

In the previous chapters, the characterisation of MSCs expanded in PLT-supplemented medium established that the cells maintain morphological, general phenotypic and functional characteristics, including trilineage differentiation and immunosuppression. Further analysis showed that in comparison to FCS-expansion of MSCs, PLT-expansion induced changes in the expression of protein markers that were mainly related to MSC proliferative and differentiation properties. Given these results, MSC-EVs were purified from MSC-PLT.

Isolation of EVs from MSC culture supernatants was carried out by culturing MSCs at passage 3 until 70-80% confluence and then conditioning these cells for 48h. To avoid contamination by EVs presented in PLT used for MSC expansion, MSCs were conditioned in EV-depleted medium. To analyse the effect of 48h conditioning on MSC viability and phenotype, cells were harvested, counted and assessed for the expression of their common markers by flow cytometry. MSCs maintained high viability (>90%) (**Fig.5.3A**) and conformed to the ISCT immunophenotype (**Fig.5.3B**).

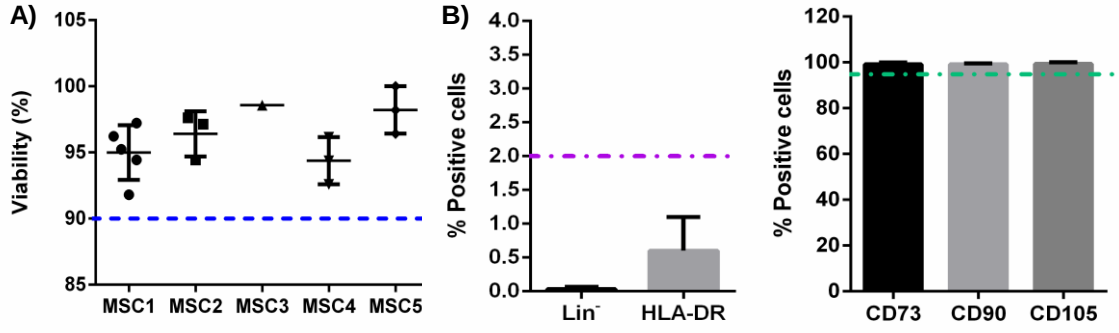

Figure 5.3: Assessment of MSC viability and phenotype after conditioning with EV-depleted medium

MSCs were conditioned with EV-depleted medium for 48h, after which (**A**) viability and (**B**) phenotype was assessed by trypan blue and flow cytometry analysis, respectively. Viability data of 15 different EV isolations from 5 different MSC samples are described. Results are expressed as mean ± SEM (n≥3). Lin^- represents CD14, CD19, CD34 and CD45

5.3.2. Purification and characterisation of MSC-EVs

Purification of MSC-EVs was performed by ultracentrifugation. This methodology relies on the collection of culture supernatant after MSC conditioning with EV-depleted medium. This supernatant goes through a series of centrifugations at 400xg, 2000xg and 10,000xg for clearing of cellular debris and contaminating proteins before pelleting MSC-EVs by centrifugation at 100,000xg. The resulting MSC-EV pellet was washed in cold PBS, spun down and re-suspended in a small volume of cold sterile PBS. The morphological and phenotypic properties of these vesicles were then analysed by quantification of protein and particle number, size range, morphology and expression of known EV markers.

MSC-EV purification from $4.24x10^7 \pm 3.05x10^6$ MSCs yielded an average of $1.16x10^{11} \pm 2.95x10^{10}$ particles/ml (**Fig. 5.4A**), with each MSC secreting 432 ± 229 particles (**Fig. 5.4B**). Additionally, the results from several MSC-EV purifications reveal that an increase in particle number is accompanied by an increase in protein concentration (R^2= 0.9473), indicating that protein increase is an effect of higher particle number (**Fig. 5.4C**). Purified MSC-EVs had a modal size of 152 ± 23 nm (**Fig.5.4D**), and exhibited the expected cup-shaped morphology, as assessed by TEM (**Fig. 5.4E**). However, their sizes ranged from 30 to 180 nm as determined based on the smallest and greatest observed vesicles in several micrographs obtained by TEM (**Fig.5.4**). This indicates that the MSC-EVs isolated from MSC culture supernatants comprise a mixture of vesicles of larger size, also known as microvesicles, and exosomes, which are usually sized at <100nm ranges.

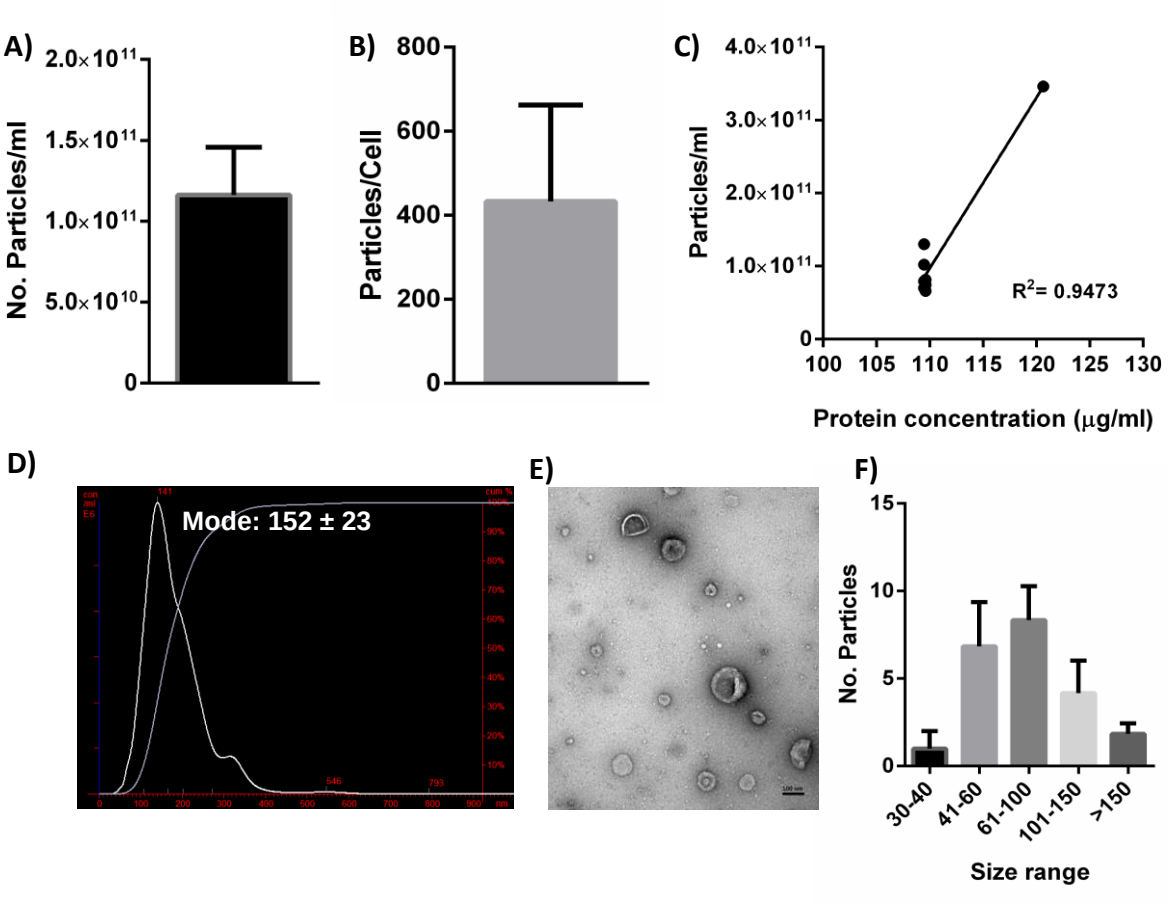

Figure 5.4: Quantification, size and morphological characterisation of MSC derived EVs.

A) Cumulative particle number as detected by NTA; **B)** Average number of particles secreted per cell; **C)** Correlation between particle number and protein concentration; **D)** Representative size distribution of MSC-EVs as determined by NTA and **E)** Representative TEM micrographs of MSC-EVs; **F)** Particle size ranges as detected by TEM. Scale bar = 100 nm (magnification of 64,000x, operating at a voltage of 100.0kV). Results are expressed as mean ± SEM (n≥4).

MSC-EVs were assessed for the expression of EV markers, CD63, CD9 and CD81. These markers are members of the tetraspanin family which plays a role in the intracellular trafficking of vesicles. CD63 is mainly expressed on the surface of exosomes (Colombo *et al.,* 2013) while CD9 is widely found on the surface of microvesicles and CD81 is both a microvesicles and exosome marker (Bobrie *et al.,* 2012).

Representative histograms show expression of CD63, CD9 and CD81 on the pellet resulting from the 100,000xg (**Fig. 5.5A**). Cumulative data of EVs derived from 4 different MSC samples demonstrate that MSC-EVs are mostly enriched in CD63, displaying an expression of 84.2% ± 6.9 in comparison to 38.0% ± 8.9 and 34.89% ± 12.6 for CD81 and CD9, respectively (**Fig. 5.5B**).

This data indicates that, despite the different size ranges detected in the various MSC-EV preparations, these are mostly composed of exosomes and contain a small percentage of microvesicles. Despite this heterogeneity, this data indicates the feasibility of isolating EVs from MSCs supernatants. The obtained MSC-EVs were used to assess their immunosuppressive potential in further experiments.

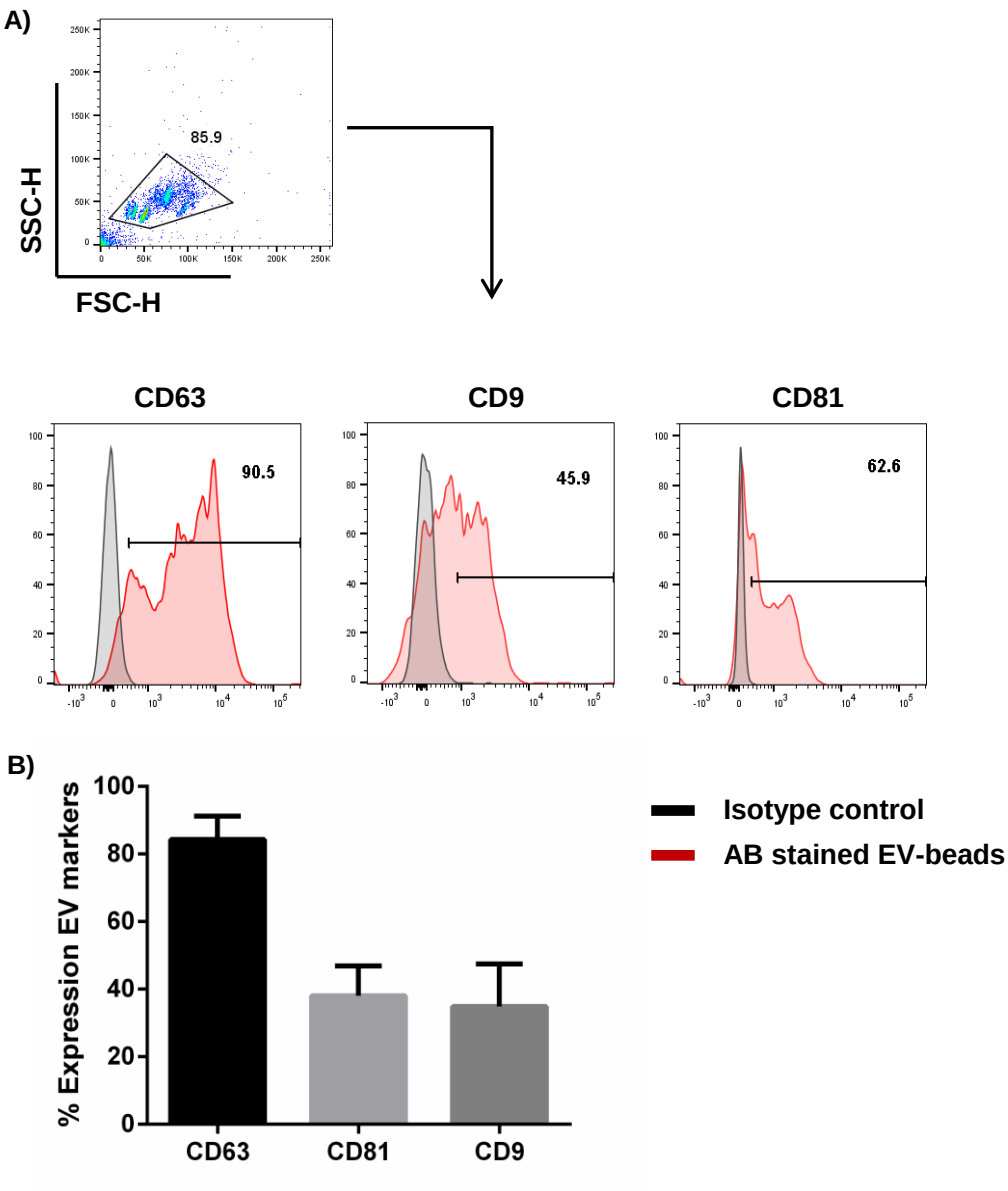

Figure 5.5: Detection of CD63, CD9 and CD81 expression in MSC-EV

A) MSC-EV bound beads were selected according to SSC-H/FSC-H characteristics and expression of CD63, CD9 and CD81 was analysed on pellets resulting from 100,000xg spin. **A)** Representative histograms show enrichment of EV markers. Positive gates were drawn based on isotype controls. **B)** Cumulative data of CD63, CD9 and CD81 expression by MSC-EVs. Results represent mean ± SEM of n=4

5.3.3. MSC-EV suppress T cell proliferation

One of the main characteristics of MSCs, is their ability to suppress T cell proliferation. In order to assess whether MSC-EVs retained the immunosuppressive capacity of the parent cells, a range of MSC-EV concentrations were added to a MLR consisting of $CD3^+$ T cells and allogeneic DCs. Co-culture was carried out for 5 days and T cell proliferation was assessed by either 3H-thymidine incorporation or CFSE dilution by flow cytometry.

Non-stimulated $CD3^+$ T cells and MLR without MSC-EVs were used as negative and positive controls, respectively. In the presence of titrated MSC-EV concentrations, a dose dependent decrease of allo-DC stimulated proliferation of T cells was observed. The inhibition rates were of 30% ± 4.5, 22.0% ± 2.5 and 11.6% ± 3.4 for the titrated concentrations of MSC-EVs as shown in **Fig. 5.6A**. In **Chapter 3**, MSCs proved to exert a strong *in vitro* inhibitory effect on the proliferation of allo-DC stimulated T cells, with an inhibition of 74.3% ± 8.5 at highest MSC concentration (**Fig. 3.7**). Altogether, these data indicate that, although MSC-EVs display an antiproliferative effect on T cells, the parent MSCs possess a significantly superior ability of inhibition (**Fig.5.6B**).

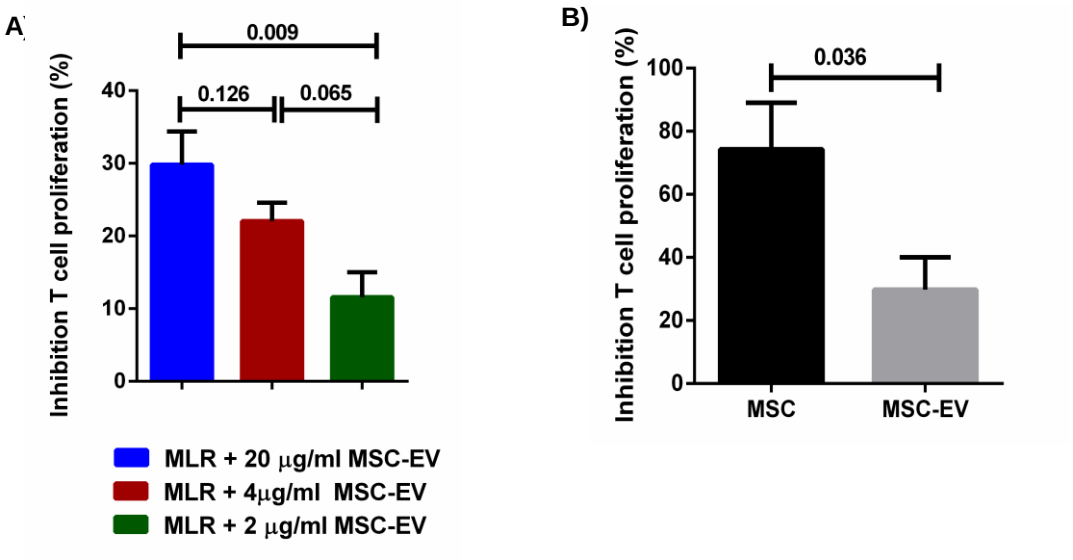

Figure 5.6: MSC-EVs suppress T cell proliferation in a dose dependent manner

A) Inhibition of T cell proliferation after treatment with a titrated dose of MSC-EVs; **B)** Comparison of antiproliferative effect of MSCs and MSC-EVs on T cells; Results are expressed as mean ± SEM of inhibition of T cell proliferation of n=3, and a p-value <0.05 was considered significant.

To further analyse if the T cell subsets, $CD4^+$ or $CD8^+$ T cells were preferentially targeted by the MSC-EVs, these experiments were repeated using flow cytometry and a fixed concentration of MSC-EVs (20 µg/ml). An inhibition of proliferation of $CD4^+$ and $CD8^+$ T cells of 27.2% ± 7.7 and 35.7% ± 13.0 was detected after MSC-EV treatment (**Fig. 5.7**).

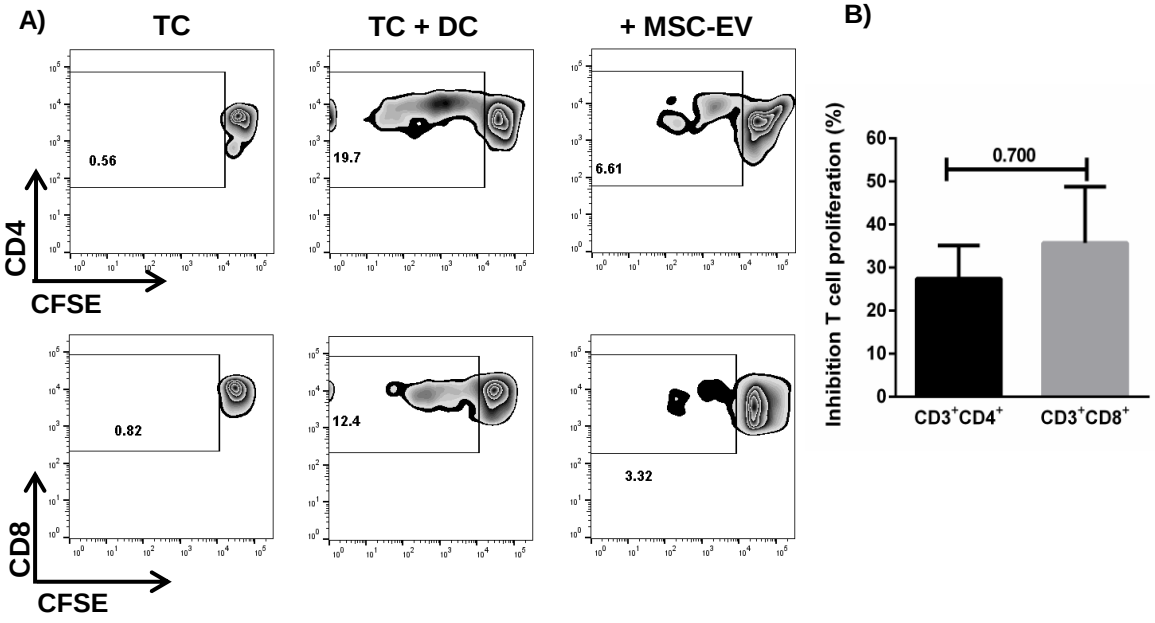

Figure 5.7: MSC-EVs equally suppress $CD4^+$ and $CD8^+$ T cells

A) Representative plots of CFSE dilution of T cells stimulated with allogeneic DCs and co-cultured with 20 µg/ml MSC-EVs. T cells alone and MLR were used as negative control respectively. **B)** Cumulative percentage of inhibition of T cell proliferation after EV co-culture of N=3. Results are expressed as mean ± SEM.

5.3.4. MSC-EVs are preferentially taken up by DC

In order to investigate the association of MSC-EVs with immune cells, PKH26 labelled MSC-EVs were incubated with a co-culture of DC and allogeneic T cells. The uptake of MSC-EVs by T cells and DCs was assessed using immunofluorescence microscopy.

The co-localisation analysis revealed a predominant association of the MSC-EVs with the HLA-DR positive DCs, as assessed by the overlapping red (PKH26) and green (HLA-DR) fluorescence (**Fig. 5.8**). No association was detected between $PKH26^+$-MSC-EVs and $CD3^+$ T cells.

Efficient uptake of MSC-EVs by DCs was further confirmed by additional experiments, in which $PKH26^+$-MSC-EVs were incubated with DCs cultured with IL-4 and GM-CSF for 24 hours. HLA-DR labelled DCs showed a strong association with $PKH26^+$-MSC-EVs as evidenced by the strong red signalling on the DCs (**Fig. 5.9**).These results have prompted investigation into the effect of MSC-EVs on DC maturation and function, which are reported in the following sections.

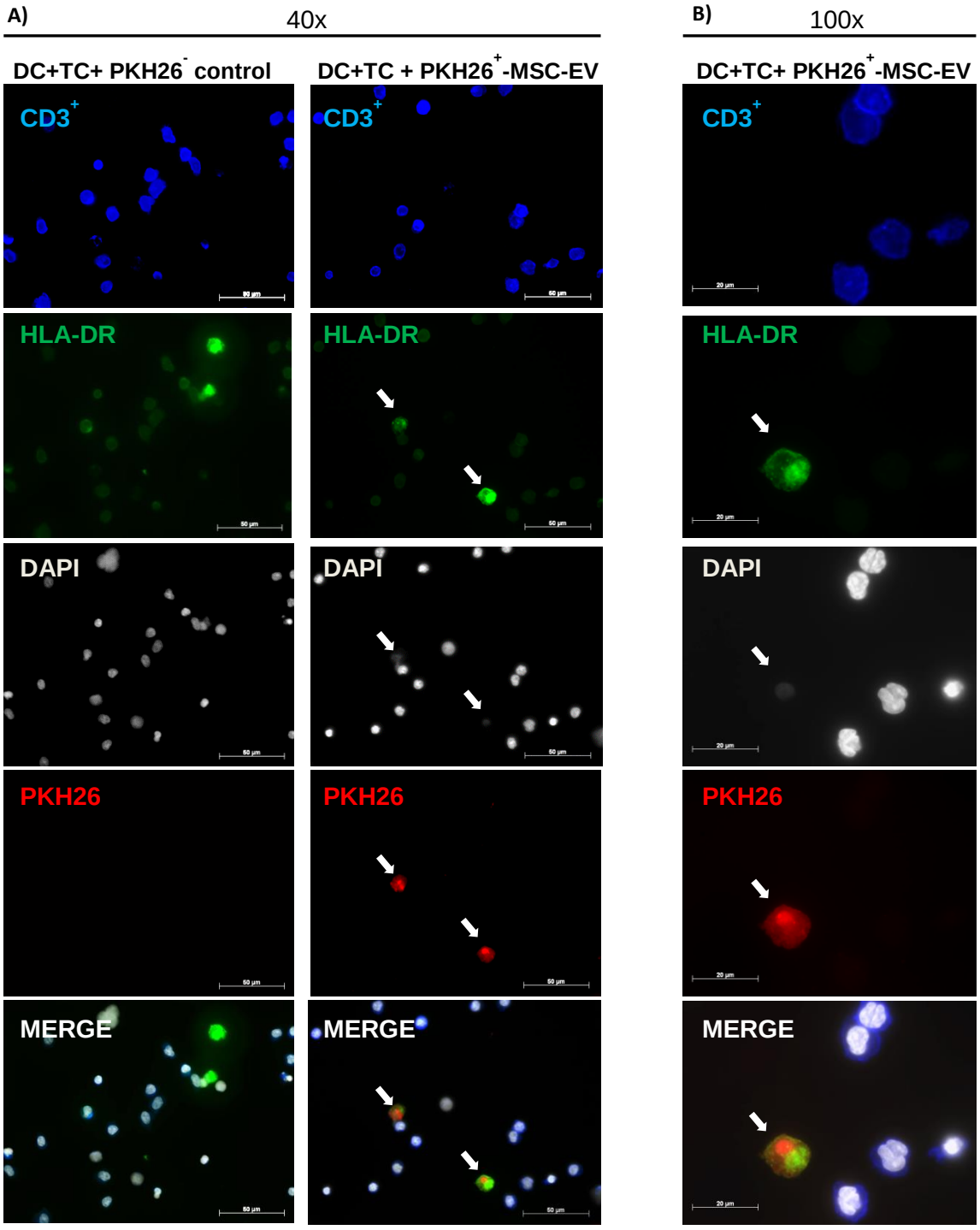

Figure 5.8: In an allogeneic-DC and CD3$^+$ T cell co-culture, MSC-EVs are preferentially taken up by DC

Representative immunofluorescence images of PKH26$^+$-MSC-EV (red) association with DCs (green). No uptake of MSC-EVs was detected by CD3 labelled T cells (blue). A PKH26 treated PBS control was used as negative control. Images were acquired using a Zeiss confocal microscope. Scale bars represent 50 (**A**) and 20 (**B**) µm.

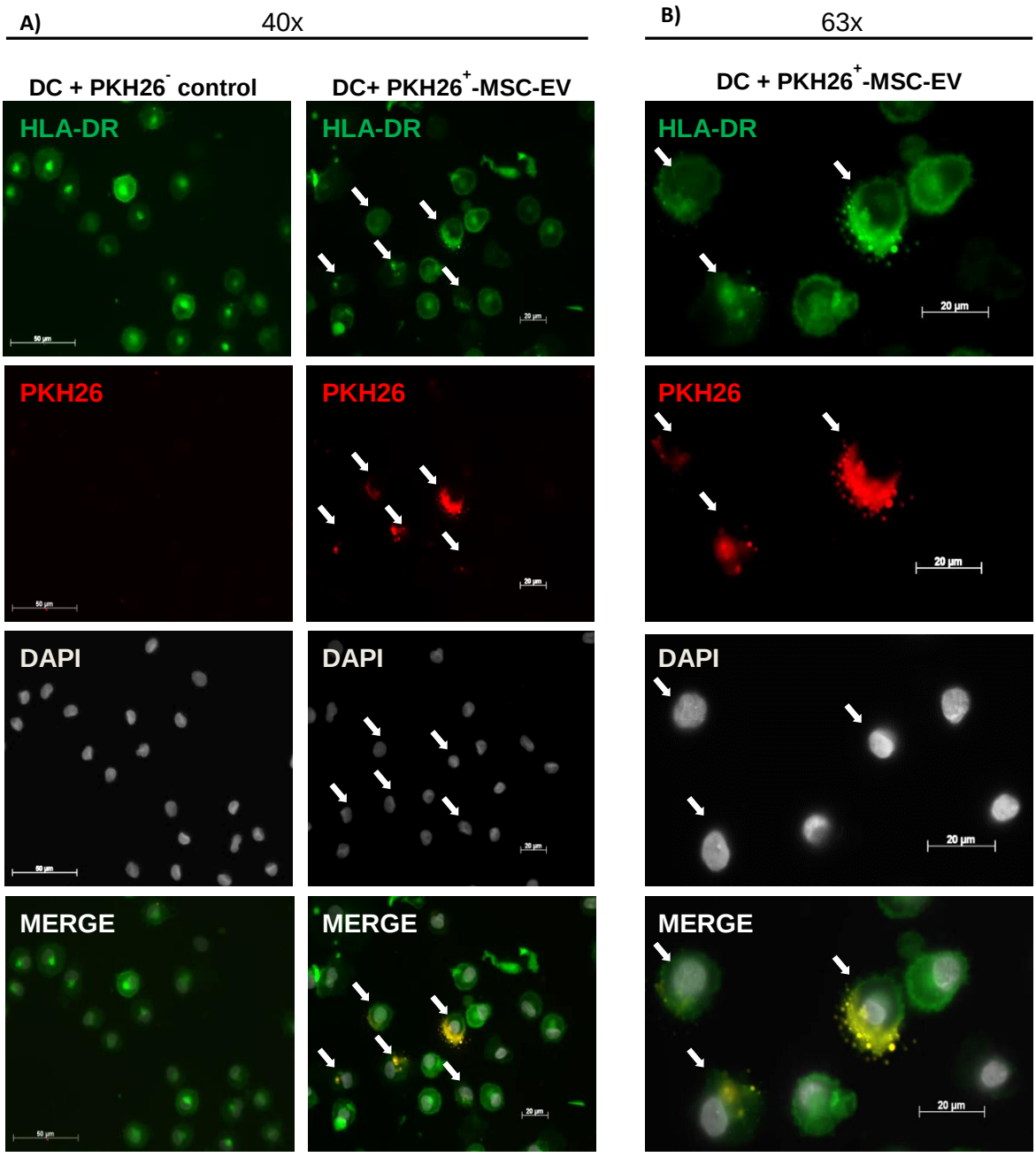

Figure 5.9: MSC-EVs are taken up by DCs during maturation

Representative immunofluorescence images of PKH26^{+}-MSC-EV (red) association with the HLA-DR^{+} DCs (green). A PKH26 treated PBS control was used as negative control. Images were acquired using a Zeiss confocal microscope. Scale bars represent 50 (**A**) and 20 µm (**B**).

5.3.5. MSC-EV treatment impairs LPS-induced maturation of DCs

Previous studies have reported that MSCs have a strong inhibitory effect on maturation and function of DCs (Chen *et al.,* 2007; Consentius *et al.,* 2015). To assess whether MSC-EVs were capable to inhibit DC maturation and function, MSC-EVs at a titrated dose of 10 and 20µg/ml were added to DCs during maturation. Immature, mature and MSC-EV treated DCs were successfully generated according to conventional protocols by culturing $CD14^+$ monocytes in RF10 supplemented with GM-CSF and IL-4 for 7 days. $CD14^+$ monocytes were successfully isolated using MACS technology to a purity of >90% (**Fig. 5.10A**). Following culture, the monocytes lost the expression of CD14 and gained the expression of CD1a, indicative of their differentiation into immature DCs (**Fig. 5.10B**). DC maturation was then induced for 24h with LPS. Maturation efficiency of DCs was confirmed by increased expression of the co-stimulatory molecules CD80, CD83, CD86 and HLA-DR (**Fig. 5.10C and D**).

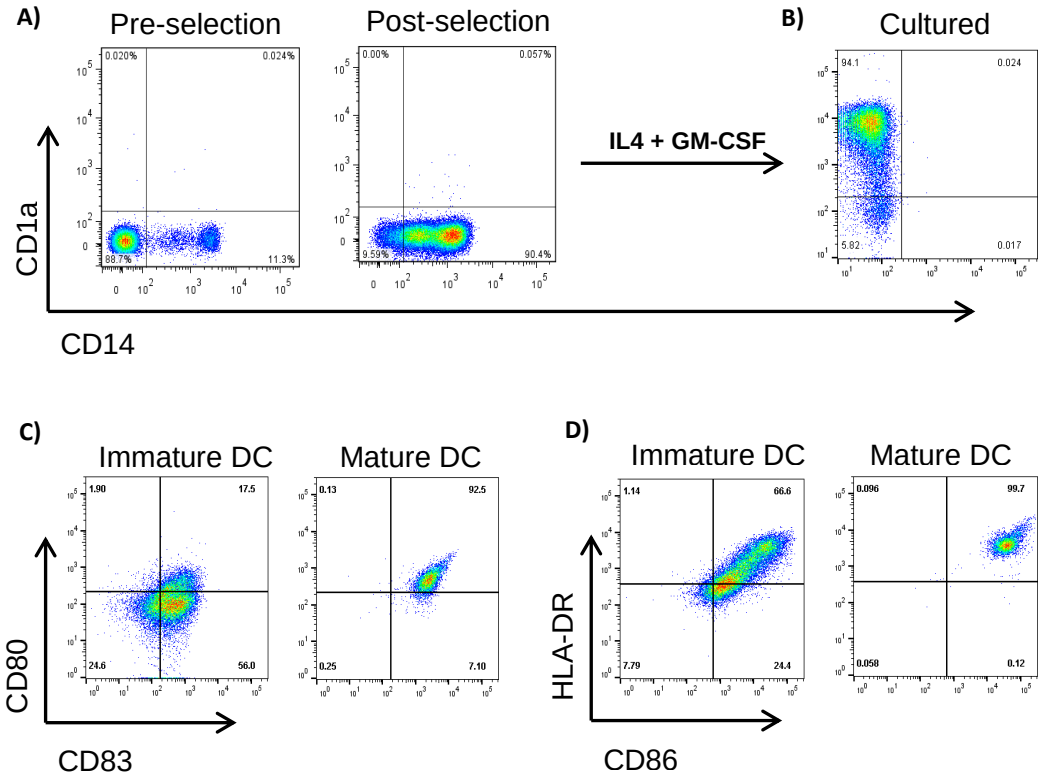

Figure 5.10: Generation of immature and mature DCs

A) Isolation of $CD14^+$ from PBMCs; **B**) Culture of $CD14^+CD1a^-$ monocytes in IL-4 and GM-CSF leads to differentiation into immature DCs. DC maturation was confirmed by expression of CD80, CD83 (**C**), HLA-DR and CD86 (**D**).

The effect of MSC-EV treatment on DC maturation was assessed by flow cytometry and analysed using the median fluorescence intensity of the maturation markers CD80, CD83, CD86, CD38 and HLA-DR. Both immature and mature DCs were used as controls. As predicted, immature DCs expressed lower levels of the abovementioned markers, which were then significantly increased upon maturation of the DCs with LPS.

The phenotype of MSC-EV-treated DCs showed significant decrease on the expression of the surface marker CD38. CD38 levels are modulated during maturation, with its expression being upregulated upon maturation of DCs (Fedele *et al.,* 2004). At 20 µg/ml MSC-EV dose, DCs displayed a MFI of 890.8 ± 264.2 in comparison to a MFI of 3233 ± 419.2 found on mature DCs ($p=0.009$). In fact, the levels of CD38 expression were closer to the ones found on immature DCs which displayed a MFI of 219.0 ± 36.5 ($p=0.248$) (**Fig. 5.11**).

MSC-EV treated DCs showed a trend for a decreased cell surface expression of CD80 and CD83, but did not reach statistical difference ($p>0.05$ for all), whilst no clear reduction in the expression of CD86 and HLA-DR were detected (**Fig. 5.11).**

Overall, the addition of MSC-EVs to DCs during their maturation results in a significant decrease of CD38 expression and marginally alters the expression of co-stimulatory markers CD80 and CD83. In the current study, due to limitations in the amount of purified MSC-EVs, the maximum concentration used was 20µg/ml. Treatment of DCs with increased concentrations of MSC-EVs may result in a significant effect on the expression of CD80 and CD83 markers by mature DCs.

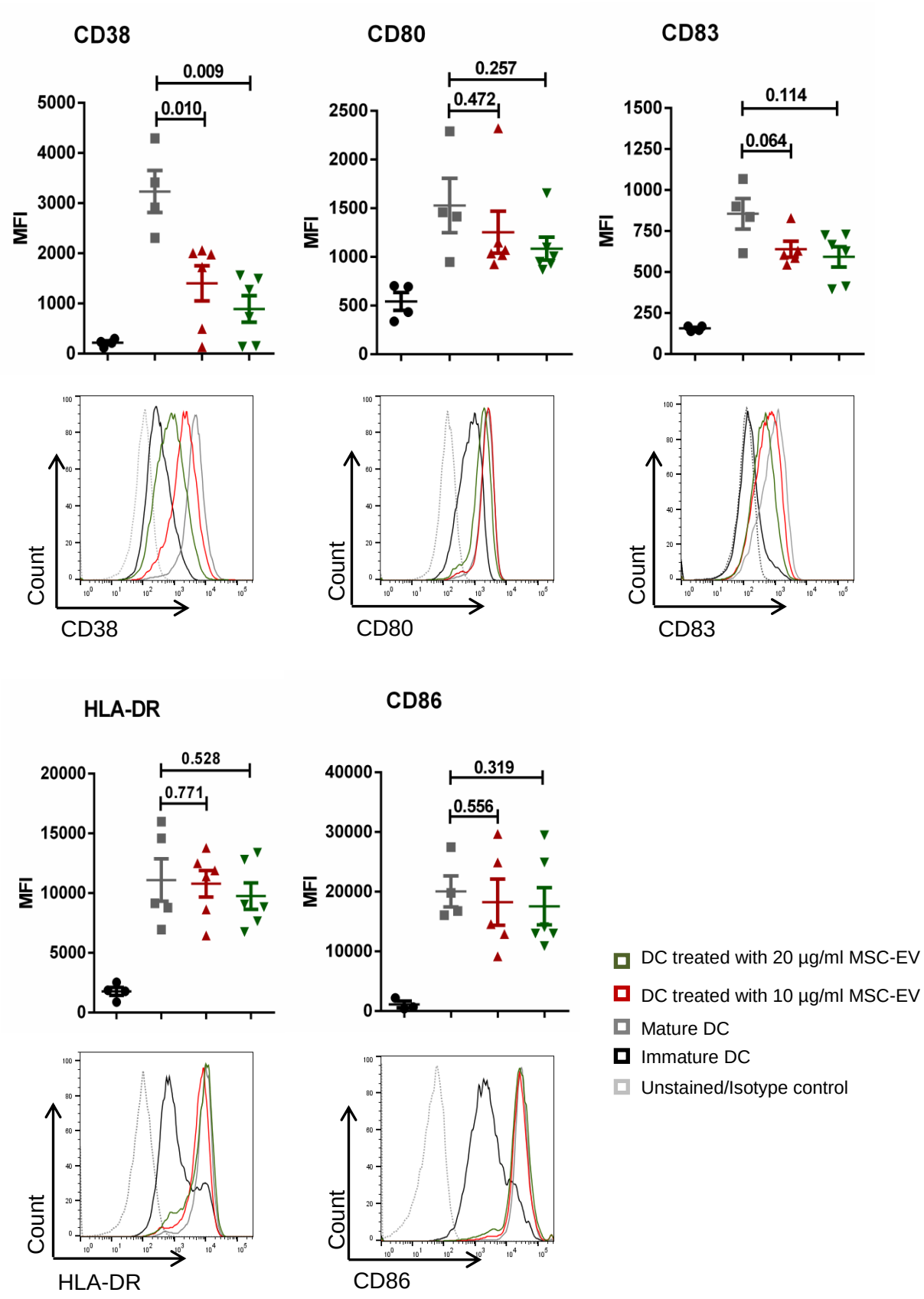

Figure 5.11: MSC-EV modulation of DC maturation

Cumulative (top) and representative (bottom) expression of surface markers CD38, CD80, CD83, CD86 and HLA-DR as determined by flow cytometry on immature, mature and MSC-EV-treated DCs. Data represents mean ± SEM of n≥4. A p-value of <0.05 was considered significant.

5.3.6. MSC-EV treatment induces impaired antigen processing by DC

To analyse whether MSC-EVs could affect antigen processing by DCs, FITC dextran uptake was used as a surrogate marker. FITC dextran uptake was assessed by flow cytometry and data is presented as fold increase in FITC MFI in comparison with the 4ºC treated control. Immature DCs have a high capacity to take up antigens. Upon LPS maturation, DCs lose this capacity and gain the ability to present antigens to effector cells (Caux and Dubois, 2001). As expected, immature DCs took up the highest amounts of FITC dextran, which was significantly higher than that exhibited by mature DCs (p=0.003). Treatment of DCs with different doses of MSC-EVs showed a decrease in the ability of immature MSC-EV-treated DCs to take up FITC dextran. While immature DCs showed a MFI fold change of 9.5 ± 0.8, MSC-EV treated immature DCs displayed a fold change of 5.9 ± 2.3 (p=0.342) and 3.3 ± 1.0 (p=0.012) for 10 and 20 µg/ml used dosage, respectively. FITC dextran uptake of the DCs treated with 20 µg/ml of MSC-EVs was similar to the one shown by mature DCs (3.4 ± 0.5; p=0.8571) (**Fig.5.12**). Overall, these results show that MSC-EV treatment impairs DC capacity to process antigens.

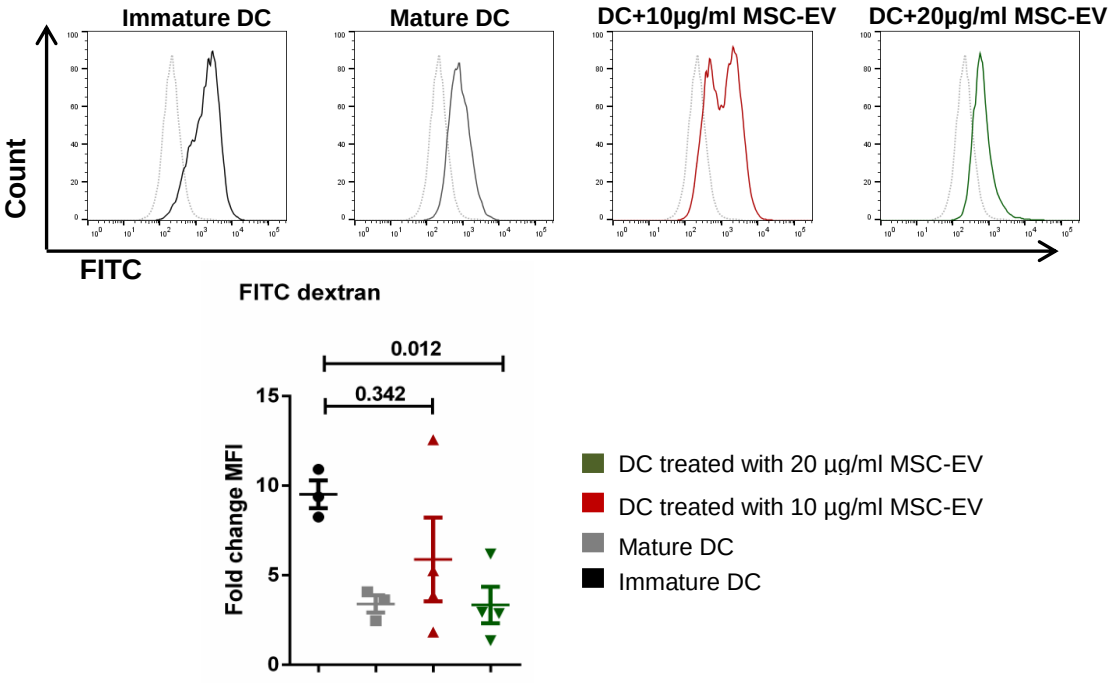

Figure 5.12: MSC-EV treated DCs have impaired FITC dextran uptake

FITC dextran uptake was used to assess antigen uptake by immature, mature and MSC-EV treated DCs. Representative histograms (top) and cumulative data (bottom) of FITC dextran, as assessed by flow cytometry. Pale grey lines in histograms represent isotype control. Results express mean ± SEM of n=4, with p-value <0.05 considered significant

5.3.7. MSC-EV treatment does not impair DC ability to induce alloreactive T cell proliferation *in vitro*

To evaluate whether MSC-EV-treated DCs had impaired ability to stimulate alloreactive T cell proliferation, MSC-EV-treated DCs were co-cultured with allogeneic T cells and $CD4^+$ and $CD8^+$ cell proliferation and activation was evaluated by flow cytometry after 5 days of culture. As expected, unstimulated T cells showed the lowest proliferation (< 1% for both CD4 and CD8). Stimulation of T cells with mature DCs resulted in a proliferation rate of 25.4% ± 5.6 and 17.6% ± 1.9 for CD4 and CD8 T cells, respectively. Unexpectedly, T cells stimulated by MSC-EV-treated DCs did not show reduced levels of proliferation. In MSC-EV-treated DCs, the proliferation rates of CD4 and CD8 were 36.6% ± 5.7 and 24.4% ± 2.7, respectively, after stimulation with DCs treated with 20 µg/ml of MSC-EVs (p>0.05 for all) (**Fig.5.13**).

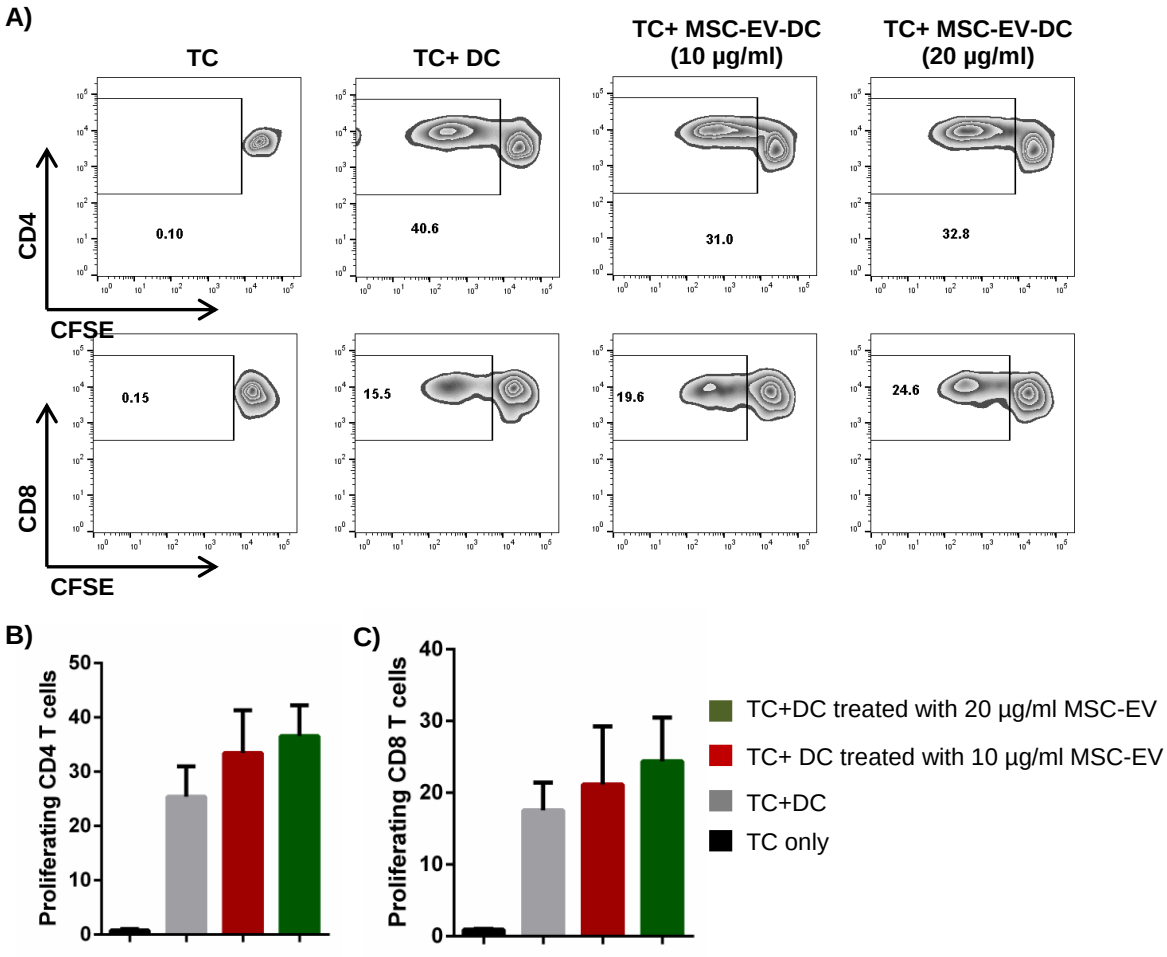

Figure 5.13: MSC-EV treatment does not impair DC ability to induce alloreactive T cell proliferation

A) Representative histograms for and **B)** cumulative data for CD4 and CD8 T cell proliferation. Results are expressed as mean ± SEM of n=4.

Concomitant analysis of T cell activation, by measure of CD25 expression, revealed similar results. CD25 expression was negligible in unstimulated T cells (less than 1% for both cell populations), and increased to 27.3% ± 5.8 and 14.3% ± 2.1 for CD4 and CD8 T cells, respectively, after stimulation with mature DCs. CD25 expression on T cells stimulated with MSC-EV-treated DCs did not show any significant difference when compared to those stimulated with mature DCs, with a percentage of $CD25^+$ cells of 37.9% ± 5.3 and 21.1% ± 3.3 being detected by CD4 and CD8 T cells, respectively, after stimulation with DCs treated with 20 µg/ml of MSC-EVs (**Fig.5.14**).

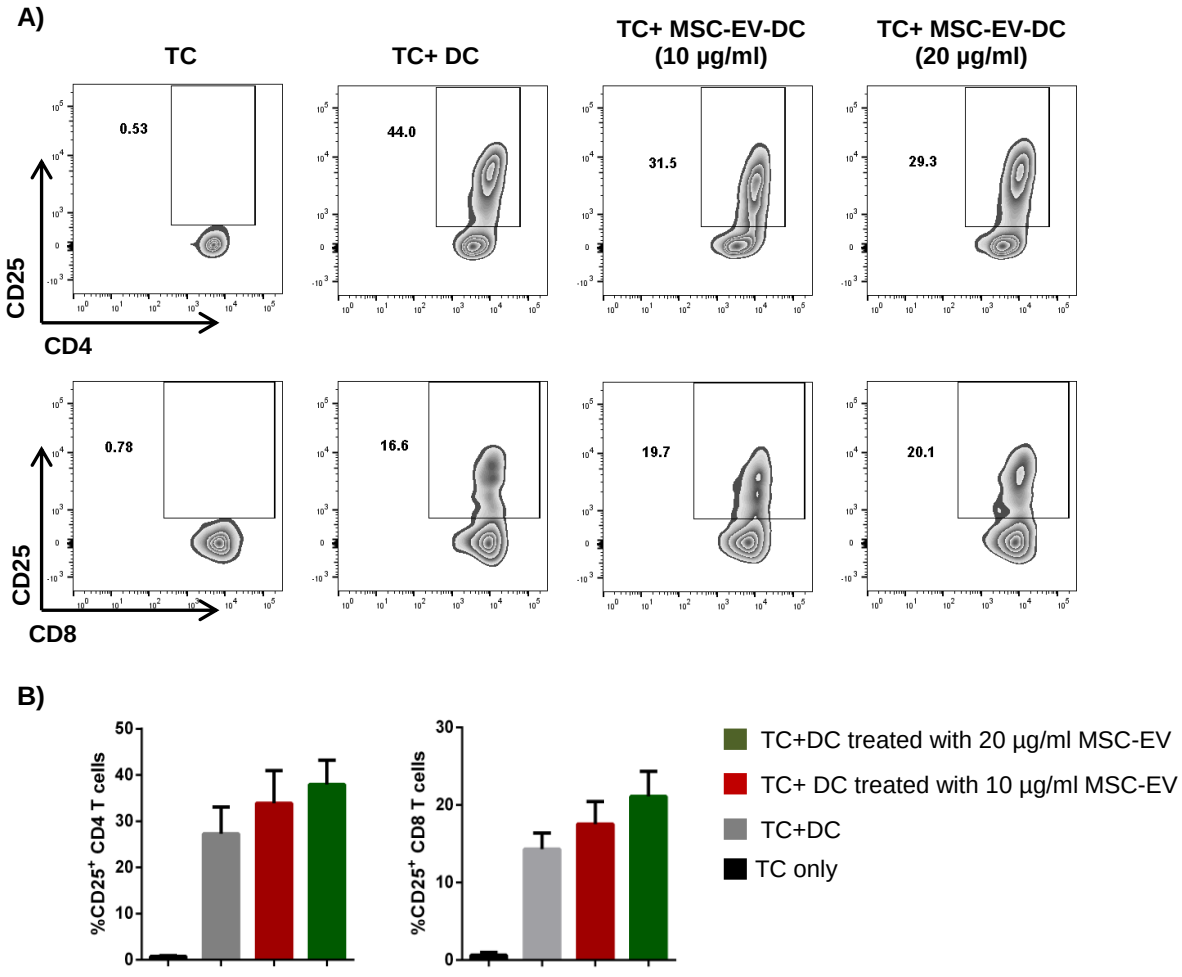

Figure 5.14: MSC-EV treatment does not impair DC ability to induce alloreactive T cell activation

A) Representative histograms and **B)** cumulative data for CD25 expression by CD4 and CD8 T cells. Results are expressed as mean ± SEM of n=4.

5.3.8. MSC-EV treatment impairs DC migration

Given the abovementioned results, further investigation was carried out to explore the importance of CD38 expression by DCs. CD38, also known as adenosine-5'-diphosphate-ribosyl cyclase 1, is a multifunctional enzyme, expressed by a variety of cells, involved in the generation of calcium-mobilizing metabolites (Hamblin, 2003). In DCs, CD38 expression by the mature cells has been linked to increased secretion of IL-12, antigen processing ability and migration to the lymph nodes for antigen presentation (Fedele *et al.,* 2004, Frasca *et al.*, 2006). Additionally, its expression is closely related to CCR7 expression after maturation (Frasca *et al.*, 2006). This has led us to evaluate CCR7 expression on MSC-EV-treated DCs. Compared to mature only, MSC-EV-treated DCs showed a dose dependent decrease of CCR7 expression (**Fig.5.15A**).

After treatment with EVs, DCs expressed reduced levels of CD38 and CCR7. CCR7 expression plays an essential role in DC homing to the lymph nodes. Upon the presence of inflammatory *stimuli* DCs mature and gain CCR7 expression. CCR7 and its ligands, CCL19 and CCL21, direct these DCs to the lymph nodes where they present antigens to the T cells (Comerford *et al.*, 2013). In the present study, the transwell system was used to confirm that the decrease in CCR7 expression after MSC-EV treatment had a functional implication in the migration of mature DCs. A pilot study was performed to determine the optimal parameters for DC migration using this experimental approach (**Supplementary Fig.S5.1**)

DCs were generated as previously described and treated with 20 µg/ml MSC-EVs. After maturation, the cells were added onto an insert at a concentration of $1x10^5$ cells/insert and CCL21 supplemented medium was added onto the bottom well and cells were incubated at 37^0C for 24h. Background migration was assessed as by adding basal medium without chemokine onto the bottom well. The migration efficiency of the DCs was calculated as a percentage of the number of cells that were found on the bottom well in relation to the input number of cells. DC migration was significantly decreased upon MSC-EV-treatment, with MSC-EV-treated DCs displaying a migration efficiency of 22.4% ± 4.0 in comparison with 73.2% ± 6.4 detected by mature DCs (p=0.008). In

fact, the migration efficiency of MSC-EV-treated DCs was negligible and presented rates similar to that detected by the background control (16.7% ± 3.5, p=0.395) (**Fig. 5.15B**).

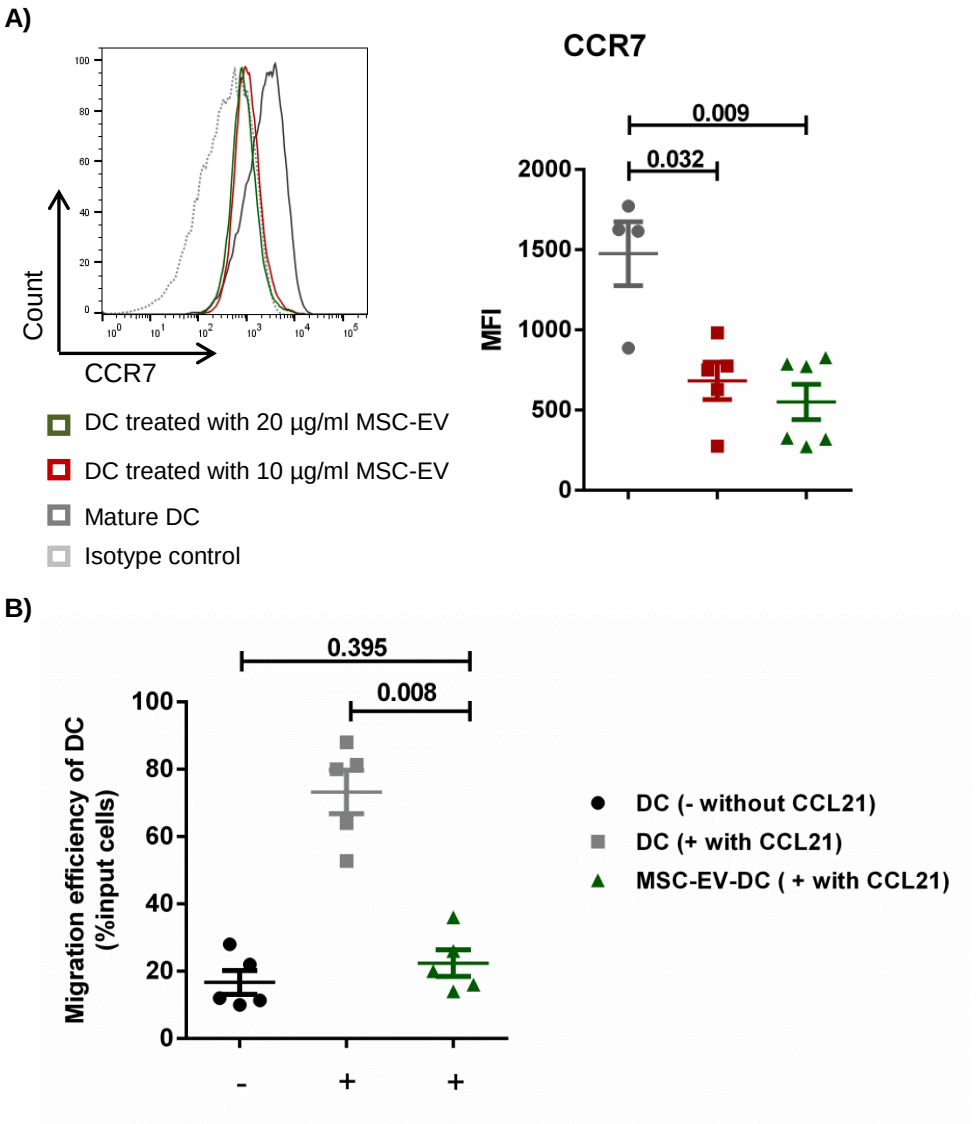

Figure 5.15: MSC-EV-treated DCs have reduced CCR7 expression and impaired migratory potential

A) Representative histograms (left) and cumulative (right) levels of expression of CCR7 by mature DCs, DCs treated with 10 µg/ml MSC-EV and DCs treated with 20µg/ml MSC-EV. Live cells were selected prior to histograms and levels of expression were compared to isotype controls. **B)** Migration efficiency of mature and MSC-EV-treated DCs. Mature DCs migrating towards medium without CCL21 was used as background control. Results express mean ± SEM of n≥4 and p-values are as illustrated.

5.3.9. MSC-EV treatment alters the profiles of cytokines produced by DCs

Upon maturation, DCs express high levels of pro-inflammatory cytokines, including IL-6 and IL-12 (Castiello *et al.,* 2011), therefore levels of IL-6 and IL-12p70 and the anti-inflammatory cytokines, TGF-β and IL-10, were measured in the co-culture supernatants after generation of DC and MSC-EV-treated DCs.

IL-6 concentration was low in the supernatants collected from immature DCs; 136.5 ± 60.6 pg/ml. The levels of IL-6 in supernatants of MSC-EV-treated DCs were higher than those detected on supernatants of immature DCs, but significantly lower than those secreted by non-MSC-EV treated mature DCs, 430.6 ± 85.9 and 5973 ± 3869 pg/ml, respectively (p=0.01) (**Fig.5.16A**).

MSC-EV-treated DCs produced 4.35 ± 0.9 pg/ml of IL-12p70, which was significantly lower than the levels detected in mature DCs (491.9 ± 482.1pg/ml, p=0.04). Very low levels of IL-12p70 were detected on supernatants from immature DCs (0.03 ± 0.03 pg/ml) (**Fig.5.16B**).

Compared to mature DCs, which produced 34.9 ± 13.0 pg/ml of soluble TGF-β, MSC-EV-treated DCs secreted significantly higher levels of this cytokine, with its concentration being comparable to the one detected by immature DCs, 181.1 ± 60.4 and 140.2 ± 37.9 pg/ml, respectively (p=0.74) (**Fig. 5.16C**).

In addition to the abovementioned cytokines, the concentration of IL-10 and IL-1β was analysed. No differences in the levels of soluble IL-10 were detected between the MSC-EV-treated DCs and the two control groups (**Fig.5.16D**), and the concentrations of IL-1β in all analysed groups were below the level of detection.

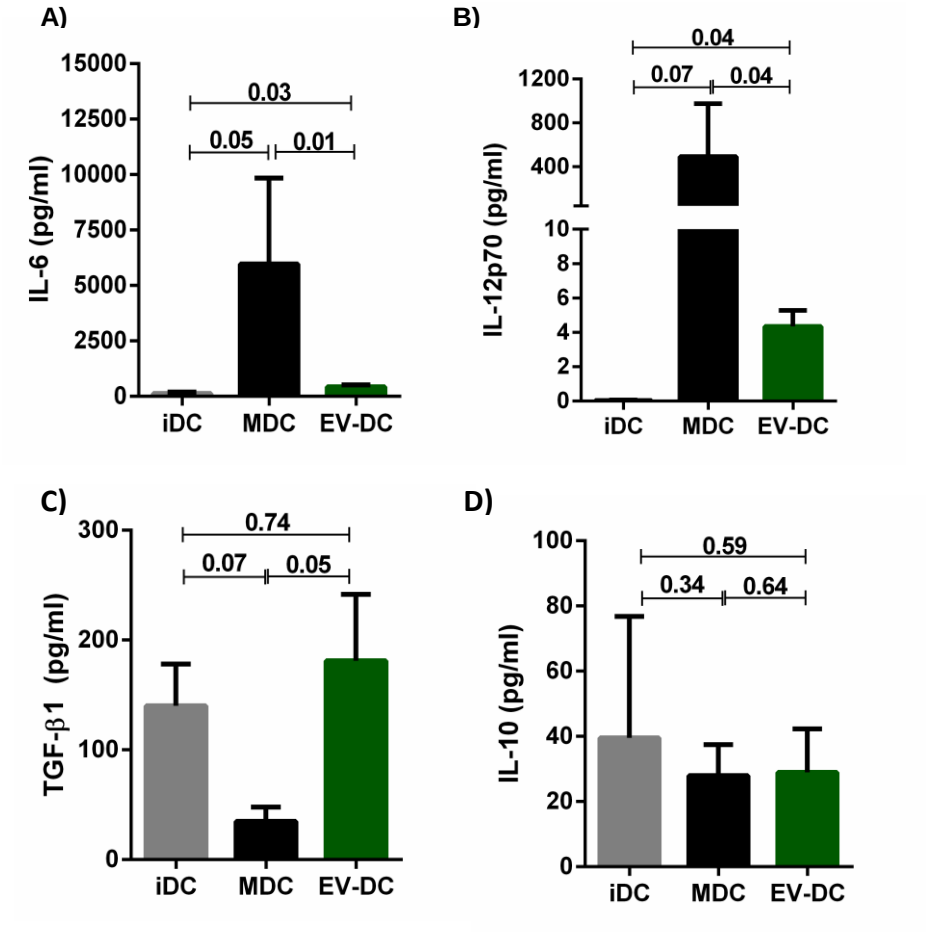

Figure 5.16: MSC-EV-treatment induces changes in the cytokine profile of DCs

Cell culture supernatants were collected on day 7 of DC generation and levels of **A)** IL-6, **B)**, IL-12p70, **C)** TGF-β and **D)** IL-10 were analysed by CBA flex. Data acquired on FACS Canto II and analysed with FCAP array. Results express mean ± SEM of 5 independent experiments.

In addition to analysis of cytokine secretion by MSC-EV-treated DCs, the cytokine profile of T cells after stimulation with MSC-EV-DCs was analysed. Secreted levels of IL-6 were lower when the T cells were stimulated with MSC-EV-DCs, 92.0 ± 25.2 pg/ml, compared to when they were stimulated with non-MSC-EV-treated mature DCs, 201.1 ± 20.4 pg/ml, but higher than the levels detected on supernatants of T cells only (27.5 ± 53 pg/ml), however, the results failed to reach statistical significance (**Fig.5.17A**).

In comparison to the supernatants collected from T cells stimulated with mature DCs (725.8 ± 322.3 pg/ml), the levels of secreted IFN-γ were lower in supernatants from T cells stimulated with MSC-EV-DCs (149.0 ± 60.3 pg/ml, p=0.054). IFN-γ was not detected in supernatants from T cells only (**Fig5.17B**).

No differences were detected in secreted TNF-α in and IL-2 supernatants collected from T cells stimulated with mature DCs or MSC-EV-treated DCs (p=0.400 and p=0.250, respectively) (**Fig.5.17C and D**). In addition to these cytokines, IL-17 levels were also analysed, however, these were not detectable with the CBA technology.

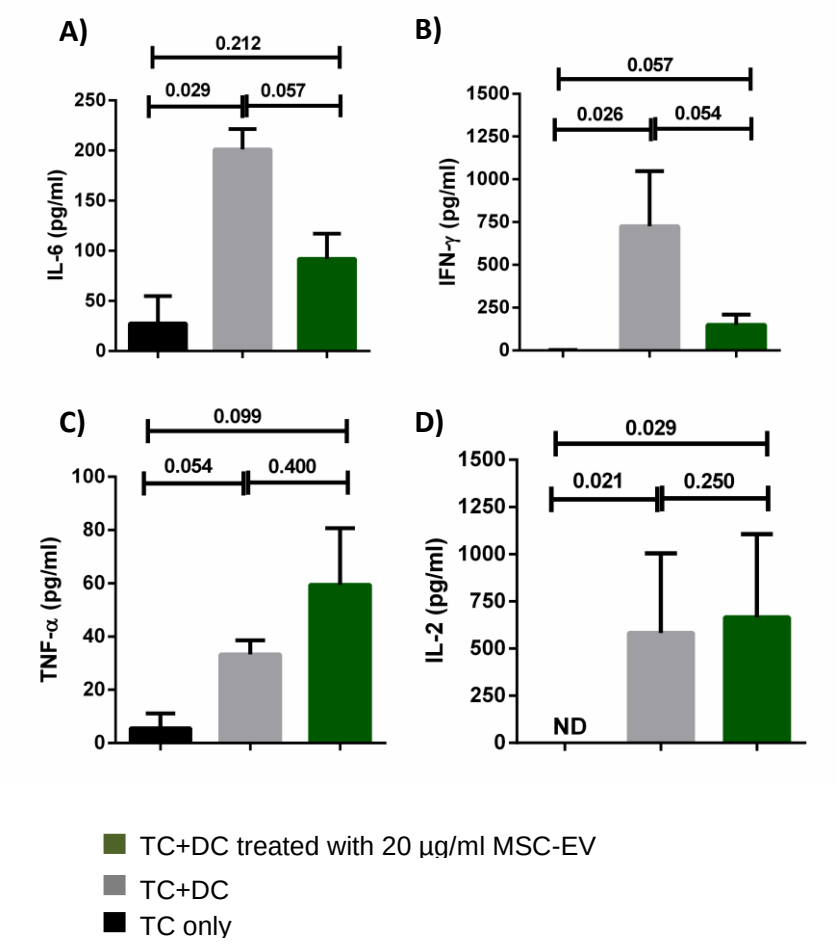

Figure 5.17: Cytokine production by T cells following stimulation with MSC-EV-treated DCs

Supernatants were collected on day 5 after co-culture of T cells with mature DCs or MSC-EV-treated DCs and analysed for the levels of **A)** IL-6, **B)** IFN-γ, **C)** TNFα and **D)** IL-2 by CBA flex. Data collected on FACS Canto II and analysed using FCAP array. Data generated from 3-4 independent experiments. ND = not detectable

5.4. Discussion

Accumulating evidence has demonstrated that the biological activity of MSCs is mediated by both cells and the release of paracrine factors, also known as, secretome. MSC secretome includes a wide variety of soluble proteins, including growth factors and cytokines, as well as extracellular vesicles. MSC-derived EVs are thought to have similar functions to MSCs. In models of myocardial infarction and acute kidney injury, these vesicles have been shown to recapitulate the effect detected upon MSC administration (Arslan *et al.*, 2013; Gatti *et al.,* 2011; Timmers *et al.,* 2007). In clinical settings, MSC-EVs have been successfully used to treat a patient with acute graft-versus-host disease, whom experienced stable improvement of symptoms over 5 months (Kordelas *et al.,* 2014). Despite MSC-EV potential, little is known about their immunomodulatory effect. The current study aimed at investigating the immunosuppressive capacity of EVs derived from xeno-free expanded MSCs. Data presented in this Chapter describes the morphological and phenotypic characteristics of EVs purified from MSC culture supernatants. Furthermore this Chapter presents evidence that MSC-EVs retain immumomodulatory properties of their parent cells and reports for the first time that treatment with these vesicles shift DC function towards an immunoregulatory phenotype and impair their migratory capacity.

MSC-derived EVs were obtained from culture supernatants by differential ultracentrifugation. This procedure was initially described to purify reticulocyte exosomes from tissue conditioned medium (Pan and Johnstone, 1987) and later described in detail by Théry *et al* (2006). This technique has currently been adopted by many laboratories worldwide to purify EVs from supernatants of many cell types, such as B lymphocytes (Escola et al., 1998), dendritic cells (Thery et al., 1999) and mesenchymal stromal cells (Di Trapani *et al.,* 2016; Ti *et al.,* 2015), among others. In comparison to other techniques, such as sucrose gradient centrifugation and ultrafiltration, differential ultracentrifugation is a more robust methodology, which allows for higher yields of EVs are relatively high purity levels (Momen-Heravi *et al.,* 2013).

EVs comprise a mixture of vesicles of distinct sizes and biogenesis. The most extensively studied, and harbouring the highest therapeutic potential, are

exosomes and microvesicles (Colombo *et al.*, 2014), with sizes ranging from 30-100nm and 100-1000nm, respectively. Initially, differential ultracentrifugation was believed to purify mainly exosomes, however, several studies have demonstrated high size heterogeneity of EV pellets obtained using this methodology (Escola *et al.,* 1998, Thery *et al.,* 1999). In this chapter, MSC-EVs purified using ultracentrifugation exhibited a size range of 20 to 180 nm. TEM analysis of the MSC-EV preparations confirmed these observations and revealed a wide heterogeneity of vesicles.

Additional characterisation of EVs includes the analysis of the expression of protein markers enriched in vesicle preparations (Lötvall *et al.,* 2014). Purified MSC-EVs in this study were rich in the expression of the tetraspanins CD63, CD9 and CD81. In most cells, CD63 is present in compartments of endosomal/lysosomal origin (Colombo *et al.,* 2013) while CD9 is mainly detected on the plasma membrane or vesicles near the cell membrane (Cramer *et al*, 1994). Altogether these two markers are discriminatory between exosomes and microvesicles. The expression of CD81 is ambiguous and has been described in vesicles of different sizes (Bobrie *et al.,* 2012). The expression of these three markers on EVs purified from MSC culture supernatants indicates MSCs secrete a variety of different vesicles, which can be pelleted using conventional ultracentrifugation protocols.

One of the most attractive characteristics of these vesicles is their ability to modify physiological processes by shuttling bioactive molecules and genetic material to recipient cells, which can be adjacent cells and distant tissues (Colombo *et al.*, 2014). Pre-clinical studies have reported on the beneficial role of MSC-derived EVs *in vivo* (Lai *et al.,* 2010; Zhang *et al.,* 2016). Data presented in this Chapter suggests that MSC-EVs partially retain the immunosuppressive capacity of their parent cells.

Mokarizadeh and colleagues investigated the immunosuppressive potential of MSC-EVs on allogeneic and syngeneic mononuclear cells. In their study, MSC-EVs were shown to have higher inhibitory potential towards the syngeneic mononuclear cells (Mokarizadeh *et al.,* 2012). Similarly, Blazquez *et al* (2014) demonstrated the ability of adipose stem cell-derived EVs to suppress T cell proliferation. However, these observations are still controversial. Gouveia de

Andrade *et al* (2015) have shown MSC-EVs were not as potent as their parent cells at inhibiting T cell proliferation, even at high concentrations and Di Trapani *et al* (2016) reported that amongst the immune cell subsets present in PBMCs, MSC-EV-mediated immunosuppression was mainly detected on B and NK cells and uptake was largely by DCs, B and NK cells. Data resulting from these studies is however, not easily comparable due to varied experimental approaches, in terms of MSC source, MSC-EV purification protocols and methods to test MSC-EV-mediated immunosuppression. Similar to results of previous studies, our study showed that MSC-EV inhibit allogeneic T cell proliferation, however, not as potently as their parent cells. The suppressive effect of MSCs on T cell proliferation has been associated to a wide variety of soluble factors and (Haddad and Saldanha-Araujo, 2014). Our data suggests that MSC-EVs are only one of many contributors that are collectively responsible for MSC-mediated suppression of T cell proliferation.

Further experiments revealed a preferential association of MSC-EVs with DCs when added to a co-culture of T cells and allogeneic DCs. They were efficiently taken up by DCs during their maturation. MSCs have been previously shown to impair differentiation of monocyte and $CD34^+$ haematopoietic stem cells into DCs *in vitro*, resulting in a reduced ability to stimulate T cells (Chen *et al.,* 2007). Documented data indicates that the mechanisms of DC modulation are mainly accounted to MSC secreted factors, with IL-6 and PGE2 playing major roles in this effect (Nauta *et al.,* 2006; Spaggiari *et al.,* 2009). Based on this data, the effect of MSC-EVs on DC maturation and function was explored. MSC-EV-treated DCs (MSC-EV-DCs) were generated as shown in the methods section of this chapter, where DCs were generated according to conventional protocols and maturation was induced by LPS. Maturation of DCs with LPS activates TLR4 signalling via the formation of a receptor complex consisting of dimerised TLR4 and the lymphocyte antigen 96 (MD-2) (Tapping, 2009). TLR4 signal transduction occurs via MyD88 dependent and independent pathways leading to the activation of NF-κB pathway. This pathway induces the secretion of pro-inflammatory cytokines, chemokines and the expression of co-stimulatory markers and constitutive antigen presentation on HLA-DR on the surface of the DCs (Tapping, 2009).

In our study, MSC-EV treatment induced a significant decrease on the expression of CD38 by mature DCs. CD38, is an ectoenzyme that catalyses the synthesis of cyclic adenosine diphosphate ribose (a second messenger for Ca^{2+} release) which initiates transmembrane signalling upon engagement with CD31 (Hamblin, 2003). In DCs, CD38 induces the expression of CD83 and IL-12 production via NF-κB pathway (Fedele *et al.,* 2004; Frasca *et al.,* 2006). This marker is laterally associated with the CCL21-specific chemokine receptor 7 (CCR7), and is therefore an important regulator of DC migratory potential (Frasca *et al.,* 2006). Both CD38 and CCR7 are upregulated upon LPS stimulation of DCs (Fedele *et al.,* 2004; Frasca *et al.,* 2006). Studies performed in a murine model showed that $CD38^{-/-}$ DCs are less efficient in taking up antigens (Lischke *et al.,* 2013). In our study, MSC-EV-treated DCs showed a reduced phagocytic capacity when compared to the untreated DCs, concomitant with a significantly reduced CD38 expression. Moreover, DC treated MSC-EVs displayed impaired expression of CCR7 resulting in a lower ability of these DCs to migrate towards CCL21 *in vitro*. Immature DCs are usually located at the primary tissues and mucosal sites. Upon antigen uptake, these cells mature and migrate to the draining lymph nodes where they effectively present antigens to the lymphocytes and initiate T cell mediated responses (Randolph *et al.,* 2005). Documented studies show that MSC inhibitory effect on CCR7 expression by DCs results in lower migration towards its ligands and consequently lack of *in vivo* priming of T cells (Chiesa *et al.,* 2011). This effect has been shown to be reproducible with MSC-culture supernatants (Chen *et al.,* 2007). This chapter suggests for the first time MSC secreted MSC-EVs are major bioactive components involved in MSC-mediated inhibition of DC homing to the lymph nodes, hence suppressing lymphocyte immune responses.

Along with these effects, MSC-EV-treated DCs were shown to secrete low levels of pro-inflammatory cytokines IL-6 and IL-12p70, and increased levels of soluble TGF-β, with the levels of these cytokines being similar to those detected in the supernatants of immature DCs. This cytokine profile resembles that of tolerogenic DCs, which are involved in the maintenance of periphery tolerance, via the inhibition of memory T cell responses and the induction of T cell anergy (Raker *et al.,* 2015). In particular, cytokines secreted by tolerogenic DCs, such

as, TGF-β and IL-10, play an important role in the induction of FoxP3 expression in naïve T cells (Raker *et al.,* 2015). Unexpectedly, the levels of IL-10 secreted by MSC-EV-DCs were not significantly different than that of mature DCs. This could be due to the timing of cell culture supernatant collection. Measuring of DC cytokine profiles following MSC-EV treatment at different time points is necessary to confirm the current finding.

Despite the decreased expression of CD38 and CCR7 and a tolerogenic cytokine profile by MSC-EV-treated DCs, the expression of DC maturation marker CD83 and the co-stimulatory molecule co-stimulatory CD80 was only marginally reduced, and no changes were detected on the expression of CD86 and HLA-DR. A recent study performed by Favaro and colleagues compared the effect of MSCs and MSC-EVs on the function of human monocyte-derived DCs. Their study showed that both MSCs and their derived EVs skewed DC maturation into a regulatory phenotype characterised by the reduced expression of DC activation markers and increased production of IL-10 and TGF-β. These effects led to the generation of Tregs after DC co-culture with allogeneic T cells and diminished T cell proliferation after co-culture with the MSC and MSC-EV treated DCs (Favaro *et al.,* 2015). In our study, MSC-EV-DCs showed similar ability to induce proliferation and activation of both CD4 and CD8 T cells as mature DCs. This observation can be explained by the fact that MSC-EV-DCs still express high levels of co-stimulatory molecules and HLA-DR. In an *in vitro* system, these cells can easily engage with T cells and stimulate their activation as efficiently as mature DCs. The discrepancy detected between Favaro *et al* (2015) and our study may be due to differences in methodology and sample variation. While in our study all experiments were performed on DCs derived from healthy donors, Favaro and colleagues tested the effect of MSC and MSC-EV treatment on DC maturation and function of samples derived type 1 diabetes patients (Favaro *et al.,* 2015).

Analysis of cytokine secretion by T cells after stimulation with MSC-EV treated DCs showed lower levels of pro-inflammatory cytokines, such as IFN-y and IL-6. In accordance to the detected T cell proliferation and activation levels, no differences in the levels of IL-2 were detected in supernatants from T cell stimulated with MSC-EV-treated and untreated DCs. IL-2 promotes proliferation

and activation of effector and memory T cells (Boyman and Sprent, 2012). Published data suggests that this cytokine is also essential for the *de novo* generation of regulatory T cells (Fontenot *et al.,* 2006). Several reports have demonstrated that one of the main mechanisms of MSC-EV immunosuppression is by inducing the generation of regulatory T cells (Blazquez *et al.,* 2014; Mokarizadeh *et al.*, 2012; Zhang *et al.,* 2014). One such study hypothesised that this effect was mediated by macrophages by showing that MSC-EVs polarized macrophages into an IL-10^{hi}IL-12^{low} M2-like phenotype in a TLR-dependent signalling manner. In turn, these M2-macrophages induced the generation of $FoxP3^{+}$ Tregs but had little influence on T cell proliferation (Zhang *et al.,* 2014). It is plausible to hypothesize that MSC-EV treatment of DCs may skew these cells into an anti-inflammatory phenotype, which in turn will induce the generation of regulatory T cells. Further work is warranted to confirm whether MSC-EV treated DCs induce the generation of regulatory T cells by analysing the polarisation of naïve T cells after stimulation with MSC-EV treated DCs.

Interestingly, in this chapter we reported a contradictory outcome of MSC-EV mediated suppression of T cell proliferation. When MSC-EVs were added to a co-culture of allo-DC stimulated T cells, suppression of T cell proliferation was detected. However, when MSC-EVs were added to DC generation culture, and these DCs were used to stimulate allogeneic T cells in a secondary culture, no suppression of T cell proliferation was detected. This data indicated MSC-EVs may have a direct effect on T cells as well. Although the mechanisms of MSC-EV mediated suppression are not fully understood, recent data suggests that these vesicles induce T cell apoptosis (Mokarizadeh *et al.,* 2012). In our study, the T cell apoptosis was not analysed, however, there was a decrease in the number of live T cells upon MSC-EV treatment (**Supplementary Fig.S5.2**). This suggests that the differences detected in the inhibition of T cell proliferation may be due to the delivery of apoptotic signals by MSC-EVs to the T cells. Further analysis of the apoptosis level of T cells after MSC-EV treatment is needed to confirm this hypothesis.

Overall, findings reported in this chapter provide novel insights underpinning the mechanisms of MSC-mediated attenuation of the immune system, and show for

the first time, the effects of MSC-EV treatment on migratory potential of DCs. Data presented in this Chapter suggests that MSC-EVs modulate DC function by impairing their ability to process antigens and to upregulate markers of maturation, such as CD38 and CCR7. Both proteins have important roles in the migration of DCs to the lymph nodes for antigen presentation to the naïve T cells. In addition, MSC-EVs skew DC cytokine production to a tolerogenic profile. As illustrated in figure **Fig.5.18**, MSC-EV induced changes in both DC phenotype and DC cytokine secretion may function in synergy.

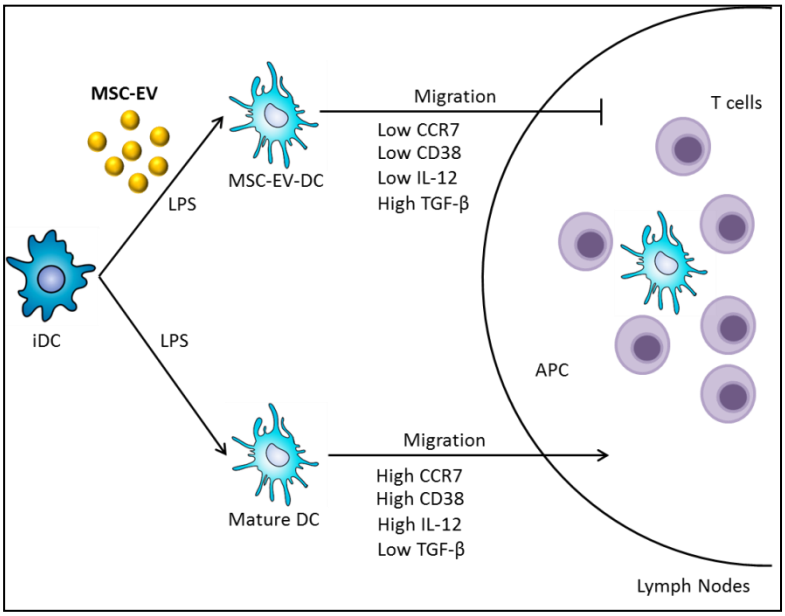

Figure 5.18: Proposed model of MSC-EV impairment of DC functions

MSC-EVs deliver signals that prevent upregulation of CD38 and CCR7 during maturation of DCs which may have important implications in the migration of DCs to the lymph nodes. MSC-EVs inhibit the secretion of pro-inflammatory cytokines, IL-12 and IL-6, and promote the secretion of anti-inflammatory cytokines, such as TGF-β by mature DCs.

In addition, it is most likely that MSC-EVs are not the sole factors contributing to MSC-mediated modulation of DC maturation and function. Other MSC-derived soluble factors, such as PGE2 and IL-6 (Nauta *et al.,* 2006; Spaggiari *et al.,* 2009), have been reported to down-regulate DC activation. It is noteworthy to mention that experiments presented in this chapter were all carried out using *in vitro* approaches, which limit the proposed output. To further confirm whether MSC-EVs impair DC migration to the lymph nodes and subsequent antigen

presentation to the naïve T cells, experiments using *in vivo* models need to be performed.

Acknowledgments

- Dr. Clotilde Théry and Joanna Kowal for hosting and training me in the isolation and characterisation of EVs from culture supernatants at Institut Curie, Paris, France
- E. Mavin for the sharing of DC generation and functional assessment protocols

Chapter 6: Profiling of microRNAs in MSC-EVs

“Science, my boy, is made up of mistakes, but they are mistakes which it is useful to make, because they lead little by little to the truth.”

- Jules Verne

Chapter 6 – Profiling of microRNAs in MSC-EVs

6.1. Introduction

Currently, it is broadly accepted amongst the MSC research community that their therapeutic effects are mainly due to the action of MSC released secretome (Liang *et al.,* 2014). Work reported in previous chapters have highlighted the fact that MSC-EVs play important roles in the mode of action of MSCs. MSC-EVs were shown to modulate the maturation, migration and cytokine secretion of monocyte derived DCs.

In recent years, increasing interest has been given to MSC-EV enclosed microRNA. MicroRNAs are small non-coding RNAs that regulate gene transcription at a post-transcriptional level by targeting mRNAs for degradation (Bartel, 2004). Despite the fact that MSC-EVs contain a complex mixture of proteins, enzymes, lipids and multiple RNA species, several reports have demonstrated the relevance of MSC-EV derived miRNAs in the modification of biological and cellular processes (De Luca *et al.,* 2015; Xin *et al.,* 2012). Recent evidence showed that upon RNase treatment, the protective effect of MSC-conditioned medium was abrogated in acute kidney injury pre-clinical models (Biancone *et al.,* 2012; Bruno and Camussi, 2013). Several MSC-EV enclosed microRNAs, such as, miR-122, miR-23b and miR-22, have been shown to contribute to the MSC protective effects and to promote tissue regeneration in several models, e.g., myocardial ischemia and acute kidney injury (Lou *et al.,* 2015; Ono *et al*., 2014; Yu *et al.,* 2015). A few reports have profiled the miRNA content of MSC-EVs. They have identified a signature of miRNAs that are commonly detected in these vesicles, but that can also be identified in the parent cells (Baglio *et al.,* 2015; Chen *et al.,* 2010; De Luca *et al.,* 2015). However, the contribution of miRNAs to the immunomodulatory effect of MSC-EVs, both *in vitro* and *in vivo*, remains unexplored.

This chapter aimed to profile the miRNA content of MSC-EVs and to investigate the influence of these miRNAs in the MSC-EV effect on DC maturation, function and migration, by the identification of relevant target genes. The specific aims of this chapter were:

- To perform a global miRNA profiling on MSC-EVs and MSCs that were expanded in PLT-supplemented medium, by Nanostring analysis.
- To identify the miRNAs that were differentially expressed in MSC-EVs and MSCs
- To identify miRNAs that were exclusively detected in MSC-EVs or MSCs
- To identify the most abundant miRNAs detected in MSC-EVs
- And to perform target and pathway enrichment analysis using bioinformatics platforms in order to identify miRNAs with the ability to modulate the effects observed in MSC-EVs in the previous chapter.

6.2. Specific Methods

The majority of the methods used in this chapter have been previously described in **Chapter 2**. Specific methods for this chapter will be herein listed.

6.2.1. Total RNA extraction from MSC-EVs

MSC-EVs were purified from conditioned medium of MSCs expanded in human PLT-supplemented medium, as described in **Chapter 2**. Total RNA was extracted from EVs using the Total Exosome RNA and Protein Isolation kit (Invitrogen). This kit uses an acid-phenol:chloroform extraction to ensure a robust RNA purification. When mixed with an aqueous solution, such as cell lysates or homogenised tissue, and centrifuged, this mixture yields two phases due to the immiscible characteristics of phenol. The lower organic phase contains hydrophobic lipids and proteins, while the nucleic acids (including other contaminants such as salts and sugar) partition in the upper aqueous phase. Because phenol may retain 10-15% of the aqueous phase after centrifugation, chloroform is used to prevent this retention and to ensure sharper phase separation. Total RNA extraction was performed as per the manufacturer's instructions. All steps are depicted in **Fig. 6.1**.

All working solutions were prepared as follows: 375 µl of 2-mercaptoethanol (Life Technologies) was added to 2X denaturing solution; 21 and 40 ml of 100% ethanol were added to miRNA wash solution 1 and wash solution 2/3, respectively.

In brief, MSC-EVs were purified from culture conditioning medium as described in **Chapter 2**. The MSC-EV fraction was re-suspended in 100-200 µl of exosome resuspension buffer. The organic extraction of RNA was carried out by mixing one volume of 2x denaturing solution to the MSC-EV lysate. After a 5 minute incubation on ice, 1 volume of acid-phenol:chloroform was added to the mixture and the samples were homogenized by vortexing for 30-60 seconds. The mixture was centrifuged for 5 minutes at 10,000xg to separate the aqueous (upper) and organic (lower) phases. The upper phase was carefully removed without disturbing the lower phase and interphase, and transferred to a new tube. The collected volume was registered for the posterior steps. Then 1.25 volumes of 100% ethanol was mixed with the aqueous solution and loaded onto

a filter cartridge and centrifuged for 15 seconds. The flow-through was discarded. Total RNA was washed by adding miRNA wash solution 1 and centrifuging at 14,000xg for 15 seconds. Wash solution 2/3 was then added and centrifuged as above. This step was repeated and the filter cartridge was centrifuged at 14,000xg for 1 minute for removal of residual fluids. Total RNA was eluted using 25-30 µl of pre-heated (95^{o}C) elution solution and centrifugation at 14,000xg for 30 seconds. RNA quantity and quality was determined using Agilent 2100 Bioanalyzer with the RNA 6000 Pico (for MSC-EV RNA) and Nano (for cellular RNA) Kit.

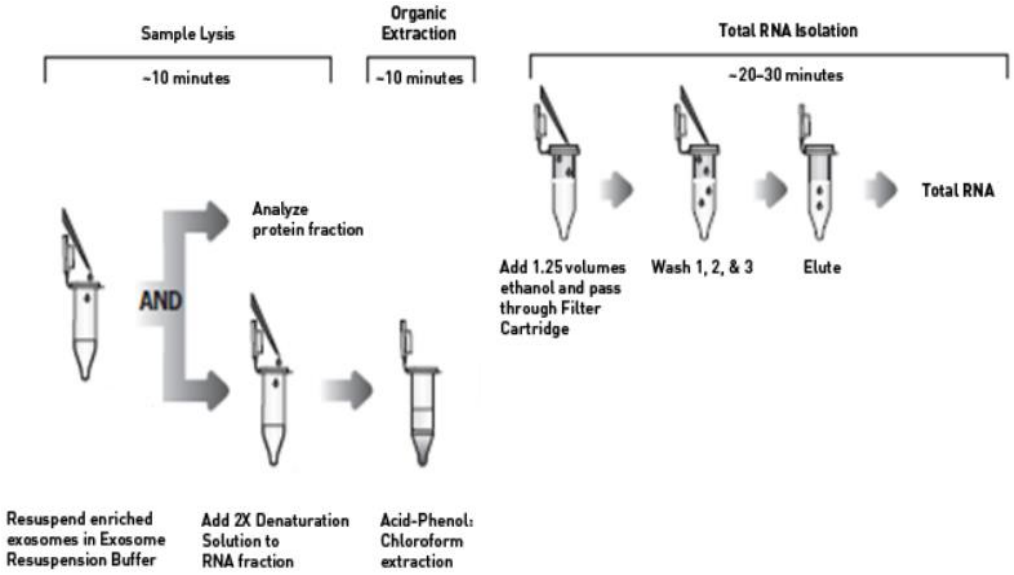

Figure 6.1: **Total RNA extraction from MSC-EVs**

MSC-EVs were suspended in exosome resuspension buffer. The EV suspension was mixed with 2X denaturing solution and then acid:phenol-chloroform. The upper phase was collected and mixed with ethanol and passed through a filter cartridge. Total RNA was washed with wash solution 1 and wash buffer 2/3. Elution was performed with preheated elution buffer (adapted from www.thermofisher.com).

6.2.2. Quality control of total RNA extracted from MSCs and MSC-EVs

Determination of RNA quality and concentration was assessed using Agilent 2100 Bioanalyzer and the RNA 6000 Nano kit and the RNA 6000 Pico kit (Agilent technologies) for MSC-EV and cellular derived RNA respectively. The Bioanalyzer separates nucleic acids (e.g. RNA and DNA) and proteins by electrophoretic and microfluidics technology. This technology allows for the analysis of 11-12 nucleic acid samples on a disposable chip in a short amount of time (~30 minutes). Chips are fabricated from glass and contain a network of fluid reservoirs and microchannels. Typically, each chip comprises 16 wells: 3 for loading the gel-dye mixture, 1 for a molecular ladder and 12 for experimental samples. The gel dye mixture consists of a linear polymer containing an intercalating fluorescent dye and the molecular ladder consists of a buffer with lower and upper molecular size markers which are used as references for sizing and quantification of the nucleic acids. After loading the samples onto the wells, the movement of the nucleic acids through the microchannels is controlled by a series of electrodes which are connected to a common power supply. The bioanalyzer presents the data as both migration-time plots and virtual gels generated by the Agilent 2100 expert software. Details about the Nano and Pico kits are summarised on **Table 6.1**.

Table 6.1: Summary of agilent bioanalyzer kit details to assess RNA quality/quantity.

Kit	Sample type	Concentration range (ng/µl)	Cat. No.
Agilent RNA 6000 Nano	Cellular Total RNA	25-500	5067-1511
Agilent RNA 6000 Pico	EV Total RNA	0.05-5	5067-1513

6.2.3. MicroRNA profiling using Nanostring technology

The microRNA content of MSCs and their derived EVs was analysed using the nCounter system (Nanostring), which is a hybridization-based digital detection method that quantifies mRNA, microRNA, DNA and proteins without the need for nucleic acid purification or enzymatic reaction, thus minimizing technical bias. This technology allows for the detection and quantification of up to 800 transcripts during a single multiplexed hybridisation reaction by the use of a two sequence-specific probe library (Geiss *et al*., 2008). Firstly, the RNA target is hybridised with a biotin-capture probe for binding onto the streptavidin-coated surface. The second probe, the reporter probe, is coupled to a colour-coded tag that provides the detection signal. This tag consists of a specific combination of seven repeats of four non-overlapping fluorophores arranged in a unique order for each RNA species (Geiss *et al.,* 2008). For microRNA screening, the total RNA is annealed with specific tags to their target miRNA thus allowing for robust detection of these short RNAs. The sample is hybridised with the multiplexed probe pair and excess probes are removed by affinity purification. The probe/target complexes are aligned and immobilised onto a streptavidin slide using a robotised protocol in the prep station. After capture, samples are aligned and elongated by the application of an electric field of 160V. The level of expression is then quantified by counting the number of colour code specific for each microRNA target. A schematic representation of the nCounter workflow is shown in **Fig. 6.2**.

In this work, the commercially available nCounter® human miRNA V3 kit (Nanostring) was used to quantify MSC-EV and MSC derived microRNAs. Due to the low concentration of MSC-EV RNA, for this assay, 33 ng/µl of Cellular and a minimum of 0.6 ng/µl of MSC-EV RNA were used as input for the analysis (n=3). In brief, sample preparation was carried out by normalising MSC total RNA samples to ~33 ng/µl using RNase free water. For the MSV-EV total RNA samples, a total of 3 µl were used as input RNA (total RNA ranged from 1.7- 8.3 ng). The miRNA assay controls were diluted at a 1:5000 by adding 499 µl of RNase free water to 1µl of the miRNA assay control in RNase free microcentrifuge tube. The annealing master mix was prepared by mixing 13 µl of annealing buffer, 26 µl of nCounter miRNA tag reagent and 6.5 µl of the

1:5000 diluted assay controls and thoroughly mixed by pipetting up and down. 3.5 µl of annealing master mix was then aliquoted into each tube of a 12 x 0.2 ml strip tube and 3 µl of RNA sample was added to each tube. Samples were mixed by flicking the tube strip and the annealing step was carried out in a thermocycler using the following settings: 94^{o}C for 1 minute, 65^{o}C for 2 minutes, 45^{o}C for 10 minutes and hold at 48^{o}C.

The ligation mix was then prepared by mixing 19.5 µl of polyethylene glycol (PEG) and 13 µl of ligation buffer. 2.5 µl of ligation master mix was added to each tube. Strip tubes were flicked, centrifuged and incubated for 5 minutes at 48^{o}C. Ligase (1.0 µl/tube) was then added to each tube, which were still incubated at 48^{o}C, and the ligation protocol was carried out as following: 48^{o}C for 3 min, 47^{o}C for 3 min, 46^{o}C for 3 min, 45^{o}C for 5 min, 65^{o}C for 10 min and hold at 4^{o}C. After ligation, 1 µl of ligation clean-up enzyme was added to each tube. The strip tube was flicked and spun down. Tubes were returned to the thermocycler and a purification protocol was performed using the following conditions: 37^{o}C for 1h, 70^{o}C for 70 min and hold at 4^{o}C. After completion of the purification protocol, 40 µl of RNAse free water was added to each sample and the samples were then used for miRNA hybridisation. A master mix was prepared by mixing 130 µl of reporter codeset and 130 µl of hybridisation buffer. This master mix was thoroughly mixed and aliquoted at 20µl/tube in a 12 tube strip. The previously prepared samples were denatured at 85^{o}C for 5 minutes, quickly cooled on ice and added at 5µl/tube to each tube containing the hybridisation mix. The capture probe set (5µl/tube) was added to each tube and the samples were then added to a 65^{o}C pre-heated thermocycler and incubated overnight. After hybridisation, samples were directly added to the nCounter prep station where the final miRNA detection and quantification was carried out.

The miRNA expression profiles were analysed according to the manufacturer's instructions using the nSolver software V2.5 (Nanostring). Briefly, data were normalised to the top 100 most highly expressed miRNAs in each sample and the average, calculated as geometric mean, of the six internal controls was used to determine the background control. A target RNA was determined as detected when the measurements obtained for each target was greater than the average counts for the negative controls, and exhibited a p-value <0.05 as

determined by the Student's t-test. A microRNA was designated as differentially expressed between MSCs and MSC-EVs when the expression in one of the sample types exhibited a fold increase >1.5 and a p-value <0.05. RStudio™ version 0.98.501 (RStudio, SPSS Inc) was used to perform unsupervised clustering and to plot the heatmaps.

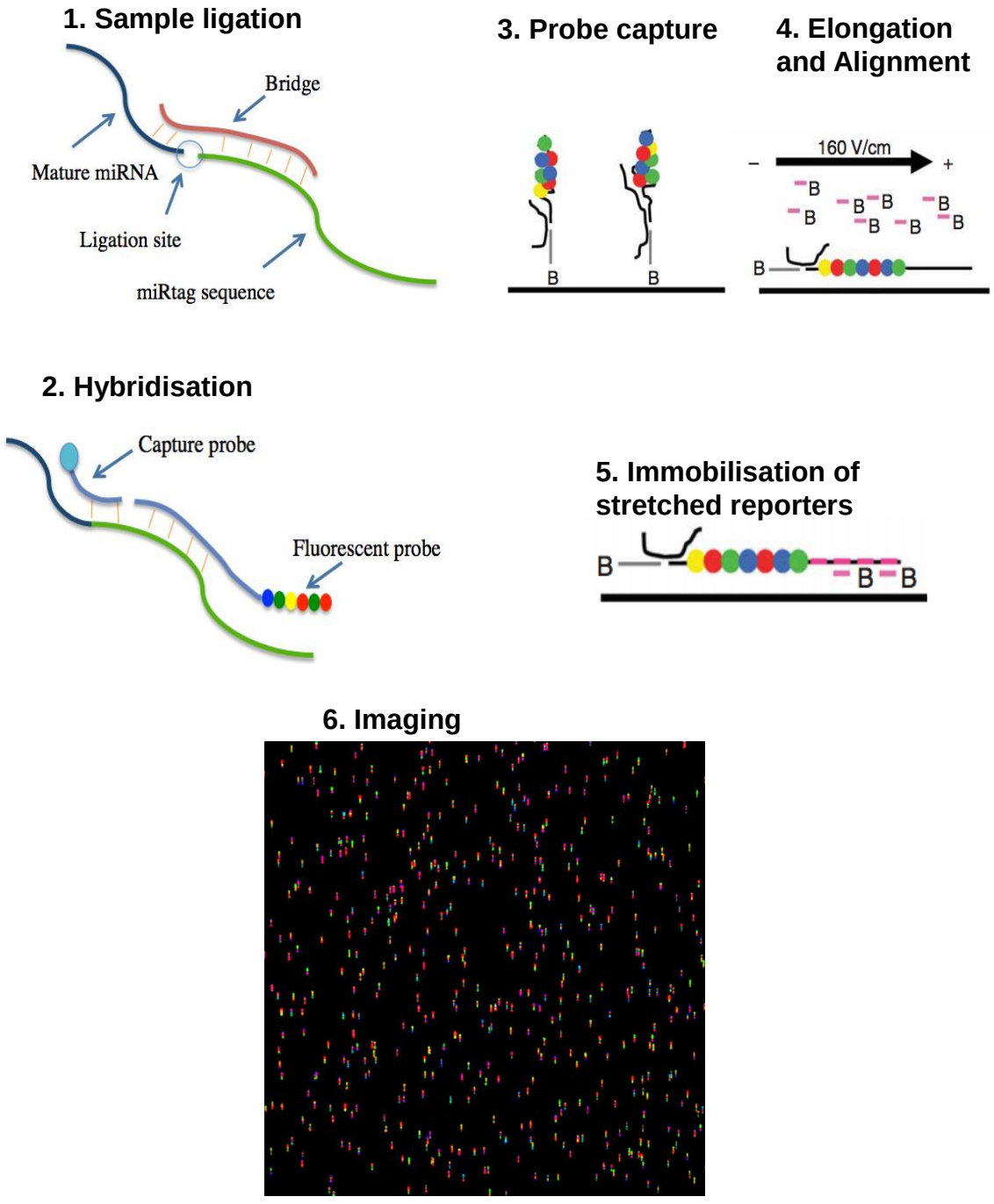

Figure 6.2: Workflow for miRNA profiling using nCounter technology (adapted from Geiss *et al.,* 2008)

6.2.4. qPCR Validation of microRNA profiling

Validation of the microRNA profiling results was performed on 7 selected microRNAs that were highly presented and/or overexpressed in MSC-EVs in comparison to their parent cells by qPCR. Details of the used microRNA primer/probes are described on **Table 6.2**. The Taqman miRNA specific primer/probe consists of a set of primers, both forward and reverse and a Taqman® probe. These probes are based on fluorescence resonance energy transfer (FRET) and they are centred on the same principles as described in **section 2.8.2** for gene expression Taqman® assays.

Table 6.2: Summary of microRNA primer/probes used for qPCR

miRNA ID	Sequence (5'-3')	Catalogue no.	Supplier
hsa-miR-21-5p	UAGCUUAUCAGACUGAUGUUGA	000397	Thermo Fisher
hsa-miR-223	UGUCAGUUUGUCAAAUACCCCA	002295	Thermo Fisher
hsa-miR-142-3p	UGUAGUGUUUCCUACUUUAUGGA	000464	Thermo Fisher
hsa-miR-29b	UAGCACCAUUUGAAAUCAGUGUU	000413	Thermo Fisher
hsa-miR-15a	UAGCAGCACAUAAUGGUUUGUG	000389	Thermo Fisher
hsa-miR-126	UCGUACCGUGAGUAAUAAUGCG	002228	Thermo Fisher
U6 snRNA control	GTGCTCGCTTCGGCAGCACATATACTA AAATTGGAACGATACAGAGAAGATTAG CATGGCCCCTGCGCAAGGATGACACG CAAATTCGTGAAGCGTTCCATATTTT	001973	Thermo Fisher

Synthesis of cDNA and real-time chemistries were performed using the Taqman miRNA reverse transcription kit (Life Technologies) and the SensiFAST™ probe Hi-ROX (Bioline) kit, which has been formulated for use with probe-detection technology, including TaqMan®. The Taqman® chemistry for quantification of microRNAs is a two-step process. The first step involves the synthesis of miRNA specific cDNA by the addition of miRNA specific stem-loop primers that bind to the -3p end of the template. The primer is then extended by the action of

the reverse transcriptase enzyme which adds nucleotides for the cDNA strand synthesis.

For the Taqman® miRNA specific cDNA synthesis 1 ng of cellular and MSC-EV total RNA was reverse transcribed in a 15 µl reaction using specific RT primers (**Table 6.2**) and the Taqman® miRNA reverse transcription kit as described by the manufacturer's protocol. Briefly, the master mix contained the miRNA specific primers, nuclease free water, buffer, reverse transcriptase, RNase inhibitor, dNTPs and diluted RNA (**Table 6.3**). All the steps were performed on ice and reverse transcription reaction was performed on a thermal cycler (applied Biosystems, 2720 Thermal Cycler) using the following settings: 16^{o}C for 30 minutes; 42^{o}C for 30 minutes and 85^{o}C for 5 minutes. The cDNA assays were stored at -80^{o}C until further use.

Table 6.3: Taqman microRNA specific cDNA synthesis master mix

Taqman cDNA master mix	Volume per reaction (µl)
100mM dNTPs	0.15
MultiScribeTM Reverse Transcriptase, 50 U/ml	1
10x Reverse transcription buffer	1.5
RNase inhibitor	0.19
Nuclease-free water	4.16
microRNA specific primer	3
Template total RNA (diluted)	5
Total volume	15

For qPCR reaction, the miRNA specific cDNAs were added to a master mix containing specific miRNA cDNA, nuclease-free water, Taqman primer-probe sets and SensiFAST^{TM} probe Hi-ROX master mix. The samples were run in duplicate at 10µl/well. The duplicate volumes included 20% excess volume to account or pipetting loss (**Table 6.4**).

Table 6.4: miRNA RT-qPCR master mix

Real-Time PCR master mix	Volume (µl) per duplicates
Taqman primer-probe	1.2
SensiFAST™ probe Hi-ROX master mix	12.0
Nuclease-free water	9.2
cDNA	1.6
Total volume	24.0

6.2.5. *In silico* Target prediction

The target genes of the miRNAs detected in MSCs and MSC-EVs were predicted by Ingenuity pathway analysis (as described in section **2.10**) and by miRSystem prediction software (http://mirsystem.cgm.ntu.edu.tw). This software allows for simple and fast analysis of miRNA target genes, biological functions and canonical pathways. This software encompasses several prediction algorithms to analyse 7 online prediction databases and 2 experimentally validated data sources (e.g. Targetscan, mirBase, miRanda, miRecords) to identify the miRNA targets and reduce false positive estimates (Lu *et al.,* 2012). A schematic representation of miRSystems is illustrated on **Fig. 6.3.** In this analysis, predicted targets and were considered when they were observed in at least 4 distinct databases. After target identification a hypergeometric test was used to predict the functions of the target genes and a p-value for each function/pathway was calculated. This was calculated out by ranking the enriched hypergeometric probability as compared with the null baseline probabilities, which was established by randomly selecting a group of miRNAs using the default values in miRSystem database to calculate the statistical significance for each function/pathway. A ranking score was then obtained by the summation of the weight of each specific miRNA in each specific pathway times its enrichment –log(P-value) from the predicted target genes $\{Score = \sum_{\forall miRNA} w_i[-\log_{10}(p_i)]\}$. In this work, miRSystem database was used to investigate pathways that were preferentially targeted by MSC-EV or MSC unique miRNAs and the pathways that are targeted by the most abundant miRNAs detected in MSC-EVs.

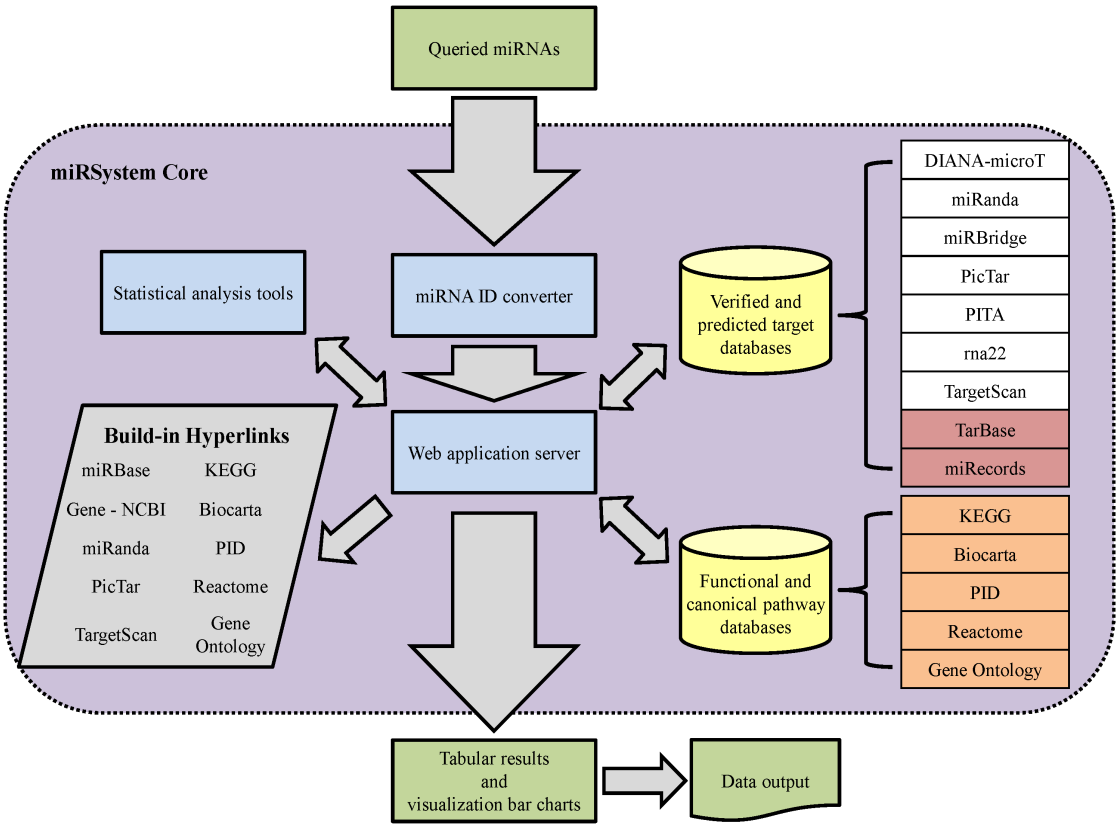

Figure 6.3: **Overview of the miRSystem software (adapted from Lu *et al.*, 2012)**

Green boxes indicate data input and output. The purple rectangle represents the miRSystem core. The three main components of the software are displayed in the blue boxes. This software queries each specific microRNA in 7 different target databases and analyses their influence in specific function/pathways by analysing online databases, including gene ontology and KEGG.

6.3. Results

6.3.1. Quality of RNA extracted from MSCs and MSC-EVs

Before performing the profiling experiment, the RNA integrity number (RIN) of the RNA extracted from MSCs and correspondent MSC-EVs was obtained using Bioanalyzer®. Results showed that RNA extracted from MSCs was of high quality with RINs greater than 7 for all analysed samples, exhibiting single narrow peaks at the 18 and 28S ribosomal RNA (**Fig. 6.4A**). Unlike the parent cells, MSC-EVs enclosed only small RNA species. RNA extracted from MSC-EVs displayed sizes equal or lower than 200nt. No RIN was calculated for the RNA extracted from MSC-EVs due to the absence of the ribosomal RNA peaks (**Fig. 6.4B**).

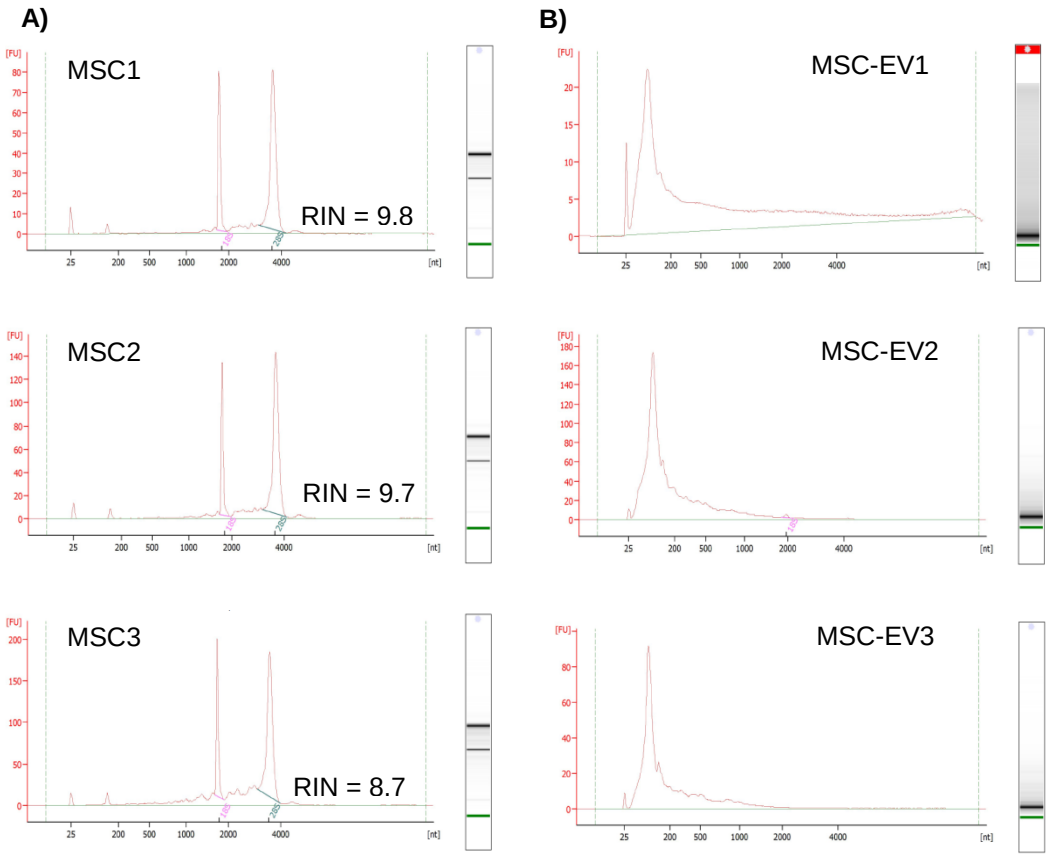

Figure 6.4: **RNA profiles of MSC and MSC-EVs**

Representative electropherograms and gel images show the size distribution in nucleotides (nt), shown on the x-axis, and fluorescence intensity (FU), shown on the y-axis, of total RNA in A) MSCs and B) MSC-EVs. In MSCs the most dominant peaks are the 18 and 28S ribosomal RNA.

6.3.2. Global microRNA profiling of MSCs and MSC-EVs

Global microRNA profiling of MSC and MSC-EVs (n=3) was performed using the nCounter® human microRNA V3 panel containing miRNA specific probes for 800 human microRNAs compiled from miRBase v21. Results were analysed using the nSolver software and microRNA was considered detected in each sample when the normalised counts were ≥10.

Of the 800 miRNAs investigated, averages of 291 ± 11.17 and 324 ± 3.48 miRNAs were detected on MSC and MSC-EVs, respectively. No significant differences in the number of miRNAs were detected among the three analysed samples in both MSCs and MSC-EVs (p=0.420) (**Fig.6.5A**). Principal component analysis (PCA) performed on the MSC and MSC-EV samples using the miRNA microarray data obtained for MSCs and MSC-EVs shows a clear segregation of these two sample types in two distinct clusters (**Fig.6.5B**). Analysis of the sample variability revealed that miRNA profiling was similar between different MSC and MSC-EV samples (sample distance values ≤0.02 for all comparisons). Differences in global miRNA profiles were only detected between MSC and MSC-EV samples (sample distance values >0.40 for all MSC/MSC-EV comparisons performed) (**Fig.6.5C**).

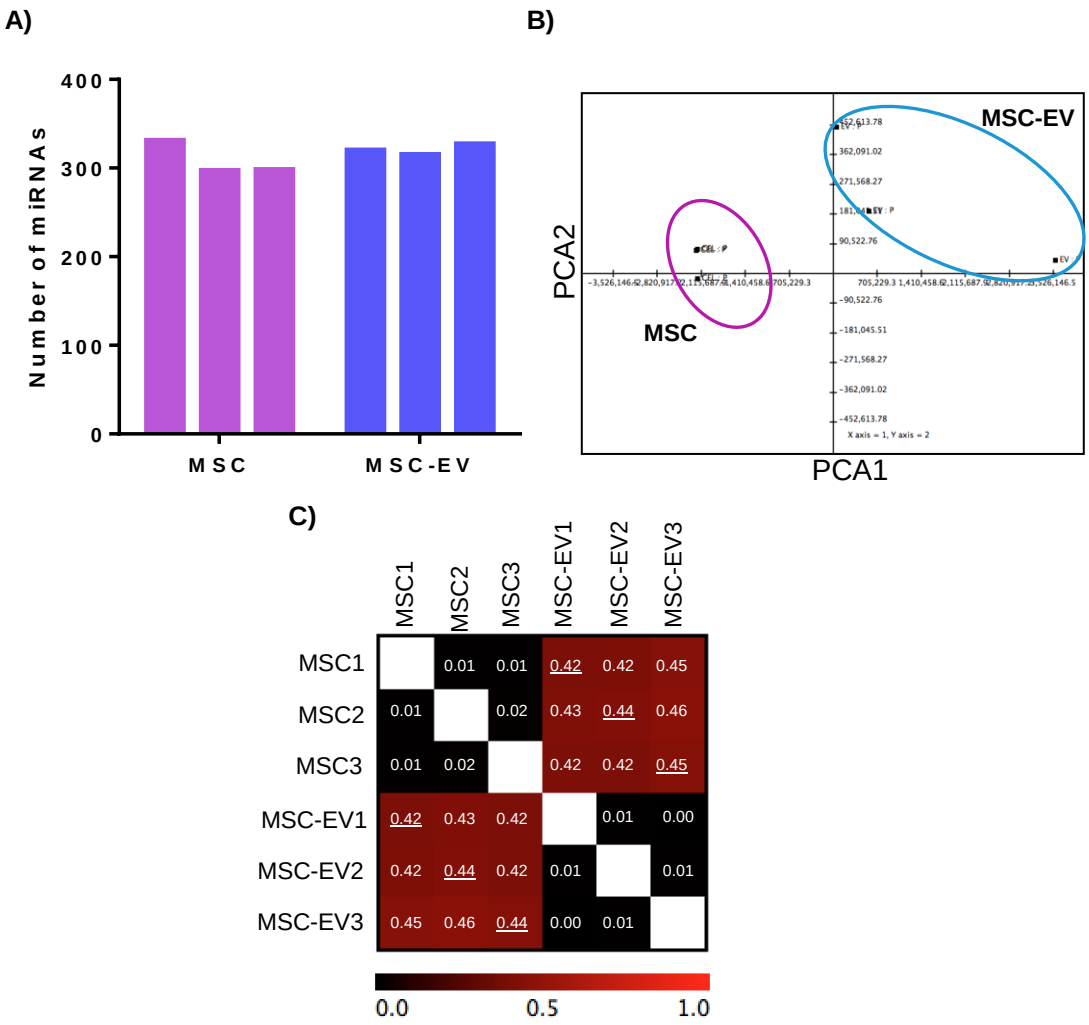

Figure 6.5: Number of microRNAs detected on MSCs and MSC-EV and sample clustering by PCA analysis and sample matrix correlation

The miRNA content of three different samples of MSC and MSC-EVs was individually assessed using nCounter® technology. A target miRNA was determined as detected when the measurements obtained for each target were greater than the average counts for the negative controls and exhibited a p-value <0.05 as assessed by Student's t-test. To account for variances in the background across our cohort, values exceeding the cut-off point of 10 counts were considered to be indicative of relevant miRNA expression. **A)** the number of microRNAs detected across all three samples; **B)** PCA analysis based on the expression patters of miRNAs detected in MSCs (pink circle) and MSC-EVs (blue circle) and **C)** scaled correlation matrices displaying sample similarity as expressed by Pearson's correlation values, for the analysed MSC and MSC-EV samples. The scale bar (0.0 to 1.0) indicates the levels of similarity (0.0) and dissimilarity (1.0) between the samples. PCA and correlation matrices were visualised using TM4 MeV, a R™ Studio based software (www.tm4.org/mev.html)

6.3.3. Differential expression profile of miRNAs in MSCs and MSC-EVs

This microarray identified various miRNAs that were differentially expressed between MSCs and MSC-EVs. A microRNA was considered as differentially expressed between MSCs and MSC-EVs when its expression on one of the sample types exhibited a fold increase >1.5 and a p-value<0.05 as assessed by one-tailed t-tests. A total of 79 miRNAs in MSCs and MSC-EVs were found to be differentially expressed between the two sample types. These differentially expressed miRNAs were used to plot a heat-map based on a hierarchical clustering analysis (**Fig.6.6**).

The heat-map shows 7 distinct expression regions, illustrating the different expression profiles (**Fig.6.6**). From these 79 miRNAs, 49 miRNAs were upregulated in MSC-EVs, of which, miR-223-3p and miR-4286 were the most upregulated, with a fold change of 1992.68 and 833.26, respectively. The remaining 30 miRNAs were up-regulated on MSCs, with miR-502-5p and miR-1253 showing the highest fold increases of 120.89 and 75.54, respectively. Details of all the differentially expressed microRNAs can be found on **Supplementary Table S6.1**.

Further analysis showed that 22/49 of miRNAs upregulated on MSC-EVs were exclusively detected in these samples, while in MSCs, 14/30 of the upregulated miRNAs were unique to the cells (**Fig. 6.7**).

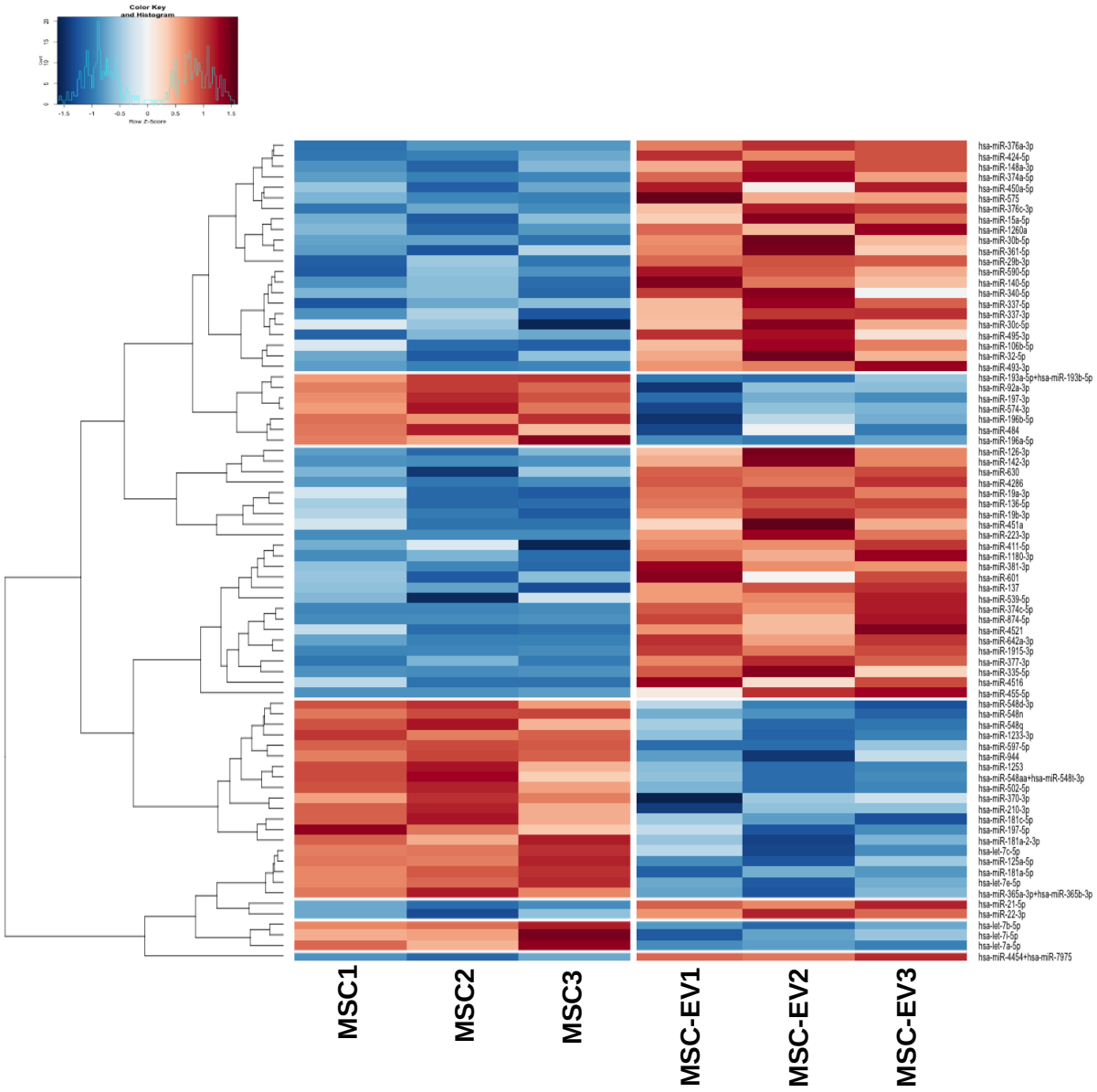

Figure 6.6: Heat-map showing the differentially expressed miRNAs between MSC and MSC-EVs

Hierarchical clustering was performed using the expression levels of the 79 differentially expressed miRNAs. Heatmap colours represent relative miRNA expression as indicated by the colour key, i.e., under-expressed (blue) and over-expressed (red). Each row is representative of one microRNA and each column represents one sample. RStudio™ was used to plot the results.

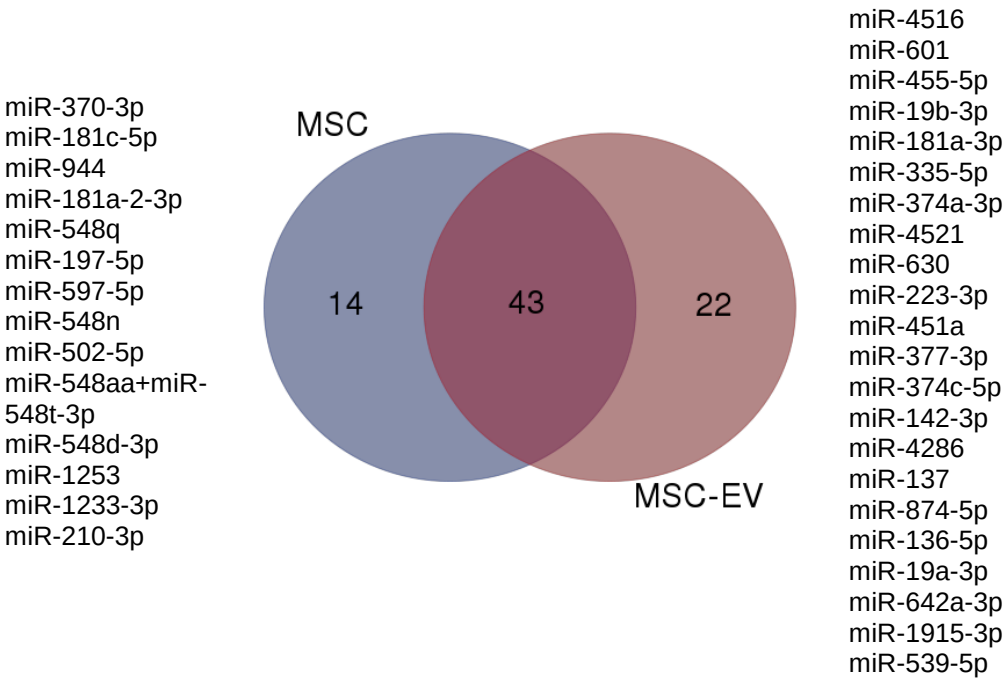

Figure 6.7: Venn diagram showing the differentially expressed miRNAs between MSC and MSC-EVs.

Of the 79 differentially expressed microRNAs, 43 were detected in both MSC and MSC-EV, 14 were unique to MSCs and 22 to MSC-EVs. A detailed list of all the miRNAs can be found on Supplementary Table 6.1. The Venn diagram was generated using the online software http://www.bioinformatics.psb.ugent.be/webtools/Venn/.

6.3.4. Top enriched miRNAs in MSC-EVs

The miRNAs that are most highly enriched in MSC-EVs, i.e., have higher copy number in these vesicles, may have greater biological significance than those differentially expressed, as a higher copy number of the same miRNA may target more genes upon uptake by the recipient cells. The 25 most abundant miRNAs in MSC-EVs are illustrated in **Table 6.5**, with respective average copy number ± SEM and fold change in expression in relation to the MSCs.

Among the top 25 miRNAs in MSC-EVs, only 9 (miR-4454+miR-7975, miR-4286, miR-21-5p, miR-223-3p, miR-142-3p, miR-22-3p, miR-29b-3p, miR-630 and miR-126-3p) showed significantly higher copy numbers in MSC-EVs in comparison to their parent cells (**Supplementary Table S6.1**). In particular, the miRNAs, miR-4286, miR-223-3p, miR-142-3p and miR-630 were exclusively detected in MSC-EVs, indicating a preferential segregation of these miRNAs into the vesicles.

MSC-EVs also contained high concentrations of miRNAs belonging to the let-7 family (let-7a-5p, let-7b-5p and let-7i-5p), however, these miRNAs were expressed in the parent cells at significantly higher levels than in MSC-EVs. The other miRNAs presented in **Table 6.5** were similarly detected in MSCs and MSC-EVs.

Table 6.5: Top 25 enriched miRNAs in MSC-EVs

Results expressed are the average counts ±SEM of miRNA copies detected in MSC-EVs as assessed by the nSolver software. Fold change of the normalised expression values of each microRNA are presented. Negative fold change values represent higher expression of the miRNA in MSC-EVs whereas positive fold change values signify higher expression of the microRNA in MSCs.

microRNA ID	Counts	SEM	FC
miR-4454+miR-7975*	173824.7	501.6	-105.3
miR-125b-5p	11704.9	586.8	6.2
miR-4286*#	8182.4	2.3	-833.3
miR-21-5p*	6957.7	122.5	-6.0
let-7a-5p+	6805.7	2772.3	2.8
miR-199a-3p+miR-199b-3p	4647.7	830.1	-1.5
miR-16-5p	3806.8	149.2	-2.2
let-7b-5p+	3362.6	1045.1	3.1
miR-23a-3p	2682.6	248.3	-1.4
let-7i-5p+	2453.6	1305.2	2.7
miR-221-3p	2167.0	398.9	1.3
miR-223-3p*#	2029.6	0.0	-1992.7
miR-145-5p	1900.4	303.6	3.2
miR-142-3p*#	1659.4	0.2	-224.2
miR-29a-3p	1637.5	69.8	-1.4
miR-22-3p*	1631.4	72.3	-2.2
miR-29b-3p*	1378.2	34.6	-14.5
miR-26a-5p	1333.1	261.0	1.5
miR-494-3p	1319.7	572.7	-12.4
miR-15b-5p	1273.6	124.3	1.7
miR-100-5p	1249.9	40.1	-1.1
miR-630*#	1232.5	4.7	-216.5
miR-130a-3p	1169.1	27.2	-5.3
miR-126-3p*	1156.7	5.2	-86.3
miR-199a-5p	1094.7	86.8	-1.5

* upregulated in MSC-EVs

+ upregulated in MSCs

*# miRNAs upregulated and unique to MSC-EV

FC = fold change of expression

Negative FC – upregulated in MSC-EV

Positive FC – upregulated in MSCs

6.3.5. Real-time quantitative PCR validation of microRNA profiling results

For further validation of the miRNA profiling results, six miRNAs (miR-21-5p, miR-142-3p, miR-29b-3p, miR-223-3p, miR-15a-5p and miR-126-3p) were validated for their expression in MSCs and MSC-EVs by qPCR. These miRNAs were chosen according to both their differential expression levels and according to their regulatory function. In **Chapter 5**, the results showed that MSC-EVs impaired DC maturation and function, by mainly inhibiting their migratory capacity *in vitro* and modifying their secreted cytokine profile. The six microRNAs chosen for qPCR validation have been experimentally validated as important regulators of DC maturation, function and cytokine secretion (Smyth *et al.,* 2015; Turner *et al.,* 2011).

The three paired MSC and MSC-EV samples used for the miRNA profiling using the nCounter® human microRNA array were subjected to qPCR analysis for the expression of the abovementioned miRNAs. The expression of U6 snRNA was used as the miRNA normalisation control for both MSC and MSC-EV miRNA levels. Overall, qPCR analysis validated the miRNA profiling results, with all of the miRNAs showing significantly higher expression levels in MSC-EVs in contrast to their parent MSCs (**Fig.6.8**).

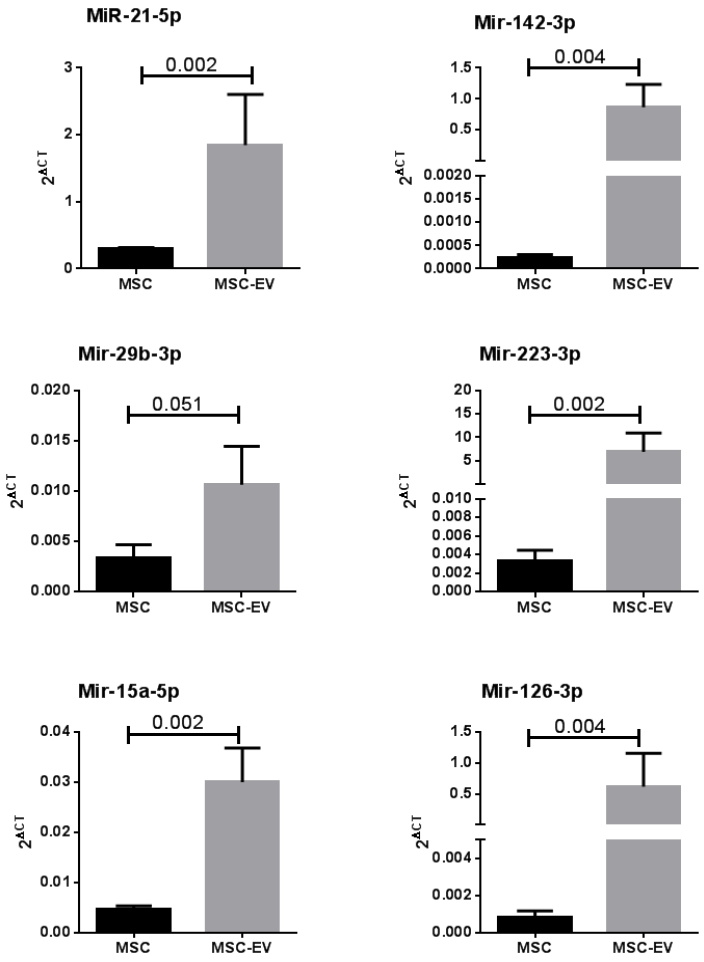

Figure 6.8: RT-qPCR validation of miRNA profiling results

The graphs depict the relative expression levels, herein conveyed as $2^{\Delta CT}$ of 6 miRNAs (miR-21-5p, miR-142-3p, miR-29b-3p, miR-223-3p, miR-15a-5p and miR-126-3p) assessed by qPCR in MSCs and MSC-EVs (n=3). Results express mean ± SEM and Mann-Whitney U tests are presented.

6.3.6. Bioinformatic identification of targets and pathway analysis of miRNA-targets

MicroRNAs can target various genes and are therefore important regulators of a variety of cellular processes. To elucidate the genes and pathways targeted by MSC-EV miRNAs, the ingenuity pathway analysis and the miRSystem online software was used. The miRSystem software retrieves both validated and predicted miRNA target genes from multiple databases (DIANA-microT, miRanda, miRBridge, PicTar, PITA, rna22, TargetScan, TarBase and miRecords), which increases prediction accuracy. Additionally, miRSystems correlated the target list of each microRNA to specific functions/pathways by retrieval of information from several pathway analysis databases, including KEGG, Biocarta and Gene Ontology, and allows for investigation of targeted pathways by a specific or a set of miRNAs. The miRNAs that were unique (n=22) to MSC-EVs and MSCs (n=14) were queried on this database to investigate for differences in targeted pathways. MicroRNA targets predicted by at least 4 distinct databases were selected. In addition, the 25 most abundant miRNAs detected on MSC-EVs were queried to investigate for putative targeted pathways. Pathway enrichment analysis revealed that the putative targets for MSC-EV unique miRNAs are mainly involved in pathways such as, “protein binding transcription factor activity”, “developmental biology” and “nerve growth factor (NGF) signalling” (**Table 6.6A**), while MSCs contain unique miRNAs that target genes involved in “TGF-β signaling pathway”, “axon guidance” and “forkhead box O (FOXO) family signalling” (**Table 6.6B**). Many pathways involved in cellular development and differentiation, migration and homing, such as, signalling by FGFR, PDGF and focal adhesion were highly predicted to be targeted by miRNAs detected in both MSC-EVs and MSCs. The results show that miRNAs that are exclusively secreted into MSC-EVs, are predicted to target “calcium signalling pathway” and “endocytosis”, with 20 and 22 of the queried miRNAs targeting 37 and 45 genes of each pathway respectively (**Table 6.6A**). Calcium signalling is an important pathway involved in the intracellular translocation of multivesicular bodies to the plasma membrane and subsequent secretion to the extracellular milieu (Savina *et al.,* 2003). Endocytosis is one of the main proposed mechanisms of EV uptake by target cells (Mulcahy *et al.,*

2014). These results indicate that MSC-EV enclosed miRNA may be important regulators of biogenesis and mechanisms of secretion and uptake of EVs.

Table 6.6: List of pathways predicted to be targeted by MSC-EV and MSC unique miRNAs. The top 20 pathways predicted to be targeted by the 22 unique MSC-EV **(A)** and the 14 unique MSC **(B)** miRNAs are presented. Pathways were selected according to their score. The number of target genes and miRNAs are presented.

A.List of pathways predicted to be targeted by MSC-EV unique miRNAs

Pathway	Score	#genes	#miRNAs
Protein binding transcription factor activity	2.7	72	22
Developmental biology	2.7	89	22
NGF signalling via TRKA	2.7	40	18
Signalling by NGF	2.6	52	18
Signalling by PDGF	2.4	34	18
Focal Adhesion	2.4	44	20
Signalling by EGFR	2.4	35	18
MAPK signalling pathway	2.2	61	22
Calcium signalling pathway	2.2	37	20
Axon guidance	2.1	56	22
Dilated cardiomyopathy	2.1	23	22
Endocytosis	2.1	45	22
Regulation of nuclear SMAD2/3 signalling	2.1	26	18
Signalling events mediated by FAK	1.9	21	20
Downstream signalling of activated FGFR	1.9	27	16
Pathways in cancer	1.9	60	22
Wnt signalling pathway	1.8	35	20
Melanogenesis	1.8	25	20
CXCR4 mediated signalling events	1.8	24	14
Signalling events mediated by HGFR (C-MET)	1.8	27	22

B. List of pathways predicted to be targeted by MSC unique miRNAs

Pathway	Score	#genes	#miRNAs
TGF-β signalling pathway	2.7	37	14
Axon Guidance	2.6	43	14
FOXO family signalling	2.4	23	12
Pathways **in** cancer	2.4	78	14
Developmental biology	2.3	107	14
Regulation of nuclear SMAD2/3 signalling	2.2	32	14
Signalling by PDGF	2.2	41	14
Transmission across chemical synapses	2.1	45	14
ERBB1 downstream signalling	2.1	35	12
NGF signalling via TRKA	2.0	42	12
Signalling by EGFR	2.0	37	12
PDGFR-β signalling pathway	1.9	37	12
Prostate cancer	1.9	30	12
Neuronal System	1.9	59	14
Downstream signalling of activated FGFR	1.9	34	12
Signalling by NGF	1.9	57	12
ALK1 Signalling events	1.9	13	10
Haemostasis	1.7	84	14
Focal adhesion	1.7	50	12
Neurotrophin signalling pathway	1.7	33	12

Further analysis of the predicted targeted pathways by the 25 most abundant miRNAs in MSC-EVs revealed a preferential targeting of “pathways in cancer”, “focal adhesion” and “developmental biology” (**Table 6.7**). Most of the pathways predicted to be targeted by these miRNAs were similar to the pathways targeted by MSC-EV and MSC unique miRNAs. Notably, MSC-EVs contained miRNAs that target genes involved in relevant pathways related to the development of immune responses, such “MAPK signalling pathway”, “direct p53 effectors”, “TGF-β signalling” and “Wnt signalling”.

Table 6.7: List of pathways predicted to be targeted by the most abundant miRNAs in MSC-EV

The top 20 pathways predicted to be targeted by the top 25 MSC-EV miRNAs are presented. Pathways were selected according to their score. The number of target genes and miRNAs are presented.

List of pathways predicted to be targeted by most abundant miRNAs in MSC-EVs			
Pathway	**Score**	**#genes**	**#miRNAs**
Pathways in Cancer	3.9	142	23
Focal adhesion	3.3	90	23
Developmental biology	3.3	169	22
MAPK signalling pathway	3.2	117	23
Axon guidance	3.2	118	21
Integrins in angiogenesis	2.6	43	22
Direct P53 effectors	2.5	64	21
Signalling by PDGF	2.4	58	22
TGF-β signaling pathway	2.4	47	21
Signalling by NGF	2.3	94	23
Melanoma	2.3	36	22
PDGFR-β signalling pathway	2.3	63	22
Wnt signalling pathway	2.2	71	21
Glioma	2.2	32	22
Prostate cancer	2.2	43	23
NGF signalling via TRKA	2.2	64	22
Endocytosis	2.2	88	22
C-MYB Transcription factor network	2.1	40	22
Protein binding transcription factor activity	2.1	124	22
Neurotrophin signalling pathway	2.1	60	22

Results presented in **Chapter 5** show that MSC-EVs modulate DC maturation and function. To further elucidate whether these effects could be due to MSC-EV enclosed miRNA, the most abundant miRNAs detected in MSC-EVs were queried for their regulatory effect on relevant genes in DC maturation and function.

Several miRNAs were shown to target genes of DC development and function. Members of the let-7 family (let-7a-5p, let-7b-5p and let-7i-5p), all detected in high copy numbers in MSC-EVs (**Table 6.5**) were observed to target genes such as *TLR4*, *CD86*, *IL-6* and *Fas* (Su *et al.,* 2012). MiR-223-3p targets the *CD83* gene, while miR-142-3p has been experimentally observed as an inhibitor of IL-6 expression (Sun *et al.,* 2011). MiR-126-3p targets genes upstream TLR signalling such as Tsc1, a negative regulator of the mTOR kinase (Agudo *et al.,* 2014) and mir-29b targets Bcl-2 gene, which is involved in the maintenance of DC longevity *in vivo* (Hong *et al.,* 2013).

One functional effect of MSC-EV treatment on DCs was the inhibition of CCR7 expression and concomitant abrogation of DC migration towards CCL21 *in vitro*. The microRNA target analysis has shown that the *CCR7* gene can be targeted by 5 different miRNAs (**Fig. 6.9**). Of these, miR-21-5p (**Fig.6.9A**), miR-145-5p (**Fig.6.9B**) and let-7a-5p (**Fig.6.9C**) were all abundantly detected in MSC-EVs, indicating that these miRNAs may be, in part, responsible for the impairment of CCR7 expression by MSC-EV treated DCs. In fact, one of the most promising miRNAs acting as a regulator of DC maturation and function is miR-21-5p. This miRNA was ranked fifth of the top 25 most abundant miRNAs in MSC-EVs (**Table 6.5**). Target analysis of this miRNA revealed that not only its inhibitory effect on CCR7 expression has been experimentally observed (Smigielska-Czepiel *et al.,* 2013); miR-21-5p also targets *IL-12A* and *IL-6* for degradation and indirectly promotes the expression of TGF-β1 and IL-10 (Barnett *et al*., 2016; Lu *et al.,* 2011; Wang *et al.,* 2012). Overall, these results complied with those obtained in **Chapter 5** and indicate miR-21-5p may play an important role in the modulation of DC maturation by inhibiting the expression of IL-12, IL-6 and CCR7 and promoting secretion of TGF-β1.

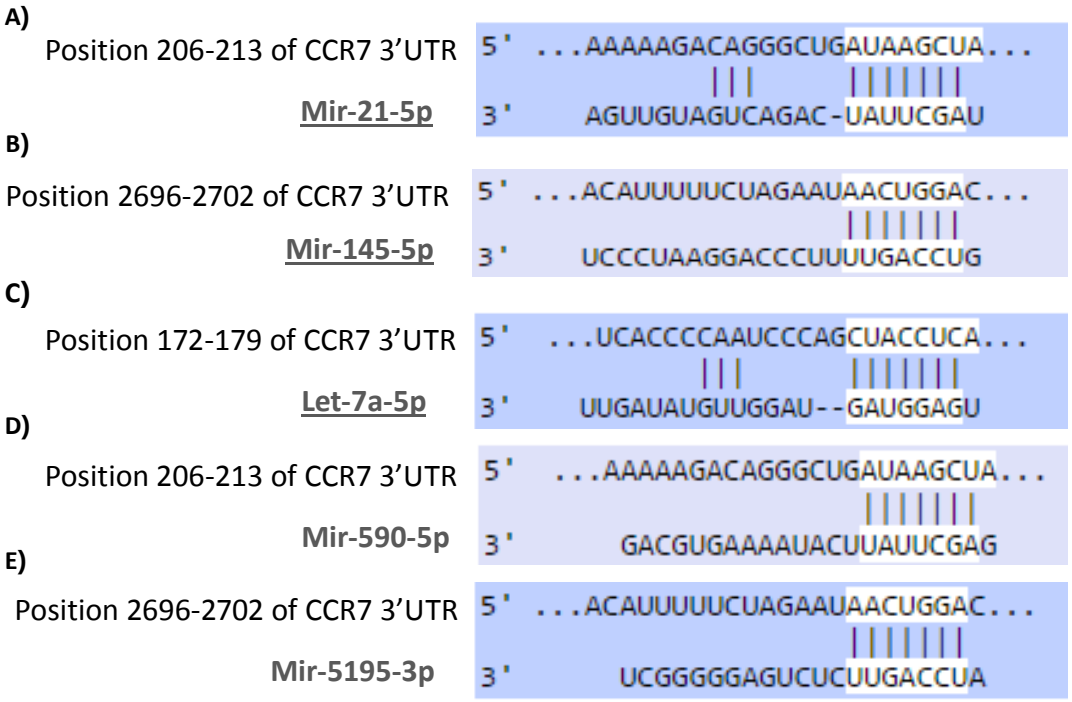

Figure 6.9: Predicted and experimentally observed miRNAs that target CCR7 expression

MiRNAs targeting *CCR7* expression were queried using miRSystems. Graphic representations and complementarity information was obtained from the online database www.targetscan.com. **A)** miR-21-5p, **B)** miR-145-5p, **C)** let-7a-5p, **D)** miR-590-5p and **E)** miR-5195-5p showed complementarity with the conserved 3'UTR regions of *CCR7* gene.

6.4. Discussion

Over the past decade, more than 1900 miRNAs have been identified in humans, and their regulatory effect has been investigated. It is well established that a single miRNA can target more than 200 mRNAs, and specific mRNA can be targeted by more than one miRNA (Bartel, 2004). In MSC research, emerging evidence suggests that MSC therapeutic effects may be largely due to MSC-EV enclosed miRNAs for example, in models of myocardial ischemia and acute kidney injury (Biancone *et al*., 2012; Lai *et al.,* 2010). These observations have prompted several groups to screen for functionally active miRNAs in MSC-EVs to elucidate on the mode of action of the latter (Baglio *et al.*, 2015; Chen *et al.,* 2010; De Luca *et al.,* 2015). The goal of this chapter was to screen for miRNAs in MSC-EVs and MSCs and to investigate miRNAs enriched in MSC-EVs with immuno-regulatory functions, specifically in their ability to regulate DC maturation and function. To our knowledge, this chapter describes the first study to profile miRNAs in MSC-EV and MSCs that were expanded under xeno-free conditions, i.e. in PLT-supplemented medium.

Global miRNA profiling was carried out by Nanostring nCounter® technology. This technology was considered the most appropriate for the investigation of miRNAs in MSC-EVs and MSCs due to its robustness and small sample requirements. This approach resolves endogenous miRNAs without amplification and allows for comparisons of miRNAs profiles within and between individual samples. In comparison to other microarrays, nCounter® technology requires less amounts of input RNA (~100ng of total RNA) and it's not as rigorous as other platforms in its requirements for sample quality (Geiss *et al.,* 2008). This system has also been shown to be as sensitive and precise as real-time Tapman PCR (Malkov *et al.,* 2009). One of the main limitations for miRNA screening from EVs is their low concentration of RNA (concentration < 2 ng/µl for all analysed samples). Prior to miRNA profiling, RNA extracted from MSC and MSC-EVs were checked for their quality and quantity, using the Bioanalyzer system. As expected, RNA extracted from MSCs had RIN>8 which indicated high purity and no degradation of the samples. MSC-EV extracted RNA was as expected, comprised of small RNA (< 200nt) and contained no detectable 18S and 28S rRNA and, as a result, it was not possible to evaluate

the quality of their RNA. Previous studies performed on EVs from other cellular origins using Nanostring technology have shown successful miRNA profiling even when using input concentration of total RNA as low as 1-1.7 ng/µl (Nakamura *et al.,* 2015; Yeh *et al.,* 2015). In this work a minimum of 0.6 ng/µl of MSC-EV RNA was used for global miRNA profiling and ~33 ng/µl were used for MSCs.

Global miRNA profiling of MSC-EVs and MSCs revealed a differential enrichment of 79 miRNAs between the two sample types, with 49 miRNAs being upregulated in MSC-EVs and 30 upregulated in MSCs. Further analysis revealed a signature of 22 and 14 unique miRNAs in MSC-EVs and MSCs, respectively. Bioinformatics analysis of targets and pathway enrichment revealed that both MSC and MSC-EVs unique microRNAs targeted genes of a plethora of pathways, including MAPK, FGF, PDGF and TGF-β, which regulate cellular mechanisms such as cell cycle progression, migration, proliferation and differentiation (Rodrigues *et al.,* 2010). Interestingly, only MSC-EVs contained miRNAs that mediate the processes of endocytosis and calcium signalling. The endocytosis pathway is one of the main pathways of EV formation and uptake by target cells (Mulcahy *et al.,* 2014). Amongst the MSC-EV unique miRNAs, miR-19a-3p and miR-19b-3p, were predicted to inhibit the expression of *RAB5B* and *RAB11FIP2*, two important regulators of the endosomal sorting complexes required for transport (ESCRT)-dependent pathway of multivesicular body formation and translocation to the plasma membrane (Ducharme *et al.,* 2011). Members of the miR-19 family (miR-19b-3p and miR-19a-3p) and miR-377-3p were also predicted to inhibit the expression of epidermal growth factor receptor substrate 15 (*EPS15)*, an integral component of the clathrin-coated pits (Benmerah *et al.,* 1999), and G protein-coupled receptor kinase 6 (*GRK6)* which regulates the mechanism of clathrin-mediated endocytosis (Khan *et al.,* 2010). MSC-EV unique miRNAs, such as miR-142-3p and miR-137 were also predicted to inhibit the expression of calcium signalling genes, such as phospholipase C beta 1 (*PLCB1*) and the erb-b2 receptor tyrosine kinase 4 (*ERBB4),* which play important roles in calcium-dependent intracellular transduction and cytoskeleton movements (Kim *et al.,* 2006; Pregno *et al.,* 2011). Overall, these observations indicate MSC-EVs contain miRNAs that may regulate both secretion and uptake of vesicles by the target cells. Moreover, this

enrichment in miRNAs involved in intracellular compartment mobility may be a direct consequence of the mechanisms of EV biogenesis within the intracellular compartments. During EV biogenesis, these miRNAs are expected to be in close proximity with these organelles in order to regulate the formation and release of these vesicles within the parent cells.

One important analysis of the miRNA profiling in MSC-EVs was to identify the most abundant miRNAs to which the regulatory effects may be more attributable rather than those less abundant miRNAs. These were not necessarily specifically upregulated in MSC-EVs, and within the top 25 most abundant miRNAs, only 9 of them were upregulated in MSC-EVs, with the remaining miRNAs showing equal or even higher concentration in the parent cells. Nonetheless, our study is in agreement with previous studies that profiled for miRNA content in MSC-EVs. Previous groups have shown that MSC-EVs are enriched in members of the let-7 family, miR-21, miR-223 and miR-630 (Baglio *et al.*, 2015; Chen *et al.,* 2010). All of these miRNAs were detected in high copy numbers in MSC-EVs in this present study. It is important to note that the abovementioned studies have been executed in EVs derived from MSCs expanded in FCS supplemented medium, while in our study MSCs were expanded in PLT-supplemented medium. This indicates that culture medium has little influence on the miRNA content of both MSCs and MSC-EVs and consolidates the feasibility of using PLT as culture supplement for MSC *in vitro* expansion.

In Chapter 5, the assessment of MSC-EV ability to modulate allogeneic immune responses has shown that these vesicles are preferentially internalised by DCs and modulate their maturation and function. One of the main detected effects of MSC-EV treatment on DCs, was the impairment of CCR7 expression and consequential inhibition of their migratory potential towards CCL21. Bioinformatics analysis has shown targeting of important genes of DC maturation by the MSC-EV miRNAs, including, miR-142-3p, members of the let-7 family, miR-223, members of the miR-29 family and miR-21-5p. Previous *in vitro* and *in vivo* studies have demonstrated that miRNAs, such as, miR-126, let-7i and miR-142 have important regulatory roles in DC maturation (Smyth et al., 2015). Knock out of let-7i has demonstrated the role of this miRNA in the

expression of co-stimulatory molecules CD80 and CD86 and the production of pro-inflammatory cytokines (Zhang *et al.,* 2011). The upregulation of this miRNA after LPS stimulation leads to the inhibition of the suppressor of cytokine signalling 1 (SOCS1), an inhibitor of Janus kinase/signal transducer which activates transcription signalling after TLR activation (Zhang *et al.,* 2011). MiR-126 is another pro-inflammatory miRNA which has been shown to control the expression of *Tsc-1*, a negative regulator of the mechanistic target of rapamycin (mTOR) signalling pathway, which is essential for the activation of the TLR signalling cascade (Agudo *et al.,* 2014). The high numbers of copies of these miRNAs in MSC-EVs indicate that they may skew DC activation into a pro-inflammatory phenotype; however, this may be counteracted by the activity of other miRNAs. MiR-142-3p and miR-223-3p were two of the most abundant miRNAs in MSC-EVs. MiR-142-3p is an important regulator of cellular development and maturation and its upregulation has been linked to an increase in $FoxP3^+$ regulatory T cells (Zhou *et al.,* 2013). In DCs, mir-142-3p is constitutively expressed in immature DCs and its expression is downregulated upon LPS activation (Mildner *et al.,* 2013). MiR-142-3p directly binds to IL-6 mRNA and inhibits its production (Sun *et al.,* 2011). In Chapter 5, it was observed that IL-6 secretion by DCs was significantly decreased after MSC-EV treatment. In addition to cytokine secretion, one other observation was the decreased phagocytic capacity of MSC-EV treated immature DCs. In previous studies, DCs from miR-223-deficient mice had reduced capacity to cross-present antigens (Mi *et al.,* 2013), indicating that this miRNA affects the antigen presentation pathways, however, the exact inhibitory mechanism has not been yet elucidated. Additionally, miR-223 inhibits the production of signal transducer and activator of transcription 3 (*STAT3*), which is essential for the production of the pro-inflammatory cytokines IL-6 and IL-1β (Chen *et al.,* 2012).

Other miRNAs, e.g. miR-29b-3p and miR-29a-3p, have also been shown to affect DC function mainly regulating their survival (Smyth *et al.,* 2015), however, one of the most interesting miRNAs detected in MSC-EVs, is miR-21-5p.

MiR-21 is one of the most highly expressed miRNAs in many mammalian cell types, and its upregulation has been associated in many diseases, including solid tumours, cardiac injury and inflamed tissue (Sheedy, 2015). This miRNA

was detected in both MSCs and MSC-EVs, however, its expression was higher in MSC-EVs. MiR-21 was also one of the most abundant miRNAs detected in the vesicles, occupying position number 4 of the top enriched miRNAs, being surpassed only by mir-454+mir-7975, mir-125b-5p and mir-4286, which are important regulators of EV biogenesis and secretion, as assessed by bioinformatics analysis. The regulation of inflammatory responses by miR-21 has been well documented by many groups. One of the main targets of miR-21 is programmed cell death protein 4 (*PDCD4*). The expression of *PDCD4* is essential to inhibit IL-10 production and promote IL-6 production via the activation of NF-kB pathway (Sheedy *et al.,* 2010). Sheedy *et al* (2010) have shown that transfection of PBMCs with miR-21 induced inhibition of PDCD4 production which in turn blocked NF-kB activation. This resulted in enhanced IL-10 induction and blockade of IL-6 production (Sheedy *et al.,* 2010). Lu *et al* (2011) demonstrated that DCs from mir-21-deficient mice had increased IL-12 production after LPS stimulation and $CD4^+$ T cells produced higher concentrations of IL-4 (Lu *et al.,* 2011). In Chapter 5, MSC-EV treated DCs secreted lower amounts of IL-6 and IL-12. It is important to note that the MSC-EVs used in the co-culture experiments with DCs were of the same source as the MSC-EVs used for miRNA global profiling. Given the high concentration of miR-21-5p detected in MSC-EVs, it is plausible to hypothesise that this miRNA may be one of the main bioactive components in the regulation of the observed effects in MSC-EV treated DCs. In addition to blocking the production of pro-inflammatory cytokines, such as IL-6 and IL-12, miR-21 also enhances TGF-β signalling (Wang *et al.,* 2012). Knock down experiments of miR-21 in glioblastoma cell lines have demonstrated a dysregulation of TGF-β signalling in these cells. MiR-21 was shown to indirectly regulate TGFB1/2 thus inducing activation of TGF-β signalling pathway (Li *et al.,* 2013). These results were further verified by Liu and colleagues who showed that mir-21 directly targeted *SMAD7*, which is an inhibitory regulator of TGF-β signalling (Liu *et al.,* 2010). In the present work, MSC-EV treated DCs were shown to produce higher concentrations of soluble TGF-β1.

One of the validated targets for this miRNA is *CCR7*. Smigielska-Czepiel *et al* (2013) demonstrated that silencing of miR-21 in activated naïve and memory T cells resulted in a significant induction of *CCR7* expression (Smigielska-Czepiel

et al., 2013). In DCs miR-21 was shown to have a highly conserved target region in *CCR7* 3'UTR and to be significantly down-regulated upon DC maturation. Lentiviral transfection of miR-21 of DCs has demonstrated a reduction of *CCR7* expression, even after LPS maturation. In our study, CCR7 was significantly decreased upon MSC-EV treatment of DCs, in the presence of LPS, which resulted in decreased migratory capacity *in vitro* (Al Akoum *et al.,* 2015).

Overall, miR-21-5p may be one of the main bioactive components of MSC-EVs in the context of DC maturation. As proof of concept, further experiments of transfection of DCs with miR-21 mimics and inhibitors are needed to confirm this hypothesis.

However, it is unlikely that the effect observed modulatory effects on DCs by MSC-EVs is solely due to the activity of miR-21-5p, and their enclosed microRNAs. MSC-EVs are complex structures enclosing a wide variety of bioactive proteins, RNAs and lipids. All of these components may be involved in the functional effects of these vesicles. Additionally, the mechanisms of EV internalisation by the target cells remains widely unexplored, and little is known about the fate of EVs after uptake. Further research is needed to investigate these issues in order to elucidate how MSC-EVs and their content modulate physiological processes in the recipient cells. Nonetheless, this work is the first to explore the role of MSC-EV derived microRNAs in their modulatory effects on DCs.

Acknowledgements:

Kile Green for assisting in the running and the analysis of Nanostring nCounter®

Chapter 7: Concluding remarks and future work

“Science never solves a problem without creating ten more”

– George Bernard Shaw

Chapter 7: Concluding remarks and future work

In the past decades, the immunomodulatory properties of MSCs have been explored in clinical trials to treat a variety of diseases. Despite the promising results, questions remain unanswered regarding their safety and mode of action. This thesis aimed at investigating the suitability of xenogeneic-free expansion of bone marrow-derived MSCs using human PLT as culture supplement, and investigating their immunosuppressive properties and especially, the regulatory properties of MSC-derived EVs.

The findings in this thesis confirm the current knowledge demonstrating that human PLT-expanded MSCs complied with the ISCT criteria. Further results showing retention of the immunosuppressive properties by PLT-expanded MSCs provide new evidence to the currently controversial literatures supporting the potential of using human PLT-expanded MSCs for the treatment of medical conditions caused by the failure of effective immune regulation.

This thesis is the first to perform a large scale phenotypic characterisation and PLT-expanded MSC using high-throughput flow cytometry. This study demonstrated that PLT-expansion upregulates the expression of surface proteins that confer enhanced proliferative and differentiation properties to MSCs (Reis *et al.*, manuscript in preparation). Current research supports the notion that human PLT is a suitable supplement for the clinical production of MSCs. MSC-PLT have now been used in clinical trials of, for example, GvHD and diabetes (Introna *et al.,* 2014; Lucchini *et al.,* 2010). Human PLT contains a variety of mitogenic factors, such as, PDGF and FGF, which contribute to the proliferation of MSCs. However, platelets enclose many other constituents, such as metabolites and complement proteins. Recent published work also highlighted the involvement of microRNAs and EVs in platelet functions (Quesenberry *et al.,* 2015). These constituents are also present in platelet derivatives (Burnouf *et al.,* 2016). Future work to unravel the interplay between each of these constituents in MSC function and general characteristics is necessary.

The enhanced proliferation rate of MSC-PLT is one of the most attractive effects of using this supplement for MSC expansion. This is of great interest for future

therapeutic use of MSCs since PLT-expansion allows for the generation of reasonable MSC numbers in less time and in conditions compliant with the current good manufacturing practice guidelines. Nonetheless, for clinical application it is adamant to understand the mechanisms behind this enhanced proliferative kinetics. The proliferation rates are intrinsically correlated to the level of senescence of MSCs, which in turn, is associated to the epigenetic changes that occur to the cells during *in vitro* expansion (Griffiths *et al.,* 2013; Li *et al.,* 2011). Future work analysing the PLT-induced epigenetic changes in MSCs, in comparison to their FCS-expanded counterparts, is warranted. This could be performed by analysing the DNA methylation profiles of both cell populations.

Current consensus within the MSC community is that their mode of action is mainly accounted to MSC-derived secretome. We therefore conducted the first study so far to investigate the characteristics and functional properties of extracellular vesicles secreted by PLT-expanded MSCs (PLT-MSC-EVs). This part of the study showed that PLT-expanded MSCs are able to secrete a large amount of EVs, which could partially mimic the immunosuppressive potential of the parent cells. Further effort focusing on their modulatory effect on DC maturation and function showed that PLT-MSC-EVs are able to impair expression of maturation markers by DCs, to skew DC cytokine secretion towards a tolerogenic profile and to inhibit the migratory potential of DCs (Reis *et al.*, manuscript in preparation). The work in this thesis revealed that PLT-MSC-EVs have an enrichment of microRNAs, with the potential to regulate the expression of genes which are upregulated during DC maturation, including CCR7, IL-12 and IL-6. DCs are major players of immune responses. Encounter with foreign antigens drives DC maturation and migration to the lymph nodes where they present the antigens to the naïve T cells (Waisman *et al.,* 2016). Our data suggest PLT-MSC-EVs may prevent the migration of DCs to the lymph nodes hence diminish antigen presentation to the naïve T cells. This effect is of great relevance in clinical applications where MSCs are used to attenuate an exacerbated immune system. To confirm the *in vitro* findings reported in this thesis it would help to test the effect of PLT-MSC-EVs on DC maturation and migration using murine models. The findings in this research could also be strengthened by investigating the PLT-MSC-EV-induced changes in the overall

gene expression profile of DCs and their effect on the activation and/or inhibition of relevant molecular pathways, such as NF-κB.

The profiles of the microRNA content of PLT-MSC-EVs have not been reported before. This thesis analysed, for the first time, the microRNA profiles of MSC-PLT and PLT-MSC-EV and identified a signature of microRNAs that are differentially expressed in PLT-expanded MSCs and their derived MSC-EVs. The work presented in this report has demonstrated selective packaging of microRNAs in PLT-MSC-EVs which regulate a variety of molecular pathways and modulate the expression of genes involved in multivesicular body biogenesis and intracellular trafficking. More investigations in this matter are warranted to identify the mechanisms of selective packaging into the vesicles. Both MSC-PLT and PLT-MSC-EVs were rich in a variety of microRNAs with the potential to modulate the expression of pathways relevant to the development of inflammatory responses. Moreover, this thesis identified microRNAs which have high copy numbers in PLT-MSC-EVs, such as miR-21-5p, with complementarity to genes involved in DC functions. Experiments where the microRNAs are overexpressed or knocked down by transfecting the DCs with mimics or inhibitors are necessary to enlighten on the weight of these microRNAs on MSC-EV biological effect.

In summary, this thesis has demonstrated that PLT-expansion maintained the general characteristics and immunosuppressive properties of MSCs. This work has provided in depth information about the effect PLT-supplemented medium on MSC overall surface protein phenotype and established the molecular basis for the enhanced proliferative properties of MSC-PLT. In addition, MSC-EVs derived from PLT-expanded MSCs were shown to maintain modulatory properties of the parent cells, and further analysis of the microRNA content of these vesicles has explored the molecular basis of the modulatory effects of PLT-MSC-EVs.

Increasing research in the last years points to the possibility of reproducing the therapeutic effects of MSCs with their derived EVs. This has prompted the research community to think about the use of these vesicles as a safer and more reproducible therapeutic tool. MSC-EV research is however still in its infancy, and little is known about their therapeutic effects, especially in

modulating the immune system. This thesis has contributed to the understanding of the modulatory effects of these vesicles, and describes a rationale of how MSCs may modulate immune responses when used in therapeutic settings.

Several questions remain unanswered, and, despite MSC-EV modulatory properties described in this thesis, further research is needed. For these vesicles to be considered for therapeutic application, some questions need to be further investigated, including:

1) Are MSC-EVs as potent as their parent cells in modulating the immune system?
2) How does the inflammatory environment influence the composition of MSC-EVs?
3) How are MSC-EVs bio-distributed *in vivo*? How long do these vesicles remain in the system after administration?
4) How are these vesicles taken up by the recipient cells and what is their "fate" upon internalisation?
5) What bioactive components, i.e, proteins, lipids, and genetic material do these vesicles contain? How does each component contribute to MSC-EV mediated effects? What is the interactome profile of MSC-EVs?
6) How do different types of vesicles contribute to the biological effects detected upon MSC-EV treatment?

One other issue to take into consideration is the feasibility of purifying enough MSC-EVs for future clinical application. Current protocols are not effective at purifying the whole population of vesicles present in the supernatants. In this project, due to the low yield of MSC-EVs, the maximum amount of 20µg/ml of MSC-EVs was used to test their modulatory effect on DCs. Further tests are needed to determine whether the concentration of MSC-EVs was sub-optimal, and enhanced suppression of DC maturation and functions could be achieved with higher MSC-EV concentrations. Future optimisation of EV purification protocols is needed to improve the yield of MSC-EVs, by, for example, performing comparative studies of the yield and characteristics of MSC-EVs purified using the standard differential ultracentrifugation protocols, and, for

example, a combination of ultracentrifugation and concentration of MSC supernatants.

Collectively, this thesis has provided new insights in the feasibility of developing future MSC therapy under xeno-free conditions. Novel evidence reported in this thesis has added new knowledge that significantly advances the understanding in the mode of action of MSC mediated immune modulation.

Appendices

Appendix I – Supplementary information for Chapter 3

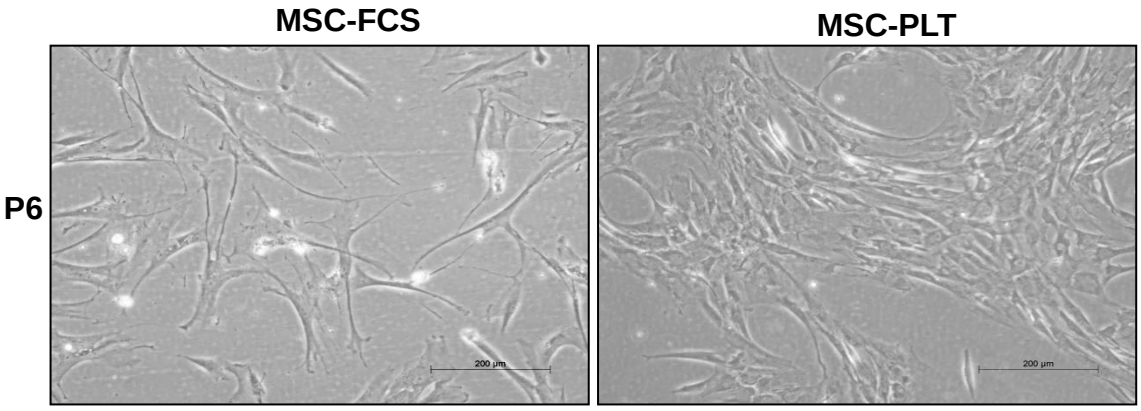

Supplementary figure S3.1: Morphology of MSC-PLT and MSC-FCS at passage 6

Representative micrographs of MSCs expanded in FCS and PLT supplemented medium. By passage 6, while MSC-PLT maintains compact and elongated morphology, MSC-FCS become flatter and exhibits a ragged morphology.

Appendix II – Supplementary information for Chapter 4

Plate 1						
Position		Marker	Fluorochrome	Clone	Isotype	Internal order Cat. No.
A	1	empty				empty
B	1	empty				empty
C	1	empty				empty
D	1	empty				empty
E	1	Mouse IgG1 – isotype control	APC	IS5-21F5		120-012-330
F	1	Anti-DLL1	APC	MHD1-314	mouse IgG1	120-009-186
G	1	Anti-DLL4	APC	MHD4-46	mouse IgG1	120-014-738
H	1	Anti-DR3	APC	JD3	mouse IgG1k	120-019-943
A	2	Anti-GITR	APC	DT5D3	mouse IgG1	120-011-653
B	2	Anti-HLA-E	APC	3D12	mouse IgG1	120-008-911
C	2	Anti-iNKT	APC	6B11	mouse IgG1	120-010-713
D	2	Anti-Jagged2	APC	MHJ2-523	mouse IgG1	120-009-173
E	2	Anti-KIR2D	APC	NKVFS1	mouse IgG1	120-014-004
F	2	Anti-LAP (TGF-β1)	APC	CH6-17E5.1	mouse IgG1	120-008-767
G	2	Anti-Melanoma (MCSP)	APC	EP-1	mouse IgG1	120-001-873
H	2	Anti-MSCA-1 (W8B2)	APC	W8B2	mouse IgG1	120-014-003
A	3	Anti-NKp80	APC	4A4.D10	mouse IgG1	120-014-800
B	3	Anti-Notch3	APC	MHN3-21	mouse IgG1	120-009-197
C	3	Anti-ROR-1	APC	2A2	mouse IgG1	120-010-756
D	3	Anti-Siglec-8	APC	7C9	mouse IgG1	120-012-105
E	3	Anti-Siglec-1	APC	5G6	mouse IgG1κ	120-018-192
F	3	Anti-TCR-Vδ2	APC	123R3	mouse IgG1	120-013-587
G	3	Anti-TCRγ/δ	APC	11F2	mouse IgG1	120-013-215
H	3	Anti-TIM-3	APC	F38-2E2	mouse IgG1	120-012-152
A	4	CD1a	APC	HI149	mouse IgG1	120-010-403
B	4	CD1b	APC	SN13	mouse IgG1	120-010-977
C	4	CD4	APC	M-T466	mouse IgG1	120-010-605
D	4	CD5	APC	UCHT2	mouse IgG1	120-014-379
E	4	CD6	APC	M-T411	mouse IgG1	120-014-663
F	4	CD9	APC	SN4 C3-3A2	mouse IgG1	120-018-644
G	4	CD10	APC	97C5	mouse IgG1	120-014-372
H	4	CD18	APC	TS1/18	mouse IgG1κ	120-016-605
A	5	CD19	APC	LT19	mouse IgG1	120-010-635
B	5	CD20	APC	LT20	mouse IgG1	120-010-122
C	5	CD23	APC	M-L23.4	mouse IgG1	120-014-691
D	5	CD24	APC	32D12	mouse IgG1	120-013-143
E	5	CD25 (3G10)	APC	3G10	mouse IgG1	120-017-010
F	5	CD27	APC	M-T271	mouse IgG1	120-010-666
G	5	CD28	APC	1.50E+09	mouse IgG1	120-012-887
H	5	CD29	APC	TS2/16	mouse IgG1κ	120-016-831
A	6	CD30	APC	Ki-2	mouse IgG1	120-011-649
B	6	CD31	APC	AC128	mouse IgG1	120-010-644
C	6	CD33	APC	AC104.3E3	mouse IgG1	120-012-463
D	6	CD35	APC	E11	mouse IgG1	120-014-067
E	6	CD39	APC	MZ18-23C8	mouse IgG1	120-014-757
F	6	CD40	APC	HB14	mouse IgG1	120-012-874
G	6	CD43	APC	DF-T1	mouse IgG1	120-009-800
H	6	CD44	APC	DB105	mouse IgG1	120-010-692
A	7	CD49a	APC	TS2/7	mouse IgG1κ	120-017-044
B	7	CD51/CD61	APC	23C6	mouse IgG1κ	120-018-217
C	7	CD55 (DAF)	APC	JS11	mouse IgG1κ	120-017-794
D	7	CD56	APC	AF12-7H3	mouse IgG1	120-010-597
E	7	CD58 (LFA-3)	APC	TS2/9	mouse IgG1κ	120-015-970
F	7	CD61	APC	Y2/51	mouse IgG1	120-011-650
G	7	CD62L	APC	145/15	mouse IgG1	120-012-804
H	7	CD63	APC	H5C6	mouse IgG1	120-014-628
A	8	CD64	APC	10.1.1	mouse IgG1	120-014-747
B	8	CD69	APC	FN50	mouse IgG1	120-012-429
C	8	CD73	APC	AD2	mouse IgG1	120-010-699
D	8	CD74	APC	5-329	mouse IgG1	120-017-230
E	8	CD79a	APC	HM47	mouse IgG1	120-011-899
F	8	CD80	APC	2D10	mouse IgG1	120-013-519
G	8	CD83	APC	HB15	mouse IgG1	120-012-457
H	8	CD84	APC	MZ18-21F6	mouse IgG1	120-004-972
A	9	CD86	APC	FM95	mouse IgG1	120-010-661
B	9	CD87	APC	VIM5	mouse IgG1	120-012-920
C	9	CD90	APC	DG3	mouse IgG1	120-010-696
D	9	CD93	APC	VIMD2	mouse IgG1	120-011-106
E	9	CD95	APC	DX2	mouse IgG1	120-013-556
F	9	CD97	APC	VIM3b	mouse IgG1	120-009-358
G	9	CD101	APC	BB27	mouse IgG1	120-006-980
H	9	CD105	APC	43A4E1	mouse IgG1	120-012-644
A	10	CD107a	APC	H4A3	mouse IgG1	120-014-677
B	10	CD111	APC	R1.302	mouse IgG1	120-018-444
C	10	CD114	APC	LMM741	mouse IgG1	120-009-602
D	10	CD117 (A3C6E2)	APC	A3C6E2	mouse IgG1	120-010-687
E	10	CD133/1 (AC133)	APC	AC133	mouse IgG1	120-012-327
F	10	CD134 (OX40)	APC	ACT35	mouse IgG1	120-007-145
G	10	CD137	APC	4B4-1	mouse IgG1	120-012-439
H	10	CD141 (BDCA-3)	APC	AD5-14H12	mouse IgG1	120-012-413
A	11	CD142	APC	HTF-1	mouse IgG1	120-012-109
B	11	CD146	APC	541-10B2	mouse IgG1	120-010-703
C	11	CD158a/h (KIR2DL1/DS1)	APC	11PB6	mouse IgG1	120-013-516
D	11	CD158e (KIR3DL1)	APC	DX9	mouse IgG1	120-013-573
E	11	CD158f (KIR2DL5)	APC	UP-R1	mouse IgG1	120-011-651
F	11	CD158i (KIR2DS4)	APC	JJC11.6	mouse IgG1	120-013-539
G	11	CD163	APC	GHI/61.1	mouse IgG1	120-014-768
H	11	CD165	APC	SN2	mouse IgG1	120-011-858
A	12	CD169 (Siglec-1)	APC	7-239	mouse IgG1	120-011-971
B	12	CD178	APC	NOK-1	mouse IgG1	120-008-354
C	12	CD180 (RP105)	APC	MHR73-11	mouse IgG1κ	120-011-193
D	12	CD197 (CCR7)	APC	FR 11-11E8	mouse IgG1	120-010-715
E	12	CD200	APC	OX-104	mouse IgG1	120-008-935
F	12	CD203c	APC	FR 3-16A11	mouse IgG1	120-012-425
G	12	CD205	APC	HD30	mouse IgG1κ	120-008-611
H	12	CD206	APC	DCN228	mouse IgG1	120-013-554

Plate 2						
Position		Marker	Fluorochrome	CLONE	Isotype	Internal order cat. no
A	1	CD207 (Langerin)	APC	MB22-9F5	mouse IgG1	120-010-769
B	1	CD209 (DC-SIGN)	APC	DCN47.5	mouse IgG1	120-013-535
C	1	CD218 (IL-18Rα)	APC	H44	mouse IgG1κ	120-015-558
D	1	CD226 (DNAM-1)	APC	DX11	mouse IgG1	120-014-764
E	1	CD229 (Ly-9)	APC	Hly9.1.25	mouse IgG1	120-014-112
F	1	CD231 (TALLA)	APC	SN1a	mouse IgG1	120-011-151
G	1	CD253	APC	RIK-2.1	mouse IgG1	120-009-527
H	1	CD262	APC	DJR2-4	mouse IgG1	120-009-322
A	2	CD263 (TRAIL-R3)	APC	DJR3	mouse IgG1κ	120-019-765
B	2	CD268	APC	11C1	mouse IgG1	120-010-073
C	2	CD271 (LNGFR)	APC	ME20.4-1.H4	mouse IgG1	120-010-620
D	2	CD273 (B7-DC)	APC	MIH18	mouse IgG1	120-011-861
E	2	CD275 (B7-H2)	APC	MIH12	mouse IgG1	120-012-112
F	2	CD283	APC	TLR 3.7	mouse IgG1	120-014-669
G	2	CD300e (IREM-2)	APC	UP-H2	mouse IgG1κ	120-017-767
H	2	CD300f (IREM-1)	APC	UP-D2	mouse IgG1	120-010-956
A	3	CD303 (BDCA-2)	APC	AC144	mouse IgG1	120-010-674
B	3	CD304 (BDCA-4/Neuropilin-1)	APC	AD5-17F6	mouse IgG1	120-012-336
C	3	CD309 (VEGFR-2/KDR)	APC	ES8-20E6	mouse IgG1	120-012-442
D	3	CD314 (NKG2D)	APC	BAT221	mouse IgG1	120-012-823
E	3	CD324 (E-Cadherin)	APC	67A4	mouse IgG1	120-013-534
F	3	CD326 (EpCAM)	APC	HEA-125	mouse IgG1	120-010-683
G	3	CD335 (NKp46)	APC	9.00E+02	mouse IgG1	120-012-515
H	3	CD336 (NKp44)	APC	2,29	mouse IgG1	120-013-196
A	4	CD337 (NKp30)	APC	AF29-4D12	mouse IgG1	120-013-239
B	4	Mouse IgG2a – isotype control	APC	S43.10		120-012-412
C	4	Anti-CLEC9A	APC	8F9	mouse IgG2a	120-014-739
D	4	Anti-CRTAM	APC	Cr24.1	mouse IgG2a	120-008-069
E	4	Anti-GLAST (ACSA-1)	APC	ACSA-1	mouse IgG2a	120-012-452
F	4	Anti-HLA-DR	APC	AC122	mouse IgG2a	120-010-647
G	4	Anti-MICA/MICB	APC	6D4	mouse IgG2a	120-015-938
H	4	Anti-Notch2	APC	MHN2-25	mouse IgG2a	120-009-164
A	5	Anti-PTK7 (CCK-4)	APC	188B	mouse IgG2a	120-014-000
B	5	CD1c (BDCA-1)	APC	AD5-8E7	mouse IgG2a	120-010-641
C	5	CD3	APC	BW264/56	mouse IgG2a	120-010-583
D	5	CD4 (VIT4)	APC	VIT4	mouse IgG2a	120-010-601
E	5	CD8 (BW135/80)	APC	BW135/80	mouse IgG2a	120-010-623
F	5	CD14	APC	TÜK4	mouse IgG2a	120-010-613
G	5	CD21	APC	HB5	mouse IgG2a	120-017-587
H	5	CD26	APC	FR10-11G9	mouse IgG2a	120-014-019
A	6	CD32	APC	2.00E+01	mouse IgG2a	120-009-773
B	6	CD34	APC	AC136	mouse IgG2a	120-010-595
C	6	CD36	APC	AC106	mouse IgG2a	120-014-687
D	6	CD38	APC	IB6	mouse IgG2a	120-012-821
E	6	CD45	APC	5B1	mouse IgG2a	120-010-510
F	6	CD45RO	APC	UCHL1	mouse IgG2a	120-013-152
G	6	CD71	APC	AC102	mouse IgG2a	120-012-801
H	6	CD88 (C5AR)	APC	S5/1	mouse IgG2a	120-019-238
A	7	CD99	APC	3B2/TA8	mouse IgG2a	120-019-136
B	7	CD123	APC	AC145	mouse IgG2a	120-012-334
C	7	CD127	APC	MB15-18C9	mouse IgG2a	120-010-614
D	7	CD152	APC	BNI3	mouse IgG2a	120-009-353
E	7	CD154	APC	5C8	mouse IgG2a	120-012-421
F	7	CD158b (KIR2DL2/DL3)	APC	DX27	mouse IgG2a	120-013-246
G	7	CD161	APC	191B8	mouse IgG2a	120-012-443
H	7	empty				empty
A	8	CD284	APC	HTA125	mouse IgG2a	120-014-384
B	8	Mouse IgG2b – isotype control	APC	IS6-11E5.11		120-012-426
C	8	Anti-FcεRIα	APC	CRA1	mouse IgG2b	120-007-695
D	8	Anti-Perforin	APC	delta G9	mouse IgG2b	120-008-703
E	8	Anti-TCRα/β	APC	BW242/412	mouse IgG2b	120-0012-467
F	8	Anti-TdT	APC	19-Mar	mouse IgG2b	120-015-444
G	8	CD1d	APC	51,1	mouse IgG2b	120-014-058
H	8	CD2	APC	LT2	mouse IgG2b	120-011-648
A	9	CD11c	APC	MJ4-27G12	mouse IgG2b	120-003-065
B	9	CD25	APC	4.00E+03	mouse IgG2b	120-010-686
C	9	CD45RA	APC	T6D11	mouse IgG2b	120-010-652
D	9	CD49d	APC	MZ18-24A9	mouse IgG2b	120-012-813
E	9	CD49e	APC	NKI-SAM1	mouse IgG2b	120-009-543
F	9	CD66abce	APC	TET2	mouse IgG2b	120-012-462
G	9	CD68	APC	Y1/82A	mouse IgG2b	120-014-664
H	9	CD85j (ILT2)	APC	GHI/75	mouse IgG2b	120-011-190
A	10	CD133/2 (293C3)	APC	293C3	mouse IgG2b	120-010-592
B	10	CD193	APC	5E8.4	mouse IgG2b	120-014-766
C	10	CD266 (FN14)	APC	ITEM-4	mouse IgG2bκ	120-019-291
D	10	CD276	APC	FM276	mouse IgG2b	120-007-430
E	10	CD279	APC	PD1.3.1.3	mouse IgG2b	120-014-760
F	10	CD338 (ABCG2)	APC	5D3	mouse IgG2bk	120-020-343
G	10	Mouse IgM – isotype control	APC	IS5-20C4		120-012-521
H	10	Anti-A2B5	APC	105HB29	mouse IgM	120-010-587
A	11	Anti-O4	APC	O4	mouse IgM	120-012-852
B	11	Anti-PSA-NCAM	APC	2-2B	mouse IgM	120-004-981
C	11	Anti-Slan (M-DC8)	APC	DD-1	mouse IgM	120-012-884
D	11	CD15	APC	VIMC6	mouse IgM	120-010-631
E	11	CD16	APC	VEP13	mouse IgM	120-010-678
F	11	CD57	APC	TB03	mouse IgM	120-014-014
G	11	Rat IgG2a- isotype control	APC	ES26-15B7.3		120-015-465
H	11	Anti-Galectin 3	APC	M3/38	rat IgG2a	120-016-611
A	12	CD49f	APC	GoH3	rat IgG2a	120-014-380
B	12	Rat IgG2b – isotype control	APC			120-016-206
C	12	Anti-CX3CR1	APC	2A9-1	rat IgG2b	120-014-009
D	12	Anti-LGR5	APC	DA03-22H2.8	rat IgG2b	120-016-270
E	12	CD11b	APC	M1/70.15.11.5	rat IgG2b	120-010-656
F	12	Rat IgM – isotype control	APC	ES26-13D3.4		120-015-791
G	12	Anti-CLA	APC	HECA-452	rat IgM	120-011-652
H	12	hamster IgG – isotype control	APC	22F6		120-018-552

Plate 3						
Position		Marker	Fluorochrome	CLONE	Isotype	Internal order Cat. No.
A	1	CD27	APC	LG.3A10	hamster IgG	120-014-759
B	1	REA Control (I)	APC	REA293		120-020-139
C	1	Anti-CCR10	APC	REA326	recombinant human IgG1	120-020-153
D	1	Anti-CLIP	APC	REA296	recombinant human IgG1	120-019-333
E	1	Anti-DCIR	APC	REA329	recombinant human IgG1	120-020-226
F	1	Anti-Fibroblast	APC	REA165	recombinant human IgG1	120-014-561
G	1	Anti-fMLP receptor	APC	REA169	recombinant human IgG1	120-015-074
H	1	Anti-GARP (LRRC32)	APC	REA166	recombinant human IgG1	120-014-965
A	2	Anti-HLA Class I B8	APC	REA145	recombinant human IgG1	120-013-337
B	2	Anti-HLA Class I Bw4	APC	REA274	recombinant human IgG1	120-018-414
C	2	Anti-HLA Class I Bw6	APC	REA143	recombinant human IgG1	120-013-309
D	2	Anti-HLA-A2 A28	APC	REA142	recombinant human IgG1	120-013-232
E	2	Anti-HLA-A9	APC	REA127	recombinant human IgG1	120-012-769
F	2	Anti-HLA-ABC	APC	REA230	REA Control (S)	120-017-199
G	2	Anti-HLA-B12	APC	REA138	REA Control (S)	120-013-101
H	2	Anti-HLA-DQ	APC	REA303	recombinant human IgG1	120-019-395
A	3	Anti-HLA-DR, DP, DQ	APC	REA332	REA Control (S)	120-020-186
B	3	Anti-KLRG1 (MAFA)	APC	REA261	recombinant human IgG1	120-017-919
C	3	Anti-SSEA-1	APC	REA321	recombinant human IgG1	120-020-389
D	3	Anti-SSEA-4	APC	REA101	recombinant human IgG1	120-010-889
E	3	Anti-TCR-Vα7.2	APC	REA179	recombinant human IgG1	120-014-585
F	3	Anti-TCR-Vδ1	APC	REA173	recombinant human IgG1	120-014-894
G	3	CD13	APC	REA263	recombinant human IgG1	120-018-283
H	3	CD22	APC	REA340	recombinant human IgG1	120-020-649
A	4	CD41b	APC	REA336	recombinant human IgG1	120-020-702
B	4	CD42a	APC	REA209	recombinant human IgG1	120-016-240
C	4	CD42b	APC	REA185	REA Control (S)	120-014-610
D	4	CD45RB	APC	REA119	recombinant human IgG1	120-014-933
E	4	CD46	APC	REA312	recombinant human IgG1	120-019-700
F	4	CD47	APC	REA220	recombinant human IgG1	120-016-567
G	4	CD49b	APC	REA188	recombinant human IgG1	120-014-981
H	4	CD51	APC	REA181	recombinant human IgG1	120-014-956
A	5	CD52	APC	REA164	recombinant human IgG1	120-013-814
B	5	CD53	APC	REA259	recombinant human IgG1	120-017-661
C	5	CD54 (ICAM-1)	APC	REA266	REA Control (S)	120-018-739
D	5	CD56	APC	REA196	recombinant human IgG1	120-015-188
E	5	CD66b	APC	REA306	recombinant human IgG1	120-019-496
F	5	CD62E (E-Selectin)	APC	REA280	recombinant human IgG1	120-019-666
G	5	CD70	APC	REA292	recombinant human IgG1	120-018-785
H	5	CD72	APC	REA231	recombinant human IgG1	120-016-971
A	6	CD79b	APC	REA120	recombinant human IgG1	120-012-285
B	6	CD82	APC	REA221	recombinant human IgG1	120-016-393
C	6	CD85a (ILT5)	APC	REA207	recombinant human IgG1	120-017-622
D	6	CD85d (ILT4)	APC	REA184	recombinant human IgG1	120-015-253
E	6	CD85h (ILT1)	APC	REA219	recombinant human IgG1	120-016-187
F	6	CD85k (ILT3)	APC	REA141	recombinant human IgG1	120-013-212
G	6	CD89	APC	REA234	recombinant human IgG1	120-016-792
H	6	CD94	APC	REA113	REA Control (S)	120-012-047
A	7	CD96 (TACTILE)	APC	REA195	recombinant human IgG1	120-015-163
B	7	CD100	APC	REA316	recombinant human IgG1	120-019-730
C	7	CD104 (Integrin β4)	APC	REA236	recombinant human IgG1	120-016-986
D	7	CD106	APC	REA269	recombinant human IgG1	120-018-377
E	7	CD110	APC	REA250	recombinant human IgG1	120-017-685
F	7	CD116	APC	REA211	recombinant human IgG1	120-016-219
G	7	CD119	APC	REA161	recombinant human IgG1	120-013-844
H	7	CD122 (IL-2Rβ)	APC	REA167	REA Control (S)	120-014-231
A	8	CD126 (IL-6Ra)	APC	REA291	recombinant human IgG1	120-018-803
B	8	CD132	APC	REA313	recombinant human IgG1	120-019-649
C	8	CD131	APC	REA249	recombinant human IgG1	120-018-534
D	8	CD137L (4-1BBL)	APC	REA254	REA Control (S)	120-017-888
E	8	CD138 (44F9)	APC	REA104	recombinant human IgG1	120-012-179
F	8	CD147	APC	REA282	recombinant human IgG1	120-019-373
G	8	CD144 (VE-Cadherin)	APC	REA199	REA Control (S)	120-015-518
H	8	CD148	APC	REA204	REA Control (S)	120-015-698
A	9	CD156c (ADAM10)	APC	REA309	recombinant human IgG1	120-019-483
B	9	CD158e1/e2	APC	REA168	recombinant human IgG1	120-019-451
C	9	CD150 (SLAM)	APC	REA151	recombinant human IgG1	120-013-287
D	9	CD151	APC	REA265	recombinant human IgG1	120-017-961
E	9	CD156a (ADAM8)	APC	REA331	recombinant human IgG1	120-020-049
F	9	CD158a (KIR2DL1)	APC	REA284	recombinant human IgG1	120-018-519
G	9	CD158b2 (KIR2DL3)	APC	REA147	recombinant human IgG1	120-014-037
H	9	CD159a (NKG2A)	APC	REA110	REA Control (S)	120-012-024
A	10	CD159c (NKG2C)	APC	REA205	recombinant human IgG1	120-015-764
B	10	CD162	APC	REA319	recombinant human IgG1	120-020-036
C	10	CD171 (L1CAM)	APC	REA163	recombinant human IgG1	120-013-950
D	10	CD172a (SIRPα)	APC	REA144	recombinant human IgG1	120-013-361
E	10	CD177	APC	REA258	recombinant human IgG1	120-017-498
F	10	CD182 (CXCR2)	APC	REA208	recombinant human IgG1	120-016-074
G	10	CD183 (CXCR3)	APC	REA232	recombinant human IgG1	120-016-735
H	10	CD185 (CXCR5)	APC	REA103	recombinant human IgG1	120-010-989
A	11	CD191 (CCR1)	APC	REA158	recombinant human IgG1	120-014-537
B	11	CD192 (CCR2)	APC	REA264	recombinant human IgG1	120-018-321
C	11	CD194 (CCR4)	APC	REA279	recombinant human IgG1	120-018-352
D	11	CD196 (CCR6)	APC	REA190	recombinant human IgG1	120-014-729
E	11	CD197 (CCR7)	APC	REA108	REA Control (I)	120-011-991
F	11	CD202b (TIE-2)	APC	REA198	recombinant human IgG1	120-016-588
G	11	CD208 (DC-LAMP)	APC	REA295	REA Control (S)	120-018-841
H	11	CD212	APC	REA242	REA Control (S)	120-017-126
A	12	CD213α2 (IL-13Rα2)	APC	REA308	recombinant human IgG1	120-019-604
B	12	CD217 (IL-17RA)	APC	REA290	recombinant human IgG1	120-019-955
C	12	CD220	APC	REA260	recombinant human IgG1	120-017-859
D	12	CD221 (IGF-1R)	APC	REA271	recombinant human IgG1	120-018-543
E	12	CD222	APC	REA187	recombinant human IgG1	120-014-711
F	12	CD230 (PrP)	APC	REA203	recombinant human IgG1	120-015-819
G	12	CD235a (Glycophorin A)	APC	REA175	recombinant human IgG1	120-015-000
H	12	CD238 (KEL)	APC	REA330	recombinant human IgG1	120-020-451

Plate 4						
Position		Marker	Fluorochrome	CLONE	isotype	Internal order cat. no
A	1	CD239 (BCAM)	APC	REA276	recombinant human IgG1	120-018-464
B	1	CD240DCE	APC	REA327	recombinant human IgG1	120-020-162
C	1	CD244 (2B4)	APC	REA112	recombinant human IgG1	120-012-041
D	1	CD258 (LIGHT)	APC	REA244	recombinant human IgG1	120-017-875
E	1	CD269 (BCMA)	APC	REA315	recombinant human IgG1	120-019-585
F	1	CD270 (HVEM)	APC	REA247	recombinant human IgG1	120-017-480
G	1	CD278 (ICOS)	APC	REA192	recombinant human IgG1	120-015-235
H	1	CD282 (TLR2)	APC	REA109	recombinant human IgG1	120-011-984
A	2	CD298	APC	REA217	recombinant human IgG1	120-016-411
B	2	CD312 (EMR2)	APC	REA302	recombinant human IgG1	120-019-682
C	2	CD317 (BST2)	APC	REA202	recombinant human IgG1	120-015-917
D	2	CD318 (CDCP1)	APC	REA194	recombinant human IgG1	120-015-846
E	2	CD319 (CRACC)	APC	REA150	recombinant human IgG1	120-013-175
F	2	CD328 (Siglec-7)	APC	REA214	recombinant human IgG1	120-016-163
G	2	CD354 (TREM-1)	APC	REA213	recombinant human IgG1	120-016-100
H	2	CD360 (IL-21R)	APC	REA233	recombinant human IgG1	120-017-160
A	3	CD184	APC	12G5	mouse IgG2a	120-010-802
B	3	Anti-DCIR	APC	REA329	recombinant human IgG1	120-020-226
C	3	Anti-DR3	APC	JD3	mouse IgG1k	120-019-943
D	3	IFN alpha/beta Receptor	APC	REA124	recombinant human IgG1	120-012-567
E	3	IL-12Rb 2	APC	REA33	recombinant human IgG1	120-020-609
F	3	CD11a (ITGAL)	APC	REA378	recombinant human IgG1	120-021-480
G	3	CD37	APC	REA366	recombinant human IgG1	120-021-039
H	3	CD41a (ITGA2b)	APC	REA386	recombinant human IgG1	120-021-761
A	4	CD49c (ITGA3)	APC	REA360	recombinant human IgG1	120-021-337
B	4	CD62P	APC	REA389	recombinant human IgG1	120-021-626
C	4	CD98	APC	REA387	recombinant human IgG1	120-021-824
D	4	CD140b	APC	REA363	recombinant human IgG1	120-021-276
E	4	CD172b	APC	B4B6	mouse IgG1κ	120-021-294
F	4	CD181 (CD128a)	APC	8F1	mouse IgG2bκ	120-021-432
G	4	CD201	APC	REA337	recombinant human IgG1	120-021-104
H	4	CD223	APC	REA351	recombinant human IgG1	120-021-321
A	5	CD234	APC	REA376	recombinant human IgG1	120-021-897
B	5	CD295	APC	REA361	recombinant human IgG1	120-020-959
C	5	CD352	APC	REA339	recombinant human IgG1	120-021-530
D	5	CD103	APC	Ber-ACT 8	mouse IgG1κ	120-017-837
E	5	CD107	APC	H4A3	mouse IgG1κ	120-018-246
F	5	CD170	APC	1A5	mouse IgG1κ	120-017-812
G	5	CD233	APC	REA368	recombinant human IgG1	120-021-969
H	5	CD256	APC	REA347	recombinant human IgG1	120-021-020
A	6	HLA-B7,B27	APC	REA176	recombinant human IgG1	120-022-044
B	6	Syk	APC	REA111	recombinant human IgG1	120-011-044
C	6	TIM-1	APC	REA384	recombinant human IgG1	120-021-933
D	6	CD158b2	APC	REA147	recombinant human IgG1	120-014-037
E	6	CD255	APC		recombinant human IgG1	120-012-159
F	6	CD307e (FcRL5)	APC	REA391	recombinant human IgG1	120-022-662
G	6	Siglec-5 / Siglec-14-APC	APC	REA393	recombinant human IgG1	120-022-254
H	6	IFNAR2	APC	REA124	recombinant human IgG1	120-022-567
A	7	HLA-DM	APC	REA406	recombinant human IgG1	120-022-567
B	7	Galectin-9	APC	REA435	recombinant human IgG1	120-022-629
C	7	CD181 (CXCR1)	APC	8F1	mouse IgG2bκ	20-023-311
D	7	Anti-Notch1	APC	REA357	recombinant human IgG1	120-021-432
E	7	CD340	APC	24D2	mouse IgG1κ	120-022-206
F	7	CD195 CCR5 APC	APC	REA245	recombinant human IgG1	120-023-492
G	7	CD286 (TLR6)	APC	REA382	recombinant human IgG1	120-022-787
H	7	Anti-SSEA-5-APC	APC	8.00E+11	mouse IgG1κ	120-022-644
A	8	CD353 (SLAMF8)	APC	REA394	recombinant human IgG1	120-022-998
B	8	CD120A (TNF-R1)	APC	REA525	recombinant human IgG1	120-022-690
C	8	CD307A (FCRL1)	APC	REA440	recombinant human IgG1	120-022-517
D	8	INTEGRIN B7	APC	REA441	recombinant human IgG1	120-023-227
E	8	CD166	APC	REA442	recombinant human IgG1	120-023-147
F	8	CD310 (VEGFR-3)	APC	REA419	recombinant human IgG1	120-023-585
G	8	PSMA	APC	REA408	recombinant human IgG1	120-023-349
H	8	CD16	APC	REA423	recombinant human IgG1	120-023-330
A	9	CD48	APC	REA426	recombinant human IgG1	120-023-377
B	9	CD66acde	APC	REA428	recombinant human IgG1	120-023-395
C	9	CD66c	APC	REA414	recombinant human IgG1	120-023-165
D	9	CD135	APC	BV10A4H2	mouse IgG1κ	120-022-895
E	9	CD246	APC	REA425	recombinant human IgG1	120-022-482
F	9	CD344	APC	CH3A4A7	mouse IgG1κ	120-023-106
G	9	CLEC12A	APC	REA431	recombinant human IgG1	120-023-548
H	9	Anti-CX3CR1	APC	REA385	recombinant human IgG1	120-023-199
A	10	CD7	APC	CD7-6B7	mouse IgG2aκ	120-021-671
B	10	CD155	APC	PV404.19	mouse IgG1	120-022-044
C	10	Anti-ACSA2	APC		mouse IgG2	120-022-080
D	10	CD81	APC	JS-81	Mouse IgG_1, κ	
E	10	CD274 (PD-L1)	APC	MIH1	Mouse IgG_1, κ	

Supplementary tables S4.1-4: Antibody list used for cell surface marker screening. Details about the antibodies used are displayed, including, position in the 96-well plates, antibody specificity, fluorochrome, clone, isotype controls and internal order catalogue number. All antibodies were supplied by, and experiments performed at Miltenyibiotec in Bergisch Gladbach, Germany.

Supplementary Table S4.5: MSC-PLT and MSC-FCS have similar expression of several markers. MSC-PLT and MSC-FCS display >70% of expression of several markers. Data represents mean ± SEM of n=3, and for all markers the fold change <1.5.

Antibody Specificity	*MSC-PLT*		*MSC-FCS*	
	MEAN	**SEM**	**MEAN**	**SEM**
CD47	99.9	0.0	99.4	0.5
CD29	99.9	0.0	99.5	0.4
CD95	100.0	0.0	99.5	0.4
CD63	100.0	0.0	99.5	0.5
CD44	99.9	0.0	99.4	0.4
CD73	99.9	0.1	99.4	0.4
CD98	100.0	0.0	99.4	0.6
CD298	99.9	0.1	99.4	0.4
CD46	99.9	0.1	99.3	0.5
CD166	99.9	0.0	99.3	0.3
CD147	99.8	0.1	99.3	0.5
CD151	99.8	0.1	99.3	0.5
CD90	99.9	0.1	99.4	0.4
CD49c	99.9	0.1	99.3	0.6
CD51	99.9	0.0	99.1	0.4
CD49e	100.0	0.0	99.2	0.5
CD140b	100.0	0.0	99.2	0.6
CD156c	100.0	0.0	98.9	0.6
CD276	99.9	0.0	99.0	0.6
HLA Class I Bw6	99.9	0.1	98.8	0.3
CD105	99.9	0.0	98.0	1.8
HLA-ABC	99.9	0.1	98.4	0.7
CD58	99.9	0.0	97.8	0.0
CD155	99.9	0.0	98.2	0.0
CD81	99.6	0.0	98.1	0.0
CD230	99.7	0.2	96.7	3.1
PTK7	99.8	0.1	96.1	3.4
CD13	99.5	0.2	97.3	2.4
CD262	99.6	0.3	96.2	1.1
CD49a	99.2	0.2	96.3	1.8
CD340	99.7	0.1	95.4	1.8
CD266	99.5	0.2	95.1	3.7
CD61	99.8	0.1	94.4	3.6
CD10	99.8	0.1	93.3	1.5
CD82	99.7	0.2	92.0	2.2
CD51/CD61	99.7	0.3	87.8	6.2
CD201	98.9	0.5	86.9	4.9
CD49b	99.4	0.2	85.6	7.8
CD222	98.9	0.2	86.1	1.4
CD55	90.8	2.0	84.4	5.7
CD273	96.5	1.8	82.7	13.6
CD49f	87.4	1.3	81.5	5.7
CD217	96.8	2.3	77.9	13.0
CD99	96.2	2.1	78.5	16.9
CD9	86.4	5.6	78.8	9.4
CD146	78.2	4.8	78.2	15.7
CD119	93.8	1.7	74.6	8.5
Fibroblast	98.3	1.3	78.4	9.9
CD71	95.2	0.9	69.5	8.6
CD274	84.7	11.1	69.5	17.6
HLA-B12	97.4	0.9	70.5	14.8

Supplementary Table S4.6: Statistics of the markers that showed variable expression between MSC-PLT and MSC-FCS. The table shows mean percentage of positive cells, standard error or mean (SEM) and coefficient of variation (%CV) of MSC-PLT and MSC-FCS (n=3). Fold increase in % positive cells in MSC-PLT and p-values are presented. A marker was considered differentially expressed when they exhibited a fold change >1.5 and a p-value<0.05.

Antibody Specificity	MSC-FCS			MSC-PLT			Fold Change	p-value
	MEAN %Pos	SEM	%CV	MEAN %Pos	SEM	%CV		
CD49d	8.3	4.5	94.5	61.2	5.4	15.2	10.3	0.0002
HLA-E	7.4	2.8	64.5	70.6	11.5	28.3	10.5	0.0221
CD106	6.8	0.5	12.5	58.7	8.0	23.6	8.6	0.0229
CD31	2.0	0.4	32.4	13.8	2.3	28.8	7.1	0.0311
MSCA-1	15.2	7.3	82.6	71.7	4.9	11.8	5.8	0.0429
Notch2	9.9	5.3	92.5	36.5	2.0	9.5	5.5	0.0220
MCSP	4.7	1.8	66.6	20.9	4.0	33.5	5.0	0.0185
CD40	4.9	1.1	40.5	18.3	1.4	13.0	4.0	0.0109
CD26	21.6	8.1	65.3	70.1	8.2	20.2	3.7	0.0030
CD312	14.5	6.0	71.1	45.6	3.9	14.9	3.6	0.0138
CD54	24.3	7.7	54.7	44.3	8.7	34.0	2.0	0.0400
CD318	58.2	5.1	15.1	97.1	1.6	2.9	1.7	0.0083
CD97	41.1	6.4	27.1	67.8	6.9	17.6	1.7	0.0057
ROR-1	30.2	10.3	59.3	60.6	13.7	39.3	2.1	0.0620
CD194	16.3	7.2	76.2	32.6	10.4	55.3	2.7	0.0729
CD319	13.7	3.4	43.1	63.9	17.3	46.9	4.5	0.0731
CD221	4.6	2.0	74.7	16.5	5.8	61.2	4.1	0.0916
CD200	7.8	2.8	62.3	35.6	12.0	58.7	4.5	0.0985
CD195	31.8	14.1	76.8	50.8	12.9	43.9	2.2	0.0991
CD56	5.8	1.4	57.4	7.9	1.6	35.5	1.5	0.0991
IFNAR2	50.2	19.9	68.5	93.4	3.8	7.0	2.3	0.1205
CD182	8.1	4.9	104.0	28.0	12.6	78.1	4.3	0.1267
CD137L	41.1	17.8	75.0	69.8	12.8	31.8	2.5	0.1314
IFNα/β receptor	51.2	19.7	66.8	95.8	1.8	3.2	2.2	0.1315
CD304	5.2	2.8	94.4	38.2	15.5	70.4	9.9	0.1351
CD120A	37.5	24.8	114.5	78.4	8.6	19.0	5.9	0.1513
CD317	7.6	2.8	64.0	36.3	15.9	75.8	4.5	0.1611
CD270	8.2	4.0	84.8	15.9	7.4	81.1	2.1	0.1635
CD132	14.2	3.5	42.3	26.9	4.2	27.1	2.0	0.2200
CD197	6.3	4.2	116.6	11.2	7.4	114.5	1.9	0.2615
KLRG1	42.7	26.5	107.3	59.9	25.8	74.4	2.8	0.2770
fMLP receptor	20.6	12.6	106.5	27.3	9.5	60.5	1.8	0.2919
CD111	2.5	1.3	89.0	10.6	7.1	115.6	3.6	0.2985
CCR10	3.3	0.3	17.9	10.9	5.6	88.9	2.6	0.3125
CD150	3.9	1.9	84.8	14.4	10.0	120.1	2.9	0.3256
CD114	9.7	9.0	161.0	22.6	21.1	161.8	2.4	0.3967
CD148	53.5	24.5	79.4	66.9	12.4	32.2	2.0	0.4884
CD107a	5.7	3.5	107.4	7.6	2.0	46.3	1.8	0.7575

Supplementary Table S4.7: Summary table showing networks associated with the 13 overexpressed markers on MSC-PLT. The 13 overexpressed markers were uploaded onto IPA software and analysed for their association with specific functions. The software predicted the involvement of these markers in three distinct networks associated with inflammatory responses, carbohydrate metabolism and cellular movement. Information about the score, focus molecules and the molecules in the network is presented.

Networks	Score	Focus Molecules	Molecules in Network
Network 1: Inflammatory response	24	9	ADRB, ATPase, CD3, **CD40**,**CSPG4**, **DPP4**, ERK1/2, HDL, Histone H4, **HLA-E**, Hsp70, **ICAM1**, IFN, IFNγ, IFNAR, IgG, IgG1, IL1, IL12 (complex), Immunoglobulin, IFNα, **ITGA4**, Jnk, LDL, NFAT, **NOTCH2**, P38 MAPK, **PECAM1**, TCR, TGF-β, TLR, TNF family, **VCAM1**
Network 2: Carbohydrate metabolism	9	4	ACP1, ADAM28, **ADGRE2**, **ADGRE5**, advanced glycation end-products, Akt, **ALPL**, **CDCP1**, Cg, CNR2, CYSLTR1, DUSP16, ERL, Focal adhesion kinase, FPR1, GAST, Gpcr, GPR4, Histone H3, HTR4, IKK (complex), Integrin, Integrin alpha 3 beta 1, MAPK, NFKb complex, P2RY1, P2RY4, P2RY6, P13K (complex), RNA polimerase II, S1PR2, SLC52A1, THBS2, VEGF
Network 3: Cellular movement	4	2	ALP, ARAP1, ARFGEF2, BIRC2, CCL11, **CD40**, CYTH1, GHRH, GNB2L1, GPS2, GTPase, IPO5, IQGAP1, ITGA6, MADD, mevalonic acid, MLLT4, NISCH, **PECAM1**, PIN1, PLXNB2, PRKG1, RALGDS, RAP1GAP, RASGRF1, RCC1, RICTOR, S1PR1, SEMA4D, THY1, TRIO, WNT5A

Abbreviations: ADRB: adrenergic receptor beta; ATPase: adenosine triphosphatase; CD3: cluster of differentiation 3; CD40: cluster of differentiation 40; CSPG4: chondroitin sulphate proteoglycan 4; DPP4: dipeptidyl-peptidase 4; ERK1/2: extracellular signal-regulated kinases 1/2; HDL: high-density lipoprotein; HLA-E: histocompatibility antigen alpha chain E; Hsp70: heat shock protein 70; ICAM1: intercellular adhesion molecule 1; IFN: interferon; IFNγ: interferon gamma; IFNAR: interferon alpha/beta receptor; IgG: immunoglobulin G; IL1: interleukin 1; IL12: interleukin 12; IFNα: interferon alpha; ITGA4: integrin alpha 4; Jnk: c-Jun N-terminal kinases; LDL: low density lipoprotein; NFAT: nuclear factor of activated T cells; P38MAKP: p38 mitogen-activated kinases; PECAM1: platelet/endothelial cell adhesion molecule 1; TCR: T cell receptor; TGF-β: transforming growth factor beta; TLR: toll-like receptor; TNF family: tumour necrosis factor family; VCAM1: vascular cell adhesion protein 1; ACP1: acid phosphatase 1; ADAM28: ADAM metallopeptidase domain 28; Akt (PKB): protein kinase B; ALPL: alkaline phosphatase, liver/bone/kidney; CDCP1: CUB domain containing protein 1; Cg: class C-G-protein coupled receptors: CNR2: cannabinoid receptor 2; CYSLTR1: cysteinyl leukotriene receptor 1; DUSP16: dual specificity phosphatase 16; ERL: endoplasmic reticulum lipid; FPR1: formyl peptide receptor 1; GAST: gastrin; Gpcr: G protein-coupled receptor; GPR4: G protein-coupled receptor 4; HTR4: 5-hydroxytryptamine (serotonin) receptor 4; IKK: IkB kinase; MAPK: mitogen-activated kinases; NFkB: nuclear factor k beta; P2RY1: purinergic receptor P2Y, G-protein coupled 1; P2RY4: purinergic receptor P2Y, G-protein coupled 4; P2RY6: purinergic receptor P2Y, G-protein coupled 6; P13K: phosphpoinositide 3-kinase; S1PR2: sphingosine-1-phosphate receptor 2; SLC52A1: solute carrier family 52 member 1; THBS2: thrombospondin 2; VEGF: vascular endothelial growth factor; ALP: alkaline phosphatase; ARAP1: arfGAP with RhoGAP domain, ankyrin repeat and PH domain 1; ARFGEF2: adenosine phosphate-ribosylation factor guanine nucleotide-exchange factor 2; BIRC2: baculoviral IAP repeat containing 2; CCL11: chemokine ligand 11; CYTH1: cytohesin 1; GHRH: growth hormone releasing hormone; GNB2L1: guanine nucleotide binding protein, beta polypeptide 1-like 1; GPS2: G protein pathway suppressr 2; GTPase: guanine triphosphatase; IPO5: importin 5; IQGAP1: IQ motif containing GTPase activating protein 1; ITGA6: integrin alpha 6; MADD: MAP-kinase activating death domain; MLLT4: myeloid/lymphoid leikemia translocated to 4; NISCH: nischarin; PIN1: peptidylpropyl cis/trans isomerase NIMA-interacting 1; PLXNB2: plexin B2; PRKG1: protein kinase, CGMP-dependent type 1; RALGDS: ral guanine nucleotide dissociation stimulator; RAP1GAP: RAP1 GTPase activating protein; RCC1: regulator of chromosome condensation 1; RICTOR: RPTOR independent companion of MTOR, complex 2; S1PR1: sphingosine-1-phosphate receptor 1; SEMA4D: sema domain, immunoglobulin domain, transmembrane domain and short cytoplasmic domain; THY1: Thy-1 cell surface antigen; TRIO: trio rho guanine nucleotide exchange factor; WNT5A: wingless-type MMTC integration site family, member 5A.

Appendix III – Supplementary information for Chapter 5

Optimisation of Transwell migration assay

The transwell assay is based on addition of cells to a porous insert which is positioned on top of a well. On the bottom well, medium with a chemokine attractant induces a migratory flux of the cells from the upper well into the bottom well. CCR7 has two known ligands, CCL19 and CCL21. To evaluate the feasibility of the assay and define the optimal parameters, for example, whether the DCs migrated more efficiently towards CCL19 or CCL21 and the ideal time of migration, a preliminary assay, with mature DCs was performed. DCs at a density of $1.5x10^5$cells/insert were seeded on an 8 µm pore insert and left to migrate towards medium supplemented with either CCL19 or CCL21 for, 2, 6 and 24h. Medium without chemokine was used to evaluate spontaneous migration of the DCs due to pore size. Results showed that the DCs had higher migration efficiency after 24h incubation. At this time point, migration efficiency was higher towards CCL21 (44.8%) than towards CCL19 (28.0%). Spontaneous migration of DCs through the pores was negligible (**Fig. 5.16**). Given these results, CCL21 and the 24h time point were used to test the effect of EV treatment on DC migration.

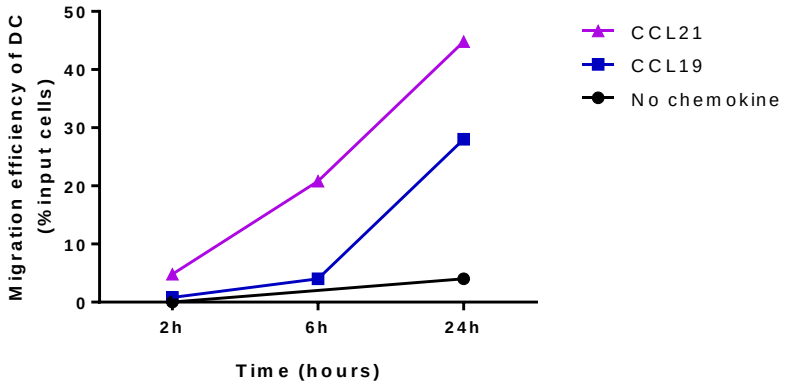

Supplementary figure S5.1: Optimisation of DC migration conditions using Transwell system

Mature DCs were seeded at a density of 1.5 x 10^5 cells on 8µm pore upper chamber. Medium supplemented with either CCL21 or CCL19 was added to the lower chamber and DC migration towards CCL21 (pink) and CCL19 (blue) was assessed at 2h, 6h and 24h. Medium without chemokine on the lower chamber was used as background control.

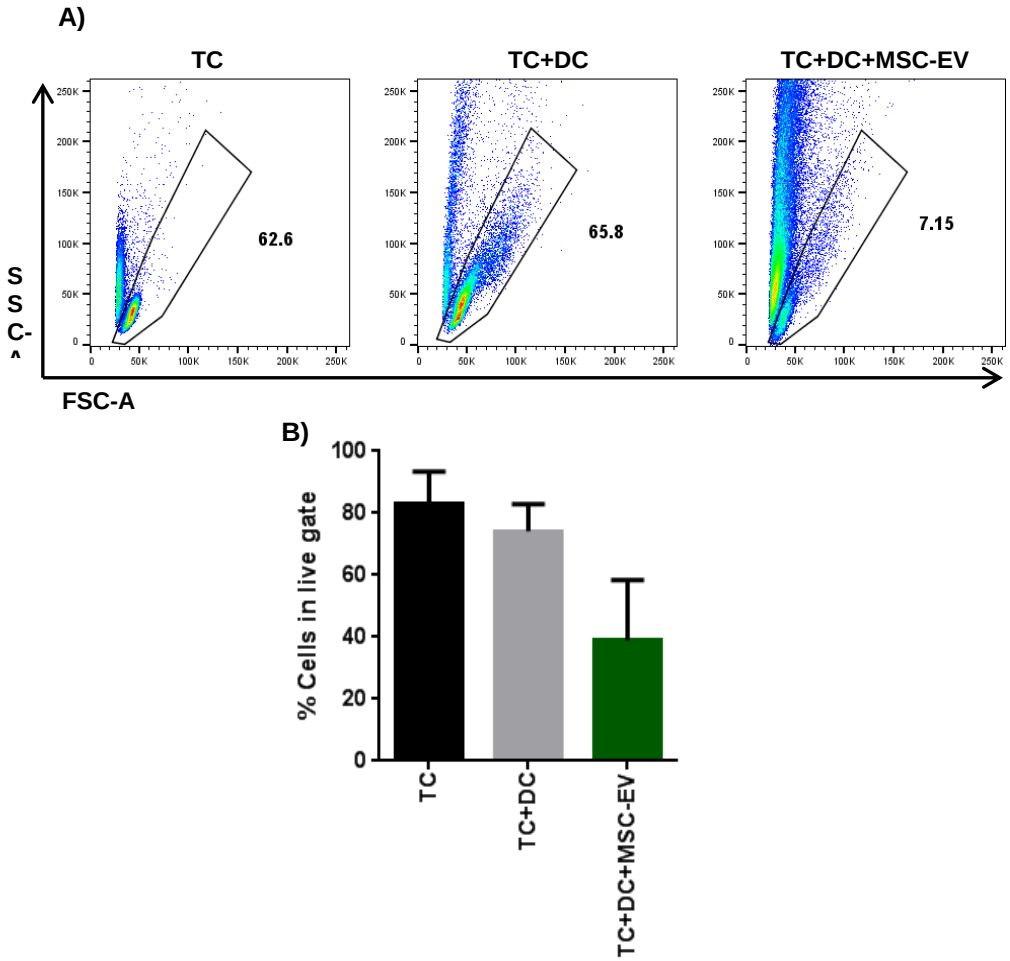

Supplementary figure S5.2: A decreased percentage of living T cells is detected after allo-DC stimulation in the presence of MSC-EVs

$CD3^+$ T cells were co-cultured with allo-DCs with or without 20 µg/ml MSC-EVs. After 5 day co-culture, T cell proliferation was analysed by flow cytometry. Live cells were selected according to SSC-A/FSC-A. **A)** Representative gates, and **B)** cumulative percentage of live T cells show a decrease in living T cells after MSC-EV treatment. Results express mean ±SEM of n=3.

Appendix IV – Supplementary information for Chapter 6

	MSC			MSC-EV				
Gene name	**Counts**	**SEM**	**CV**	**Counts**	**SEM**	**CV**	**P-value**	**FC**
hsa-miR-223-3p	1.0	0.0	0.0	2029.6	2945.4	2.5	0.014	-1992.7
hsa-miR-4286	9.8	2.3	0.4	8182.4	2492.0	0.5	0.000	-833.3
hsa-miR-142-3p	7.4	0.2	0.0	1659.4	2201.1	2.3	0.024	-224.2
hsa-miR-630	5.7	4.7	1.4	1232.5	139.3	0.2	0.023	-216.5
hsa-miR-136-5p	1.8	1.5	1.4	209.9	28.3	0.2	0.008	-117.5
hsa-miR-4454+hsa-miR-7975	1651.5	501.6	0.5	173824.7	47161.3	0.5	0.000	-105.3
hsa-miR-4516	1.9	1.8	1.7	172.5	148.0	1.5	0.018	-90.9
hsa-miR-642a-3p	1.2	0.2	0.3	105.9	31.8	0.5	0.004	-88.8
hsa-miR-126-3p	13.4	5.2	0.7	1156.7	1447.1	2.2	0.019	-86.3
hsa-miR-1915-3p	1.0	0.0	0.0	86.5	12.3	0.2	0.002	-84.9
hsa-miR-19b-3p	5.3	4.6	1.5	420.9	114.0	0.5	0.008	-80.0
hsa-miR-19a-3p	2.5	3.4	2.3	174.3	40.8	0.4	0.021	-68.7
hsa-miR-451a	2.1	2.7	2.2	142.1	294.3	3.6	0.036	-66.7
hsa-miR-377-3p	1.3	0.4	0.5	79.1	20.5	0.4	0.000	-59.9
hsa-miR-335-5p	1.0	0.0	0.0	59.8	42.7	1.2	0.029	-57.4
hsa-miR-374c-5p	1.0	0.0	0.0	34.5	10.1	0.5	0.008	-33.8
hsa-miR-874-5p	1.0	0.0	0.0	26.7	9.0	0.6	0.017	-26.3
hsa-miR-539-5p	3.9	2.8	1.3	86.8	30.3	0.6	0.030	-22.4
hsa-miR-4521	1.6	0.9	1.0	27.3	15.3	1.0	0.013	-17.3
hsa-miR-29b-3p	95.0	34.6	0.6	1378.2	47.2	0.1	0.012	-14.5
hsa-miR-374a-5p	7.0	1.5	0.4	22.5	12.4	1.0	0.010	-13.5
hsa-miR-493-3p	12.1	0.7	0.1	137.6	39.6	0.5	0.012	-11.4
hsa-miR-106b-5p	14.1	8.3	1.0	145.5	48.6	0.6	0.016	-10.3
hsa-miR-137	4.0	1.1	0.5	36.7	5.1	0.2	0.005	-9.3
hsa-miR-32-5p	12.8	3.0	0.4	112.7	51.8	0.8	0.019	-8.8
hsa-miR-381-3p	10.2	2.1	0.4	86.1	22.6	0.5	0.004	-8.5
hsa-miR-376a-3p	81.5	6.4	0.1	585.9	55.1	0.2	0.000	-7.2
hsa-miR-601	7.7	1.8	0.4	50.3	19.4	0.7	0.041	-6.5
hsa-miR-376c-3p	47.2	4.3	0.2	289.4	55.4	0.3	0.012	-6.1
hsa-miR-21-5p	1151.0	122.5	0.2	6957.7	794.8	0.2	0.001	-6.1
hsa-miR-1180-3p	10.4	1.2	0.2	57.2	11.9	0.4	0.008	-5.5
hsa-miR-575	42.0	3.7	0.2	220.9	68.4	0.5	0.027	-5.3
hsa-miR-424-5p	99.9	7.6	36.7	472.7	0.1	0.1	0.000	-4.7
hsa-miR-148a-3p	88.9	11.5	0.2	386.0	55.3	0.2	0.003	-4.3
hsa-miR-337-5p	35.9	5.6	0.3	145.9	25.5	0.3	0.007	-4.1
hsa-miR-411-5p	12.6	4.4	0.6	51.2	4.8	0.2	0.048	-4.1
hsa-miR-140-5p	32.5	3.9	0.2	131.3	28.8	0.4	0.016	-4.0
hsa-miR-340-5p	40.5	5.3	0.2	161.6	44.5	0.5	0.047	-4.0
hsa-miR-590-5p	40.5	5.8	0.2	158.0	20.0	0.2	0.003	-3.9
hsa-miR-1260a	173.3	19.3	0.2	675.9	117.9	0.3	0.009	-3.9
hsa-miR-450a-5p	83.7	12.0	0.2	286.9	60.1	0.4	0.032	-3.4
hsa-miR-15a-5p	190.8	24.5	0.2	631.2	116.9	0.3	0.014	-3.3

	MSC			MSC-EVs			P-value	FC
Gene name	**Counts**	**SEM**	**CV**	**Counts**	**SEM**	**CV**		
hsa-miR-30b-5p	149.4	8.3	0.1	419.4	70.2	0.3	0.024	-2.8
hsa-miR-337-3p	50.5	6.8	0.2	134.0	12.3	0.2	0.006	-2.7
hsa-miR-495-3p	70.4	5.2	0.1	160.6	19.9	0.2	0.021	-2.3
hsa-miR-22-3p	752.7	72.3	0.2	1631.4	91.9	0.1	0.005	-2.2
hsa-miR-30c-5p	56.8	8.9	0.3	102.8	10.8	0.2	0.048	-1.8
hsa-miR-361-5p	174.7	14.5	0.1	302.7	27.7	0.2	0.018	-1.7
hsa-miR-196a-5p	160.8	21.8	0.2	66.0	1.7	0.0	0.016	2.4
hsa-let-7i-5p	6601.6	1305.2	0.3	2453.6	234.5	0.2	0.014	2.7
hsa-let-7a-5p	18788.4	2772.3	0.3	6805.7	143.8	0.0	0.017	2.8
hsa-miR-197-3p	292.6	23.8	0.1	100.7	5.7	0.1	0.001	2.9
hsa-let-7c-5p	1610.4	117.1	0.1	540.2	81.5	0.3	0.016	3.0
hsa-miR-484	136.1	22.2	0.3	44.1	11.3	0.4	0.035	3.1
hsa-let-7b-5p	10477.6	1045.1	0.2	3362.6	210.6	0.1	0.001	3.1
hsa-miR-574-3p	304.1	38.8	0.2	95.8	12.0	0.2	0.006	3.2
hsa-miR-125a-5p	1639.4	160.6	0.2	515.8	61.1	0.2	0.004	3.2
hsa-let-7e-5p	1391.1	131.6	0.2	361.1	35.2	0.2	0.001	3.9
hsa-miR-92a-3p	464.2	33.0	0.1	118.7	19.7	0.3	0.019	3.9
hsa-miR-193a-5p+ hsa-miR-193b-5p	669.3	78.5	0.2	149.4	19.6	0.2	0.002	4.5
hsa-miR-365a-3p+ hsa-miR-365b-3p	2574.7	377.9	0.3	548.2	68.3	0.2	0.002	4.7
hsa-miR-196b-5p	196.2	25.9	0.2	41.4	9.8	0.4	0.023	4.7
hsa-miR-181c-5p	12.0	2.4	0.3	2.4	0.4	0.3	0.005	5.1
hsa-miR-210-3p	49.0	11.0	0.4	6.5	1.6	0.4	0.011	7.5
hsa-miR-370-3p	70.3	14.6	0.4	9.3	3.6	0.7	0.049	7.5
hsa-miR-197-5p	15.8	6.8	0.7	1.7	0.6	0.6	0.013	9.1
hsa-miR-181a-2-3p	24.2	7.2	0.5	2.1	0.6	0.5	0.008	11.6
hsa-miR-597-5p	57.4	2.8	0.1	4.4	1.1	0.4	0.009	13.2
hsa-miR-548d-3p	46.6	10.0	0.4	3.0	1.2	0.7	0.010	15.8
hsa-miR-548n	39.4	4.0	0.2	2.4	0.4	0.3	0.002	16.7
hsa-miR-944	62.3	9.4	0.3	2.9	1.5	0.9	0.028	21.4
hsa-miR-548q	40.8	16.6	0.7	1.6	0.6	0.7	0.004	25.6
hsa-miR-1233-3p	66.0	13.5	0.4	1.7	0.6	0.6	0.002	38.2
hsa-miR-548aa+ hsa-miR-548t-3p	81.2	53.7	1.1	1.7	0.6	0.6	0.011	47.0
hsa-miR-1253	130.5	71.0	0.9	1.7	0.6	0.6	0.004	75.5
hsa-miR-502-5p	208.8	101.3	0.8	1.7	0.6	0.6	0.001	120.9

Supplementary Table S6.1: Statistics of the miRNAs that showed differential expression between MSCs and MSC-EVs.

The table shows geometric means of the counts, standard error or mean (SEM) and coefficient of variation (%CV) of MSC and MSC-EVs (n=3). Fold increase in number of copies and p-values are presented. A miRNA was considered differentially expressed when they exhibited a fold change >1.5 and a p-value<0.05. Negative FC represent upregulation in MSC-EVs and positive FC values represent upregulation of the miRNAs in MSCs.

Appendix V – Abstracts and publications

Published abstracts:

- ***Reis M**, Nicholson L, Mavin E, Dickinson A, Wang XN. The modulatory potential of Mesenchymal Stem cells is mediated by the release of immunologically active extracellular vesicles. UKEV 2015 (Cardiff, UK) Oral Presentation*
- *Mavin M, Nicholson L, **Reis M**, Crossland R, Dickinson A, Wang XN. Regulatory T cell derived extracellular vesicles are able to modulate dendritic cell maturation and function. UKEV 2015 (Cardiff, UK) Poster presentation.*
- ***Correia dos Reis M**, Nicholson L, Dickinson A, Nong-Wang X. "MSC-derived Microparticles – characterisation and functional evaluation"(Abstract) 2015. Cytotherapy, Supplement Vol. 1 (6S): Page S24 (ISCT2015, Las Vegas)*
- ***Correia dos Reis M**, Nicholson L, Dickinson A, Nong-Wang X.*Human Platelet Lysate promotes Proliferation and Maintains Immunomodulatory capacity of Mesenchymal Stromal Cells. (2015) In: 41st European Group for Bone and Marrow Transplantation. Istanbul, Turkey: Nature Publishing Group

Other abstracts:

- *Mardiasmo D, **Reis M**, Wang XN. Phenotypic and functional characteristics of xeno-free Mesenchymal Stem Cells. NEPG 2015 (Newcastle, UK)*
- Reis M, Nicholson L, Mavin E, Green K, Dickinson AM, Wang XN. Evaluation of the immunoregulatory effect of MSC-derived Extracellular vesicles", ICM director's research day, June, 2016

Manuscripts (submitted & in preparation):

- **Reis M,** Ogonek J, Qesari M, Nicholson L, Borges N, Preußner L, Dickinson AM, Wang XN, Weissinger EM, Richter A. Recent

developments in cellular therapy for the treatment of hematological malignancies. Frontiers of Immunology (2016) – submitted

- **Reis M,** Nicholson L, Godthardt K, Filby A, Richter A, Dickinson AM, Knöbel S, Wang XN. Phenotypic characterisation of xeno-free MSCs by high-throughput flow cytometry. Nature Communications, to be submitted
- **Reis M,** Nicholson L, Mavin E, Green K, Dickinson AM, Wang XN. MSC derived extracellular vesicles modulate DC function and migratory potential (preliminary title). Stem Cells, in preparation.

Appendix VI – Personal development

Oral presentations

- Celleurope midterm review: project overview, Newcastle July 2014
- Department research meeting: Overview on Curie Institute internship – Isolation and characterisation of extracellular vesicles, Newcastle, September 2014
- Celleurope consortium meeting: project update meeting, Munich, January 2015
- Miltenyi Stem Cells group meeting: overview on secondment, Miltenyi Bitoec, Bergisch Gladbach, Germany, March 2015
- ICM research Seminar: “Characterisation and assessment of immunosuppressive capacity of xeno-free expanded Mesenchymal Stromal Cells”, Newcastle, April 2015
- Department Research meeting: Overview on Miltenyi Secondment, Newcastle, April 2015
- Reis, M. *et al* (2015). The modulatory potential of Mesenchymal stromal cells is mediated by the release of immunologically active extracellular vesicles. UKEV forum, Cardiff 2015
- Department research meeting – Overview on research project, January, 2016
- Celleurope consortium meeting, March 2016
- ICM research seminar: “Evaluation of the immunoregulatory effect of MSC-derived extracellular vesicles”, April, 2016

Meetings and Conferences attended:

- Celleurope consortium meeting, Goettingen, Germany, October 2013
- 7th UK Mesenchymal stem cell meeting - Aston University, Birmingham. September 2013
- North east postgraduate conference (NEPG), Newcastle University, Newcastle. October 2013
- Practicalities of Cellular Analysis “Omics and Informatics”, Centre for Life, Newcastle, February 2014
- GvH-GvL meeting, Regensburg, Germany, March 2014
- Northeast postgraduate conference (NEPG), Newcastle, October 2014
- UK extracellular vesicle (UKEV) forum, London, December 2014
- European bone marrow transplantation (EBMT), Istanbul, Turkey, March 2015
- NESCI research day, stem cell epigenetics, Newcastle, April 2015
- International Society for cellular therapies (ISCT) annual meeting, Las Vegas, USA, May 2015
- GvH/GvL meeting, Regensburg, Germany, March 2016
- SelectBio extracellular vesicle symposium, Cambridge, UK, June 2016

Courses/workshops attended:

- Flow Cytometry training
- Basic Immunology and Immunogenetics
- ePortfolio and Personal Development training
- Managing your PhD, MD or MPhil
- Introduction to Statistical Considerations in Experimental Research
- Learning Agreement
- Endnote
- Chemical Safety training
- UELA test
- Basic fire training induction
- ICM induction morning
- Public speaking

- Risk assessment
- Biological Agents and GMO
- Insights from industry, Good manufacturing practice
- Recording your research (Lab books, research diaries, etc)
- Robust research methodologies for Literature Review
- Very basic Stats
- Basic Stats ISRU
- Haematology department sample tracking system training
- Academic writing
- Convincing CVs and Covering Letters
- Research ethics
- Thesis writing
- Human Tissue Act training
- ISIS database training
- Biotech and Environment Yes workshop
- Celleurope transferable skills week
- Celleurope Immunohistochemistry workshop
- Database training
- Basic Rad protection workshop
- Second year annual review: your research outputs
- Chairing at a scientific meeting
- Communication and presentation skills
- Celleurope workshop on chronic GvHD, Istanbul, March 2015

Additional activities:

- Celleurope newsletter issue 2 – article on Paris internship and experience
- Secondment to Alcyomics, May-June 2014,
- Internship at Institut Curie to learn how to isolate and characterise EVs, August 2014, Paris, France (Fully funded by Newcastle's doctoral awards scheme, supported by Welcome Trust)
- Secondment to Miltenyi Biotec, Germany, January-February 2015

- Co-supervisor of MRes student; Project title: Phenotypic and functional characteristics of xeno-free Mesenchymal stem cells. 2015
- Co-supervisor of MRes student, Project title: Functional dissection of mesenchymal stem cell subpopulations. 2016
- Celleurope newsletter issue – article on ISCT conference
- Small grant writing

Appendix VII – Ethics approval

The Newcastle upon Tyne Hospitals NHS
NHS Foundation Trust

Regent Point
Regent Farm Road
Gosforth
Newcastle upon Tyne
NE3 3HD

Tel: (0191) 233 6161

AJ/AJ/MS

10 September 2015

Professor Matthew Collin,
Newcastle University,
Institute of Cellular Medicine,
Leech Building,
Framlington Place,
Newcastle upon Tyne.
NE2 4HH

Dear Professor Collin,

Trust R&D Project:	**6980**
Title of Project:	**Improving haematopoeitic stem cell outcome through studies of alloreactivity, immune reconstitution, biomarkers and novel therapies**
Principal Investigator	**Professor Collin**
Number of patients:	**300**
Funder:	**NUTH**
Sponsor:	**NUTH**
REC number:	**14/NE/1136**
IRAS Project Code:	**129780**
First participant to be recruited by:	**10 October 2015**

After completing the necessary risk and site assessments for the above research project, The Newcastle upon Tyne Hospitals NHS Foundation Trust grants NHS Management Permission for this research to take place at this Trust dependent upon:

(i) you, as Principal Investigator, agreeing to comply with the Department of Health's Research Governance Framework for Health and Social Care, and confirming your understanding of the responsibilities and duties of Principal Investigators by signing the Investigator Responsibilities Document. A copy of this document will be kept on file within the Joint Research Office.

(ii) you, as Principal Investigator, ensuring compliance of the project with all other legislation and guidelines including Caldicott Guardian approvals and compliance with the Data Protection Act 1998, Health and Safety at Work Act 1974, any requirements of the MHRA (*eg* CTA, EudraCT registration), and any other relevant UK/European guidelines or legislation (*eg* reporting of suspected adverse incidents).

(iii) where applicable, you, as Principal Investigator, should also adhere to the GMC supplementary guidance *Good practice in research* and *Consent to research* which sets out the good practice principles that doctors are expected to understand and follow if they are involved in research – see http://www.gmc-uk.org/guidance/ethical_guidance/5991.asp

The NIHR requires NHS organisations to recruit patients to CLRN Portfolio studies within 30 days from the date of this letter. The 30 day deadline for recruiting the first patient is therefore 10 October 2015.

Please note: the Department of Health 70 day bench mark requires recruitment within 70 days of a valid SSI submission. Therefore, recruiting within the NIHR 30 day target will ensure compliance with both targets.

Sponsorship

The Newcastle upon Tyne Hospitals NHS Foundation Trust will act as Sponsor for this project, under the Department of Health's guidelines for research in health and social care.

In addition, the Trust has a Research Governance Implementation Plan, agreed with the Department of Health, in order to fully comply with Research Governance and fulfil the responsibility of a Sponsor.

As the Trust is acting as Sponsor for the research and where some of the research is taking place outside of Newcastle upon Tyne, then all costs must be met for research governance audit visits to those sites. It is the responsibility of the PI to provide confirmation to the Trust of who will pay these costs. Audit is required under the Research Governance Framework for Health and Social Care. (Please note that the Trust randomly audits 10% of approved research projects annually.)

NHS Permission applies to the research described in the protocol and related documentation as listed on the favourable ethical opinion(s) from NRES Committee North East – Newcastle & North Tyneside 2, dated 25 November 2014 and 23 January 2015. Specifically, the following versions of the key documents are approved:

Document	Version	Date
Participant Information Sheet (PIS) [Donors]	V10	16 January 2015
Participant Information Sheet (PIS) [Patient]	V10	16 January 2015
Participant Information Sheet (PIS) [Healthy volunteer	V10	16 January 2015
Research Protocol or project proposal[improving HSCT outcome v2.2]	V2.2	23 July 2014
Participant Consent Form [Consent- Donor_ improving HSCT outcome v4]	V4	14 November 2014
Participant Consent Form [Consent – healthy Volunteer_ improving HSCT outcome v4]	V4	14 November 2014
Participant Consent Form [Consent –Patient improving HSCT outcome v4]	V4	14 November 2014
Copies of advertisement materials for research participants [Healthy Volunteer Recruitment Leaflet 2]	V2	14 November 2014

Any changes to these documents, or any other amendments to the study must be submitted to the Research Ethics Committee and MHRA (if relevant) for review – see http://www.nres.npsa.nhs.uk/applications/after-ethical-review/amendments/ for guidance). All amendments must be submitted to the R&D office for review in parallel with ethical and regulatory review so that implications of the amendment can be assessed. You must send a copy of all amendment documents to the R&D office and if the changes or amendments to the study have implications for costs or use of resources, you must also submit details of these changes.

It is the Principal Investigator's responsibility to ensure that all staff involved in the research have Honorary Research Contracts or the necessary Letters of Access. These must be issued prior to commencing the research.

In addition, unless otherwise agreed with the Trust, the research will be covered for negligence under the CNST (Clinical Negligence Scheme for Trusts), however cover for no-fault harm is the responsibility of the Principal Investigator to arrange if required.

Please also note that for any NHS employee who generates Intellectual Property *in the normal course of their duties*, it is recognised that the Intellectual Property Rights remain with the employer and not the employee.

Yours sincerely

Andrew Johnston
Research Management & Governance (RM&G) Manager

CC: Ms Carolyn Robinson, Finance Department, Level 2, Regents Point
Ian Pedley, Clinical Director Cancer Services and Haematology, NCCC
Mr Andrew Johnston Sponsor Representative NUTH
Jo Wincup Research Team Lead
Katie Nurowski Trial co-ordinator Newcastle University

References

Abdelrazik, H., Spaggiari, G.M., Chiossone, L. and Moretta, L. (2011b) 'Mesenchymal stem cells expanded in human platelet lysate display a decreased inhibitory capacity on T- and NK-cell proliferation and function', *European Journal of Immunology*, 41(11), pp. 3281-3290.

Aggarwal, S. and Pittenger, M.F. (2005) '*Human mesenchymal stem cells modulate allogeneic immune cell responses*.', Blood, 105(4); pp.1815-1822.

Agudo, J., Ruzo, A., Tung, N., Salmon, H., Leboeuf, M., Hashimoto, D., Becker, c., Garrett-Sinha, L.A., Baccarini, A., Merad, M. and Brown, B.D. (2014) 'The miR-126-VEGFR2 axis controls the innate response to pathogen-associated nucleic acids.', *Nat Immunol,* 15, pp.54–62

Aktas, E., Kucuksezer, U.C., Bilgic, S., Erten, G. and Deniz, G. (2009) 'Relationship between CD107a expression and cytotoxic activity', *Cell Immunol*, 254, pp.149-54

Al Akoum, C., Akl, I., Rouas, R., Fayyad-Kazan, M., Falha, L., Renno, T., Burny, A., Lewalle, P., Fayyad-Kazan, H., Badran, B. (2015) 'NFAT-1, Sp-1, Sp-3, and miR-21: New regulators of chemokine C receptor 7 expression in mature human dendritic cells', *Hum Immunol*, 76(5), pp.307-17

Alter, G., Malenfant, J.M. and Altfeld, M. (2004) 'CD107a as a functional marker for the identification of natural killer cell activity. *J Immunol Methods*, 294, pp.15-22

Amarnath, S., Foley, J.E., Farthing, D.E., Gress, R.E., Laurence, A., Eckhaus, M.A., Metais, J.Y., Rose, J.J., Hakim, F.T., Felizardo, T.C., Cheng, A.V., Robey, P.G., Stroncek, D.E., Sabatino, M., Battiwalla, M., Ito, S., Fowler, D.H. and Barrett, A.J. (2015) 'Bone marrow-derived mesenchymal stromal cells harness purinergenic signaling to tolerize human Th1 cells in vivo', *Stem Cells*, 33(4), pp. 1200-12.

Anderson, A.E., Swan, D.J., Sayers, B.L., Harry, R.A., Patterson, A.M., von Delwig, A., Robinson, J.H., Isaacs, J.D. and Hilkens, C.M. (2009) 'LPS activation is required for migratory activity and antigen presentation by tolerogenic dendritic cells', *J Leukoc Biol*, 85(2), pp.230-50

Anderson, J. D., Johansson, H. J., Graham, C. S., Vesterlund, M., Pham, M. T., Bramlett, C. S., Montgomery, E.N., Mellema, M.S., Bardini, R.L., Contreras, Z., Hoon, M., Bauer, C., Fink, B., Hendrix, K.J., Chedin, F., El-Andaloussi, S., Hwang, B., Mulligan, M.S., Lehtio, J. and Nolta, J. A. (2016). *Comprehensive proteomic analysis of mesenchymal stem cell exosomes reveals modulation of angiogenesis via nuclear factor-kappaB signaling*. *Stem Cells*, *34*(3), pp. 601-613. DOI:10.1002/stem.2298

Appleman, L.J. and Boussiotis, V.A. (2003) 'T cell anergy and costimulation', *Immunol Rev*, 192, pp. 161-80.

Arslan, F., Lai, R.C., Smeets, M.B., Akeroyd, L., Choo, A., Aguor, E.N.E., Timmers, L., van Rijen, H.V., Doevendans, P.A., Pasterkamp, G., Lim, S.K. and de Kleijn, D.P. (2013) 'Mesenchymal stem cell-dericed exosomes increase ATP levels, decrease oxidative stress and activate PI3K/Akt pathway to enhance myocardial viability and prevent adverse remodeling after myocardial ischemia/reperfusion injury', *Stem Cell Research*, 10(3), pp.301-312

Azouna, N.B., Jenhani, F., Regaya, Z., Berraeis, L., Othman, T.B., Ducrocq, E. and Domenech, J. (2012) 'Phenotypical and functional characteristics of mesenchymal stem cells from bone marrow: comparison of culture using different media supplemented with human platelet lysate or fetal bovine serum', *Stem Cell Research & Therapy*, 3(1), pp. 1-14.

Baer, P.C., Kuci, S., Krause, M., Kuci, Z., Zielen, S., Geiger, H., Bader, P. and Schubert, R. (2013) 'Comprehensive phenotypic characterization of human adipose-derived stromal/stem cells and their subsets by a high throughput technology', *Stem Cells Dev*, 22(2), pp. 330-9.

Baglio, S.R., Rooijers, K., Koppers-Lalic, D., Verweij, F.J., Perez Lanzon, M., Zini, N., Naaijkens, B., Perut, F., Niessen, H.W., Baldini, N. and Pegtel, D.M. (2015) 'Human bone marrow- and adipose-mesenchymal stem cells secrete exosomes enriched in distinctive miRNA and tRNA species', *Stem Cell Res Ther*, 6, p. 127.

Baj-Krzyworzeka, M., Szatanek, R., Weglarczyk, K., Baran, J., Urbanowicz, B., Branski, P., Ratajczak, M. Z., Zembala, M. (2006) ‘Tumour-derived microvesicles carry several surface determinants and mRNA of tumour cells and transfer some of these determinants to monocytes’, Cancer Immunol Immunother, 55(7), pp.808-818

Ball, S.G., Shuttleworth, C.A. and Kielty, C.M. (2007) 'Vascular endothelial growth factor can signal through platelet-derived growth factor receptors', *J Cell Biol*, 177(3), pp. 489-500.

Barnett, R.E., Conklin, D.J., Ryan, L., Keskey, R.C., Ramjee, V., Sepulveda, E.A., Srivasava, S., Bhatnagar, A. and Chadle, W.G. (2016) ‘Anti-inflammatory effects of miR-21 in the macrophage response to peritonitis’, *J Leukoc Biol*, 99(2), pp. 361-371

Bartel, D.P. (2004) ‘MicroRNAs: genomics, biogenesis, mechanism and function’, *Cell*, 116(2), pp.281-97

Bartholomew, A., Sturgeon, C., Siatskas, M., Ferrer, K., McIntosh, K., Patil, S., Hardy, W., Devine, S., Ucker, D., Deans, R., Moseley, A. and Hoffman, R. (2002) 'Mesenchymal stem cells suppress lymphocyte proliferation in vitro and prolong skin graft survival in vivo', *Exp Hematol*, 30(1), pp. 42-8.

Bassi EJ, Aita CA, Câmara NO. (2011) ‘Immune regulatory properties of multipotent mesenchymal stromal cells: Where do we stand?’ *World J Stem Cells*, 3, pp.1–8.

Battula, V.L., Treml, S., Bareiss, P.M., Gieseke, F., Roelofs, H., de Zwart, P., Muller, I., Schewe, B., Skutella, T., Fibbe, W.E., Kanz, L. and Buhring, H.J. (2009) 'Isolation of functionally distinct mesenchymal stem cell subsets using antibodies against CD56, CD271, and mesenchymal stem cell antigen-1', *Haematologica*, 94(2), pp. 173-84.

Benmerah, A., Bayrou, M., Cerf-Bensussan, N. and Dautry-Varsat, A. (1999) ‘Inhibition of clathrin-coated pit assembly by an Eps15 mutant’, *Journal of Cell Science*, 112, pp.1303-1311

Benvenuto, F., Ferrari, S., Gerdoni, E., Gualandi, F., Frassoni, F., Pistoia, V., Mancardi, G. and Uccelli, A. (2007) 'Human Mesenchymal Stem Cells

Promote Survival of T Cells in a Quiescent State', *STEM CELLS*, 25(7), pp. 1753-1760.

Bernardo, M.E., Avanzini, M.A., Perotti, C., Cometa, A.M., Moretta, A., Lenta, E., Del Fante, C., Novara, F., de Silvestri, A., Amendola, G., Zuffardi, O., Maccario, R. and Locatelli, F. (2007) 'Optimization of in vitro expansion of human multipotent mesenchymal stromal cells for cell-therapy approaches: Further insights in the search for a fetal calf serum substitute', *Journal of Cellular Physiology*, 211(1), pp. 121-130.

Bernardo, M.E., Cometa, A.M., Pagliara, D., Vinti, L., Rossi, F., Cristantielli, R., Palumbo, G. and Locatelli, F. (2011) 'Ex vivo expansion of mesenchymal stromal cells', *Best Practice & Research Clinical Haematology*, 24(1), pp. 73-81.

Bernardo, M.E. and Fibbe, W.E. (2013) 'Mesenchymal stromal cells: sensors and switchers of inflammation'. *Cell Stem Cell*, 13, pp.392–402.

Bianco, P. and Gehron Robey, P. (2000) 'Marrow stromal stem cells', *J Clin Invest*, 105(12), pp. 1663-8.

Biancone, L., Bruno, S., Deregibus, M.C., Tetta, C. and Camussi, G. (2012) 'Therapeutic potential of mesenchymal stem cell-derived microvesicles', *Nephrology Dialysis Transplantation*, 27(8), pp. 3037-3042.

Bieback, K. (2013) 'Platelet Lysate as Replacement for Fetal Bovine Serum in Mesenchymal Stromal Cell Cultures', *Transfusion Medicine and Hemotherapy*, 40(5), pp. 326-335.

Bieback, K., Hecker, A., Kocaömer, A., Lannert, H., Schallmoser, K., Strunk, D. and Klüter, H. (2009) 'Human Alternatives to Fetal Bovine Serum for the Expansion of Mesenchymal Stromal Cells from Bone Marrow', *STEM CELLS*, 27(9), pp. 2331-2341.

Bieback, K., Hecker, A., Schlechter, T., Hofmann, I., Brousos, N., Redmer, T., Besser, D., Klüter, H., Müller, A.M. and Becker, M. (2012) 'Replicative aging and differentiation potential of human adipose tissue-derived mesenchymal stromal cells expanded in pooled human or fetal bovine serum', *Cytotherapy*, 14(5), pp. 570-583.

Black, C.B., Duensing, T.D., Trinkle, L.S. and Dunlay, R.T. (2011) 'Cell-based screening using high-throughput flow cytometry', *Assay Drug Dev Technol*, 9(1), pp. 13-20.

Blazquez R, Sanchez-Margallo FM, de la Rosa O, Dalemans W, Alvarez V, Tarazona R. (2014) 'Immunomodulatory Potential of Human Adipose Mesenchymal Stem Cells Derived Exosomes on in vitro Stimulated T Cells.' Frontiers in immunology, 5:556.

Bobrie, A., Colombo, M., Krumeich, S., Raposo,G. and Thery, C. (2012) 'Diverse subpopulations of vesicles secreted by different intracellular mechanisms are present in exosome preparations obtained by differential ultracentrifugation', *J Extracell Vesicles*, 1

Bocelli-Tyndall, C., Zajac, P., Di Maggio, N., Trella, E., Benvenuto, F., Iezzi, G., Scherberich, A., Barbero, A., Schaeren, S., Pistoia, V., Spagnoli, G., Vukcevic, M., Martin, I. and Tyndall, A. (2010) 'Fibroblast growth factor 2 and platelet-derived growth factor, but not platelet lysate, induce proliferation-dependent, functional class II major histocompatibility complex antigen in human mesenchymal stem cells', Arthritis Rheum, 62(12), pp.3815-25

Bonab, M.M., Alimoghaddam, K., Talebian, F., Ghaffari, S.H., Ghavamzadeh, A. and Nikbin, B. (2006) 'Aging of mesenchymal stem cell in vitro.' *BMC Cell Biol,* 7:14

Boyman, O. and Sprent, J. (2012) 'The role of interleukin-2 during hemostasis and activation of the immune system'*, Nat Rev Immunol*, 12, pp.180-190

Brunner, D., Frank, J., H., A. and al, e. (2010) 'Serum-free cell culture: the serum-free media interactive online database', *ALTEX*, 27(53-62).

Bruno, S. and Camussi, G. (2013) 'Role of mesenchymal stem cell-derived microvesicles in tissue repair', *Pediatr Nephrol*, 28, pp.2249

Budoni, M., Fierabracci, A., Luciano, R., Petrini, S., Di Ciommo, V. and Muraca, M. (2013) 'The immunosuppressive effect of mesenchymal stromal cells on B lymphocytes is mediated by membrane vesicles', *Cell Transplant*, 22(2), pp. 369-79.

Bunnell, B.A., Betancourt, A.M. and Sullivan, D.E. (2010) 'New concepts on the immune modulation mediated by mesenchymal stem cells', *Stem Cell Res Ther*, 1(5), p. 34.

Bunnell, B.A., Estes, B.T., Guilak, F. and Gimble, J.M. (2008) 'Differentiation of adipose stem cells', *Methods Mol Biol*, 456, pp. 155-71.

Burnouf, T., Strunk, D., Koh, M.B. and Schallmoser, K. (2016) 'Human platelet lysate: Replacing fetal bovine serum as a gold standard for human cell propagation?', *Biomaterials*, 76, pp. 371-87.

Cantaert, T., Baeten, D., Tak, P.P. and van Baarsen, L.G.M. (2010) 'Type I IFN and TNFα cross-regulation in immune-mediated inflammatory disease: basic concepts and clinical relevance', *Arthritis Research & Therapy*, 12(5), pp. 1-10.

Caplan, A.I. (1991) 'Mesenchymal stem cells', *Journal of Orthopaedic Research*, 9(5), pp. 641-650.

Caplan, A.I. (2010) 'What's in a name?', *Tissue Eng Part A*, 16(8), pp. 2415-7.

Caplan, A.I. and Bruder, S.P. (2001) 'Mesenchymal stem cells: building blocks for molecular medicine in the 21st century', *Trends Mol Med*, 7(6), pp. 259-64.

Casado JG, Tarazona R, Sanchez-Margallo FM. (2013) 'NK and MSCs crosstalk: the sense of immunomodulation and their sensitivity. *Stem Cell Rev*., 9, pp.184–189.

Cashman, T., Gouon-Evans, V. and Costa, K. (2013) 'Mesenchymal Stem Cells for Cardiac Therapy: Practical Challenges and Potential Mechanisms', *Stem Cell Reviews and Reports*, 9(3), pp. 254-265.

Castiello, L., Sabatino, M., Jin, P., Clayberger, C., Marincola, F. M., Krensky, A. M., and Stroncek, D. F. (2011). 'Monocyte-derived DC maturation strategies and related pathways: a transcriptional view.' *Cancer Immunology, Immunotherapy : CII*, *60*(4), 457–466.

Castro-Manrreza, M.E. and Montesinos, J.J. (2015) 'Immunoregulation by Mesenchymal Stem Cells: Biological Aspects and Clinical Applications', *Journal of Immunology Research*, 2015, p. 20.

Caux, C. and Dubois, B. (2001) ‘Antigen uptake by dendritic cells’, *Methods Mol Med*, 64, pp.369-76

Chen, L., Zhang, W., Yue, H., Han, Q., Chen, B., Shi, M., Li, J., Li, B., You, S., Shi, Y. and Zhao, R. C. (2007). ‘Effects of human mesenchymal stem cells on the differentiation of dendritic cells from CD34+ cells.’ Stem Cells Dev, 16(5), pp. 719-731

Chen, L. and Flies, D.B. (2013) 'Molecular mechanisms of T cell co-stimulation and co-inhibition', *Nat Rev Immunol*, 13(4), pp. 227-42.

Chen, T.S., Lai, R.C., Lee, M.M., Choo, A.B., Lee, C.N. and Lim, S.K. (2010) 'Mesenchymal stem cell secretes microparticles enriched in pre-microRNAs', *Nucleic Acids Res*, 38(1), pp. 215-24.

Chen, Q., Wang, H., Liu, Y., Song, Y., Lai, L., Han, Q., Cao, X. and Wang, Q. (2012) ‘Inducible microRNA-223 down-regulation promotes TLR-triggered IL-6 and IL-1beta production in macrophages by targeting STAT3’*, PLoS One*, 7(8), e42971

Chiara Barsotti, M., Losi, P., Briganti, E., Sanguinetti, E., Magera, A., Al Kayal, T., Feriani, R., Di Stefano, R. and Soldani, G. (2013) 'Effect of Platelet Lysate on Human Cells Involved in Different Phases of Wound Healing', *PLoS ONE*, 8(12), p. e84753.

Chiesa, S., Morbelli, S., Morando, S., Massollo, M., Marini, C., Bertoni, A., Frassoni, F., Bartolome, S.T., Sambuceti, G., Traggiai, E. and Uccelli, A. (2011). Mesenchymal stem cells impair in vivo T-cell priming by dendritic cells. *Proceedings of the National Academy of Sciences of the United States of America*, *108*(42), 17384–17389.

Choi, H.Y., Saha, S.K., Kim, K., Kim, S., Yang, G.-M., Kim, B., Kim, J.-h. and Cho, S.-G. (2015) 'G protein-coupled receptors in stem cell maintenance and somatic reprogramming to pluripotent or cancer stem cells', *BMB Reports*, 48(2), pp. 68-80.

Chong, P.P., Selvaratnam, L., Abbas, A.A. and Kamarul, T. (2012) 'Human peripheral blood derived mesenchymal stem cells demonstrate similar characteristics and chondrogenic differentiation potential to bone marrow derived mesenchymal stem cells', *J Orthop Res*, 30(4), pp. 634-42.

Choo, S.Y. (2007) 'The HLA System: Genetics, Immunology, Clinical Testing, and Clinical Implications', *Yonsei Medical Journal*, 48(1), pp. 11-23.

Ciccocioppo, R., Cangemi, G. C., Kruzliak, P., Gallia, A., Betti, E., Badulli, C., Martinetti, M., Cervio, M., Pecci, A., Bozzi, V., Dionigi, P., Visai, L., Gurrado, A., Alvisi, C., Picone, C., Monti, M., Bernardo, M. E., Gobbi, P. and Corazza, G. R. (2015) 'Ex vivo immunosuppressive effects of mesenchymal stem cells on Crohn's disease mucosal T cells are largely dependent on indoleamine 2,3-dioxygenase activity and cell-cell contact' *Stem Cell Res Ther*, 6, pp.137

Clark, E.A., Kalomoiris, S., Nolta, J.A. and Fierro, F.A. (2014) 'Concise review: MicroRNA function in multipotent mesenchymal stromal cells', *Stem Cells*, 32(5), pp.1074-82

Cogle, C.R., Yachnis, A.T., Laywell, E.D., Zander, D.S., Wingard, J.R., Steindler, D.A. and Scott, E.W. (2004) 'Bone marrow transdifferentiation in brain after transplantation: a retrospective study', *The Lancet*, 363(9419), pp. 1432-1437.

Collino, F., Deregibus, M.C., Bruno, S., Sterpone, L., Aghemo, G., Viltono, L., Tetta, C. and Camussi, G. (2010) 'Microvesicles derived from adult human bone marrow and tissue specific mesenchymal stem cells shuttle selected pattern of miRNAs', *PLoS ONE,* 5, e11803

Colombo, M., Moita, C., van Niel, G., Kowal, J., Vigneron, J., Benaroch, P., Manel, N., Moira, L.F., Thery, C. and Raposo, G. (2013) 'Analysis of ESCRT functions in exosome biogenesis, composition and secretion highlights the heterogeneity of extracellular vesicles', *Journal of Cell Science*, doi: 10.1242/jcs.128868

Colombo, M., Raposo, G., and Thery, C. (2014) ‘Biogenesis, secretion and intercellular interactions of exosomes and other extracellular vesicles’ Annu Red Cell Dev Biol, 30, pp.255-289

Colonna, M. and Facchetti, F. (2003) 'TREM-1 (Triggering Receptor Expressed on Myeloid Cells): A New Player in Acute Inflammatory Responses', *Journal of Infectious Diseases*, 187(Supplement 2), pp. S397-S401.

Comerford I., Harata-Lee Y., Bunting M.D., Gregor C., Kara E.E. and McColl S.R. (2013) ‘A myriad of functions and complex regulation of the CCR7/CCL19/CCL21 chemokine axis in the adaptive immune system.’, *Cytokine Growth Factor Rev.,*24, 269–283.

Conforti, A., Scarsella, M., Starc, N., Giorda, E., Biagini, S., Proia, A., Carsetti, R., Locatelli, F. and Bernardo, M.E. (2014) 'Microvescicles derived from mesenchymal stromal cells are not as effective as their cellular counterpart in the ability to modulate immune responses in vitro', *Stem Cells Dev*, 23(21), pp. 2591-9.

Consentius, C., Akyuz, L., Schmidt-Lucke, J. A., Tschope, C., Pinzur, L., Ofir, R., Reinke, P., Volk, H. D. and Juelke, K. (2015) ‘Mesenchymal stromal cells prevent allostimulation in vivo and control checkpoints of Th1 priming: migration of human DC to lymph nodes and NK cell activation’, Stem Cells, 33(10), pp. 3087-99

Copland, I.B., Garcia, M.A., Waller, E.K., Roback, J.D. and Galipeau, J. (2013) 'The effect of platelet lysate fibrinogen on the functionality of MSCs in immunotherapy', *Biomaterials*, 34(32), pp. 7840-7850.

Corradetti, B., Correani, A., Romaldini, A., Marini, M.G., Bizzaro, D., Perrini, C., Cremonesi, F. and Lange-Consiglio, A. (2014) 'Amniotic Membrane-Derived Mesenchymal Cells and Their Conditioned Media: Potential Candidates for Uterine Regenerative Therapy in the Horse', *PLoS ONE*, 9(10), p. e111324.

Cortés, J.R., Sanchez-Diaz, R., Bovolenta, E.R., Barreiro, O., Lasarte, S., Matesanz-Marin, A., Toribio, M.L., Sanchez-Marid, F. and Martin, P. (2014) ‘Maintenance of immune tolerance by FoxP3+ regulatory T cells requires CD69 expression’, *J Autoimmun*, 55, pp. 51-62

Cox, G., Boxall, S.A., Giannoudis, P.V., Buckley, C.T., Roshdy, T., Churchman, S.M., McGonagle, D. and Jones, E. (2012) 'High abundance of CD271(+) multipotential stromal cells (MSCs) in intramedullary cavities of long bones', *Bone*, 50(2), pp. 510-517.

Couper, K.N., Blount, D.G and Riley, E.M (2008) 'IL-10:the master regulator of immunity to infection', *The Journal of Immunology*, 180(9), pp.5771-5777

Cramer, E.M., Berger, G. and Berndt, M.C. (1994) 'Platelet alpha-granule and plasma membrane share two new components: CD9 and PECAM-1', *Blood,* 84 (6), pp.1722-30

Crespo-Diaz, R., Behfar, A., Butler, G.W., Padley, D.J., Sarr, M.G., Bartunek, J., Dietz, A.B. and Terzic, A. (2011) 'Platelet lysate consisting of a natural repair proteome supports human mesenchymal stem cell proliferation and chromosomal stability', *Cell Transplant*, 20(6), pp. 797-811.

Dahl, J.A., Duggal, S., Coulston, N. and al, e. (2008) 'Genetic and epigenetic instability of human bone marrow mesenchymal stem cells expanded in autologous serum or fetal bovine serum.', *Int J Dev Biol*, 52, pp. 1033-1042.

Dazzi, F. and Marelli-Berg, F.M. (2008) 'Mesenchymal stem cells for graft-versus-host disease: close encounters with T cells', *Eur J Immunol*, 38(6), pp. 1479-82.

De Bari, C., Dell'Accio, F., Tylzanowski, P. and Luyten, F.P. (2001) 'Multipotent mesenchymal stem cells from adult human synovial membrane', *Arthritis & Rheumatism*, 44(8), pp. 1928-1942.

De Luca, L., Trino, S., Laurenzana, I., Simeon, V., Calice, G., Raimondo, S., Podesta, M., Santodirocco, M., Di Mauro, L., La Rocca, F., Caivano, A., Morano, A., Frassoni, F., Cilloni, D., Del Vecchio, L. and Musto, P. (2015) 'MiRNAs and piRNAs from bone marrow mesenchymal stem cell extracellular vesicles induce cell survival and inhibit cell differentiation of cord blood hematopoietic stem cells: a new insight in transplantation', *Oncotarget*.

Del Fattore, A., Luciano, R., Pascucci, L., Goffredo, B.M., Giorda, E., Scapaticci, M., Fierabracci, A. And Muraca, M. (2015) 'Immunoregulatory

effects of mesenchymal stem cell-derived extracellular vesicles on T lymphocytes', *Cell Transplant*, 24(12), pp. 2615-27

Deng, Z.L., Sharff, K.A., Tang, N., Song, W.X., Luo, J., Luo, X., Chen, J., Bennett, E., Reid, R., Manning, D., Xue, A., Montag, A.G., Luu, H.H., Haydon, R.C. and He, T.C. (2008) 'Regulation of osteogenic differentiation during skeletal development', *Front Biosci*, 13, pp. 2001-21.

Dennis, J.E., Merriam, A., Awadallah, A., Yoo, J.U., Johnstone, B. and Caplan, A.I. (1999) 'A quadripotential mesenchymal progenitor cell isolated from the marrow of an adult mouse', *J Bone Miner Res*, 14(5), pp. 700-9.

Di Nicola, M., Carlo-Stella, C., Magni, M., Milanesi, M., Longoni, P.D., Matteucci, P., Grisanti, S. and Gianni, A.M. (2002) 'Human bone marrow stromal cells suppress T-lymphocyte proliferation induced by cellular or nonspecific mitogenic stimuli.' *Blood*, 99, pp.3838–3843.

Di Trapani, M., Bassi, G., Midolo, M., Gatti, A., Kamga, P. T., Cassaro, A., Carusone, R., Adamo, A. and Krampera, M. (2016) 'Differential and transferable modulatory effects of mesenchymal stromal cell-derived extracellular vesicles on T, B and NK cell functions', Sci Rep, 6, pp. 24120

Dominici, M., Le Blanc, K., Mueller, I., Slaper-Cortenbach, I., Marini, F., Krause, D., Deans, R., Keating, A., Prockop, D. and Horwitz, E. (2006) 'Minimal criteria for defining multipotent mesenchymal stromal cells. The International Society for Cellular Therapy position statement', *Cytotherapy*, 8(4), pp. 315-7.

Donnenberg, A.D., Meyer, E.M., Rubin, J.P. and Donnenberg, V.S. (2015) 'The cell-surface proteome of cultured adipose stromal cells', *Cytometry A*, 87(7), pp. 665-74.

dos Santos, F., Andrade, P.Z., Boura, J.S., Abecasis, M.M., da Silva, C.L. and Cabral, J.M.S. (2010) 'Ex vivo expansion of human mesenchymal stem cells: A more effective cell proliferation kinetics and metabolism under hypoxia', *Journal of Cellular Physiology*, 223(1), pp. 27-35.

Doucet, C., Ernou, I., Zhang, Y., Llense, J.R., Begot, L., Holy, X. and Lataillade, J.J. (2005) 'Platelet lysates promote mesenchymal stem cell expansion: a safety substitute for animal serum in cell-based therapy applications', *J Cell Physiol*, 205.

Doze, V.A. and Perez, D.M. (2013) 'GPCRs in Stem Cell Function', *Progress in molecular biology and translational science*, 115, pp. 175-216.

Ducharme, N. A., Ham, A.-J. L., Lapierre, L. A., and Goldenring, J. R. (2011). 'Rab11-FIP2 influences multiple components of the endosomal system in polarized MDCK cells.' *Cellular Logistics*, 1(2), 57–68.

Duffy, M.M., Pindjakova, J., Hanley, S.A., McCarthy, C., Weidhofer, G.A., Sweeney, E.M., English, K., Shaw, G., Murphy, J.M., Barry, F.P., Mahon, B.P., Belton, O., Ceredig, R. and Griffin, M.D. (2011) 'Mesenchymal stem cell inhibition of T-helper 17 cell- differentiation is triggered by cell–cell contact and mediated by prostaglandin E2 via the EP4 receptor', *European Journal of Immunology*, 41(10), pp. 2840-2851.

Dugrillon, A., Eichler, H., Kern, S. and Klüter, H. (2002) 'Autologous concentrated platelet-rich plasma (cPRP) for local application in bone regeneration', *International Journal of Oral and Maxillofacial Surgery*, 31(6), pp. 615-619.

Eastment, C. and Sirbasku, D. (1980) 'Human platelet lysate contains growth factor activities for established cell lines derived from various tissues of several species.', *In Vitro*, 16(8), pp. 694-705.

Elgueta, R., Benson, M.J., de Vries, V.C., Wasiuk, A., Guo, Y. and Noelle, R.J. (2009) 'Molecular mechanism and function of CD40/CD40L engagement in the immune system', *Immunological reviews*, 229(1), pp. 10.1111/j.1600-065X.2009.00782.x.

Eliopoulos, N., Stagg, J., Lejeune, L., Pommey, S. and Galipeau, J. (2005) 'Allogeneic marrow stromal cells are immune rejected by MHC class I- and class II-mismatched recipient mice', *Blood*, 106(13), pp. 4057-65.

EMEA, Committee for Advanced therapies (CAT), (2003) 'Note for Guidance on the Use of Bovine Serum in the Manufacture of Human Medicinal Products.', *EMEA*, CPMP/BWP/1793/02.

English, K., Barry, F.P. and Mahon, B.P. (2008) 'Murine mesenchymal stem cells suppress dendritic cell migration, maturation and antigen presentation', *Immunol Lett*, 115(1), pp.50-8

English, K. (2013) 'Mechanisms of mesenchymal stromal cell immunomodulation', *Immunology and Cell Biology*, 91, pp. 19-26.

English, K., Barry, F.P., Field-Corbett, C.P. and Mahon, B.P. (2007) 'IFN-γ and TNF-α differentially regulate immunomodulation by murine mesenchymal stem cells', *Immunology Letters*, 110(2), pp. 91-100.

English, K. and Wood, K.J. (2013) 'Mesenchymal Stromal Cells in Transplantation Rejection and Tolerance', *Cold Spring Harbor Perspectives in Medicine*, 3(5).

Escola, J.M., Kleijmeer, M.J., Stoorvogel, W., Griffith, J.M., Yoshie, O. and Geuze, H.J. (1998), 'Selective enrichment of tetraspan proteins on the internal vesicles of multivesicular endosomes and on exosomes secreted by human B-lymphocytes.' *J. Biol. Chem*, 273, pp.20121–20127.

Estève, D., Galitzky, J., Bouloumié, A., Fonta, C., Buchet, R., and Magne, D. (2016). 'Multiple Functions of MSCA-1/TNAP in Adult Mesenchymal Progenitor/Stromal Cells.' *Stem Cells International*, *2016*, 1815982.

Favaro, E., Carpanetto, A., Caorsi, C., Giovarelli, M., Angelini, C., Cavallo-Perin, P., Tetta, C., Camussi, G. and Zanone, M.M. (2016) 'Human mesenchymal stem cells and derived extracellular vesicles induce regulatory dendritic cells in type 1 diabetic patients', *Diabetologia*, 59(2), pp. 325-33.

Fedele, G., Frasca, L., Palazzom R., Ferrero, E., Malavasi, F. And Ausiello, C.M. (2004) 'CD38 is expressed on human mature monocyte-derived dendritic cells and is functionally involved in CD83 expression and IL-12 production', *Eur J Immunol,* 34(5), pp.1342-50

Flemming, A., Schallmoser, K., Strunk, D., Stolk, M., Volk, H.-D. and Seifert, M. (2011) 'Immunomodulative Efficacy of Bone Marrow-Derived Mesenchymal Stem Cells Cultured in Human Platelet Lysate', *Journal of Clinical Immunology*, 31(6), pp. 1143-1156.

Fontenot, J. D., Rasmussen, J. P., Gavin, M. A. and Rudensky, A. Y. (2006) ' A function for interleukin 2 in Foxp3-expressing regulatory T cells.' *Nature Immunol.* 6, pp.1142–1151.

François, M., Romieu-Mourez, R., M., L. and Galipeau, J. (2012) 'Human MSC Suppression Correlates With Cytokine Induction of Indoleamine 2,3-Dioxygenase and Bystander M2 Macrophage Differentiation', *Molecular Therapy*, 20(1), pp. 187-185.

Frank, F., Sonenberg, N. and Nagar, B. (2010)' Structural basis for 5′ nucleotide base-specific recognition of guide RNA by human AGO2', **Nature**, 465, pp. 818–822

Frasca, L., Fedele, G., Deaglio, S., Capuano, C., Palazzo, R., Viasitti, T., Malavasi, F. And Ausiello, C.M. (2006) 'CD38 orchestrates migration, survival, and Th1 immune response of human mature dendritic cells', *Blood*, 107(6), pp.2392-9

Friedenstein, A.J., Chailakhjan, R.K. and Lalykina, K.S. (1970) 'THE DEVELOPMENT OF FIBROBLAST COLONIES IN MONOLAYER CULTURES OF GUINEA-PIG BONE MARROW AND SPLEEN CELLS', *Cell Proliferation*, 3(4), pp. 393-403.

Friedenstein, A.J., Chailakhyan, R.K. and Gerasimov, U.V. (1987) 'Bone marrow osteogenic stem cells: in vitro cultivation and transplantation in diffusion chambers', *Cell Proliferation*, 20(3), pp. 263-272.

Friedenstein, A.J., Chailakhyan, R.K., Latsinik, N.V., Panasyuk, A.F. and Keiliss-Borok, I.V. (1974) 'STROMAL CELLS RESPONSIBLE FOR TRANSFERRING THE MICROENVIRONMENT OF THE HEMOPOIETIC TISSUES: Cloning In Vitro and Retransplantation In Vivo', *Transplantation*, 17(4).

Friedenstein, A.J., Piatetzky-Shapiro, I.I. and Petrakova, K.V. (1966) 'Osteogenesis in transplants of bone marrow cells', *Journal of Embryology and Experimental Morphology*, 16(3), pp. 381-390.

Friedman, M.S., Long, M.W. and Hankenson, K.D. (2006) 'Osteogenic differentiation of human mesenchymal stem cells is regulated by bone morphogenetic protein-6', *J Cell Biochem*, 98(3), pp. 538-54.

Frings, K.R.S.V.V.d.C.P. (2012) 'Comparison between antibodies from different providers: determination of median fluorescent intensities and stain indices', *MACS & More*, 14(1).

Fu, X., Chen, Y., Xie, F.N., Dong, P., Liu, W.B., Cao, Y., Zhang, W.J. and Xiao, R. (2015) 'Comparison of immunological characteristics of mesenchymal stem cells derived from human embryonic stem cells and bone marrow', *Tissue Eng Part A*, 21(3-4), pp. 616-26.

Fuhlbrigge, R.C., Kieffer, J.D., Armerding, D. and Kupper, T.S. (1997) ’Cutaneous lymphocyte antigen is a specialized form of PSGL-1 expressed on skin-homing T cells’, *Nature*, 389(6654), pp.978-981

Gatti, S., Bruno, S., Deregibus, M.C., Sordi, A., Cantaluppi, V., Tetta, C. and Camussi, G. (2011) 'Microvesicles derived from human adult mesenchymal stem cells protect against ischaemia-reperfusion-induced acute and chronic kidney injury', *Nephrol Dial Transplant*, 26(5), pp. 1474-83.

Gedye, C.A., Hussain, A., Paterson, J., Smrke, A., Saini, H., Sirskyj, D., Pereira, K., Lobo, N., Stewart, J., Go, C., Ho, J., Medrano, M., Hyatt, E., Yuan, J., Lauriault, S., Kondratyev, M., van den Beucken, T., Jewett, M., Dirks, P., Guidos, C.J., Danska, J., Wang, J., Wouters, B., Neel, B., Rottapel, R. and Ailles, L.E. (2014) 'Cell Surface Profiling Using High-Throughput Flow Cytometry: A Platform for Biomarker Discovery and Analysis of Cellular Heterogeneity', *PLoS ONE*, 9(8), p. e105602.

Germain, R.N. (2002) 'T-cell development and the CD4-CD8 lineage decision', *Nat Rev Immunol*, 2(5), pp. 309-22.

Gholamrezanezhad A, Mirpour S, Bagheri M, Mohamadnejad M, Alimoghaddam K, Abdolahzadeh L. (2011) ‘In vivo tracking of 111In-oxine

labelled mesenchymal stem cells following infusion in patients with advanced cirrhosis'. *Nuclear medicine and biology,* 38(7), pp.961-7

Geiss, G.K., Bumgarner, R.E., Birditt, B., Dahl, T., Dowidar, N., Dunaway, D.L., Fell, H.P., Ferree, S., George, R.D., Grogan, T., James, J.J., Maysuria, M., Mitton, J.D., Oliveri, P., Osborn, J.L., Peng, T., Ratcliffe, A.L., Webster, P.J., Davidson, E.H., Hood, L. and Dimitrov, K. (2008), 'Direct multiplexed measurement of gene expression with color-coded probe pairs', *Nat Biotechnol*, 26, pp.317-325

Giuliani, N., Lisignoli, G., Magnani, M., Racano, C., Bolzoni, M., Dalla Palma, B., Spolzino, A., Manferdini, C., Abati, C., Toscani, D., Facchini, A. and Aversa, F. (2013) 'New Insights into Osteogenic and Chondrogenic Differentiation of Human Bone Marrow Mesenchymal Stem Cells and Their Potential Clinical Applications for Bone Regeneration in Pediatric Orthopaedics', *Stem Cells International*, 2013, p. 312501.

Giuliani, M., Bennaceur-Griscelli, A., Nanbakhsh, A., Oudrhiri, N., Chouaib, S., Azzarone, B., Durrbach, A. and Lataillade, J. J (2014) 'TLR ligands stimulation protects MSC from NK killing', *Stem Cells*, 32(1), pp.290-300

Gottipamula, S., Ashwin, K.M., Muttigi, M., Kannan, S., Kolkundkar, U. and Seetharam, R. (2014) 'Isolation, expansion and characterization of bone marrow-derived mesenchymal stromal cells in serum-free conditions', *Cell and Tissue Research*, 356(1), pp. 123-135.

Gouveia de Andrade, A. V., Bertolino, G., Riewaldt, J., Bieback, K., Karbanova, J., Odendahl, M., Bornhauser, M., Schmitz, M., Corbeil, D. and Tonn, T. (2015) 'Extracellular vesicles secreted by bone marrow- and adipose tissue-derived mesenchymal stromal cells fail to suppress lymphocyte proliferation', Stem Cells Dev, 24(11), pp.1374-1376

Granéli, C., Thorfve, A., Ruetschi, U., Brisby, H., Thomsen, P., Lindahl, A. and Karlsson, C. (2014) 'Novel markers of osteogenic and adipogenic differentiation of human bone marrow stromal cells identified using a quantitative proteomics approach', *Stem Cell Research*, 12(1), pp. 153-165.

Griffiths, S., Baraniak, P.R., Copland, I.B., Nerem, R.M. and McDevitt, T.C. (2013) 'Human platelet lysate stimulates high-passage and senescent human multipotent mesenchymal stromal cell growth and rejuvenation in vitro', *Cytotherapy*, 15(12), pp. 1469-83.

Grove, J.E., Bruscia, E. and Krause, D.S. (2004) 'Plasticity of bone marrow-derived stem cells', *Stem Cells*, 22(4), pp. 487-500.

Grzesiak, J., Krzysztof, M., Karol, W. and Joanna, C. (2011) 'Isolation and morphological characterisation of ovine adipose-derived mesenchymal stem cells in culture', *Int J Stem Cells*, 4(2), pp. 99-104.

Gyorgy B, Szabo TG, Pasztoi M, Pal Z, Misjak P, Aradi B. (2011) 'Membrane vesicles, current state-of-the-art: emerging role of extracellular vesicles. *Cellular and molecular life sciences : CMLS*, 68(16), pp.2667-88.

Haddad, H and Saldanha-Araujo, F. (2014) 'Mechanisms of T-Cell Immunosuppression by Mesenchymal Stromal Cells: What Do We Know So Far?*' BioMed Research International*, vol. 2014, doi:10.1155/2014/216806

Hamblin, T.J. (2003) 'CD38: what is it there for?', *Blood*, 102(6), pp. 1939-1940

Herlaar, E. and Brown, Z. (1999) 'p38 MAPK signalling cascades in inflammatory disease', *Molecular Medicine Today*, 5(10), pp. 439-447.

Heyer, M.P., Pani, A.K., Smeyne, R.J., Kenny, P.J. and Feng, G. (2012) 'Normal midbrain dopaminergic neuron development and function in mir-133b mutant mice', *The Journal of Neuroscience*, 32(32), pp.10887-10894

Hong, Y., Wu, J., Zhao, J., Wang, H., Chen, T., Kan, X., Tao, Q., Shen, X., Yan, K. and Zhai, Z. (2013) 'miR-29b and miR-29c are involved in Toll-like receptor control of glucocorticoid-induced apoptosis in human plasmacytoid dendritic cells.', *PLoS One*, 8:e69926.

Horwitz, E.M., Gordon, P.L., Koo, W.K., Marx, J.C., Neel, M.D., McNall, R.Y., Muul, L. and Hofmann, T. (2002) 'Isolated allogeneic bone marrow-derived mesenchymal stem cells engraft and stimulate growth in children with osteogenesis imperfecta: implications for cell therapy of bone', *Proc Natl Acad Sci USA,* 99(13), pp.8932-8937

Horwitz, E.M., Le Blanc, K., Dominici, M., Mueller, I., Slaper-Cortenbach, I., Marini, F.C., Deans, R.J., Krause, D.S. and Keating, A. (2005) 'Clarification of the nomenclature for MSC: The International Society for Cellular Therapy position statement', *Cytotherapy*, 7(5), pp. 393-395.

Horwitz, E.M., Prockop, D.J., Fitzpatrick, L.A., Koo, W.W.K., Gordon, P.L., Neel, M., Sussman, M., Orchard, P., Marx, J.C., Pyeritz, R.E. and Brenner, M.K. (1999) 'Transplantability and therapeutic effects of bone marrow-derived mesenchymal cells in children with osteogenesis imperfecta', *Nat Med*, 5(3), pp. 309-313.

Huang, X.P., Sun, Z., Miyagi, Y., McDonald Kinkaid, H., Zhang, L., Weisel, R.D. and Li, R.K. (2010) 'Differentiation of allogeneic mesenchymal stem cells induces immunogenicity and limits their long-term benefits for myocardial repair', *Circulation*, 122(23), pp. 2419-29.

Introna, M., Lucchini, G., Dander, E., Galimberti, S., Rovelli, A., Balduzzi, A., Longoni, D., Pavan, F., Masciocchi, F., Algarotti, A., Micò, C., Grassi, A., Deola, S., Cavattoni, I., Gaipa, G., Belotti, D., Perseghin, P., Parma, M., Pogliani, E., Golay, J., Pedrini, O., Capelli, C., Cortelazzo, S., D'Amico, G., Biondi, A., Rambaldi, A. and Biagi, E. (2014) 'Treatment of Graft versus Host Disease with Mesenchymal Stromal Cells: A Phase I Study on 40 Adult and Pediatric Patients', *Biology of Blood and Marrow Transplantation*, 20(3), pp. 375-381.

Iudicone, P., Fioravanti, D., Bonanno, G., Miceli, M., Lavorino, C., Totta, P., Frati, L., Nuti, M. and Pierelli, L. (2013) 'Pathogen-free, plasma-poor platelet lysate and expansion of human mesenchymal stem cells', *Journal of Translational Medicine*, 12(1), pp.1-14

Ivanova-Todorova E, Bochev I, Mourdjeva M, Dimitrov R, Bukarev D, Kyurkchiev S, Tivchev P, Altunkova I, Kyurkchiev DS. (2009) 'Adipose tissue-derived mesenchymal stem cells are more potent suppressors of dendritic cells differentiation compared to bone marrow-derived mesenchymal stem cells.' Immunol Lett,126, pp.37–42.

Ivanova-Todorova, E., Bochev, I., Dimitrov, R., Belemezova, K., Mourdjeva, M., Kyurkchiev, S., Kinov, P., Altankova, I. and Kyurkchiev, D. (2012) ‘Conditioned medium from adipose tissue-derived mesenchymal stem cells induces CD4+FOXP3+ cells and increases IL-10 secretion.’ *J Biomed Biotechnol*, 2012:295167.

Jacobs, S.A., Pinxteren, J., Roobrouck, V.D., Luyckx, A., van't Hof, W., Deans, R., Verfaillie, C.M., Waer, M., Billiau, A.D. and Van Gool, S.W. (2013a) 'Human multipotent adult progenitor cells are nonimmunogenic and exert potent immunomodulatory effects on alloreactive T-cell responses', *Cell Transplant*, 22(10), pp. 1915-28.

Jacobs, S.A., Roobrouck, V.D., Verfaillie, C.M. and Van Gool, S.W. (2013b) 'Immunological characteristics of human mesenchymal stem cells and multipotent adult progenitor cells', *Immunol Cell Biol*, 91(1), pp. 32-9.

Jeon, E.J., Lee, K.Y., Choi, N.S., Lee, M.H., Kim, H.N., Jin, Y.H., Ryoo, H.M., Choi, J.Y., Yoshida, M., Nishino, N., Oh, B.C., Lee, K.S., Lee, Y.H. and Bae, S.C. (2006) 'Bone morphogenetic protein-2 stimulates Runx2 acetylation', *J Biol Chem*, 281(24), pp. 16502-11.

Jiang, Y., Jahagirdar, B.N., Reinhardt, R.L., Schwartz, R.E., Keene, C.D., Ortiz-Gonzalez, X.R., Reyes, M., Lenvik, T., Lund, T., Blackstad, M., Du, J., Aldrich, S., Lisberg, A., Low, W.C., Largaespada, D.A. and Verfaillie, C.M. (2002) 'Pluripotency of mesenchymal stem cells derived from adult marrow', *Nature*, 418(6893), pp. 41-9.

Kalra, H., Simpson, R. J., Ji, H., Aikawa, E., Altevogt, P., Askenase, P., Bond, V. C., Borras, F. E., Breakefield, X., Budnik, V., Buzas, E., Camussi, G., Clayton, A., Cocucci, E., Falcon-Perez, J. M., Gabrielsson, S., Gho, Y. S., Gupta, D., Harsha, H. C., Hendrix, A., Hill, A. F., Inal, J. M., Jenster, G., Kramer-Albers, E. M., Lim, S. K., Llorente, A., Lotvall, J., Marcilla, A., Mincheva-Nilsson, L., Nazarenko, I., Nieuwland, R., Nolte-'t Hoen, E. N., Pandey, A., Patel, T., Piper, M. G., Pluchino, S., Prasad, T. S., Rajendran, L., Raposo, G., Record, M. Reid, G. E., Sanchez-Madrid, F., Schiffelers, R. M., Siljander, P., Stensballe, A., Stoorvogel, W., Taylor, D., Thery, C., Valadi, H., van Balkom, B. W., Vazquez, J., Vidal, M., Wauben, M. H.,

Yanez-Mo, M., Zoeller, M., Mathivanan, S. (2012) ‘Vesiclepedia: a compendium for extracellular vesicles with continuous community annotation’, *PLoS Biol*, 10(12), e1001450

Katakowski, W., Buller, B., Zheng, X., Lu, Y., Rogers, T., Osabamiro, O., Shu, W., Jiang, F. and Chopp, M. (2013) ‘Exosomes from marrow stromal cells expressing miR-146b inhibit glioma growth’, *Cancer letters*, 335(1), pp.201-04

Katare R, Riu F, Mitchell K, Gubernator M, Campagnolo P, Cui Y, Fortunato, O., Avolio, E., Cesselli, D., Beltrami, A.P., Angelini, G., Emanueli, E. and Madeddu, P. (2011) ‘Transplantation of human pericyte progenitor cells improves the repair of infarcted heart through activation of an angiogenic program involving micro-RNA-132.’ *Circ Res.*, 109, pp.894–906

Keerthikumar, S., Chisanga, D., Ariyaratne, D., Al Saffar, H., Anand, S., Zhao, K., Samuel, M., Pathan, M., Jois, M., Chilamkurti, N., Gangoda, L., Mathivanan, S. (2016) ‘ExoCarta: a web-based compendium of exosomal cargo’, J Mol Biol, 428(4), pp.688-692

Khan, S. Y., McLaughlin, N. J. D., Kelher, M. R., Eckles, P., Gamboni-Robertson, F., Banerjee, A. and Sillman, C.C. (2010). ‘Lysophosphatidylcholines activate G2A inducing Gαi-1-/Gαq/11-Ca2+ flux, Gβγ-Hck activation and clathrin/β-arrestin-1/GRK6 recruitment in PMNs.’ *The Biochemical Journal,* 432(1), pp. 35–45.

Kilpinen, L., Impola, U., Sankkila, L., Ritamo, I., Aatonen, M., Kilpinen, S., Tiumala, J., Valmu, L., Levijoki, J., Finckenberg, P., Siljander, P., Kankuri, E., Mervaala, E., Laitinen, S. (2013) ’Extracellular membrane vesicles from umbilical cord blood-derived MSC protect against ischemic acute kidney injury, a feature that is lost after inflammatory conditioning.’ *Journal of Extracellular Vesicles***,** [S.l.]

Kim, H.S., Choi, D.Y., Yun, S.J., Choi, S.M., Kang, J.W., Jung, J.W., Hwang, D., Kim, K.P. and Kim, D.W. (2012) 'Proteomic analysis of microvesicles derived from human mesenchymal stem cells', *J Proteome Res*, 11(2), pp. 839-49.

Kim, D. K., Kang, B., Kim, O. Y., Choi, D. S., Lee, J., Kim, S. R., Go, G., Yoon, Y. J., Kim, J. H., Jang, S. C., Park, K. S., Choi, E. J., Kim, K. P., Desiderio, D. M., Kim, Y. K., Lotvall, J., Hwang, D. and Gho, Y. S. (2013) EVpedia: an integrated database of high-throughput data for systemic analysis of extracellular vesicles', *J Extracell Vesicles*, 2

Kim, G.G., Donnberg, V.S., Donnberg, A.D., Gooding, W. and Whiteside, T.L. (2007) 'A novel multiparametric flow cytometry-based cytotoxicity assay simultaneously immunophenotypes effector cells: comparisons to a 4h 51Cr-release assay.' *J Immunol Methods*, 325, pp.51-66

Kim, S.M., Moon, S.H., Lee, Y., Kim, G.J., Chung, H.M. and Choi, Y.S. (2013) 'Alternative Xeno-Free Biomaterials Derived from Human Umbilical Cord for the Self-Renewal Ex-vivo Expansion of Mesenchymal Stem Cells', *Stem Cells and Development*, 22(22), pp. 3025-3038.

Kim, Y. H., Song, M., Oh, Y. S., Heo, K., Choi, J. W., Park, J. M., Kim, S. H., Lim, S., Kwon, H. M., Ryu, S. H. and Suh, P. G. (2006) 'Inhibition of phospholipase C-beta1-mediated signaling by O-GlcNAc modification', *J Cell Physiol*, 207(3), pp.689-96

Kinzebach, S. and Bieback, K. (2013) 'Expansion of Mesenchymal Stem/Stromal Cells under Xenogenic-Free Culture Conditions', in Weyand, B., Dominici, M., Hass, R., Jacobs, R. and Kasper, C. (eds.) *Mesenchymal Stem Cells - Basics and Clinical Application I*. Springer Berlin Heidelberg, pp. 33-57.

Kmiecik, G., Niklinska, W., Kuc, P., Pancewicz-Wojtkiewicz, J., Fil, D., Karwowska, A., Karczewski, J. and Mackiewicz, Z. (2013) 'Fetal membranes as a source of stem cells', *Adv Med Sci*, 58(2), pp. 185-95.

Kobayashi, T., Watanabe, H., Yanagawa, T., Tsutsumi, S., Kayakabe, M., Shinozaki, T., Higuchi, H. and Takagishi, K. (2005) 'Motility and growth of human bone-marrow mesenchymal stem cells during ex vivo expansion in autologous serum', *Journal of Bone & Joint Surgery, British Volume*, 87-B(10), pp. 1426-1433.

Kocaoemer, A., Kern, S., Klüter, H. and Bieback, K. (2007) 'Human AB Serum and Thrombin-Activated Platelet-Rich Plasma Are Suitable Alternatives to Fetal Calf Serum for the Expansion of Mesenchymal Stem Cells from Adipose Tissue', *STEM CELLS*, 25(5), pp. 1270-1278.

Koppers-Lalic, D., Hackenberg, M., Bijnsdorp, I.V., van Eijndhoven, M.A., Sadek, P., Sie, D., Zini, N., Middeldorp, J.M., Ylstra, B., de Menezes, R.X., Wurdinger, T., Meijer, G.A. and Pegtel, D.M. (2014) 'Nontemplated nucleotide additions distinguish the small RNA composition in cells from exosomes' Cell Rep, 8, pp. 1649–1658

Kordelas L, Rebmann V, Ludwig AK, Radtke S, Ruesing J, Doeppner TR, et a. (2014).' MSC-derived exosomes: a novel tool to treat therapy-refractory graft-versus-host disease, Leukemia, 28(4), pp.970-3.

Kosaka, N., Iguchi, H., Yoshioka, Y., Takeshita, F., Matsuki, Y. and Ochiya, T. (2013) Neutral sphingomyelinase 2 (nSMase2)-dependent exosomal transfer of angiogenic microRNAs regulate cancer cell metastasis.' J Biol Chem, 288 (10), pp.849-59

Krampera, M., Cosmi, L., Angeli, R., Pasini, A., Liotta, F., Andreini, A., Santarlasci, V., Mazzinghi, B., Pizzolo, G., Vinante, F., Romagnani, P., Maggi, E., Romagnani, S. and Annunziato, F. (2005) 'Role of the IFN-γ in the immunomodulatory activity of human mesenchymal stem cells', *Stem Cells*, 24.

Krampera, M., Glennie, S., Dyson, J., Scott, D., Laylor, R., Simpson, E. and Dazzi, F. (2003) 'Bone marrow mesenchymal stem cells inhibit the response of naive and memory antigen-specific T cells to their cognate peptide', *Blood*, 101(9), pp. 3722-9.

Kronsteiner, B., Peterbauer-Scherb, A., Grillari-Voglauer, R., Redl, H., Gabriel, C., van Griensven, M. and Wolbank, S. (2011) 'Human mesenchymal stem cells and renal tubular epithelial cells differentially inflience monocyte-derived dendritic cell differentiation and maturation', *Cell Immunol*, 267(1), pp.30.38

Kuci, S., Kuci, Z., Kreyenberg, H., Deak, E., Putsch, K., Huenecke, S., Amara, C., Koller, S., Rettinger, E., Grez, M., Koehl, U., Latifi-Pupovci, H., Henschler, R., Tonn, T., von Laer, D., Klingebiel, T. and Bader, P. (2010) 'CD271 antigen defines a subset of multipotent stromal cells with immunosuppressive and lymphohematopoietic engraftment-promoting properties', *Haematologica*, 95(4), pp. 651-9.

Kupcova, S.K. (2013) 'Proteomic techniques for characterisation of mesenchymal stem cell secretome', *Biochimie,* 95(12), pp.2196-211

Kyurkchiev, D., Bochev, I., Ivanova-Todorova, E., Mourdjeva, M., Oreshkova, T., Belemezova, K., & Kyurkchiev, S. (2014). Secretion of immunoregulatory cytokines by mesenchymal stem cells. *World Journal of Stem Cells*, *6*(5), 552–570. http://doi.org/10.4252/wjsc.v6.i5.552

Lai, R.C., Arslan, F., Lee, M.M., Sze, N.S., Choo, A., Chen, T.S., Salto-Tellez, M., Timmers, L., Lee, C.N., El Oakley, R.M., Pasterkamp, G., de Kleijn, D.P. and Lim, S.K. (2010) 'Exosome secreted by MSC reduces myocardial ischemia/reperfusion injury', *Stem Cell Res*, 4(3), pp. 214-22.

Lai, R. C., Tan, S. S., Yeo, R. W. Y., Choo, A. B. H., Reiner, A. T., Su, Y., Shen, Y., Fu, Y., Alexander, L., Sze, S.K. and Lim, S. K. (2016). MSC secretes at least 3 EV types each with a unique permutation of membrane lipid, protein and RNA. *Journal of Extracellular Vesicles*, *5*, 10.3402/jev.v5.29828. http://doi.org/10.3402/jev.v5.29828

Lavoie, J.R. and Rosu-Myles, M. (2013) 'Uncovering the secretes of mesenchymal stem cells', *Biochimie*, 95(12), pp. 2212-21.

Lazarus, H.M., Haynesworth, S.E., Gerson, S.L., Rosenthal, N.S. and Caplan, A.I. (1995) 'Ex vivo expansion and subsequent infusion of human bone marrow-derived stromal progenitor cells (mesenchymal progenitor cells): implications for therapeutic use', *Bone Marrow Transplant*, 16.

Le Blanc, K., Frassoni, F., Ball, L., Locatelli, F., Roelofs, H., Lewis, I., Lanino, E., Sundberg, B., Bernardo, M.E., Remberger, M., Dini, G., Egeler, R.M., Bacigalupo, A., Fibbe, W. and Ringden, O. (2008) 'Mesenchymal stem cells

for treatment of steroid-resistant, severe, acute graft-versus-host disease: a phase II study', *Lancet*, 371(9624), pp. 1579-86.

Le Blanc, K., Rasmusson, I., Gotherstrom, C., Seidel, C., Sundberg, B., Sundin, M., Rosendahl, K., Tammik, C. and Ringden, O. (2004) 'Mesenchymal stem cells inhibit the expression of CD25 (interleukin-2 receptor) and CD38 on phytohaemagglutinin-activated lymphocytes', *Scand J Immunol*, 60(3), pp. 307-15.

Le Blanc, K., Tammik, C., Rosendahl, K., Zetterberg, E. and Ringden, O. (2003) 'HLA expression and immunologic properties of differentiated and undifferentiated mesenchymal stem cells', *Exp Hematol*, 31(10), pp. 890-6.

Lee, K. S., Cha, S.-H., Kang, H. W., Song, J.-Y., Lee, K. W., KO, K. B., & Lee, H. T. (2013). 'Effects of Serial Passage on the Characteristics and Chondrogenic Differentiation of Canine Umbilical Cord Matrix Derived Mesenchymal Stem Cells.' *Asian-Australasian Journal of Animal Sciences*,, *26*(4), pp. 588–595.

Lee, J.K., Park, S.R., Jung, B.K., Jeon, Y.K., Lee, Y.S., Kim, M.K., Kim, Y.G., Jang, J.Y. and Kim, C.W. (2014) 'Exosomes derived from mesenchymal stem cells suppress angiogenesis by down-regulating VEGF expression in breast cancer cells' *PLoS ONE*, 8(12), pp. e84256

Lennon, D. P., Schluchter, M. D., & Caplan, A. I. (2012). 'The Effect of Extended First Passage Culture on the Proliferation and Differentiation of Human Marrow-Derived Mesenchymal Stem Cells.' *Stem Cells Translational Medicine*, *1*(4), pp.279–288.

Li, Q., Zhang, D., Wang, Y., Sun, P., Hou, X., Larner, J., Xiong, W. and Mi, J. (2013) 'MiR-21/Smad 7 signaling determines TGF-β1-induced CAF formation', *Scientific Reports*, 3, pp.2038

Li, Z., Liu, C., Xie, Z., Song, P., Zhao, Robert, C. H., Guo, L., Liu, Z. and Wu, Y. (2011) 'Epigenetic Dysregulation in Mesenchymal Stem Cell Aging and Spontaneous Differentiation', *PLoS One*, 6(6), e20526

Liang, X., Ding, Y., Zhang, Y., Tse, H.F. and Lian, Q. (2014) ‘Paracrine mechanisms of mesenchymal stem cell-based therapy: current status and perspectives’, *Cell Transplantation*, 23(9), pp.1045-1059

Lim, I.J. and Phan, T.T. (2014) 'Epithelial and mesenchymal stem cells from the umbilical cord lining membrane', *Cell Transplant*, 23(4-5), pp. 497-503.

Lin, F., Zhang, W., Xue, D., Zhu, T., Li, J., Chen, E., Yao, X. and Pan, Z. (2016) 'Signaling pathways involved in the effects of HMGB1 on mesenchymal stem cell migration and osteoblastic differentiation', *Int J Mol Med*, 37(3), pp. 789-97.

Lin, H.T., Tarng, Y.W., Chen, Y.C., Kao, C.L., Hsu, C.J., Shyr, Y.M., Ku, H.H. and Chiou, S.H. (2005) 'Using Human Plasma Supplemented Medium to Cultivate Human Bone Marrow–Derived Mesenchymal Stem Cell and Evaluation of Its Multiple-Lineage Potential', *Transplantation proceedings*, 37(10), pp. 4504-4505.

Lischke, T., Heesch, K., Schumacher, V., Schneider, M., Haag, F., Koch-Nolte, F. and Mittrucker, H.W. (2013) ‘CD38 controls the innate immune response against Listeria monocytogenes’, *Infect Immun, 81* (11), pp.4091-4099

Liu, G., Friggeri, A., Yang, Y., Milosevic, J., Ding, Q., Thannickal, V.J., Kaminski, N. and Abraham, E. (2010) ‘miR-21 mediates fibrogenic activation of pulmonary fibroblasts and lung fibrosis’ *The Journal of Experimental Medicine*, 207(8), pp.1589-1597

Liu, L., Eckert, M.A., Riazifar, H., Kang, D.-K., Agalliu, D. and Zhao, W. (2013) 'From Blood to the Brain: Can Systemically Transplanted Mesenchymal Stem Cells Cross the Blood-Brain Barrier?', *Stem Cells International*, 2013, p. 7.

Liu, F.J., Lim, K.Y., Kaur, P., Sepramniam, S., Armugam, A., Wong, P.T. and Jeyaseelan, K. (2013) ‘MicroRNAs involved in regulating spontaneous recovery in embolic stroke model’*, PLoS ONE*, 8, e66393

Liu, L., Sun, Z., Chen, B., Han, Q., Liao, L., Jia, M., Cao, Y., Ma, J., Sun, Q., Guo, M., Liu, Z., Ai, H. and Zhao, R.C. (2006) 'Ex vivo expansion and in vivo infusion of bone marrow-derived Flk-1+CD31-CD34- mesenchymal

stem cells: feasibility and safety from monkey to human', *Stem Cells Dev*, 15(3), pp. 349-57.

Lötvall, J., Hill, A. F., Hochberg, F., Buzás, E. I., Di Vizio, D., Gardiner, C., Gho, Y.S., Kurochkin, I.V., Mathivanan, S., Quesenberry, P., Sahoo, S., Tahara, H., Wauben, M.H., Witwer, K.W. and Théry, C. (2014). Minimal experimental requirements for definition of extracellular vesicles and their functions: a position statement from the International Society for Extracellular Vesicles. *Journal of Extracellular Vesicles*, *3*, 10.3402/jev.v3.26913.

Lou, G., Song, X., Yang, F., Wu, S., Wang, J., Chen, Z., Liu, Y. (2015) 'Exosomes derived from miR-122-modified adipose tissue-derived MSCs increase chemosensitivity of hepatocellular carcinoma' *J Hematol Oncol*, 8, pp.122

Lozzio, C.B. and Lozzio, B.B. (1975) 'Human chronic myelogenous leukemia cell-line with positive Philadelphia chromosome', *Blood*, 45, pp.321-324

Lu, T.P., Lee, C.Y., Tsai, M.H., Chiu, Y.C., Hsiao, C.K., Lai, L.C. and Chuang, E.U. (2012) 'miRSystem: an integrated system for characterizing enriched functions and pathways of microRNA targets', *PLoS One*, http://dx.doi.org/10.1371/journal.pone.0042390

Lu, T.X., Hartner, J., Lim, E.J., Fabry, V., Mingler, M.K., Cole, E.T., Orkin, S.H., Aronow, B.J. and Rothenberg, M.E. (2011) 'MicroRNA-21 limits in vivo immune response-mediated activation of the IL-12/IFN-gamma pathway, Th1 polarization, and the severity of delayed-type hypersensitivity.' *J Immunol*, 187, pp.3362–73.10.4049/jimmunol.1101235

Lu, T. X., Hartner, J., Lim, E.-J., Fabry, V., Mingler, M. K., Cole, E. T., Orkin, S.H., Aronow, B.J. and Rothenberg, M.E. (2011). MicroRNA-21 limits in vivo immune response-mediated activation of the IL-12/interferon gamma pathway, Th1 polarization, and the severity of delayed-type hypersensitivity. *Journal of Immunology (Baltimore, Md. : 1950)*, 187(6), pp. 3362–3373.

Lucchini, G., Introna, M., Dander, E., Rovelli, A., Balduzzi, A., Bonanomi, S., Salvadè, A., Capelli, C., Belotti, D., Gaipa, G., Perseghin, P., Vinci, P., Lanino, E., Chiusolo, P., Orofino, M.G., Marktel, S., Golay, J., Rambaldi, A., Biondi, A., D'Amico, G. and Biagi, E. (2010) 'Platelet-lysate-Expanded Mesenchymal Stromal Cells as a Salvage Therapy for Severe Resistant Graft-versus-Host Disease in a Pediatric Population', *Biology of Blood and Marrow Transplantation*, 16(9), pp. 1293-1301.

Maleki, M., Ghanbarvand, F., Reza Behvarz, M., Ejtemaei, M. and Ghadirkhomi, E. (2014) 'Comparison of Mesenchymal Stem Cell Markers in Multiple Human Adult Stem Cells', *International Journal of Stem Cells*, 7(2), pp. 118-126.

Malkov, V. A., Serikawa, K. A., Balantac, N., Watters, J., Geiss, G., Mashadi-Hossein, A., and Fare, T. (2009). 'Multiplexed measurements of gene signatures in different analytes using the Nanostring nCounter™ Assay System.' *BMC Research Notes*, *2*, 80.

Maltman, D.J., Hardy, S.A. and Przyborski, S.A. (2011) 'Role of mesenchymal stem cells in neurogenesis and nervous system repair', *Neurochemistry International*, 59(3), pp. 347-356.

Martens, T.P., See, F., Schuster, M.D., Sondermeijer, H.P., Hefti, M.M., Zannettino, A., Gronthos, S., Seki, T. and Itescu, S. (2006) 'Mesenchymal lineage precursor cells induce vascular network formation in ischemic myocardium', *Nat Clin Pract Cardiovasc Med*, 3 Suppl 1, pp. S18-22.

Martin, P., Gomez, M., Lamana, A., Cruz-Adalia, A., Ramirez-Huesca, M., Ursa, M. A., Yanez-Mo, M. And Sanchez-Madrid, F. (2010) 'CD69 association with Jak3/Stat5 proteins regulates Th17 cell differentiation.' Mol Cell Biol, 30(20), pp. 4877-89

Maynard, D.M., Heijnen, H.F.G., Horne, M.K., White, J.G. and Gahl, W.A. (2007) 'Proteomic analysis of platelet α-granules using mass spectrometry', *Journal of Thrombosis and Haemostasis*, 5(9), pp. 1945-1955.

Melo, C.A and Melo, S.A (2014) 'Biogenesis and physiology of MicroRNAs', *Springer New York*, pp.5-24

Melo, S.A., Sugimoto, H., O'Connell, J.T., Kato, N., Villanueva, A., Vidal, A., Qiu, L., Vitkin, E., Perelman, L.T., Melo, C.A., Lucci, A., Cristina Ivan, C., Calin, G.A. and Kalluri, R. (2014)' Cancer exosomes perform cell-independent microRNA biogenesis and promote tumorigenesis' *Cancer Cell*, 26, pp. 707–721

Mellor, A.L. and Munn, D.H. (1999) 'Tryptophan catabolism and T-cell tolerance: immunosuppression by starvation?', *Immunology Today*, 20(10), pp. 469-473.

Mi, Q.S., Xu, Y.P., Wang, H., Qi, R.Q., Dong, Z. and Zhou, L. (2013) 'Deletion of microRNA miR-223 increases Langerhans cell cross-presentation.' *Int J Biochem Cell Biol*, 45, pp.395–400.

Mifune, Y., Matsumoto, T., Murasawa, S., Kawamoto, A., Kuroda, R., Shoji, T., Kuroda, T., Fukui, T., Kawakami, Y., Kurosaka, M. and Asahara, T. (2013) 'Therapeutic superiority for cartilage repair by CD271-positive marrow stromal cell transplantation', *Cell Transplant*, 22(7), pp. 1201-11.

Mildner, A., Chapnik, E., Manor, O. Yona, S., Kim, K.W., Aychek, T., Varol, D., Beck, G., Itzhaki, Z.B., Feldmesser, E., Amit, O., Hornstein, E. and Jung, S. (2013) 'Mononuclear phagocyte miRNome analysis identifies miR-142 as critical regulator of murine dendritic cell homeostasis.',*Blood*, 121, pp.1016–27.

Mokarizadeh, A., Delirezh, N., Morshedi, A., Mosayebi, G., Farshid, A.A. and Mardani, K. (2012) 'Microvesicles derived from mesenchymal stem cells: potent organelles for induction of tolerogenic signaling', *Immunol Lett*, 147(1-2), pp. 47-54.

Momen-Heravi, F., Balaj, L., Alian, S., Mantel, P. Y., Halleck, A. E., Trachtenberg, A. J., Soria, C. E., Oquin, S., Bonebreak, C. M., Saracoglu, E., Skog, J. and Kuo, W. P. (2013) 'Current methods for the isolation of extracellular vesicles', Biol Chem, 394(10), pp.1253-262

Moreira Teixeira, L.S., Leijten, J.C., Wennink, J.W., Chatterjea, A.G., Feijen, J., van Blitterswijk, C.A., Dijkstra, P.J. and Karperien, M. (2012) 'The effect of

platelet lysate supplementation of a dextran-based hydrogel on cartilage formation', *Biomaterials*, 33(14), pp. 3651-61.

Mou, X.Z., Lin, J., Chen, J.Y., Li, Y.F., Wu, X.X., Xiang, B.Y., Li, C.Y., Ma, J.M. and Xiang, C. (2013) 'Menstrual blood-derived mesenchymal stem cells differentiate into functional hepatocyte-like cells', *J Zhejiang Univ Sci B*, 14(11), pp. 961-72.

Mulcahy, L. A., Pink, R. C., and Carter, D. R. F. (2014). 'Routes and mechanisms of extracellular vesicle uptake.' *Journal of Extracellular Vesicles*, *3*, 10.3402/jev.v3.24641.

Müller, A., Davenport, M., Verrier, S., Droeser, R., Alini, M., Bocelli-Tyndall, C., Schaefer, D., Martin, I. and Scherberich, A. (2009) 'Platelet lysate as a serum substitute for 2D static and 3D perfusion culture of stromal vascular fraction cells from human adipose tissue.', *Tissue Eng Part A*, 15(4), pp. 869-875.

Murali, A. and Rajalingam, K. (2014) 'Small Rho GTPases in the control of cell shape and mobility', *Cell Mol Life Sci*, 71(9), pp. 1703-21.

Muralidharan-Chari, V., Clancy, J., Plou, C., Romao, M., Chavrier, P., Raposo, G. and D'Souza-Schorey, C. (2009)'ARF6-regulated shedding of tumour cell-derived plasma membrane microvesicles', Curr Bio, 19(22), pp-1875-1887

Murphy, M.B., Blashki, D., Buchanan, R.M., Yazdi, I.K., Ferrari, M., Simmons, P.J. and Tasciotti, E. (2012) 'Adult and umbilical cord blood-derived platelet-rich plasma for mesenchymal stem cell proliferation, chemotaxis, and cryo-preservation', *Biomaterials*, 33(21), pp. 5308-16.

Murray, I., West, C., Hardy, W., James, A., Park, T., Nguyen, A., Tawonsawatruk, T., Lazzari, L., Soo, C. and Péault, B. (2014) 'Natural history of mesenchymal stem cells, from vessel walls to culture vessels', *Cellular and Molecular Life Sciences*, 71(8), pp. 1353-1374.

Nakamura, Y., Miyaki, S., Ishitobi, H., Matsuyama, S., Nakasa, T., Kamei, N., Akimoto, T., Higashi, Y. and Ochi, M. (2015) 'Mesenchymal-stem-cell-

derived exosomes accelerate skeletal muscle regeneration., *FEBS Letters*, 589(11), pp.1257-1265

Nauta, A.J., Westerhuis, G., Kruisselbrink, A.B., Lurvink, E.G., Willemze, R., and Fibbe, W.E. (2006). 'Donor-derived mesenchymal stem cells are immunogenic in an allogeneic host and stimulate donor graft rejection in a nonmyeloablative setting.', *Blood*, 108, pp.2114–2120

Neubauer, M., Wegmeyer, H. and Huss, R. (2012) 'The Biology and Regenerative Potential of Stem Cells and Their Mesenchymal Progeny', in Hayat, M.A. (ed.) *Stem Cells and Cancer Stem Cells, Volume 6*. Springer Netherlands, pp. 143-160.

Ng, F., Boucher, S., Koh, S., Sastry, K.S., Chase, L., Lakshmipathy, U., Choong, C., Yang, Z., Vemuri, M.C., Rao, M.S. and Tanavde, V. (2008) 'PDGF, TGF-beta, and FGF signaling is important for differentiation and growth of mesenchymal stem cells (MSCs): transcriptional profiling can identify markers and signaling pathways important in differentiation of MSCs into adipogenic, chondrogenic, and osteogenic lineages', *Blood*, 112(2), pp. 295-307.

Noone, C., Kihm, A., English, K., O'Dea, S. and Mahon, B.P. (2013) IFN-gamma stimulated human umbilical-tissue-derived cells potently suppress NK activation and resist NK-mediated cytotoxicity in vitro', *Stem Cells Dev*, 22(22), pp.3003-3014

Nuttall, M.E. and Gimble, J.M. (2004) 'Controlling the balance between osteoblastogenesis and adipogenesis and the consequent therapeutic implications', *Curr Opin Pharmacol*, 4(3), pp. 290-4.

Ode, A., Schoon, J., Kurtz, A., Gaetjen, M., Ode, J.E., Geissler, S. and Duda, G.N. (2013) 'CD73/5'-ecto-nucleotidase acts as a regulatory factor in osteo-/chondrogenic differentiation of mechanically stimulated mesenchymal stromal cells', *Eur Cell Mater*, 25, pp. 37-47.

Olsen, B.R., Reginato, A.M. and Wang, W. (2000) 'Bone development', *Annu Rev Cell Dev Biol*, 16, pp. 191-220.

Ono, M., Kosaka, M., Tominanga, N., Yoshioka, N., Takeshita, F., Takahashi, R.U., Yoshida, M., Tsuda, H., Tamura, K. and Ochiya, T. (2014) ‘Exosomes from bone marrow mesenchymal stem cells contain a microRNA that promotes dormancy in metastic breast cancer cells’, *Sci Signal*, 7(332), pp. ra63

Pan, B.T. and Johnstone, R.M. (1983) ‘Fate of the transferrin receptor during maturation of sheep reticulocytes in vitro: selective externalization of the receptor’, *Cell*, 33(3), pp.967-978

Park, C.W., Kim, K.S., Bae, S., Son, H.K., Myung, P.K., Hong, H.J. and Kim, H. (2009) ‘Cytokine secretion profiling of human mesenchymal stem cells by antibody array.’ *Int J Stem Cells*, 2, pp.59–68

Patki, S., Kadam, S., Chandra, V. and Bhonde, R. (2010) 'Human breast milk is a rich source of multipotent mesenchymal stem cells', *Hum Cell*, 23(2), pp. 35-40.

Pende, D., Bottino, C., Castriconi, R., Cantoni, C., Marcenaro, S., Rivera, P., Spaggiari, G.M., Dondero, A., Carnemolla, B., Reymond, N., Mingari, M.C., Lopez, M., Moretta, L. and Moretta, A. (2005) 'PVR (CD155) and Nectin-2 (CD112) as ligands of the human DNAM-1 (CD226) activating receptor: involvement in tumor cell lysis', *Mol Immunol*, 42(4), pp. 463-9.

Pérez-Ilzarbe, M., Díez-Campelo, M., Aranda, P., Tabera, S., Lopez, T., del Cañizo, C., Merino, J., Moreno, C., Andreu, E.J., Prósper, F. and Pérez-Simón, J.A. (2009) 'Comparison of ex vivo expansion culture conditions of mesenchymal stem cells for human cell therapy', *Transfusion*, 49(9), pp. 1901-1910.

Pers, Y.M., Rackwitz, L., Ferreira, R., Pullig, O., Delfour, C., Barry, F., Sensebe, L., Casteilla, L., Fleury, S., Bourin, P., Noel, D., Canovas, F., Cyteval, C., Lisignoli, G., Schrauth, J., Haddad, D., Domergue, S., Noeth, U. and Jorgensen, C. (2016) 'Adipose Mesenchymal Stromal Cell-Based Therapy for Severe Osteoarthritis of the Knee: A Phase I Dose-Escalation Trial', *Stem Cells Transl Med*, 5(7), pp. 847-56.

Phinney, D.G., Di Giuseppe, M., Njah, J., Sala, E., Shiva, S., St Croix, C.M., Stolz, D.B., Watkins, S.C., Di, Y.P., Leikauf, G.D., Kolls, J., Riches, D.W., Deiuliis, G. and Kaminski, N. (2015) 'Mesenchymal stem cells use extracellular vesicles to outsource mitophagy and shuttle microRNAs', *Nat Commun*, 6, pp.8472

Pietila, M., Lehtonen, S., Tuovinen, E., Lahteenmaki, K., Laitinen, S., Leskela, H.V., Natynki, A., Pesala, J., Nordstrom, K. and Lehenkari, P. (2012) 'CD200 positive human mesenchymal stem cells suppress TNF-alpha secretion from CD200 receptor positive macrophage-like cells', *PLoS One*, 7(2), p. e31671.

Pijnappels, D.A., Schalij, M.J., Ramkisoensing, A.A., van Tuyn, J., de Vries, A.A.F., van der Laarse, A., Ypey, D.L. and Atsma, D.E. (2008) 'Forced Alignment of Mesenchymal Stem Cells Undergoing Cardiomyogenic Differentiation Affects Functional Integration With Cardiomyocyte Cultures', *Circulation Research*, 103(2), pp. 167-176.

Pittenger, M.F., Le Blanc, K., Phinney, D.G. and Chan, J.K. (2015) 'MSCs: Scientific Support for Multiple Therapies', *Stem Cells Int*, 2015, p. 280572.

Pittenger, M.F., Mackay, A.M., Beck, S.C., Jaiswal, R.K., Douglas, R., Mosca, J.D., Moorman, M.A., Simonetti, D.W., Craig, S. and Marshak, D.R. (1999) 'Multilineage potential of adult human mesenchymal stem cells', *Science*, 284(5411), pp. 143-7.

Polchert, D., Sobinsky, J., Douglas, G., Kidd, M., Moadsiri, A., Reina, E., Genrich, K., Mehrotra, S., Setty, S., Smith, B. and Bartholomew, A. (2008) 'IFN-gamma activation of mesenchymal stem cells for treatment and prevention of graft versus host disease', *Eur J Immunol*, 38(6), pp. 1745-55.

Pregno, G., Zamburlin, P., Gambarotta, G., Farcito, S., Licheri, V., Fregnan, F., Perroteau, I., Lovisolo, D. and Bovolin, P. (2011) 'Neuregulin1/ErbB4-induced migration in ST14A striatal progenitors: calcium-dependent mechanisms and modulation by NMDA receptor activation', *BMC Neuroscience*, 12(1), pp.1-14

Prockop, D.J. (1997) 'Marrow Stromal Cells as Stem Cells for Nonhematopoietic Tissues', *Science*, 276(5309), pp. 71-74.

Psaltis, P.J., Paton, S., See, F., Arthur, A., Martin, S., Itescu, S., Worthley, S.G., Gronthos, S. and Zannettino, A.C. (2010) 'Enrichment for STRO-1 expression enhances the cardiovascular paracrine activity of human bone marrow-derived mesenchymal cell populations', *J Cell Physiol*, 223(2), pp. 530-40.

Quesenberry, P. J., Aliotta, J., Deregibus, M. C. and Camussi, G. (2015). 'Role of extracellular RNA-carrying vesicles in cell differentiation and reprogramming.' *Stem Cell Research & Therapy*, 6, pp. 153.

Radulovic K., Manta C., Rossini V., Holzmann K., Kestler H.A., Wehenka, U.M., Nakayama, T. and Niess, J.H. (2012) 'CD69 regulates type I IFN-induced tolerogenic signals to mucosal CD4 T cells that attenuate their colitogenic potential.' J Immunol 188: 2001–2013

Raker, V. K., Domogalla, M. P., and Steinbrink, K. (2015). Tolerogenic Dendritic Cells for Regulatory T Cell Induction in Man. *Frontiers in Immunology*, *6*, 569.

Ramirez, S., Aiken, C.T., Andrzejewski, B., Sklar, L.A. and Edwards, B.S. (2003) 'High-throughput flow cytometry: validation in microvolume bioassays', *Cytometry A*, 53(1), pp. 55-65.

Randolph, G.J., Angeli, V. and Swartz, M.A. (2005) 'Dendritic-cell trafficking to lymph nodes through lymphatic vessels', *Nat Rev Immunol*, 5, pp.617-628

Rani, S., Ryan, A.E., Griffin, M.D. and Ritter, T. (2015) 'Mesenchymal stem cell-derived extracellular vesicles: toward cell-free therapeutic applications', *Mol Ther,* 23(5), pp.812-823

Raposo G, Nijman HW, Stoorvogel W, Liejendekker R, Harding CV, Melief CJ. (1996) 'B lymphocytes secrete antigen-presenting vesicles.' *The Journal of experimental medicine*, 183(3), pp.1161-72.

Raposo, G. and Stoorvogel, W., (2013) 'Extracellular vesicles: exosomes, microvesicles and friends.' *J Cell Biol*, 200, pp.373-383

Rasmusson I, Ringdén O, Sundberg B and Le Blanc K (2003). Mesenchymal stem cells inhibit the formation of cytotoxic T lymphocytes, but not activated cytotoxic T lymphocytes or natural killer cells. Transplantation **76**(8): 1208.

Rasmusson, I., Uhlin, M., Le Blanc, K. and Levitsky, V. (2007) 'Mesenchymal stem cells fail to trigger effector functions of cytotoxic T lymphocytes', J Leukoc Biol, 82, pp.887-893

Rauch, C., Feifel, E., Amann, E., Spötl, H., Schennach, H., Pfaller, W. and Gstraunthaler, G. (2011) 'Alternatives to the use of fetal bovine serum: human platelet lysates as a serum substitute in cell culture media', *ALTEX*, 28(4), pp. 305-316.

Reinders, M. E. and Hoogduijn, M. J. (2014). 'NK Cells and MSCs: Possible Implications for MSC Therapy in Renal Transplantation.' *Journal of Stem Cell Research & Therapy*, *4*(2), pp. 1000166.

Ren, G., Zhang, L., Zhao, X., Xu, G., Zhang, Y., Roberts, A.I., Zhao, R.C. and Shi, Y. (2008) 'Mesenchymal Stem Cell-Mediated Immunosuppression Occurs via Concerted Action of Chemokines and Nitric Oxide', *Cell Stem Cell*, 2(2), pp. 141-150.

Ren, G., Zhao, X., Zhang, L., Zhang, J., L'Huillier, A., Ling, W., Roberts, A.I., Le, A.D., Shi, S., Shao, C. and Shi, Y. (2010) 'Inflammatory cytokine-induced intercellular adhesion molecule-1 and vascular cell adhesion molecule-1 in mesenchymal stem cells are critical for immunosuppression', *J Immunol*, 184(5), pp. 2321-8.

Richard, D.E., Vouret-Craviari, V. and Pouyssegur, J. (2001) 'Angiogenesis and G-protein-coupled receptors: signals that bridge the gap', *Oncogene*, 20(13), pp. 1556-62.

Rider, D.A., Nalathamby, T., Nurcombe, V. and Cool, S.M. (2007) 'Selection using the alpha-1 integrin (CD49a) enhances the multipotentiality of the mesenchymal stem cell population from heterogeneous bone marrow stromal cells', *J Mol Histol*, 38(5), pp. 449-58.

Ringden, O., Uzunel, M., Rasmusson, I., Remberger, M., Sundberg, B. and Lonnies, H. (2006) 'Mesenchymal stem cells for treatment of therapy-

resistant graft-versus-host disease.' *Transplantation.* 2006, 81(10), pp.1390-7

Rodrigues, M., Griffith, L.G. and Wells, A. (2010) 'Growth factor regulation of proliferation and survival of multipotential stromal cells' *Stem Cell Res & Ther*, 1, pp.32

Roelen, B.A. and Dijke, P. (2003) 'Controlling mesenchymal stem cell differentiation by TGFBeta family members', *J Orthop Sci*, 8(5), pp. 740-8.

Rogers, I. and Casper, R.F. (2004) 'Umbilical cord blood stem cells', *Best Practice & Research Clinical Obstetrics & Gynaecology*, 18(6), pp. 893-908.

Rosen, E.D., Hsu, C.H., Wang, X., Sakai, S., Freeman, M.W., Gonzalez, F.J. and Spiegelman, B.M. (2002) 'C/EBPalpha induces adipogenesis through PPARgamma: a unified pathway', *Genes Dev*, 16(1), pp. 22-6.

Rosen, E.D., Walkey, C.J., Puigserver, P. and Spiegelman, B.M. (2000) 'Transcriptional regulation of adipogenesis', *Genes Dev*, 14(11), pp. 1293-307.

Rosová, I., Dao, M., Capoccia, B., Link, D. and Nolta, J.A. (2008) 'Hypoxic Preconditioning Results in Increased Motility and Improved Therapeutic Potential of Human Mesenchymal Stem Cells', *STEM CELLS*, 26(8), pp. 2173-2182.

Rozengurt, E., Sinnett-Smith, J. and Kisfalvi, K. (2010) 'Crosstalk between Insulin/IGF-1 and GPCR Signaling Systems: A Novel Target for the Anti-diabetic Drug Metformin in Pancreatic Cancer', *Clinical cancer research : an official journal of the American Association for Cancer Research*, 16(9), pp. 2505-2511.

Sacchetti, B., Funari, A., Michienzi, S., Di Cesare, S., Piersanti, S., Saggio, I., Tagliafico, E., Ferrari, S., Robey, P.G., Riminucci, M. and Bianco, P. (2007) 'Self-renewing osteoprogenitors in bone marrow sinusoids can organize a hematopoietic microenvironment', *Cell*, 131(2), pp. 324-36.

Sakaguchi, S., Yamaguchi, T., Nomura, T. and Ono, M. (2008) 'Regulatory T Cells and Immune Tolerance', *Cell*, 133(5), pp. 775-787.

Saldanha-Araujo, F., Haddad, R., Farias, K. C., Souza Ade, P., Palma, P. V., Araujo, A. G., Orellana, M. D., Voltarelli, J. C., Covas, D. T., Zago, M. A. and Panepucci, R. A. (2012) 'Mesenchymal stem cells promote the sustained expression of CD69 on activated T lymphocytes: roles of canonical and non-canonical NF-kappaB signalling', J Cell Mol Med, 16(6), pp.1232-44

Savina, A., Furlan, M., Vidal, M. and Colombo, M. (2003) 'Exosome release is regulated by a calcium-dependent mechanism in K562 cells' *The Journal of Biological Chemistry,* 278, pp.20083-20090

Schwartz, R.E., Reyes, M., Koodie, L., Jiang, Y., Blackstad, M., Lund, T., Lenvik, T., Johnson, S., Hu, W.-S. and Verfaillie, C.M. (2002) 'Multipotent adult progenitor cells from bone marrow differentiate into functional hepatocyte-like cells', *The Journal of Clinical Investigation*, 109(10), pp. 1291-1302.

Selmani, Z., Naji, A., Zidi, I., Favier, B., Gaiffe, E., Obert, L., Borg, C., Saas, P., Tiberghien, P., Rouas-Freiss, N., Carosella, E.D. and Deschaseaux, F. (2008) 'Human Leukocyte Antigen-G5 Secretion by Human Mesenchymal Stem Cells Is Required to Suppress T Lymphocyte and Natural Killer Function and to Induce CD4+CD25highFOXP3+ Regulatory T Cells', *STEM CELLS*, 26(1), pp. 212-222.

Sensebé, L., Gadelorge, M. and Fleury-Cappellesso, S. (2013) 'Production of mesenchymal stromal/stem cells according to good manufacturing practices: a review', *Stem Cell Research & Therapy*, 4(3), pp. 1-6.

Sheedy, F. J. (2015). 'Turning 21: Induction of miR-21 as a Key Switch in the Inflammatory Response.' *Frontiers in Immunology*, 6, 19.

Sheedy, F.J., Palsson-McDermott, E., Hennessy, E.J., Martin, C., O'Leary, J.J., Ruan, Q., Johnson, D.S., Chen, Y. and O'Neill, L.A.J. (2010) 'Negative regulation of TLR4 via targeting of the proinflammatory tumor suppressor PDCD4 by the microRNA miR-21', *Nat Immunol*, 11(2), pp.141-147

Sherwin, S.Y., William, R.T., Gunes, U., Zhihui, X., Buer, S., Maya, S., Keith, B. and Janet, E.R. (2014) 'The RhoA Gtpase Activating Protein ARHGAP18

Regulates Mesenchymal Stem Cell Lineage Commitment', in *Novel Signaling Mechanisms and Bone Cell Biology*. Endocrine Society, pp. OR31-3-OR31-3.

Sheyn, D., Ben-David, S., Shapiro, G., De Mel, S., Bez, M., Ornelas, L., Sahabian, A., Sareen, D., Da, X., Pelled, G., Tawackoli, W., Liu, Z., Gazit, D. and Gazit, Z. (2016) 'Human iPSCs Differentiate Into Functional MSCs and Repair Bone Defects', *Stem Cells Transl Med*.

Shi, S. and Gronthos, S. (2003) 'Perivascular Niche of Postnatal Mesenchymal Stem Cells in Human Bone Marrow and Dental Pulp', *Journal of Bone and Mineral Research*, 18(4), pp. 696-704.

Sibov, T.T., Severino, P., Marti, L.C., Pavon, L.F., Oliveira, D.M., Tobo, P.R., Campos, A.H., Paes, A.T., Amaro, E., Jr., L, F.G. and Moreira-Filho, C.A. (2012) 'Mesenchymal stem cells from umbilical cord blood: parameters for isolation, characterization and adipogenic differentiation', *Cytotechnology*, 64(5), pp. 511-21.

Siegel, G., Kluba, T., Hermanutz-Klein, U., Bieback, K., Northoff, H. and Schafer, R. (2013) 'Phenotype, donor age and gender affect function of human bone marrow-derived mesenchymal stromal cells', *BMC Med*, 11, p. 146.

Silva, G.V., Litovsky, S., Assad, J.A., Sousa, A.L., Martin, B.J., Vela, D., Coulter, S.C., Lin, J., Ober, J., Vaughn, W.K., Branco, R.V., Oliveira, E.M., He, R., Geng, Y.J., Willerson, J.T. and Perin, E.C. (2005) 'Mesenchymal stem cells differentiate into an endothelial phenotype, enhance vascular density, and improve heart function in a canine chronic ischemia model', *Circulation*, 111(2), pp. 150-6.

Smigielska-Czepiel, K., van den Berg, A., Jellema, P., Slezak-PRochazka, I., Maat, H., van den Bos, H., van der Lei, R.J., Kluiver, J., Brouwer, E., Boots, A.M. and Kroesen, B.J. (2013) ‘Dual role of in CD4+ T cells: acivation-induced miR-21 promotes survival of memory T-cells and regulates CCR7 expression in naïve T-cells’, PLoS One, 8(10), doi: 10.1371/journal.pone.0076217

Smyth, L.A., Boardman, D.A., Tung, S.L., Lechler, R. and Lombardi, G. (2015) 'MicroRNAs affect dendritic cell function and phenotype', *Immunology*, 144(2), pp.197-205

Sobiesiak, M., Sivasubramaniyan, K., Hermann, C., Tan, C., Orgel, M., Treml, S., Cerabona, F., de Zwart, P., Ochs, U., Muller, C.A., Gargett, C.E., Kalbacher, H. and Buhring, H.J. (2010) 'The mesenchymal stem cell antigen MSCA-1 is identical to tissue non-specific alkaline phosphatase', *Stem Cells Dev*, 19(5), pp. 669-77.

Spaggiari, G.M., Abdelrazik, H., Becchetti, F. and Moretta, L. (2009) 'MSCs inhibit monocyte-derived DC maturation and function by selectively interfering with the generation of immature DCs: central role of MSC-derived prostaglandin E2.' *Blood* 2009; 113: 6576–6583.

Spaggiari, G.M., Capobianco, A., Becchetti, S., Mingari, M.C. and Moretta, L. (2006). 'Mesenchymal stem cell-natural killer cell interactions: Evidence that activated NK cells are capable of killing MSCs, whereas MSCs can inhibit IL-2-induced NK-cell proliferation.' *Blood* 107(4): 1484.

Spaggiari G.M., Capobianco, A., Abdelrazik, H., Becchetti, F., Mingari, M.C. and Moretta, L. (2008) 'Mesenchymal stem cells inhibit natural killer-cell proliferation, cytotoxicity, and cytokine production: role of indoleamine 2,3-dioxygenase and prostaglandin E2'. *Blood*, 111, pp.1327–1333.

Spees, J.L., Gregory, C.A., Singh, H., Tucker, H.A., Peister, A., Lynch, P.J., Hsu, S.C., Smith, L. and Prockop, D.J. (2004) 'Internalized antigens must be removed to prepare hypoimmunogenic mesenchymal stem cells for cell and gene therapy', *Mol Ther*, 9, pp.747-756

Stewart, K., Monk, P., Walsh, S., Jefferiss, C.M., Letchford, J. and Beresford, J.N. (2003) 'STRO-1, HOP-26 (CD63), CD49a and SB-10 (CD166) as markers of primitive human marrow stromal cells and their more differentiated progeny: a comparative investigation in vitro', *Cell Tissue Res*, 313(3), pp. 281-90.

Stute, N., Holtz, K., Bubenheim, M., Lange, C., Blake, F. and Zander, A.R. (2004) 'Autologous serum for isolation and expansion of human

mesenchymal stem cells for clinical use', *Experimental hematology*, 32(12), pp. 1212-1225.

Su, J.L., Chen, P.S., Johansson, G. and Kuo, M.L. (2012) 'Function and regulation of let-7 family of microRNAs', *Microrna*, 1(1), pp.34-39

Sun, Y., S. Varambally, C. A. Maher, Q. Cao, P. Chockley, T. Toubai, C. Malter, E. Nieves, I. Tawara, Y. Wang, Ward, P.A., Chinnaiyan, A. and Reddy, P. (2011) 'Targeting of microRNA-142-3p in dendritic cells regulates endotoxin-induced mortality.', *Blood*, 117, pp.6172–6183.

Sudres, M., Norol, F., Trenado, A., Gregoire, S., Charlotte, F., Levacher, B., Lataillade, J.J., Bourin, P., Holy, X., Vernant, J.P., Klatzmann, D. and Cohen, J.L. (2006) 'Bone marrow mesenchymal stem cells suppress lymphocyte proliferation in vitro but fail to prevent graft-versus-host disease in mice', *J Immunol*, 176(12), pp. 7761-7.

Talwadekar, M.D., Kale, V.P. and Limaye, L.S. (2015) 'Placenta-derived mesenchymal stem cells possess better immunoregulatory properties compared to their cord-derived counterparts-a paired sample study', *Sci Rep*, 5, p. 15784.

Tamai, K., Yamazaki, T., Chino, T., Ishii, M., Otsuru, S., Kikuchi, Y., Iinuma, S., Saga, K., Nimura, K., Shimbo, T., Umegaki, N., Katayama, I., Miyazaki, J., Takeda, J., McGrath, J.A., Uitto, J. and Kaneda, Y. (2011) 'PDGFRalpha-positive cells in bone marrow are mobilized by high mobility group box 1 (HMGB1) to regenerate injured epithelia', *Proc Natl Acad Sci U S A*, 108(16), pp. 6609-14.

Tan, S.S., Yin, Y., Lee, T., Lai, R.C., Yeo, R.W., Zhang, B., Choo, A. and Lim, S.K. (2013) 'Therapeutic MSC exosomes are derived from lipid raft microdomains in the plasma membrane', *J Extracell Vesicles*, 2.

Tapping, R.I. (2009) 'Innate immune sensing and activation of cell surface Toll-like receptors', Seminars in Immunology, 21(4),pp. 175-184.

Tekkatte, C., Gunasingh, G.P., Cherian, K.M. and Sankaranarayanan, K. (2011) '"Humanized" Stem Cell Culture Techniques: The Animal Serum Controversy', *Stem Cells Int*, 2011, p. 504723.

Théry C, Clayton A, Amigorena S, Raposo G (2006) Isolation and Characterization of Exosomes from Cell Culture Supernatants and Biological Fluids. *Current Protocols in Cell Biology,* 3(22), 1–3.22.29.

Théry, C. (2011). Exosomes: secreted vesicles and intercellular communications. *F1000 Biology Reports*, *3*, 15. http://doi.org/10.3410/B3-15,

Théry, C., Regnault, A., Garin, J., Wolfers, J., Zitvogel, L., Ricciardi-Castagnoli, P., Raposo, G. and AmigorenaS. (1999) 'Molecular characterization of dendritic cell-derived exosomes. Selective accumulation of the heat shock protein hsc73.' *J. Cell Biol*. 147:599–610.

Thielens, A., Vivier, E., and Romagne, F. (2012) 'NK cell MHC class I specific receptors (KIR): from biology to clinical intervention', *Curr Opin Immunol*, 24(2), pp.239-245

Ti, D., Hao, H., Tong, C., Liu, J., Dong, L., Zheng, J., Zhao, Y., Liu, H., Fu, X. and Han, W. (2015) 'LPS-preconditioned mesenchymal stromal cells modify macrophage polarization for resolution of chronic inflammation via exosome-shuttled let-7b', *J Transl Med*, 13(1), p. 308.

Toma, J.G., Akhavan, M., Fernandes, K.J.L., Barnabe-Heider, F., Sadikot, A., Kaplan, D.R. and Miller, F.D. (2001) 'Isolation of multipotent adult stem cells from the dermis of mammalian skin', *Nat Cell Biol*, 3(9), pp. 778-784.

Tomasoni, S., Longaretti, L., Rota, C., Morigi, M., Conti, S., Gotti, E., Capelli, C., Introna, M., Remuzzi, G. and Benigni, A. (2013) 'Transfer of growth factor receptor mRNA via exosomes unravels the regenerative effect of mesenchymal stem cells', *Stem Cells Dev*, 22(5), pp. 772-80.

Tropel, P., Platet, N., Platel, J.-C., Noël, D., Albrieux, M., Benabid, A.-L. and Berger, F. (2006) 'Functional Neuronal Differentiation of Bone Marrow-Derived Mesenchymal Stem Cells', *STEM CELLS*, 24(12), pp. 2868-2876.

Tsai, M.S., Lee, J.L., Chang, Y.J. and Hwang, S.M. (2004) 'Isolation of human multipotent mesenchymal stem cells from second-trimester amniotic fluid using a novel two-stage culture protocol', *Human Reproduction*, 19(6), pp. 1450-1456.

Turner, M.L., Schnorfeil, F.M. and Brocker, T. (2011) 'MicroRNAs regulate dendritic cell differentiation and function', *J Immunol*, 187 (8), pp.3911-3917

Uccelli, A., Moretta, L. and Pistoia, V. (2008) 'Mesenchymal stem cells in health and disease', *Nat Rev Immunol*, 8(9), pp. 726-736.

Van, P.P. (2011) 'Stem Cell therapy for Islet Regeneration, Stem Cells in Clinic and Research', Dr. Ali Gholamrezanezhad (Ed.), InTechm, DOI: Phuc Pham Van (2011). Stem Cell Therapy for Islet Regeneration, Stem Cells in Clinic and Research, Dr. Ali Gholamrezanezhad (Ed.), InTech, DOI: 10.5772/17588. Available from: http://www.intechopen.com/books/stem-cells-in-clinic-and-research/stem-cell-therapy-for-islet-regeneration

Vellasamy, S., Sandrasaigaran, P., Vidyadaran, S., Abdullah, M., George, E. and Ramasamy, R. (2013) 'Mesenchymal stem cells of human placenta and umbilical cord suppress T-cell proliferation at G0 phase of cell cycle', *Cell Biol Int*, 37(3), pp. 250-6.

Villarroya-Beltri, C., Gutierrez-Vazquez, C., Sanchez-Cabo, F., Perez-Hernandez, D., Vazquez, J., Martin-Cofreces, N., Martinez-Herrera, D.J., Pascual-Montano, A., Mittelbrunn, M. and Sanchez-Madrid, F. (2013) 'Sumoylated hnRNPA2B1 controls the sorting of miRNAs into exosomes through binding to specific motifs', *Nat Commun*, 4, p. 2980

Vivier, E., Tomasello, E., Baratin, M., Walzer, T., Ugolini, S. (2008) 'Functions of natural killer cells', *Nat Immunol*, 9(5), pp.503-51

von Bahr L, Batsis I, Moll, G., Hagg, M., Szakos, A., and Sundberg, B. Analysis of tissues following mesenchymal stromal cell therapy in humans indicates limited long-term engraftment and no ectopic tissue formation. Stem cells. 2012;30(7):1575-8

von Bahr, L., Sundberg, B., Lonnies, L., Karbach, H., Hagglund, H., Ljungman, P., Gustafsson, B., Karlsson, H., Le Blanc, K., Ringden, O. (2012) 'Long-Term complications, immunological effects, and role of passage for outcome in mesenchymal stromal cell therapy'. *Biology of Blood and Bone Marrow Transplantation*, 18(4), pp.557-564

Waisman, A., Lukas, D., Clausen, B.E. and Yogev, N., (2016) 'Dendritic cells as gatekeepers of tolerance', *Semin Immunopathol*, doi: 10.1007/s00281-016-0583-z

Walmsley, G.G., Atashroo, D.A., Maan, Z.N., Hu, M.S., Zielins, E.R., Tsai, J.M., Duscher, D., Paik, K., Tevlin, R., Marecic, O., Wan, D.C., Gurtner, G.C. and Longaker, M.T. (2015) 'High-Throughput Screening of Surface Marker Expression on Undifferentiated and Differentiated Human Adipose-Derived Stromal Cells', *Tissue Eng Part A*, 21(15-16), pp. 2281-91.

Wang, S., Qu, X. and Zhao, R. (2012) 'Clinical applications of mesenchymal stem cells', *Journal of Hematology & Oncology*, 5(1), p. 19.

Wang, T., Zhang, L., Shi, C., Sun, H., Wang, J., Li, R., Zou, Z., Ran, X. and Su, Y. (2012). 'TGF-beta-induced miR-21 negatively regulates the antiproliferative activity but has no effect on EMT of TGF-beta in HaCaT cells.', *Int J Biochem Cell Biol*, 44(2), pp. 366-276

Wang, Y., Chen, X., Cao, W. and Shi, Y. (2014) 'Plasticity of mesenchymal stem cells in immunomodulation: pathological and therapeutic implications', *Nat Immunol*, 15(11), pp. 1009-16.

Waterman, R.S., Tomchuck, S.L., Henkle, S.L. and Betancourt, A.M. (2010) 'A New Mesenchymal Stem Cell (MSC) Paradigm: Polarization into a Pro-Inflammatory MSC1 or an Immunosuppressive MSC2 Phenotype', *PLoS ONE*, 5(4), p. e10088.

Webber, J. and Clayton, A. (2013) 'How pure are your vesicles?', *J Extracell Vesicles*, 2.

Werfel, T., Boeker, M. and Kapp, A. (1997) 'Rapid expression of the CD69 antigen on T cells and natural killer cells upon antigenic stimulation of peripheral blood mononuclear cell suspensions', *Allergy*, 53(4), pp. 465-569

Wexler, S.A., Donaldson, C., Denning-Kendall, S., Rice, C., Bradley, B. and Hows, J.M. (2003) ‘Adult bone marrow is a rich source of human mesenchymal ‘stem’ cells but umbilical cord and mobilized adult blood are not’, *Br J Haematol,* 121(2), pp.368-374

Wiesmann, A., Buhring, H.J., Mentrup, C. and Wiesmann, H.P. (2006) 'Decreased CD90 expression in human mesenchymal stem cells by applying mechanical stimulation', *Head Face Med*, 2, p. 8.

Winter, J., Jung, S., Keller, S., Gregory, R.I. and Diederichs, S. (2009) ‘Many roads ro maturity: microRNA biogenesis pathways and their regulation’, *Nat Cell Biol*, 11(3), pp.228-234

Wouters, G., Grossi, S., Mesoraca, A., Bizzoco, D., Mobili, L., Cignini, P. and Giorlandino, C. (2007) 'Isolation of amniotic fluid-derived mesenchymal stem cells', *Journal of Prenatal Medicine*, 1(3), pp. 39-40.

Wu, X. and Tao, R. (2012) 'Hepatocyte differentiation of mesenchymal stem cells', *Hepatobiliary Pancreat Dis Int* 11(4), pp. 360-371.

Xin, H., Li, Y., Buller, B., Katakowski, M., Zhang, Y., Wang, X., Shang, X., Zhang, Z.G. and Chopp, M. (2012) ‘Exosome-mediated transfer of miR-133b from multipotent mesenchymal stromal cells to neural cells contributes to neurite outgrowth’, *Stem Cells*, 30(83), pp.1556-1564

Xu, Y., Malladi, P., Wagner, D.R. and Longaker, M.T. (2005) *Adipose-derived mesenchymal cells as a potential cell source for skeletal regeneration*.

Yang, Z.X., Han, Z.-B., Ji, Y.R., Wang, Y.W., Liang, L., Chi, Y., Yang, S.G., Li, L.N., Luo, W.F., Li, J.P., Chen, D.D., Du, W.J., Cao, X.C., Zhuo, G.S., Wang, T. and Han, Z.C. (2013) 'CD106 Identifies a Subpopulation of Mesenchymal Stem Cells with Unique Immunomodulatory Properties', *PLoS ONE*, 8(3), p. e59354.

Yeh, Y.Y., Ozer, H.T., Lehman, A.M., Maddocks, K., Yu, L., Johnson, A.J. and Byrd, J.C. (2015) ‘Characterisation of CLL exosomes reveals a distinct microRNA signature and enhanced secretion by activation of BCR signaling’, *Blood,* 125, pp.3297-3305

Yu, D.-A., Han, J. and Kim, B.S. (2012) 'Stimulation of Chondrogenic Differentiation of Mesenchymal Stem Cells', *International Journal of Stem Cells*, 5(1), pp. 16-22.

Yu B, Kim HW, Gong M, Wang J, Millard RW, Wang Y, Ashraf, M. and Xu, M. (2015) 'Exosomes secreted from GATA-4 overexpressing mesenchymal stem cells serve as areservoir of anti-apoptotic microRNAs for cardioprotection.' *Int J Cardiol*, 182, pp.349–60

Zappia, E., Casazza, S., Pedemonte, E., Benvenuto, F., Bonanni, I., Gerdoni, E., Giunti, D., Ceravolo, A., Cazzanti, F., Frassoni, F., Mancardi, G. and Uccelli, A. (2005) 'Mesenchymal stem cells ameliorate experimental autoimmune encephalomyelitis inducing T-cell anergy', *Blood*, 106(5), pp. 1755-61.

Zhang, B., Yin, Y., Lai, R.C., Tan, S.S., Choo, A.B. and Lim, S.K. (2014) 'Mesenchymal stem cells secrete immunologically active exosomes', *Stem Cells Dev*, 23(11), pp.1233-44

Zhang, G., Zou, X., Huang, Y., Wang, F., Miao, S., Liu, G., Chen, M. and Zhu, Y. (2016) 'Mesenchymal Stromal Cell-Derived Extracellular Vesicles Protect Against Acute Kidney Injury Through Anti-Oxidation by Enhancing Nrf2/ARE Activation in Rats.', *Kidney Blood Press Res*, 41, pp.119-128

Zhang, M., Liu, F., Jia, H., Zhang, Q., Yin, L., Liu, W., Li, H., Yu, B. and Wu, J. (2011) 'Inhibition of microRNA let-7i depresses maturation and functional state of dendritic cells in response to lipopolysaccharide stimulation via targeting suppressor of cytokine signaling 1', *J Immunol*, 187(4), pp.1674-83

Zhang, Y., Chopp, M., Meng, Y., Katakowski, M., Xin, H., Mahmood, A. and Xiong, Y. (2015) 'Effect of exosomes derived from multipluripotent mesenchymal stromal cells on functional recovery and neurovascular plasticity in rats after traumatic brain injury', *J Neurosurg*, 122(4), pp. 856-67.

Zheng, Z.H., Li, X.Y., Ding, J., Jia, J.F. and Zhu, P. (2007) 'Allogeneic mesenchymal stem cell and mesenchymal stem cell-differentiatied

chondrocyte suppress the responses of type II collagen-reactive T cells in rheumatoid arthritis’*, Rheumatology*, 47(1), pp.22-30

Zhou, Q., Haupt, S., Prots, I., Thummler, K., Kremmer, E., Lipsky, P. E. Schulze-Koops, H. and Skapenko, A. (2013) ‘miR-142-3p is involved in CD25+ CD4 T cell proliferation by targeting the expression of glycoprotein A repetitions predominant’, *J Immunol*, 190(12), pp.6579-88

Zuk, P.A., Zhu, M., Ashjian, P., De Ugarte, D.A., Huang, J.I., Mizuno, H., Alfonso, Z.C., Fraser, J.K., Benhaim, P. and Hedrick, M.H. (2002) 'Human Adipose Tissue Is a Source of Multipotent Stem Cells', *Molecular Biology of the Cell*, 13(12), pp. 4279-4295.